Degree PhD Year 2006 Name of Author CALA, S. G.

NOD2 GENE EXPRESSION IN PANETH CELLS AND MONOCYTES

by

Sanjay Govind Lala

A thesis submitted in partial fulfilment of the requirements for the degree of:

Doctor of Philosophy

Royal Free & University College Medical School,
University of London

2006

ProQuest LLC
789 East Eisenhower Parkway
P.O. Box 1346
Ann Arbor, MI 48106-1346

Declaration

I, Sanjay Govind Lala, confirm that the work presented in this thesis is my own. Where information has been derived from other sources, I confirm that this has been indicated in the thesis. I can confirm that I performed all experiments, with assistance from Miss Sok-Ying Hor, Dr Annabel Bromfield and Dr Satish Keshav.

Abstract

Introduction: Mutations in the NOD2 gene are associated with the development of Crohn's disease, an inflammatory disorder of the gastrointestinal tract. The NOD2 protein induces cellular activation in response to the bacterial antigen muramyl dipeptide (MDP). The NOD2 gene is mainly expressed by circulating blood monocytes although NOD2-associated Crohn's disease involves mainly the terminal ileum. Paneth cells, which are most numerous in the terminal ileum, are specialised intestinal epithelial cells that secrete antimicrobial peptides in response to bacterial products and are critically important in enteric antibacterial defence. I hypothesised that Paneth cells express the NOD2 gene: this thesis describes the expression and quantification of the NOD2 gene in Paneth cells in inflammatory diseases such as Crohn's disease and necrotizing enterocolitis. I also identified factors that regulate NOD2 gene expression in intestinal epithelial cells and peripheral blood mononuclear cells (PBMC).

Methods: *In situ* hybridisation and immunohistochemistry were used to localize NOD2 mRNA and protein expression in intestinal tissue. Laser capture microdissection (LCM), and calcium chelation followed by mechanical disruption were used to isolate intestinal crypt and villus epithelial cells. Real-time RT-PCR was used to determine NOD2 gene expression in intestinal epithelial cells and PBMC.

Results: NOD2 mRNA and protein expression was readily detected in Paneth cells in normal and Crohn's disease affected terminal ileum; NOD2 was also expressed by monocytes, but not by mature macrophages in the lamina propria or within granulomas. NOD2 mRNA levels were enriched in isolated crypt compared to villous epithelial cells, and NOD2 expression was mainly detected in LCM-acquired Paneth cells but not villous epithelial cells. *In vitro*, tumour necrosis factor alpha (TNFα) up-regulates NOD2 gene expression in intestinal epithelial cells. There is a possibility that Paneth cell antimicrobials are reduced in patients with NOD2-related Crohn's disease.

Conclusions: Paneth cells express NOD2 and could therefore play an important and hitherto unrecognized role in the development of NOD2-associated Crohn's disease.

Table of contents

List of Figures

List of Tables

Dedication

To Jessica

and

Kiran and Divya

Acknowledgements

I would like to sincerely thank the following individuals for their help:

- Dr. Satish Keshav, my supervisor, for his guidance, support and expert training in laboratory methodology.
- Prof. Humphrey Hodgson of the Centre for Hepatology and Dr. Alan Phillips of the Centre for Paediatric Gastroenterology, Royal Free and University College Medical School, for kindly reading my thesis and suggesting improvements.
- Mr. Ed Hall, of the Unilever Foundation (South Africa) and Ms. Sue Adler, of the Canon Collins Educational Trust for Southern Africa (CCETSA), for providing invaluable financial and administrative support.
- My colleagues in the laboratory, Dr. Annabel Bromfield, Ms. Sok-Ying Hor, Dr. Manisha Abeya and Dr. Caroline Osborne, for providing invaluable assistance and friendship. Dr. Penny Moore, Mr. Dave Brown, and Dr. Silke Schepelmann, for sharing expertise and friendship.
- Mr. Olagunju Ogunbiye, of the Department of Surgery, Royal Free Hospital, for assisting with the provision of clinical samples.
- Dr. Yasunori Ogura and Professor Gabriel Nunez, of the University of Michigan, for providing valuable reagents.
- Dr. Pete Simpson and Professor Sunil Lakhani, of the Institute for Cancer Research, for training and allowing me to perform laser capture microdissection in their laboratory.
- Dr. Dianne Turton, pathologist at the Chris Hani-Baragwanath Hospital, for assisting with the provision of clinical material from South Africa.
- Dr. Tim Harrison and Prof. Jim Owen, post-graduate tutors at the Royal Free and University College Medical School, for their guidance and support during the completion of this thesis.
- Ms. Ethel de Keyser (1926-2004), campaigner against apartheid and former Director of CCETSA, and Mr. Nelson Mandela, patron of the Nelson Mandela Scholarship, were constant sources of inspiration and motivation.

I would especially like to thank my mother, Savita Lala and my brother, Shaylesh Lala for the sacrifices that they have made that has enabled my family and me to travel to the United Kingdom so that I could complete my PhD.

Finally, I would like to thank my wife Jessica. For everything.

List of common abbreviations

ABC	ATP-binding cassettes
ANG	Angiogenin
Ang-4	Angiogenin-4
APC	Antigen-presenting cell
BMDM	Bone marrow-derived macrophages
c.f.u.	Colony Forming Units
cagPAI	'cag' pathogenicity island
CARD	Caspase-recruitment domain
CATERPILLER	CARD, transcription enhancer, R (purine)-binding, pyrin, lots of leucine repeats
CD	Cluster of differentiation
cDNA	Complementary deoxyribonucleic acid
DEPC	Diethylpyrocarbonate
DMSO	Dimethylsulphoxide
DNA	Deoxyribonucleic acid
DSS	Dextran sodium sulphate
DTT	Dithiothreitol
EDTA	Ethylenediaminetetra-acetate
GAPDH	Glyceraldehyde-3-phosphate dehydrogenase
G-CSF	Granulocyte-colony stimulating factor
GM-CSF	Granulocyte monocyte colony stimulating factor
GvHD	Graft versus Host disease
HD5	Human alpha defensin 5
HD6	Human alpha defensin 6
HIV	Human immunodeficiency virus
IκB	Inhibitor of NF-κB
IBD	Inflammatory bowel disease
IFNγ	Interferon gamma

IKK	IκB kinase
IL	Interleukin
IL-1β	Interleukin 1 beta
LCM	Laser Capture Microdissection
LPS	Lipopolysaccharide
LRR	Leucine-rich repeats
LTA	Lipoteichoic acid
MAPK	Mitogen-activated protein kinase
MAT	Matrilysin
M-CSF	Macrophage-colony stimulating factor
MDP	Muramyl dipeptide
mRNA	Messenger ribonucleic acid
NADPH	Nicotinamide adenine dinucleotide phosphate
NBD	Nucleotide-binding domain
NEC	Necrotizing enterocolitis
NF-κB	Nuclear factor kappa B
NK cell	Natural killer cell
NOD	Nucleotide Oligomerisation Domain
PAMP	Pathogen associated molecular pattern
PBMC	Peripheral blood mononuclear cells
PBS	Phosphate buffered saline
PCR	Polymerase chain reaction
PGN	Peptidoglycan
PRR	Pathogen recognition receptor
RICK	RIP-like interacting CLARP kinase
RIP	Receptor-interacting protein 2
RNA	Ribonucleic acid
RT-PCR	Reverse transcriptase polymerase chain reaction
SCT	Stem cell transplantation
SIRS	Systemic inflammatory response syndrome
SNP	Single nucleotide polymorphisms

*s*PLA$_2$	Secretory phospholipase A$_2$ Group IIA
TAK1	Transforming growth factor-β-activated kinase
T-cell	T-lymphocyte
TCF4	Transcription factor 4
TCR	T cell receptor
TGF-β	Transforming growth factor-beta
T_H1	T helper 1
T_H2	T helper 2
TLC	Thin Layer Chromatography
TLR	Toll-like receptor
TNFα	Tumour necrosis factor alpha
TRM	Transplant related mortality

Chapter One

1. Introduction

Crohn's disease and ulcerative colitis are the major forms of inflammatory bowel disease (IBD), and are recognised as important causes of gastrointestinal disease in children and adults (Hendrickson 2002). Both illnesses are chronic and although medical therapy alleviates symptoms in many patients, it does not cure illness. The aetiology of IBD remains unknown, although a common postulate states that IBD develops as a consequence of an excessive or unregulated mucosal inflammatory reaction mounted in response to intestinal microflora (Bouma 2003). Interestingly, some forms of IBD develop in genetically susceptible individuals: for example, individuals carrying mutations in the *NOD2* gene are predisposed to develop Crohn's disease (Hugot 2001, Ogura 2001). It is postulated that NOD2 proteins, which sense bacterial antigens, play a role in the protective immune responses against pathogens (Inohara 2005). Nonetheless, the reasons why individuals with NOD2 mutations are predisposed to develop Crohn's disease remain unknown.

In the present thesis, I will determine whether Paneth cells express the NOD2 gene. Paneth cells are specialised for innate intestinal defence (Wilson 1999, Salzman 2003) and may also play a role in intestinal inflammation (Porter 2002): mutant NOD2 proteins may therefore disrupt normal Paneth cell function and predispose to the development of intestinal inflammation.

1.1 Crohn's disease

Crohn's disease, an inflammatory disorder affecting any part of the gastrointestinal tract from the oropharynx to the perianal area, is prevalent in about 10-200 per 100 000 individuals in Western countries (Kurata 1992, Probert 1996). Crohn's disease is a chronic disorder that is characterised by alternating periods of active intestinal inflammation and resolution.

The clinical features of Crohn's disease vary as any region of the gastrointestinal tract can be involved. The clinical presentation also depends on the extent and severity of inflammation. In Crohn's disease, inflammation of the terminal ileum (ileitis) and colon (colitis) is most frequent and often co-exist. In patients with ileocolonic involvement, abdominal pain is usually postprandial and may be referred to the periumbilical area, especially in children. On abdominal examination, tenderness often localises to the right lower quadrant, and an inflammatory mass may occasionally be palpated (Hendrickson 2002). Ileitis may be complicated by intestinal stricturing that causes intestinal obstruction, or intestinal fistulae that may communicate with other intestinal and pelvic organs, or develop into enterocutaneous fistulae (Keshav 2004).

Colitis causes diarrhoea, which usually contains blood, mucus and pus. Patients with colitis usually have cramp-like abdominal pain that is often relieved by defecation. Patients with gastroduodenal involvement often experience early satiety, nausea and vomiting, epigastric pain and dysphagia. Extensive small bowel disease causes diffuse abdominal pain, anorexia, diarrhoea and weight loss, and may result in lactose malabsorption (Hendrickson 2002).

In IBD, fever, malaise and weight loss may occur due to systemic inflammatory responses, and these symptoms are often more severe in patients with Crohn's disease. Extra-intestinal manifestations of Crohn's disease include arthralgia and arthritis, pyoderma gangrenosum and erythema nodosum, and iritis and uveitis. As there is no curative therapy for Crohn's disease, patients usually require long term therapy with immunosuppressive therapy to reduce intestinal inflammation (Keshav 2004). Surgical resection of the inflamed intestine is usually performed in those patients that do not respond to medical therapy (Podolsky 1991).

1.1.1 Pathophysiology of Crohn's disease

The aetiology of Crohn's disease is unknown. Many investigators, however, hypothesise that IBD develops from an unregulated mucosal immune response to the intestinal microbiota that is, in part, genetically determined (Podolsky 2002, Bouma 2003). It is postulated that microbiota initiate different types of

inflammatory responses in Crohn's disease and ulcerative colitis (Bouma 2003). In Crohn's disease, mucosal inflammation is mediated by an excessive T helper 1 (T_H1)-cell response that is associated with increased secretion of interleukin-12 (IL-12), interferon γ (IFNγ) and tumour necrosis factor α (TNFα) (Bouma 2003). Evidence from experimental models of intestinal inflammation, as well as from patients with IBD supports the hypothesis that inflammation in Crohn's disease is mediated by T_H1-cells. For example, macrophages isolated from intestinal tissue produce increased amounts of inflammatory cytokines such as interleukin (IL)-12 (IL-12) (Monteleone 1997, Parronchi 1997, Liu 1999), and patients treated with anti-IL-12 antibody demonstrate clinical improvement (Mannon 2004).

In murine models of IBD, intestinal inflammation can develop in several ways, and Bouma (2003) has categorised these models into four broad groups. Firstly, inflammation may occur spontaneously as a result of naturally occurring genetic abnormalities (Madara 1985, Sundberg 1994, Matsumoto 1998, Rivera-Nieves 2003). Secondly, inflammation may occur as a consequence of targeted disruption of a specific gene or introduction of a transgene (Panwala 1998, Mashimo 1996, Sadlack 1993, Willerford 1995, Spencer 1998, Shull 1992, Hahm 2001, Rudolph 1995, Watanabe 1997, Mombaerts 1993, Erdman 2001, Beg 1995, Lee 2000, Hammer 1990, Snapper 1998, Steinhoff 1999, Kontoyiannis 1999, Wirtz 1999, Kuhn 1993, Hermiston 1995). In the third group, inflammation may be induced by exogenous agents (Boirivant 1998, Morris 1989, MacPherson 1978, Yamada 1993, Okayasu 1990, Stewart 1980, Marcus 1969). Finally, transfer of T-cell populations lacking regulatory cells into a severely lymphopenic host that lacks endogenous regulatory cells, causes colitis in the recipient (Powrie 1994, Hollander 1995).

The information garnered from these murine studies highlights several important and widely accepted concepts or principles that are relevant to human IBD. Bouma (2003) has proposed that seven principles are important in understanding the pathogenesis of IBD. The first principle states that entirely different genetic abnormalities can lead to the clinical features of intestinal inflammation. The second principle states that the host genetic background determines the susceptibility to intestinal inflammation, even when a major genetic defect that

predisposes to inflammation is present. Thirdly, the normal mucosal microflora is required to initiate or sustain the inflammatory response (Sartor 1997). The fourth principle states that experimental inflammation is due to either excessive effector T-cell function or deficient regulatory T-cell function. Also, despite the wide variety of causes, intestinal inflammation is usually mediated by excessive T helper 1 (T_H1)-cell or T_H2- cell responses (the fifth principle). The sixth principle states that the epithelium of the intestinal mucosa has an essential role in the physical separation of potentially stimulating microflora and the reactive cells of the immune system (Podolsky 1999, Hermiston 1995). Finally, the seventh principle states that mucosal inflammation can also arise due to specific defects in the innate immune system and genetic abnormalities of innate immunity involving the function of antigen-presenting cells (APCs), macrophages, or natural killer (NK) cells cause mucosal inflammation (Takeda 1999). In the present thesis, I will propose that Paneth cells, which are likely to be integral to intestinal innate defence, also play a role in the pathogenesis of Crohn's disease.

1.1.2 Intestinal inflammation in patients with Crohn's disease

Although murine models provide insights into the pathogenesis of mucosal inflammation, an analysis of mucosal inflammation in patients with Crohn's disease is essential to provide an unequivocal understanding of the disease. In Crohn's disease, a substantial body of evidence suggest that disease results from an excessive T_H1-cell-mediated inflammation (Bouma 2003). Mucosal inflammation, however, may also be caused by a defect in regulatory T-cell function although functional tests of this hypothesis are difficult to perform in patients with Crohn's disease. In patients, excessive T_H1-cell-mediated inflammation is the best characterised pathophysiologic feature of Crohn's disease although it is possible that the inflammation occurs in response to an, as yet, undefined trigger or infectious agent.

There is emerging evidence to suggest that defects in innate immunity may predispose patients to IBD. Wehkamp and colleagues (2004) have reported that expression of the antimicrobial peptides alpha defensin 5 (HD5) and 6 (HD6) is lower in patients with Crohn's disease as compared to patients with ulcerative

colitis. In Crohn's disease, HD5 and HD6 expression is especially low in those patients carrying mutations in their NOD2 gene. Some studies assessing the role of innate immunity in intestinal inflammation have analysed toll-like receptor (TLR) expression in intestinal epithelial cells as it is hypothesised that pro-inflammatory cellular pathways are initiated by putative interaction between TLR and bacterial antigens in intestinal epithelial cells (Cario 2000, Abreu 2002, Abreu 2005). There are no studies that show that a functional innate defect predisposes patients to IBD; for example, the respiratory burst capacity of macrophages does not appear to be defective in macrophages isolated from IBD-affected colon and ileum (Mahida 1989).

There is, however, firm epidemiologic evidence that environmental and genetics factors predispose to the development of Crohn's disease (Bonen 2003). Out of the potentially relevant environmental risk factors implicated in Crohn's disease, smoking or tobacco exposure predicts an adverse outcome in patients (Calkins 1989). The identification of other environmental risk factors has proved difficult although, on the other hand, there is an accumulating body of evidence that has identified potential genetic defects that may predispose to the development of Crohn's disease.

1.1.3 The genetic epidemiology of Crohn's disease

Crohn's disease is usually diagnosed in early adulthood, with a peak incidence occurring between 15 and 30 years. The incidence of Crohn's disease is also dependant on racial or ethnic backgrounds, and on geographical locations. Crohn's disease is most prevalent in Caucasians (approximately 6-8 per 100 000), and rarer amongst African and Asian populations (Bonen 2003).

Epidemiologic data strongly suggest a genetic predisposition to Crohn's disease. There are racial and ethnic differences in Crohn's disease incidence and prevalence, and familial aggregation because there is an increased risk among first-degree relatives of affected individuals with a low prevalence in spouses (Bonen 2003). Twin studies support the role of genetic susceptibility in Crohn's disease as concordance rates in monozygotic twins are higher than dizygotic twins

(Tysk 1988, Thompson 1996). Furthermore, Crohn's disease is associated with other genetic syndromes resembling IBD, and with diseases with recognised genetic susceptibility such as ankylosing spondylitis and psoriasis (Bonen 2003).

Crohn's disease clusters within families, and in population-based studies, approximately 5-10% of all IBD-affected patients report a positive family history, indicating that the greatest risk factor for developing IBD is having other family members with the disease (Farmer 1980, Monsen 1991, Russel 1997). Cohort and case-control studies indicate that first-degree relatives have 14- to 15-fold increased risk of developing Crohn's disease (Orholm 1991, Satsangi 1994, Peeters 1996). Also, about 75% of multiply affected families with IBD are concordant with disease type (Binder 1998), confirming the importance of genetic factors in disease pathogenesis.

Disease aggregation in families may, however, be due to shared genetic and environmental factors. Twin concordance studies, however, provide stronger evidence to evaluate genetic and environmental factors in Crohn's disease. The monozygotic twin concordance for Crohn's disease ranges from 42% to 58%, whereas the dizygotic twin concordance rate (7%) is not significantly different from that of all siblings (Tysk 1988, Thompson 1996). Although the concordance among monozygotic twins is significantly less than 100%, which indicates that there is a reduced penetrance for the Crohn's disease genotype that is most likely due to non-genetic factors such as environmental triggers, these observations establish the role of genetic predisposition in the pathogenesis of Crohn's disease (Bonen 2003).

Overall, multiple lines of epidemiological evidence favour genetic predisposition to Crohn's disease, and two broad and complementary approaches, namely genetic linkage and candidate gene association studies, have been used to identify genetic determinants of IBD susceptibility. Using genetic linkage studies, numerous genome-wide scans and replication studies have identified at least nine IBD susceptibility loci (Hugot 1996, Satsangi 1996, Cho 1998, Duerr 1998, Ma 1999, Rioux 2000, Duerr 2000). The gene in the IBD1 gene locus has been recently

identified (Hugot 2001, Ogura 2001), and this discovery promises further insight into the pathogenesis of Crohn's disease.

1.1.4 The identification of the NOD2 gene in the IBD1 gene locus

In 1996, Hugot and colleagues, using genetic linkage studies, identified a gene locus on chromosome 16q12, named IBD1, which is specifically associated with Crohn's disease (Hugot 1996). Numerous other investigators have subsequently confirmed the IBD1 gene linkage with Crohn's disease (Ohmen 1996, Brant 1998, Cavanaugh 1998, Annese 1999, Curran 1998 and Cavanaugh 2001). In 2001, two groups of investigators working independently, identified the *NOD2* gene in the IBD1 gene locus, and showed that mutations of the *NOD2* gene are strongly associated with Crohn's disease (Hugot 2001, Ogura 2001). Hugot and colleagues (2001) screened 235 Crohn's disease families to identify the *NOD2* gene on the IBD1 locus using a positional-cloning strategy, based on linkage analysis followed by linkage disequilibrium mapping, then on pedigree disequilibrium mapping, and finally on very extensive sequence analysis of the best candidate gene. Three independent associations with Crohn's disease, a frameshift variant and two missense variants of *NOD2* were identified by this approach. Ogura and colleagues (2001), on the other hand, identified the *NOD2* gene whilst investigating apoptotic proteins, and intuitively considered *NOD2* a candidate gene on the IBD1 locus as this gene is located in the peak region of linkage on chromosome 16. Using the transmission disequilibrium test and case-control analysis, these investigators identified a frameshift mutation that is associated with Crohn's disease (Ogura 2001).

1.1.5 Mutations in the NOD2 gene associated with Crohn's disease

There are three common genetic variants of the *NOD2* gene that are associated with Crohn's disease. The frameshift mutation, identified by Hugot (2001) and Ogura (2001), is caused by a cytosine insertion in exon 11 at nucleotide position 3020 (3020insC), which results in a frameshift at the second nucleotide of codon 1007, and substitutes proline for leucine in the tenth LRR, followed by a premature stop codon. This mutation (Leu1007fsinsC) encodes for a NOD2

protein containing 1007 amino acids, instead of 1040. Hugot and colleagues (2001) identified two other single nucleotide polymorphisms (SNP), designated with the marker names SNP8 (a point mutation, substituting C for T, at nucleotide position 2104) and SNP12 (a point mutation, substituting G for C, at nucleotide position 2722), which are associated with Crohn's disease. These missense mutations encode the amino acid substitutions, Arg702Trp (tryptophan substituted for arginine at codon 702) and Gly908Arg (arginine substituted for glycine at codon 908), and occur within or near the leucine-rich repeats (LRRs)-encoding region of the gene (Figure 1.1). All three common variants occur together with a background mutation, Pro268Ser (serine substituted for proline at codon 268). Hugot and colleagues (2001) also describe over 30 other amino acid polymorphisms occurring near or within the LRRs-encoding region of the gene. These mutations, however, are rare and the study sample size did not permit the investigators to reliably determine an association with Crohn's disease.

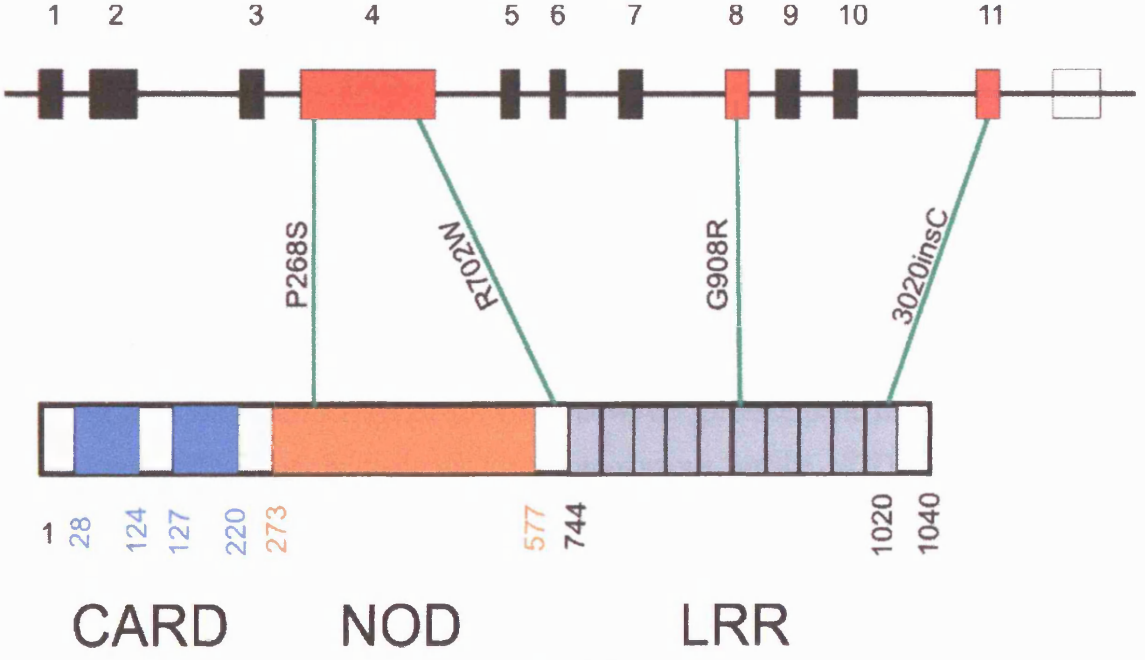

Figure 1.1. The genomic structure of the NOD2 gene, showing the location of Crohn's disease-associated variants, and predicted structural domains. *The three major coding region polymorphisms Arg702Trp (R702W), Gly908Arg (G908R), and Leu1007fsinsC (3020insC) are indicated. All three common variants occur together with a background mutation, Pro268Ser (P268S). CARD: Caspase-recruitment domains; NOD: Nucleotide-binding domain; LRR: Leucine rich repeats. Figure adapted from Bonen (2003).*

Individuals with *NOD2* mutations are at increased risk of developing Crohn's disease. Possessing one copy of a *NOD2* risk allele confers a small risk of 1.5- to 4-fold for developing Crohn's disease. Possessing two copies of the *NOD2* risk alleles, however, confers an increased risk of 20- to 40-fold for developing Crohn's disease (Hugot 2001, Bonen 2003, Hampe 2001, Cuthbert 2002, Vermeire 2002, Ahmad 2002, Vavassori 2002). The risk of developing Crohn's disease is much greater in individuals who are homozygous or compound heterozygotes for the *NOD2* mutations, which suggests that NOD2 functions in an autosomal recessive manner (Bonen 2003), or that the risk alleles confer 'loss-of-function' to NOD2 (Kelsall 2005).

Subsequently, more than thirty other studies have consistently shown the presence of higher allelic frequencies for Arg702Trp, Gly908Arg, and Leu1007fsinsC in Caucasian Crohn's disease-affected patients (shown in Appendix A). Overall, approximately 8 to 17% of Crohn's disease-affected patients carry two copies of the major NOD2 risk alleles compared to less than 1% of the control Caucasian population. About 27% to 32% of Caucasians patients carry one copy of these risk alleles compared with about 20% of controls (Economou 2004). The genetic association between the rarer polymorphisms and Crohn's disease is difficult to ascertain due to the infrequent occurrence of these mutations.

Even with these defined genotypic risks, however, disease penetrance is modest as less than 10% of individuals who are homozygous for the *NOD2* mutations will develop Crohn's disease (Bonen 2003). Also, it is likely that a complex interaction of other, as yet unidentified, genetic factors play a role in disease progression - for example, in a Flemish cohort, paternal transmission of *NOD2* risk alleles was associated with a higher proportion of Crohn's disease-affected patients compared to maternal transmission (Esters 2004). This suggests that the genetic regulation of other, as yet undefined, factors that interact with NOD2 will be important in determining the pathogenesis of NOD2-associated Crohn's disease.

1.1.6 The NOD2 genotype and ulcerative colitis

The overwhelming majority of published reports indicated that carriage of the *NOD2* variant haplotype does not confer increased susceptibility to ulcerative colitis. Andriulli and colleagues (2004), however, report a significant association between Leu1007fsinsC mutation and ulcerative colitis in Italian patients. The frameshift mutation occurs at a lower frequency in comparison to Crohn's disease-affected patients, and there are no associations between the Arg702Trp and Gly908Arg alleles and ulcerative colitis. These investigators have previously reported an ulcerative colitis-associated susceptibility locus in the pericentromeric region of chromosome 16, although it is uncertain whether this is due to the presence of rarer *NOD2* single nucleotide polymorphisms or variations of a completely independent gene (Annese 2003). McGovern and colleagues (2003) have also reported that the Leu1007fsinsC mutation occurs at a higher frequency in ulcerative colitis compared to healthy controls and, in addition, these investigators report an association between *NOD1* polymorphisms and IBD (McGovern 2005). Although other studies are required to confirm the role of other *NOD2* and *NOD1* polymorphisms and IBD, these findings suggest that there may be shared genetic predisposition to inflammation in Crohn's disease and ulcerative colitis.

1.1.7 Racial and ethnic differences in NOD2 genotypic expression

In specific racial populations, the three common variant *NOD2* alleles occur at much lower frequency and are not associated with an increased risk of developing Crohn's disease. In the Oriental and Australian populations, *NOD2* gene mutations do not appear to make a significant contribution to the development of Crohn's disease. In Japan, Inoue and colleagues (2002) were unable to detect any of the common *NOD2* mutations in 350 patients with Crohn's disease, and Yamakazi and colleagues (2002) identified one patient with the Arg702Trp variant allele from a cohort of 483 patients. In China, the three common *NOD2* variants alleles are either undetectable or occur at frequencies of less than 1% in patients with Crohn's disease (Leong 2003, Guo 2004). In some population groups, such as

Australians and Tunisians, the common variant alleles occur at lower frequencies in patients with Crohn's disease (Cavanaugh 2003, Zouiten-Mekki 2005). The Leu1007fsinsC allele also occurs at a low frequency and is not associated with Crohn's disease in Cretan (Roussomoustakaki 2003) and Scottish populations (Crichton 2002).

1.1.8 NOD2 genotype and the clinical course of Crohn's disease

Crohn's disease, a complex heterogeneous disorder, is usually classified according to the Vienna classification by defining subgroups on the basis of disease localisation, age of diagnosis, disease behaviour and surgical history (Gasche 2000). Disease site is generally categorised into four broad groups: upper gastrointestinal (involvement of the oesophagus, stomach, duodenum or jejunum without ileal disease), ileal, ileo-colonic or colonic only. In addition, perianal disease may be associated with any disease site, although it occurs most frequently in patients with colonic Crohn's disease. Disease behaviour is usually categorised as fistulizing (penetrating), stricturing or inflammatory (non-stricturing non-penetrating) and age of diagnosis based on whether the diagnosis is made before or after 40 years (Appendix B).

Several investigators have correlated *NOD2* genotype with the phenotypic manifestations of Crohn's disease to determine the influence of the common *NOD2* variant alleles on the clinical course of this disorder. Of the clinical variables, disease localisation is the major determinant of disease behaviour (Louis 2001) and ileal involvement is associated with an earlier age of onset and family history of Crohn's disease. For this reason, many investigators determined whether an association between disease localisation and carriage of the variant *NOD2* alleles existed.

1.1.8.1 Disease localisation

Numerous studies have established that *NOD2* variant allele carriage is associated with ileal disease, not colitis, in patients (Ahmad 2002, Cuthbert 2002, Lesage 2002). In European patients, the frequency of the *NOD2* variant alleles is

significantly higher in patients with exclusive ileal disease (26.9%), intermediate in those with ileocolitis (19.7%), and lowest in those with colonic disease (12.7%) (Cuthbert 2002). Lesage and colleagues (2002) have reported that in French patients with Crohn's disease, colonic involvement is significantly less common in individuals carrying two copies of the variant *NOD2* alleles than in individuals carrying wild-type alleles.

This site specific association has been confirmed in an analysis of American patients with Crohn's disease (Brant 2003). Using logistic regression analysis, these investigators determined that carriage of two *NOD2* variant alleles, either homozygous or compound heterozygous carriage, was the strongest predictor of ileal disease. *NOD2* mutations were associated with a 10-fold risk of developing ileal disease, after adjusting for the risks associated with cigarette smoking and age at diagnosis.

Other studies have subsequently confirmed that the *NOD2* variant alleles specifically confer risk for ileal disease. In a recent meta-analysis, Economou and colleagues (2004) assessed the effects of *NOD2* variants alleles on Crohn's disease phenotype in non-Jewish Caucasian populations, and showed that the strongest genetic effect of *NOD2* mutations was predisposition to small bowel or ileal disease. This meta-analysis showed that the presence of at least one *NOD2* variant allele does not confer any large risk for Crohn's disease when cases with only colonic disease are considered.

1.1.8.2 Age at diagnosis

The *NOD2* variant haplotype is associated with an earlier age of diagnosis in Crohn's disease, and the disorder is diagnosed on average 3-5 years earlier in European and American patients who are homozygous or compound heterozygotes for the *NOD2* mutations. A meta-analysis of 13 studies showed that the presence of at least one high-risk variant allele increases the risk of familial disease 1.4-fold (Economou 2004).

1.1.8.3 Disease behaviour

Disease behaviour is difficult to study as it changes over time, and a longer duration of inflammation makes it more likely that stricturing or penetrating complications will develop in an individual with Crohn's disease. This difficulty is exacerbated by the different approaches used by investigators in categorising disease behaviour. Given these caveats, some studies have shown an association between *NOD2* variant allele carriage and stricturing or fistulizing (penetrating) phenotype (Lesage 2002, Brandt 2003, Heliö 2003). A meta-analysis of 13 studies showed that the presence of at least one high-risk variant allele increases the risk of stricturing disease 1.9-fold (Economou 2004).

Most studies have also shown that the *NOD2* variant haplotype does not influence the need for surgery independently of disease location (Economou 2004). In conclusion, patients carrying the *NOD2* mutations are more likely to have stricturing disease, be diagnosed at a younger age, but most likely to have ileal disease.

1.1.9 *NOD2* variant allele associations with other diseases

Since the association between *NOD2* variants haplotypes and Crohn's disease, other investigators have therefore determined whether similar associations exist between *NOD2* variant haplotypes and other inflammatory diseases. Mutations in the NOD-encoding region of the *NOD2* gene are associated with Blau syndrome, a rare autosomal-dominant disorder characterised by arthritis, uveitis, skin rash and granulomatous inflammation (Miceli-Richard 2001, Kurokawa 2003, Rose 2005, van Duist 2005). There is also a strong possibility that Crohn's disease-associated NOD2 mutations may be associated with intestinal graft-versus-host disease (GvHD) and colorectal carcinoma (Holler 2004, Kurzawski 2004, Papaconstantinou 2005).

Holler and colleagues (2004) analysed *NOD2* mutations in a cohort of 169 recipients of allogeneic blood stem cell transplantation (SCT) and their respective donors. *NOD2* mutations were associated with an increased frequency of intestinal GvHD, overall GvHD, and transplant-related mortality (TRM).

Multivariate analysis showed that the *NOD2* mutations were highly significant independent risk factors for the development of GvHD and TRM. The presence of *NOD2* mutations in both recipients and their respective donors was associated with increased TRM, which increased from 24% in patients without the mutations to 60% in cases where both the donor and recipient harboured *NOD2* mutations. These authors speculate that the *NOD2* mutations allow for increased bacterial translocation across the gastrointestinal epithelium, which results in septicaemia and multi-organ failure (The putative role of NOD2 will be discussed later).

Some reports indicate that the Leu1007fsinsC mutation may be associated with colorectal cancer in Polish and Greek populations (Kurzawski 2004, Papaconstantinou 2005), although this association in not seen in Finnish patients (Alhopuro 2004). A preliminary study reports an association between individuals with the Leu1007fsinsC allele and early-onset breast cancer (Huzarski 2005). Additional studies are therefore required to confirm a link between carcinoma and Crohn's disease-associated *NOD2* mutations.

Published reports suggest that there is no association between *NOD2* gene mutations and systemic lupus erythematosus (Ferreiros-Vidal 2003), Wegener's granulomatosis (Newman 2003), Behcet's disease (Uyar 2004), sarcoidosis (Martin 2003), psoriasis (Young 2003, Plant 2004), multiple sclerosis (Sawcer 2003), rheumatoid arthritis (Steer 2003, Ferreiros-Vidal 2003a) and ankylosing spondylitis (Ferreiros-Vidal 2003b). With regard to infectious diseases, there is no association between *NOD2* gene mutations and pulmonary tuberculosis (Stockton 2004) and periodontitis (Folwaczny 2004, Laine 2004), although a preliminary report suggests that *NOD2* mutations may predispose very low birth weight infants to neonatal septicaemia (Ahrens 2004).

In summary, the presence of *NOD2* mutations is most strongly associated with Crohn's disease and Blau syndrome. The role of *NOD2* mutations in neonatal septicaemia and colorectal carcinoma needs further clarification, whereas the association between Crohn's disease-associated *NOD2* mutations and GvHD needs urgent investigation.

1.2 NOD2

1.2.1 Identification of the NOD2 gene

NOD2 (also known as CARD15) was initially identified by Ogura and colleagues (2001a), during a search of public genomic data bases for genes encoding proteins with homology to NOD1 (CARD4). The NOD2 protein is encoded by a gene, containing 12 exons, that is located at the q12 region of chromosome 16. The NOD2 nucleotide sequence contains two in-frame translation initiation sites that are separated by 81 nucleotides, and expression studies using mammalian cells show that the longer reading frame, encoding an additional 27 amino acids, is preferentially translated (Ogura 2001a).

1.2.2 The structure of the NOD2 protein

The NOD2 protein, comprising of 1040 amino acids, is composed of two N-terminal caspase-recruitment domains (CARD) (residues 28-220) fused to a centrally located nucleotide binding domain (NBD) (residues 273-577) containing consensus nucleotide-binding motifs followed by 10 tandem leucine-rich repeats (LRRs) (residues 744-1020) (Figure 1.1). The NOD2 LLR, which contain α helix and β sheet sequences, are prototypically horseshoe shaped.

The NOD2 protein belongs to the family of NOD (nucleotide-binding oligomerization domain) proteins. Over 20 NOD containing proteins, with a structure similar to NOD1 and NOD2, have been identified in humans, nematodes and *Arabidopsis* (plants) (Inohara 2005). Some of these proteins are shown in Figure 1.2. This family of proteins includes Apaf-1 (apoptotic protease activating factor 1), Ipaf, Cryopyrin, and NALP1, and are also referred to as the NOD-LRR proteins (Inohara 2002). The NOD-LRR proteins are alternatively classed as belonging to the CATERPILLER [CARD, transcription enhancer, R (purine)-binding, pyrin, lots of leucine repeats] family of proteins (Ting 2005). In this classification, the central domain is referred to as the NATCH domain. The majority of animal and plant NOD-LRR proteins are comprised of three distinct domains: an amino-terminal effector domain, a centrally located regulatory NOD domain, and a carboxyl-terminal LRR domain.

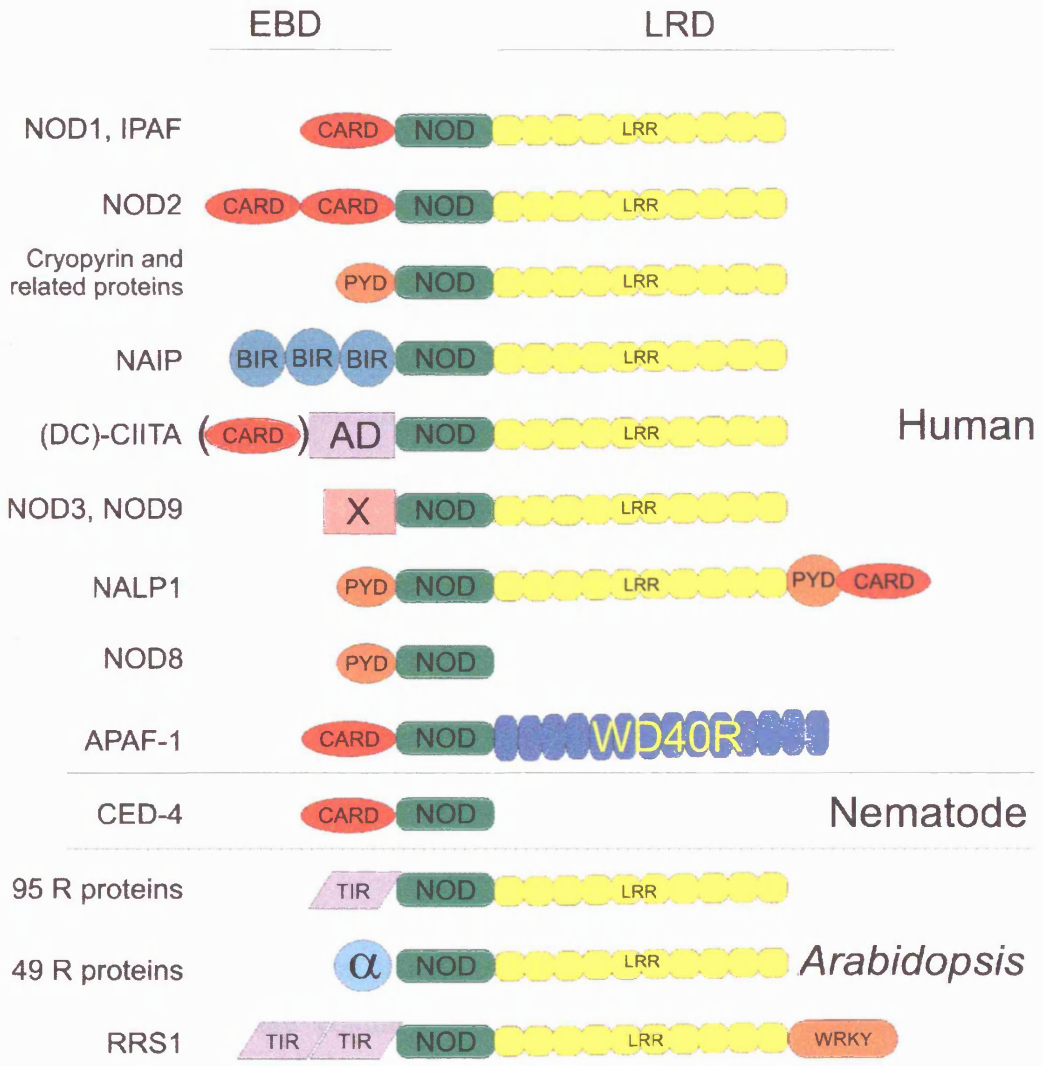

Figure 1.2. The domain structure of the NOD proteins found in humans, nematodes and Arabidopsis share structural homology. *Most NOD proteins are composed of variable amino-terminal effector-binding domains (EBD), a centrally located nucleotide-binding oligomerization domain (NOD) that mediates self-oligomerization, and a carboxyl-terminal ligand-recognition domain (LRD). The putative EBD of NOD3 and NOD9 (represented by X) do not share significant homology with any known protein. The caspase-recruitment domain (CARD) shown in parenthesis is present in CIITA expressed in dendritic cells. An incomplete pyrin domain (PYD) is present in the carboxyl-terminal region of terminus of NALP1. The number of leucine-rich repeats (LRRs) varies in NOD proteins. The WRKY domain is a zinc finger-like domain found in plant W-box-binding transcription factors. Other abbreviations: α, α-helix/coiled-coil rich; NC, NALP1/CARDINAL expanded homology domain; WD40R, WD40 repeat; BIR, baculoviral inhibitor-of-apoptosis repeat; TIR, Toll interleukin-1 receptor domain. Figure adapted from Inohara (2005)*

The CARD domains of NOD2 share significant sequence similarity with CARD motifs found in a variety of apoptotic signalling molecules, such as CED-4 and Apaf-1 (Bertin 1999). The CARD domain is a protein fold consisting of a tightly packed, six-membered α-helical bundle, and was first identified in a subset of caspases and caspase adaptor proteins by Hofmann and colleagues (1997). The CARD motif functions as effector domains that mediate specific homophilic interactions with down-stream CARD-containing signalling molecules. It is believed that proteins with CARD domains are centrally involved in assembling protein complexes that drive activation of either caspases or IκB kinase (IKK) by facilitating close proximity of the latter molecules (Martin 2001). It is therefore assumed that CARD-containing proteins play a role in the regulation of apoptosis and nuclear factor kappa B (NF-κB) activation.

The centrally located nucleotide oligomerization domain (NOD) of NOD2, which contains near its amino-terminal region a P-loop and the Mg^{2+}-binding site, is thought to mediate self-oligomerization. The NOD region has residues at catalytic sites which are essential for binding and hydrolysis of Mg^{2+}-ATP or –GTP, and are predicted to share common nucleotide binding folds with ATP-binding cassettes (ABC) of members of the ABC ATPase/GTPase superfamily (Inohara 2000). Point mutations in the phosphate chain binding site (also known as Walker's A box or P-loop) are predicted to result in loss-of-function of NOD2, since corresponding point mutations in NOD1 P-loop result in loss-of-function. (Inohara 1999).

Each of the NOD2 LRRs have structural homology to LRRs of the plant disease resistance (R) proteins, and each LRR contains a predicted α helix and β sheet sequence that is consistent with the prototypical horseshoe-shaped structure of R protein LRRs (Ogura 2003). There are 5 classes of plant R proteins, of which two have extracellular LRR domains (Dangl 2001). The LRRs of these proteins recognise distinct effector molecules from pathogenic bacteria, and it is currently inferred that the NOD2 LRRs perform a similar function. The NOD- and LRR-containing proteins, however, are relatively abundant and functionally diverse in

mammalian cells, and an interaction between the LRRs and bacterial products in mammalian cells has never been proven (Beutler 2001).

1.2.3 Signalling pathways induced through NOD2

1.2.3.1 NOD2 induces NF-κB activation

The gene sequences for NOD2 and for its closest related homolog NOD1 were identified after searching the human genomic database for sequences that shared homology with the CARD-containing apoptotic regulator, Apaf-1, and it was assumed that these proteins would perform a similar function. However, after cloning the open reading frames of the genes into expression vectors that were then transiently transfected into HEK293T mammalian cells, it was noted these cells did not undergo apoptosis, as was the case for Apaf-1 expressing cells. Instead, overexpression of either NOD2 or NOD1 induced marked NF-κB activation in HEK293T cells (Inohara 1999, Ogura 2001a).

The transcription factor nuclear factor-κB (NF-κB) is present in the cytoplasm in an inactive form, bound to the inhibitory protein called IκB (or inhibitor of NF-κB). Phosphorylation of IκB, mediated by IκB kinase (IKK; a complex of IKKα, IKKβ, and IKKγ) results in degradation of IκB, and translocation of NF-κB to the nucleus where it induces gene transcription (Li 2002). NOD2-induced NF-κB activation was inhibited in mammalian cells expressing mutant forms of IKKα, IKKβ, IKKγ, and IκBα which indicates that NOD2 acts upstream of the IKK complex. This was verified by expression studies using parental Rat1 fibroblasts and 5R cells, a Rat1-derivative cell line that does not contain the IKKγ protein (Yamaoka 1998). These studies showed that NOD2 expression induced NF-κB activation in Rat1 but not 5R cells. However, co-expression of IKKβ (which functions downstream of IKKγ) in 5R cells restored NOD2-induced NF-κB activation, confirming that NOD2 acts up-stream of IKK (Inohara 2000).

Further analysis revealed that NOD2 interacts with RICK (a protein identified by Inohara and colleagues in 1998), upstream of the IKK complex, before inducing

NF-κB activation (Inohara 2000). Firstly, NOD2-induced NF-κB activation was inhibited in cells expressing mutant RICK proteins. Then, the association between NOD2 and RICK proteins was proven in a series of experiments where cellular extracts from mammalian HEK293T cells, which were cotransfected with plasmids expressing wild-type or mutant forms of NOD2 and RICK, were analysed by immunoprecipitation and immunoblotting. However, this association was only evident between native RICK and wild-type or mutant NOD2 protein that contained both CARD domains. Similarly, native NOD2 only interacted with either wild-type or mutant RICK proteins containing the CARD domain. In addition, NOD2 did not associate with other CARD-containing proteins including as Apaf-1, caspase-1 and procaspase-9, indicating that the NOD2-RICK interaction is specific and mediated by a homophilic CARD-CARD interaction (Ogura 2001a).

Ogura and colleagues (2001a) determined the essential motifs from the NOD2 molecule required for NF-κB activation by expressing variant NOD2 proteins, genetically engineered so that they lacked one or more of the major structural motifs, in HEK293T cells. These investigations showed that both CARD domains were essential for NF-κB activation, as variant proteins containing only one CARD domain, NOD or LRRs motifs could not induce cellular activation. In addition, these studies also suggested that the LRR motif may play a regulatory role, as engineered NOD2 proteins lacking the LRR motif caused more profound activation of NF-κB than wild type protein. Interestingly, expression studies performed using equivalent amounts of expression-vectors show that the mutated proteins encoded by the three major Crohn's disease-associated NOD2 mutations, all of which involve the LRR motif, do not change NF-κB activation significantly in comparison to wild-type protein in mammalian cells (Ogura 2001, Bonen 2003a).

1.2.3.2 NOD2 interacts with the TAK1 signalling pathway

There is evidence that NOD2 activation of NF-κB is dependant on transforming growth factor-β-activated kinase 1 (TAK1), a MAP kinase kinase enzyme (Chen

2004). The complex of NF-κB proteins is inhibited by I-kappa-B (IκB) proteins, which inactivate NF-κB by trapping it in the cytoplasm. Phosphorylation of the IκB proteins by IκB kinases marks them for destruction via the ubiquitination pathway, thereby allowing activation and nuclear translocation of the NF-κB complex. By transfecting HEK293 cells with NOD2 and dominant negative forms of various enzymes that phosphorylate IκB proteins, Chen and colleagues (2004) showed that the dominant negative form of TAK1 (TAK1DN) inhibited NOD2-induced NF-κB activation. TAK1DN also inhibited MDP-induced NF-κB activation in HEK293T cells that expressed NOD2. These investigators showed further that TAK1 induces NF-κB activation in RICK-deficient embryonic fibroblasts, which suggests that TAK1-induced NF-κB activation is not dependant on RICK. In RICK-deficient embryonic fibroblasts, NOD2 inhibited TAK1-induced NF-κB activation, suggesting that NOD2 negatively regulates TAK1-induced NF-κB activation.

Using immunoblot detection of immunoprecipitated cell lysates and confocal microscopy, these investigators showed an interaction between NOD2 and TAK1 proteins. It would appear that the LRR motif of NOD2 interacts with TAK1. Interestingly, whilst the wild-type NOD2-LRR motif inhibits TAK1-induced NF-κB activation, the mutant NOD2 protein encoded by the 3020insC mutation causes less inhibition of NF-κB activation (Chen 2004).

TAK1 mediates NF-κB activation induced by bacterial products, such as LPS, and pro-inflammatory cytokines, such as IL-1, TNFα, and IL-18 (Wang 2001). Additionally, there is some evidence to suggest that TAK1 may play a role in innate defence. In flies, null mutations in the Drosophila *dTAK1* gene result in diminished production of antibacterial peptides *in vivo*, resulting in increased susceptibility to gram-negative bacterial infection (Vidal 2001). Chen and colleagues (2004) used *in vitro* systems that relied on overexpression of proteins to demonstrate an association between NOD2 and TAK1 proteins. Nevertheless, their results suggest that TAK1 may mediate interactions between bacterial products, inflammatory cytokines and NOD2. Using RICK-deficient embryonic fibroblasts, Chen and colleagues showed that NOD2 inhibited TAK1-induced NF-κB activation. This study also suggests that NOD2 interacts with TAK1 through

its LRR domain to mediate its inhibitory effect on TAK1-induced NF-κB activation. Interestingly, mutant NOD2 proteins that are encoded by the 3020insC mutation caused less inhibition of TAK1-induced NF-κB activation as compared to wild-type NOD2 proteins. This study offers an alternative explanation to disease pathogenesis in NOD2-affected Crohn's disease by suggesting that mutant NOD2 proteins do not down-regulate NF-κB activation.

1.2.3.3 Role in apoptosis

Beutler (2001) has suggested that NOD2 may play a role in Crohn's disease-pathogenesis through altered regulated of apoptotic pathways. There is, however, no evidence to suggest that overexpression of NOD2 induces apoptosis in cell transfectants, although NOD2 enhances apoptosis induced by caspase-9 expression in these cells (Ogura 2001a). NOD2 and NOD1 promote activation of caspases, however, and their role in apoptosis needs to be evaluated under more physiological conditions including knock-out mice. Indeed, Maeda and colleagues (2005) have shown that, in colitis, an increase in apoptotic lamina propria macrophages is observed in $NOD2^{2939iC}$ mice, which encode for a truncated protein homologous to the Leu1007fsinsC protein (discussed later). Thus, there remains a possibility that NOD2-dependent apoptosis plays a role in the development of intestinal inflammation, but this remains to be confirmed.

1.2.4 Proposed functions of the NOD2 protein

1.2.4.1 Interactions with bacterial products: lipopolysaccharide (LPS)

To elucidate the function(s) of NOD2, Ogura and colleagues (2001a) reasoned that the assumed structural assembly of the molecule will yield clues to its function. Functional analyses, based largely on NOD1-HEK293T transfectants, suggest that the NOD domain is essential for oligomerization, and that self-association of NOD molecules mediates proximity to RICK (Inohara 2000). The NOD molecules, i.e. NOD1 and NOD2, then interact with RICK through homophilic CARD-CARD interactions. RICK associates with the γ subunit of IκB kinase (IKKγ) that complexes with IKKα and IKKβ to induce the degradation of IκB which, subsequently results in NF-κB activation (Inohara 2000).

In mammalian cells, toll-like receptors (TLR) are signalling receptors of the innate immune system and initiate intracellular signalling cascades. For example, LPS binds to the extracellular LRR motif of TLR4, with subsequent NF-κB activation (Poltorak 1998, Beutler 2001). It was therefore reasoned that NOD2 binds LPS as the LRRs of NOD2 and TLR4 bear structural homology. Inohara and colleagues (2001a) stimulated NOD1-expressing mammalian cells with various bacterial molecules to determine a role for NOD1 in bacterial detection. The bacterial products, which included lipopolysaccharide (LPS), lipoteichoic acid (LTA), peptidoglycan (PGN), mannan and synthetic bacterial lipoprotein (sBLP), were introduced into the cells by simultaneous transfection with the NOD1 expression plasmid, and a NF-κB reporter construct. These experiments showed that NF-κB activation was increased in response to LPS stimulation and not in response to stimulation with other bacterial antigens. In NOD2-expressing transfectants, NF-κB activation increased in response to LPS stimulation and, to a lesser extent, to PGN stimulation (Inohara 2001a).

Using mutational analyses, Inohara and colleagues (2001a) showed that the LRR domain of NOD1 and NOD2 was essential for mediating NF-κB activation in mammalian cells exposed to LPS. These studies suggest that the LRR motifs are essential for enabling the NOD proteins to respond to LPS, which was consistent

with the prevailing view that LPS interacts with LRR domains of R proteins and mammalian toll-like receptors (Inohara 2001a). These transfection-based studies suggested that NOD1 is associated with an LPS binding activity in the cytosolic fraction of mammalian cells, although a direct interaction between NOD1 and LPS could not be demonstrated (Inohara 2001a). Interestingly, in mammalian cells transfected with an expression plasmid encoding the mutant Leu1007fsinsC-NOD2 protein, LPS induced less NF-κB activation and it was therefore postulated that mutant NOD2 proteins fail to mediate cellular activation in response to LPS (Ogura 2001). Based on these findings, it was widely accepted at the time that NOD1 and NOD2 were 'intracellular receptors' for LPS (Hugot 2001).

The role of NOD1 and NOD2 as intracellular receptors for LPS was, however, questioned by Beutler (2001). He cautioned that simultaneous transfection of mammalian cells with LPS and an expression vector does not ensure that LPS enters the cells. In addition, HEK294T cells that were used for transfection, do not express TLR4, and the vast majority of mammalian cells are unresponsive to LPS that is presented extracellularly. Furthermore, even if LPS is internalised and reaches the cytosol within a cell, which occurs if LPS is presented to a cell in an aggregated form, TLR4 mutations abrogate cellular responses to LPS. Beutler (2001) reasoned that while it is conceivable that, *in vivo*, epithelial cells should possess mechanisms to sense and respond to LPS, few studies have addressed this issue. Studies that determine the presence of a putative intracellular LPS receptor would require an exclusive route of presentation of LPS, for example, by microinjection, and are technically difficult to perform.

Inohara and colleagues (2001a) used high doses of LPS during transfection when determining whether NOD2 functions as an intracellular receptor for LPS. Again, Beutler (2001) cautions that treatment with exceedingly high doses of LPS (10 μg/mL) is fraught with difficulty. In similar studies using HEK293T cells transfected with a TLR2 expression vector, it was initially thought that LPS binds TLR2 (Yang 1998, Kirschning 1998). Later, it became apparent that contaminants in the LPS preparations mediated these cellular responses that were initially ascribed to LPS (Hirschfeld 2000).

In the NOD2 studies, LPS binding was not shown to be of high affinity or specificity and, therefore, to test the hypothesis that NOD2 acts as an intracellular receptor for LPS, would require microinjection of chemically synthesised LPS into cells lacking TLR4. Subsequently, Beutler's (2001) criticisms proved to be valid and Inohara and colleagues (2003), using purified preparations of LPS, showed that LPS does not interact with NOD1 or NOD2. It appears that the stimulatory effects ascribed to LPS were due to the presence of a contaminant in the LPS preparations, namely peptidoglycan (Inohara 2003a).

1.2.4.2 Interactions with bacterial products: Peptidoglycan (PGN) and muramyl dipeptide (MDP)

Bonen and colleagues (2003a), using HEK293T transfectants, first showed that PGN, as well as unpurified LPS, mediated NOD2-induced cellular activation. Later, two independent groups of investigators showed that a component of bacterial peptidoglycan (PGN), called muramyl dipeptide (MDP), induces NOD2-mediated cellular activation (Girardin 2003, Inohara 2003).

Girardin and colleagues (2003) showed that PGN, treated with polymixin B and Proteinase K, and boiled to remove LPS and lipo-proteins, activates NF-κB in mammalian cells that were simultaneously transfected with NOD2 expression plasmids. They subsequently determined that cellular activation mediated by NOD2 was due to MDP, a component of gram-positive and -negative bacteria. Using chemically synthesised MDP (or MDP-LD) and its isomer MDP-LL, they verified that MDP mediates NOD2-induced NF-κB activation. These investigators showed that macrophages, but not epithelial cells, were responsive to extracellular stimulation with MDP *in vitro*. Furthermore, epithelial cells remained unresponsive to MDP introduced into these cells by microinjection. As MDP did not induce cellular activation in cells expressing NOD1, TLR1, TLR2 and TLR6, Girardin and colleagues (2003) described NOD2 as the first protein that mediates cellular activation in response to MDP.

Inohara and colleagues (2003) used various purified LPS preparations to further characterise the bacterial moiety that interacts with NOD2. They demonstrated that purified LPS did not result in NOD2-mediated NF-κB activation, and also showed that MDP induces NOD2-mediated cellular activation in mammalian cells. Using a variety of synthetic muropeptides, they showed that only MDP specifically induces NOD2-mediated NF-κB activation.

1.2.4.3 The structure of peptidoglycan (PGN) and muramyl dipeptide (MDP)

Peptidoglycan (PGN) is a major constituent of the cell wall of gram positive bacteria and consists of glycan chains of alternating N-acetylglucosamine (GlcNAc) and N-acetylmuramic acid (MurNAc) that are cross-linked to each other by short peptides, forming a rigid polymer surrounding the bacterial cell. In gram-negative bacteria, a thinner layer of PGN is located in the periplasmic space (Figure 1.3) (Girardin 2003a). During the bacterial life cycle, PGN is constantly degraded by specific hydrolases and newly synthesized subunits, called muropeptides, are integrated into the polymeric structure, enabling biological processes, such as cell division, to occur. Apart from the thickness and the degree of stem peptide cross-linking, an important difference between gram-positive and gram-negative PGN resides in the nature of the third amino acid of the peptidic moiety (Figure 1.3). In gram-positive bacteria, this amino acid is commonly a lysine, whereas a diaminopimelic acid is found in most gram-negative bacteria.

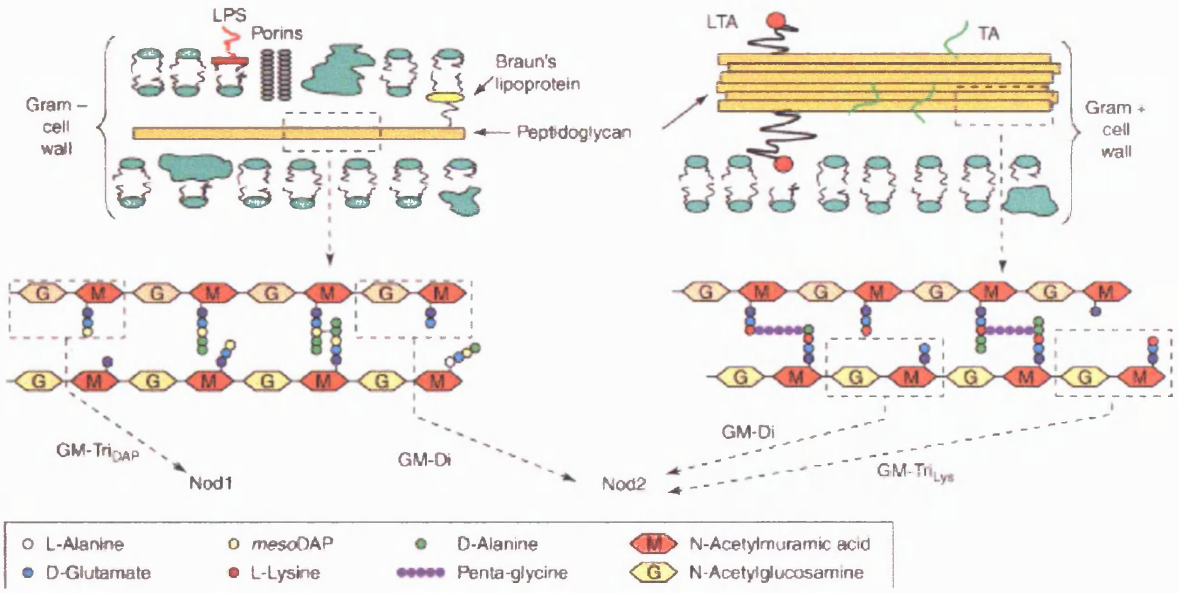

Figure 1.3. The structure of peptidoglycan showing the muropeptides that are postulated to interact with NOD1 and NOD2. *A thin layer of peptidoglycan is found in the periplasmic space of gram-negative bacterial cell walls (left). Cross-linking of two parallel glycan strands through stem peptides occurs at low frequency. This cross-linking is made by a direct link between a mesoDAP amino acid and the D-Alanine in position four from a peptide anchored on a parallel glycan strand.*

In gram-positive bacteria, peptidoglycan represents a thick structure that surrounds the bacterial membrane (right). Glycan strands are generally cross-linked to a high degree. In contrast to gram-negative bacteria, the cross-linking requires additional bridging amino acids, for example, through penta-glycine bridges, which are a characteristic of Staphylococcus aureus peptidoglycan (shown in the figure). The structure 'sensed' by NOD1, GM-TriDAP (GlcNAc-MurNAc-L-Ala-D-Glu-mesoDAP), is a muropeptide found mostly in gram-negative bacterial peptidoglycan. NOD2 'senses' two types of muropeptides: GM-Di (GlcNAc-MurNAc-L-Ala-D-Glu, also known as GMDP) present in peptidoglycans from gram-negative and gram-positive bacteria, and GM-TriLys (GlcNAc-MurNAc-L-Ala-D-Glu-L-Lys), a muropeptide found only in peptidoglycans from gram-positive bacteria. Abbreviations: LTA, lipoteichoic acid; LPS, lipopolysaccharide; TA, teichoic acid. Figure from Girardin (2003a)

1.2.5 NOD2 interacts with the PGN motif, muramyldipeptide (MDP)

Specific components of PGN induce cellular activation in transfectants expressing either NOD1 or NOD2 (Girardin 2003, Inohara 2003). NOD1 mediates cellular activation in reponse to stimulation with a single muropeptide from gram-negative bacterial peptidoglycan, GM-TriDAP (GlcNAc-MurNAc-L-Ala-D-Glu-mesoDAP). GM-TriDAP, which contains the motif γ-D-Glu-mesoDAP, with a terminal mesoDAP, is a naturally occurring muropeptide generated by the action of lytic enzymes from either the host or the bacteria (Girardin 2003b).

NOD2 senses GM-TriLys (GlcNAc-MurNAc-L-Ala-D-Glu-L-Lys) and muramyl dipeptide (MDP), whose corresponding natural muropeptide is GM-Di (GlcNAc-MurNAc-L-Ala-D-Glu). The MDP motif is not found as a naturally occurring bacterial product but the corresponding muropeptide, GM-Di, is. In contrast to NOD1, NOD2-mediated cellular activation is dependent on the presence of the MurNAc sugar moiety (Girardin 2003c). With regard to NOD1-mediated cellular activation in response to muropeptide stimulation, the mesoDAP has to be in terminal position, but the terminal amino acid of the MDP motif (i.e D-Glu) can be substituted at the C-terminus with an L-Lysine or an L-Ornithine but not a mesoDAP (Girardin 2003c). GM-Di is found in all bacteria (with the exception of the few bacteria that do not display peptidoglycan in their cell wall, such as Mycoplasma spp.), whereas GM-TriLys only occurs in gram-positive bacteria.

Although it is widely stated that NOD1 and NOD2 are "intracellular bacterial receptors" that detect muropeptides, there is no evidence showing direct interaction between muropeptides and NOD1 or NOD2 molecules (Murray 2005). NOD1 and NOD2 are intracellular proteins with motif similarity, not necessarily primary structural homology, to defensive proteins of plants – NOD1 and NOD2 do mediate cellular responses, for example NF-κB activation, in response to muropeptide stimulation and are commonly referred to as "intracytoplasmic microbial sensors" (Girardin 2004).

1.2.5.1 MDP and mammalian cell interactions

It is widely accepted that the synthetic muropeptide MDP induces NOD2-dependant NF-κB activation. What remains unclear, however, is the process or mechanisms by which MDP or other muropeptides enter the cytosol of cells. *In vivo*, MDP is believed to be generated by proteolysis in phagocytic cells, although non-specific uptake through pinocytosis may occur. Thus far, two mechanisms have been proposed to account for the internalisation of MDP and/or peptidoglycan into epithelial cells. These mechanisms suggest that muropeptides are internalised into cells by epithelial surface receptors or bacterial secretion systems (Vavricka 2004, Viala 2004).

Recently, Vavricka and colleagues (2004) have shown that the apical di-/tripeptide transporter, hPepT1, transports MDP into intestinal epithelial cells. hPepT1 transports various peptides with H^+, but also transports peptide-derived drugs and the bacterial chemotactic peptide, N-formyl-Methionyl-Leucyl-Phenylalanine. In Caco-2/bbe (C2) cells, MDP competitively inhibits uptake of glycosylsarcosine (Gly-Sar), a substrate of hPepT1. Furthermore, the physiologically inactive isomers of MDP (MDP-LL and MDP-DD) do not inhibit glycosylsarcosine uptake. MDP uptake by hPepT1 was confirmed using [^{3}H]-MDP that was later recovered from the cytosol of C2 cells. The binding affinity of MDP is similar to glycosylsarcosine, and MDP or glycosylsarcosine uptake is inhibited by decreasing hPepT1 expression with silencing RNA (siRNA). Moreover, both NOD2 and hPepT1 siRNA reduced IL-8 secretion in MDP-stimulated C2 cells, suggesting a role for hPepT1 in MDP uptake by intestinal epithelial cells (Vavricka 2004).

Next, Vavricka and colleagues (2004) demonstrated the presence of MDP *in vivo* in intestinal contents by high-performance liquid chromatography and TLC. MDP could be recovered from faecal and colonic fluid, but not from duodenum, where bacterial colonisation is minimal. These investigators show that the affinity of hPepT1 for MDP is higher than the predicted levels of MDP in the normal colon. Nonetheless, as hPepT1 expression is increased in intestinal inflammation, these findings suggest that hPepT1 may play a role in MDP-mediated innate responses.

In comparison, Viala and colleagues (2004) described a mechanism by which a non-invasive bacterial pathogen initiates innate immune signalling in epithelial cells through 'cag' pathogenicity island (cagPAI)-dependant presentation of PGN to intracellular NOD1. cagPAI is a cluster of approximately 30 genes in *Helicobacter pylori* that are proposed to encode a type VI secretion system (T4SS), a complex of about 30 proteins that assembles into a 'needle', which extends through the bacterial cell wall envelope as an external spike that can be inserted into the plasma membrane of host cells. The secretion apparatus allows for the translocation of specific bacterial effectors into the cytoplasm of target cells. *H pylori* strains containing cagPAI are more virulent, and induce NF-κB activation in gastric epithelial cells (Fischer 2001).

Viala and colleagues (2004) showed that cagPAI-positive *H pylori* induce NOD1-mediated NF-κB activation in HEK293T transfectants. Transfecting cagPAI-positive H pylori-infected cells with a dominant negative NOD1 construct abrogated NF-κB activation by up to 90%. Using radio-labelled PGN, these investigators confirmed that a functional *cag* PAI is required for the delivery of *H. pylori* PGN into host cells. They showed that PGN detection is based on recognition of a peptidoglycan-derived muropeptide, *meso*-diaminopimelate (mDAP), the structure specifically detected by NOD1. In addition, NOD1-deficient mice have an increased susceptibility to infection with cagPAI-positive *H. pylori*, demonstrating a function for NOD1 in host defence against virulent *H. pylori*. These results raise the possibility that secretion systems may not only deliver mDAP into host target cells, but could be a widespread mechanism allowing for MDP delivery from other bacteria.

1.2.5.2 Effect of Crohn's disease-associated NOD2 mutations on PGN- and MDP-mediated cellular responses

Bonen and colleagues (2003a) showed that PGN-induced cellular activation is diminished in mammalian cells expressing mutant NOD2 proteins. Using HEK293T cells that were transfected with expression plasmids encoding for wild-

type or mutant NOD2 protein, they showed that NF-κB activation was reduced or absent in PGN-treated cells that expressed mutant NOD2 proteins encoded by the Leu1007fsinsC, Arg702Trp and Gly908Arg mutations. In a similar way, Girardin and colleagues (2003) showed that mutant NOD2 proteins do not mediate NF-κB activation in response to PGN and MDP stimulation. Both groups showed that no MDP-induced NF-κB activation was noted in HEK293T cells expressing the Leu1007fsinsC-encoded NOD2 mutant protein whereas lesser degrees of activation were noted in cells expressing the Arg702Trp- and Gly908Arg-encoded NOD2 proteins.

Inohara and colleagues (2003) verified this finding by showing that MDP-induced NF-κB activation was abrogated in mammalian cells encoding mutant NOD2 proteins. These investigators obtained primary peripheral blood mononuclear cells (PBMC) from healthy volunteers and Crohn's disease-affected patients that were either homozygous or heterozygous for the Leu1007fsinsC mutation. Using an electrophoretic mobility shift assay, they showed that MDP did not induce NF-κB activation in PBMC obtained from patients homozygous for NOD2 mutations. In contrast, MDP-induced NF-κB activation was demonstrated in PBMC obtained from normal controls or patients who were heterozygous for the NOD2 mutations. Using quantitative real-time PCR, they showed that transcription of IL-1β and A1 (NF-κB target genes) was diminished in MDP-stimulated mononuclear cells obtained from patients who were homozygous for the L1007fsinsC mutation. In contrast, LPS stimulation induced IL-1B and A1 gene transcription in all PBMC, suggesting that NOD2 mediates cellular responses to MDP.

These studies show that the bacterial product MDP induces NF-κB activation, which appears to be solely mediated by NOD2. These studies highlight a new role for NOD2 and many investigators have accepted that NOD2 functions as a 'pathogen recognition receptor' (PRR). There are, however, many unanswered questions regarding the role of NOD2 as a PRR. There is no evidence to show a direct interaction between MDP and NOD2, and an explanation is sought to account for the discrepancy between the size of the much smaller MDP molecule and the binding site of the NOD2 LRRs. It is proposed that digestion of the PGN

backbone by muramidases generates MDP molecules *in vivo*, but evidence for this is lacking. Nevertheless, despite these limitations, emerging evidence from human studies and *in vivo* models confirm the role of MDP in mediating NOD2-dependant cellular responses.

1.2.5.3 *In vivo* studies assessing NOD2 function

The role of MDP in the pathogenesis of NOD2-associated Crohn's disease has been demonstrated by Maeda and colleagues (2005) using homozygous $NOD2^{2939iC}$ mice. $NOD2^{2939iC}$ mice encode for a truncated NOD2 protein lacking the last 33 amino acids, which is homolog of the human NOD2 protein that is encoded by the 3020insC mutation. In this model, MDP stimulation caused increased levels of NF-κB activation in macrophages isolated from $NOD2^{2939iC}$ mice relative to macrophages from control wild-type mice. Furthermore, the expression of several NF-κB target genes was increased in MDP-treated $NOD2^{2939iC}$ macrophages relative to wild-type controls.

IL-1β, a proinflammatory cytokine, is overexpressed in lamina propria macrophages in Crohn's disease, and MDP induced increased secretion of IL-1β from $NOD2^{2939iC}$ macrophages relative to wild-type controls. Furthermore, MDP was the only microbial product that stimulated IL-1β secretion by $NOD2^{2939iC}$ macrophages.

Maeda and colleagues (2005) showed, for the first time, that truncated NOD2 proteins influence the development of intestinal inflammation *in vivo*. Using dextran sodium sulphate (DSS) to disrupt the intestinal barrier, these investigators assessed the effects of NOD2 on intestinal inflammation in $NOD2^{2939iC}$ and control wild-type mice. DSS administration clearly caused more severe colitis in $NOD2^{2939iC}$ mice than wild-type controls: $NOD2^{2939iC}$ mice suffered from greater body weight loss and exhibited greater mortality relative to wild type mice. The severity and extent of inflammatory lesions, as assessed by the degree of mucosal ulceration and macrophage infiltration of the lamina propria, was greater in $NOD2^{2939iC}$ mice compared to wild-type controls. Following DSS exposure,

$NOD2^{2939iC}$ mice expressed greater amounts of IL-1β, I L-6 and cyclooxygenase-2 (Cox-2) protein and mRNA.

Furthermore, these investigators suggest that bacteria or their products initiate the development of intestinal inflammation in DSS-treated $NOD2^{2939iC}$ mice. Oral antibiotic therapy dramatically reduces DSS-induced intestinal inflammation. Both wild-type and $NOD2^{2939iC}$ mice died after receiving high doses of DSS, but mice that received oral antibiotics with DSS developed mild inflammation, without any genotype-linked differences. These observations support the hypothesis that bacteria or their products induce the development of intestinal inflammation, which is, in part, mediated by NOD2 (Maeda 2005).

Maeda and colleagues (2005) suggest that NOD2 also regulates apoptosis and IL-1β secretion in lamina propria macrophages. DSS treatment induced greater apoptosis of macrophages in $NOD2^{2939iC}$ mice than wild-type controls. Activation of caspase-1, an enzyme required for IL-1β secretion (Thornberry 1998, Greten 2004), is associated with an increase in macrophage apoptosis (Le Feuvre 2002). Interestingly, DSS treatment induced greater IL-1β secretion in $NOD2^{2939iC}$ macrophages than wild-type controls. Furthermore, although various bacterial products such as LPS, PGN, and Pam_3Cys induced comparable increases in IL-1α, IL-6 and TNFα secretion in $NOD2^{2939iC}$ and wild-type macrophages, MDP induced a significant increase in IL-1β release from $NOD2^{2939iC}$ macrophages only. Treatment with an IL-1 receptor antagonist (IL-1-RA) reduced DSS-induced intestinal inflammation in $NOD2^{2939iC}$ mice, and no differences in weight loss and histological inflammatory scores were seen in $NOD2^{2939iC}$ and wild-type mice. Overall, these results suggest that IL-1β contributes to increased intestinal inflammation in $NOD2^{2939iC}$ mice (Maeda 2005).

Human studies, on the other hand, show that MDP does not stimulate IL-1β secretion in PBMC (Li 2004). Li and colleagues (2004) show that MDP and TNFα synergistically induce IL-1β secretion in PBMC from wild-type normal and Crohn's disease-affected patients. In contrast, MDP and TNFα did not induce IL-1β secretion in PBMC isolated from patients homozygous for the NOD2

1007insC mutation. IL-1β gene transcription is appropriately increased in MDP and TNFα-stimulated PBMC from NOD2 homozygotes, and the authors suggest that post-translational processing of IL-1β secretion is defective in NOD2 homozygotes. Thus, the results from human and murine studies show that IL-1β secretion is altered, and suggest that this cytokine plays a role in the pathogenesis of NOD2-associated Crohn's disease.

1.2.6 The potential role of NOD2 as an antibacterial factor in intestinal epithelial cells

In addition to inducing NF-κB activation, NOD2 may also act as an antibacterial factor in intestinal epithelial cells. It is hypothesised that NOD2 functions as an intracellular bacterial sensor and is a component of the innate cellular defence mechanisms (Ogura 2001). Hisamatsu and colleagues (2003) therefore determined if the survival of intracellular bacteria is altered in cells expressing mutant NOD2 protein encoded by the Crohn's disease-associated Leu1007fsinsC mutation sequence. Caco-2 cells that were stably transfected with vectors encoding either wild-type or truncated NOD2 proteins were infected with *Salmonella typhimurium* for 60 minutes. Thereafter viable intracellular bacteria were cultured from cell extracts using a gentamicin protection assay. These results showed that the survival of intracellular bacteria was significantly diminished in those cells expressing wild-type NOD2 compared to untransfected Caco-2 cells or those transfected with a control vector. In contrast, there was no significant difference in the percentage of viable bacteria recovered from cellular lysates obtained from Caco-2 cells expressing truncated NOD2 (Leu1007fsinsC-encoded) and untransfected Caco-2 cells and those transfected with control vector only. These results suggest that NOD2 expression protects intestinal epithelial cells by enhancing the clearance of intracellular *S. typhimurium* bacteria, and that this antibacterial property is defective in intestinal cells expressing mutant NOD2 proteins.

To gain further insight into the mechanism of NOD2-mediated antibacterial function, Barnich and colleagues (2005) showed that GRIM-19, a protein with

homology to the NADPH dehydrogenase complex, interacts with endogenous NOD2 in intestinal epithelial cell lines such as HT29 and Caco-2 cells. These investigators showed, using transfected HEK293 cells, that GRIM-19 is required for NF-kB activation following NOD2 mediated recognition of bacterial muramyl dipeptide (MDP). In Caco-2 cells that were transfected with GRIM-19 and NOD2 expression plasmids, and then infected with *Salmonella typhimurium* (as described before), increased GRIM-19 expression was associated with lower numbers of intracellular bacteria within these transfected cells and the authors suggest that GRIM-19 controls pathogen invasion of intestinal epithelial cells. In patients with IBD, GRIM-19 mRNA expression was decreased in inflamed mucosal tissue as compared to uninflamed and healthy mucosal tissue. Therefore, these authors suggest that GRIM-19 plays a key role in NOD2-mediated innate mucosal responses.

1.2.7 Expression of NOD2

Ogura and colleagues (2001a) initially determined the tissue expression of *NOD2* by northern blot analysis. Using commercially available membranes, which contained purified polyadenylated mRNA obtained from various human adult and foetal organs and tissues, they localised NOD2 expression to peripheral blood leukocytes, with little or no expression in other tissues. They also fractionated peripheral blood leukocytes into its granulocytic, monocytic and lymphocytic components and established, by PCR analysis, that NOD2 expression was most abundant in monocytes (Ogura 2001a).

Other investigators have, however, showed that NOD2 mRNA is also expressed in myelomonocytic haematopoietic cell lineages and in intestinal epithelial cells. Gutierrez and colleagues (2002) have shown that NOD2 is also expressed in monocyte-derived haematopoietic cell lines, such as monoblastic U937 cells and mature monocyte-like THP-1 cells. NOD2 is also weakly expressed in CD34+ progenitor cells isolated from human peripheral blood, and the level of expression in these cells increases as they are differentiated towards granulocytes and monocytes using G-CSF and M-CSF. These *in vitro* studies suggest that NOD2 is up-regulated in differentiating myelomonocytic cells. In peripheral blood cells, quantitative real-time PCR analysis showed that granulocytes, monocytes and

dendritic cells expressed the highest levels of NOD2 mRNA. T cells weakly expressed NOD2 and no expression could be detected in B cells.

Using RT-PCR analysis, several investigators have shown that NOD2 is expressed in intestinal epithelial cells (Hisamatsu 2003, Rosenstiel 2003). Rosenstiel and colleagues (2003) have also detected NOD2 protein in inflamed intestinal tissue from patients with Crohn's colitis. The cellular sources of NOD2, however, remain undefined and it is not known whether NOD2 is prominently expressed in epithelial cells or tissue macrophages. Nonetheless, it is postulated that, within intestinal epithelial cells, NOD2 interacts with bacterial products to modulate cellular responses to infection (Inohara 2002, Inohara 2003a).

In the present thesis, I will seek to identify the cells that express NOD2 in intestinal tissue. In particular, I will determine if NOD2 is expressed in Paneth cells, which are discussed further in the next section.

1.3 Paneth cells

1.3.1 Introductory comments and description

Paneth cells, described over a century ago, are located at the bases of the crypts of Lieberkühn in the small intestinal tract (Paneth 1888, Schwalbe 1872) with each crypt containing approximately 5-15 Paneth cells (Bry 1994, Porter 2002). These cells are found in the small intestines of humans, primates, rodents, horses, and pigs (Porter 2002). Paneth cells are distributed throughout the length of the small intestine, and are most numerous in the terminal ileum (Bry 1994, Porter 2002). In the developing human embryo, Paneth cells are detected at 12 - 13.5 weeks gestation and gradually increase in number throughout gestation although these cells are less numerous in newborn infants than adults (Moxey 1978, Mallow 1996).

1.3.2 Structural characteristics

Paneth cells are pyramidal shaped columnar epithelial cells that originate from the multipotent intestinal stem cells that are located within the intestinal crypts (Booth 2000, Bach 2000). Intestinal stem cells give rise to the other intestinal epithelial cell lineages (absorptive enterocytes, goblet cells and enteroendocrine cells) that migrate upwards to form the villous epithelium. Differentiating Paneth cells, on the other hand, migrate downwards towards the crypt base and fill with granules so that mature Paneth cells are characterised by the presence of prominent apical granules. Paneth cells are easily identified as their apical granules stain intensively with eosin, phloxine-tartrazine (Figure 1.4) (Lendrum 1947), and periodic acid Schiff's stain (Porter 2002).

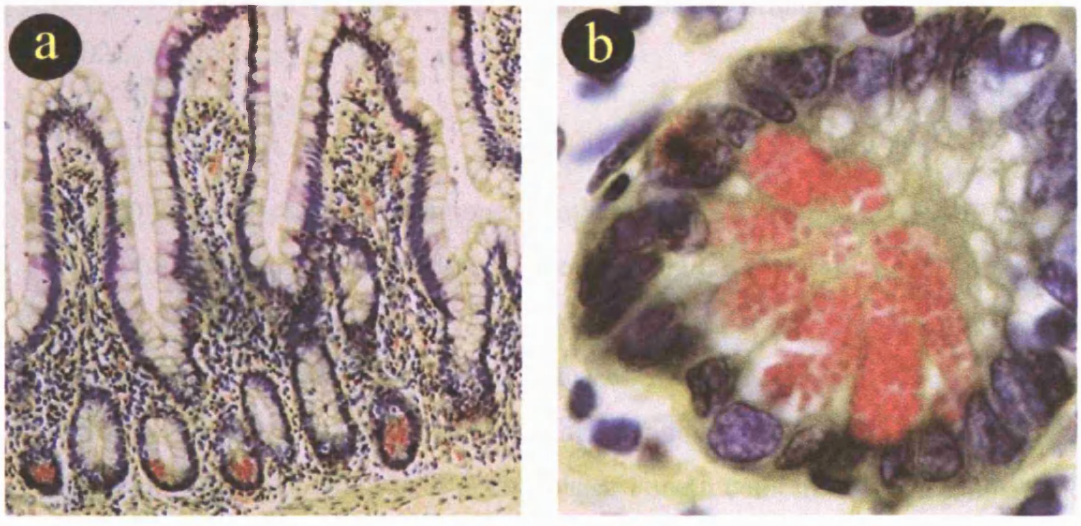

Figure 1.4. Human terminal ileal tissue stained with phloxine-tartrazine. *Prominent apical secretory granules are noted in Paneth cells that are located at the bases of the intestinal crypt. The section is viewed under the 20x objective (a) and 100x objective (b).*

Paneth cells have the morphological characteristics of secretory cells. Paneth cells have an extensive endoplasmic reticulum and Golgi network, and contain large secretory granules in the apical region of the cell (Lehrer 2004). Under electron microscopy, the granules can be visualised discharging their contents onto the intestinal lumen (Satoh 1986). In humans, the granules of Paneth cells contain an array of antimicrobial peptides including alpha defensins, lysozyme and secretory phospholipase A_2 Group IIA (sPLA$_2$). The alpha defensins are the most abundant antimicrobial peptides found in Paneth cells (Bevins 2004). Other granule proteins, such as secretory leukocyte inhibitor (SLI) (Bergenfeldt 1996), hepatocarcinoma-intestine-pancreas protein (HIP; also known as pancreatitis-associated protein, PAP) (Christa 1996), and immunoglobulins G (Rodning 1976) and A (Satoh 1986), may potentially have antimicrobial properties. In the non-granule cell region, Paneth cells contain numerous molecules such as guanylin (de Sauvage 1992), epidermal growth factor (Poulsen 1986), pancreatic lipase related-protein 2 (Lowe 2000), and tumour necrosis factor alpha (TNFα) (Keshav 1990, Beil 1995, Schmauder-Chock 1994, Tan 1993). These components suggest that Paneth cells are potentially involved in the regulation of luminal ionic

composition, crypt development, digestion and intestinal inflammation (Porter 2002).

1.3.3 Function

Paneth cells are essential components of the innate intestinal defences and have been proposed to play a regulatory role in intestinal inflammation (Porter 2002, Bevins 2004). The secretory granules in Paneth cells contain an array of antimicrobial peptides which, when released into the gut lumen, are thought to provide protection to the stem cells that are found above Paneth cells in the intestinal crypt. Nonetheless, it is the role of Paneth cells in mediating innate host defences in response to ingested intestinal pathogens that is more clearly defined (Wilson 1999, Salzman 2003). Paneth cell antimicrobials may regulate the composition and number of the intestinal microflora, thus creating unfavourable conditions for the growth of pathogenic bacteria. Paneth cells also mediate intestinal angiogenesis (Stappenbeck 2002), indicating that these cells have a broader range of functions than appreciated.

1.3.3.1 Innate immunity

A role for Paneth cells in innate immunity was alluded to by histological observations showing Paneth cells discharging their granules into the crypt lumen in response to bacterial infection (Satoh 1986). Moreover, a role for Paneth cells in innate intestinal defences was inferred from *in vitro* studies, which demonstrated the antimicrobial properties of Paneth cell granule peptides (Selsted 1992, Porter 1997, Laine 1999, Laine 2000, Gronroos 2001). In particular, the alpha defensins, or cryptdins, are potent antimicrobial peptides. Initial attempts, however, to confirm the role of Paneth cells in innate immunity *in vivo* by targeted disruption ('knockout') of alpha defensin genes was not feasible as a large number (>20) of similar genes encode for these peptides in the mouse (Ganz 2000). Nonetheless, two elegant studies have shown that, *in vivo*, Paneth cell defensins are crucial in mediating host defence against potentially lethal intestinal pathogens (Wilson 1999, Salzman 2003).

In the first study, Wilson and colleagues (1999) identified the enzyme responsible for cleaving anionic peptide segments from inactive defensin precursors to yield active defensin peptides. This enzyme, a matrix metalloproteinase 7, or matrilysin (MMP-7) localises to Paneth cells, and is secreted together with defensin molecules into the crypt lumen. By disrupting matrilysin gene expression, these investigators engineered matrilysin 'knockout' ($MAT^{-/-}$) mice that lacked mature alpha defensins but contained abundant precursor molecules. Crypt secretions isolated from $MAT^{-/-}$ mice were less bactericidal than secretions isolated from wild-type mice, and *in vivo*, exogenously administered *E coli* survived in greater numbers and were more virulent in $MAT^{-/-}$ mice. In addition, $MAT^{-/-}$ strains were more susceptible to infection by invasive pathogens such as *Salmonella typhimurium*, in comparison to wild-type mice (Wilson 1999). Although it is possible that matrilysin-dependant systemic responses may render mice resistant to oral infection with intestinal pathogens, these results strongly suggest that matrilysin-processed defensins play a pivotal role in mediating innate defences against oral pathogens.

Salzman and colleagues (2003) developed a transgenic mouse model using a 2.9-kilobase human alpha-defensin 5 (HD5) minigene containing 2 HD5 exons and 1.4 kilobases of 5'-flanking sequence. In the HD5 transgenic mice, HD5 mRNA and protein expression faithfully localises to Paneth cells, thereby implying that the flanking sequence contains tissue-specific promoter elements. This transgenic murine model allowed investigators to determine whether Paneth cell-specific HD5 conferred protection against intestinal pathogens, and this 'knock-in'-like model avoided potential confounding (systemically mediated) effects that are inherent in 'knockout' models. Following oral inoculation with *Salmonella typhimurium* (1.5×10^9 c.f.u.), a striking difference was noted in the HD5 transgenic mice and wild-type control strains. The HD5 trangenic mice showed some initial signs of illness but consistently recovered with no mortality or morbidity whereas all control mice succumbed to infection i.e. 100% mortality. Also, after oral inoculation with sub lethal doses of *S typhimurium*, increased bacterial translocation was observed in the wild-type strain. HD5 mediates innate responses to luminal intestinal pathogens as there was no difference in survival in HD5 transgenic and control mice following intraperitoneal infection with *S.*

typhimurium (Salzman 2003). It is not entirely clear why the HD5 transgenic mice are resistant to infection by *S. typhimurium* as, *in vitro*, HD5 and endogenous mouse cryptdin peptides have comparable killing activity against *S typhimurium* (Ouellette 2005). It is therefore possible that Paneth cell secretions mediate protection by direct killing of bacterial pathogens or by influencing the composition of the resident microflora by selecting for commensal species that release bactericides which protect against *S typhimurium* (Ouellette 2005). The HD5 transgenic mice is a model, however, that can be used to analyse human defensin expression and function to more precisely define the role of Paneth cells as key mediators of innate defence against intestinal pathogens.

In addition to the potent antimicrobial alpha defensin peptides, Paneth cells express angiogenin, a newly described family of endogenous antimicrobial proteins (Hooper 2003). Human angiogenin (ANG) was initially isolated based on its ability to stimulate vasculogenesis; however, more recent observations suggest that it may be involved in human defence. Hooper and colleagues (2003), using laser capture microdissection and quantitative real time RT-PCR, have shown that murine Paneth cells express angiogenin-4 (Ang4). Using immunoblot analysis, these investigators showed that Paneth cells release Ang4 into the crypt lumen in response to bacterial products. Ang4, a member of the RNase superfamily, is bactericidal against specific intestinal pathogens although, interestingly, it does not have major bactericidal activity against *Beta thetaiotamicron*, a dominant intestinal commensal microbe. Indeed, colonisation with intestinal microbiota, including *Beta thetaiotamicron*, increases Ang4 expression in Paneth cells *in vivo*. During the weaning period, which is associated with changes in the intestinal microbiota, Ang4 expression is increased in conventionally raised mice but not in mice raised in germ-free conditions. These observations provide further evidence of Ang4 regulation by intestinal microbiota. In humans, ANG is bactericidal against systemic pathogens such as *Streptococcus pneumoniae* and *Candida albicans* although it is not certain whether ANG is expressed in Paneth cells *in vivo* (Hooper 2003). These investigations suggest that Paneth cell antimicrobials have the potential to regulate the composition of the intestinal microbiota, allowing commensal bacteria to populate the intestinal lumen whilst affording protection against intestinal pathogens.

1.3.3.2 Angiogenesis

Paneth cells, in addition to their role in intestinal innate immune system, also regulate the growth of new blood vessels within the intestinal villous. Using quantitative three-dimensional imaging analysis in germ-free and conventionally raised mice, Stappenbeck and colleagues (2002) determined that the growth of the intestinal villous capillary network coincides with bacterial colonisation of the intestinal tract. Adult mice that were raised in germ-free environments have arrested villous capillary network formation. Next, using transgenic mice that lacked Paneth cells (Garabedian 1997), these investigators showed that the microbial regulation of villous angiogenesis is also dependant on Paneth cells. The capillary networks in germ-free Paneth cell-deficient mice were less developed as compared to germ-free control mice, suggesting that Paneth cells produce factors that regulate the growth of the villous microvasculature. The growth of the villous capillary network was increased in germ-free control and Paneth cell-deficient mice that were colonised with *Beta thetaiotamicron*, a prominent commensal in murine intestine. The most dramatic increase in vascular growth was observed in Paneth cell-containing control mice, suggesting that Paneth cells promote villous capillary maturation by producing factors that act directly on the villous microvasculature, or indirectly by regulating expression of angiogenic factors in other intestinal cells (Stappenbeck 2002). These findings, which highlight the multifunctional role of Paneth cells, suggest that these cells play a role in the regulation of angiogenesis.

1.3.3.3 Inflammation

Paneth cells may also be involved in the regulation of inflammation, and there is emerging, although speculative, evidence that Paneth cells play a role in intestinal inflammation. Paneth cells produce a variety of cytokines and mediators of inflammation (Porter 2002) and there is evidence to suggest that Paneth cell-α-defensins may also function as paracrine agonists by regulating inflammatory responses in intestinal epithelial cells (Lin 2004). A role for Paneth cells in inflammation is also suggested by reports describing the induction of pro-

inflammatory cytokines in these cells in haemorrhagic shock (Tani 2000) and the regulation of Paneth cell numbers by mucosal T cells in intestinal infection (Kamal 2001).

Murine alpha defensins, or cryptdins, kill microbes by forming pores in their limiting membranes (Ouellette 1994, Ouellette 1997). Certain cryptdin isoforms, such as cryptdins 2 and 3, also form apical anion-conductive channels in eukaryotic cell membranes of crypt epithelial cells. This channel causes a salt and water secretory response that flushes the intestinal crypt of noxious agents (Lencer 1997). Pore formation in eukaryotic cells, however, may also cause cytokine release in these cells, and Lin and colleagues (2004) determined if cryptdins could induce cytokine release in intestinal epithelial cells. Using an *in vitro* cell culture model, these investigators show that cryptdin-3 induces IL-8 secretion from T84 intestinal epithelial cells, presumably after forming channels in the apical membranes of these cells. Signal transduction in epithelial cells treated with cryptdin-3 are likely to occur through pathways involving the transcription factor NF-κB and the kinase MAPK as these factors are activated in cryptdin-3-stimulated cells. However, as NF-κB and MAPK are activated a few hours after cryptdin-3 stimulation, as compared to rapid activation after TNFα-stimulation, it is possible that other signal transduction pathways are invoked in response to cryptdin-3 stimulation. In addition to inducing IL-8 secretion, cryptdin-3 also induces the secretion of other pro-inflammatory cytokines such as macrophage inhibitory protein (MIP)-1-alpha, MIP-1-beta, MIP-1-delta, IL-17, IL-12 p70 and IL-8 from epithelial cells. Although it is unclear if HD5 and HD6 exert similar effects, these observations suggest that cryptdins may further enhance innate defences by triggering the secretion of epithelial cell cytokines that may recruit inflammatory cells, including neutrophils, into the lamina propria.

Paneth cells may also contribute to the development of systemic inflammatory responses following local intestinal injury. It is hypothesised that bacterial translocation across the intestinal epithelial barrier, which occurs in conditions such as haemorrhagic shock, is a major contributor to the development of systemic inflammatory responses (Chen 2003). TNFα is an important mediator of

these systemic inflammatory responses and Tani and colleagues (2000), using a murine model of haemorrhagic shock, have shown that increased tissue TNFα production is solely observed in those animals with evidence of bacterial translocation. Interestingly, increased TNFα production was only noted in Paneth cells and leukocytes present in the mesenteric lymph nodes and spleen, and not detected in hepatic, renal or pulmonary tissue. As TNFα over-production is implicated in the pathogenesis of systemic inflammatory response syndrome (SIRS) following gut ischaemia and bacterial translocation, these findings suggest that Paneth cells may play an important role in initiating inflammation.

Paneth cell products, such as TNFα and cryptdins, may also play a role in intestinal and systemic inflammation by regulating NF-κB activation in enterocytes (Tani 2000, Lin 2004, Chen 2003). In animal models, intestinal ischaemia can trigger acute systemic inflammation, which manifests clinically as systemic inflammatory response syndrome (SIRS). In this scenario, increased NF-κB activity is typically observed in enterocytes. Chen and colleagues (2003), using *Cre-loxP* technology to silence NF-κB activity specifically in murine intestinal epithelial cells, have elegantly shown that NF-κB activation in intestinal enterocytes is required for the initiation and development of systemic inflammation and is not just a marker of inflammation. The abrogation of NF-κB activation in intestinal epithelial cells prevents the development of systemic inflammation in response to intestinal ischaemia. Crucially, however, abrogation of NF-κB activation also results in an increased rate of apoptosis and tissue damage in intestinal epithelial cells. These results show that NF-κB regulation is crucially important to maintain intestinal homeostasis and prevent systemic inflammation, and Paneth cell products, such as TNFα and alpha-defensins, can potentially regulate NF-κB activation in intestinal epithelial cells.

There is evidence to suggest that Paneth cell-derived TNFα plays a role in maintaining the integrity of the epithelial barrier (Seno 2002). In rats treated with diphenylthiocarbazone (dithizone), Seno and colleagues (2002) noted increased NF-κB activation in intestinal epithelial cells. Dithizone, a zinc chelator, reportedly induces the selective killing of Paneth cells that results in the release of

Paneth cell contents, including antimicrobial proteins and TNFα into the crypt lumen. Seno and colleagues suggest that Paneth cell-derived TNFα mediates NF-κB activation in intestinal epithelial cells, as prior administration of neutralising anti-TNFα antibody or pentoxifylline, which inhibits TNFα synthesis, abrogates NF-κB activation in epithelial cells in dithizone-treated rats. Using immunohistochemistry, these investigators suggest that TNFα localises to the secretory granules of Paneth cells, and demonstrated exfoliated Paneth cells that are immunoreactive for TNFα protein in the crypt lumen in dithizone-treated rats. Seno and colleagues showed that increased NF-κB activation was associated with intestinal epithelial cell proliferation, which is consistent with the results reported by Chen and colleagues (2003). Further studies, however, are needed to confirm that this effect is mediated by Paneth cell- derived TNFα.

Kamal and colleagues (2002) have shown that Paneth cell numbers are increased in mice that are infected with parasites such as *Nippostrongylus brasiliensis*, *Heligmosomoides polygyrus*, *Schistosoma mansoni* and *Trichinella spiralis*. Furthermore, Paneth cell numbers were increased in athymic mice that were infected with *T. spiralis*, but not in infected mice deficient in the T-cell antigen receptor TCR $(\beta/\delta)^{-/-}$ (Kamal 2001). Interestingly, transfer of mesenteric lymph node cells from wild-type mice results in an increase in Paneth cell numbers in *T. spiralis*-infected TCR $(\beta/\delta)^{-/-}$ mice, suggesting that Paneth cells numbers are regulated by a specific population of mucosal T cells in response to enteric infection. Although the functional consequences of these changes in Paneth cell number are unclear, it is possible that Paneth cells act in concert with T-cell mediated immune responses to eradicate intestinal parasitic infection.

Various other cytokines and mediators of inflammation are expressed in Paneth cells although the functional significance of these observations is not known. Several investigators have shown, using *in situ* hybridisation and immunohistochemistry, that transforming growth factor (TGF)-β, TNFα, prostaglandin E2 (a pleiotropic mediator of inflammation) and osteopontin (a glycosylated phosphoprotein with proposed functions in cell-mediated immunity) are expressed by Paneth cells (Hauer-Jensen 1998, Keshav 1990, Schmauder-

Chock 1992, Qu 1997). A role for Paneth cells in antigen presentation is postulated as these cells express CD1 (Lacasse 1992). Paneth cells also express FAS ligand (or CD95) at their basolateral membrane (Moller 1996, Lee 1999), which suggests that these cells could induce apoptosis in FAS+ immune cells of the surrounding tissue. If this is true, then Paneth cells could also enhance host defence by removing diseased cells and down regulating immune responses through apoptosis. Fukuzawa and colleagues (2003) have shown Paneth cells express GM-CSF. GM-CSF enhances the expression of the co-stimulatory molecules such as CD80 and CD86 in antigen-presenting cells and increases the capacity of these cells to stimulate T cells (Holowachuk 2001). GM-CSF increases CD80 and CD86 expression in intestinal epithelial cells, which are capable of presenting MHC Class II antigens. As the GM-CSF receptor β-chain is present in both Paneth and non-Paneth cells, it is possible that GM-CSF secreted from Paneth cells acts via autocrine and paracrine mechanisms to enhance expression of costimulatory molecules in epithelial cells of the intestinal crypts. Although the functional significance of these observations is unclear, partly due to a lack of a Paneth cell-like cell line and suitable reagents, these results suggest that Paneth cells may have a repertoire of functions beyond the provision of antimicrobial defence.

1.3.4 Paneth cells and Crohn's disease

The role of Paneth cells in the pathogenesis of intestinal inflammation has not been suitably investigated in animal models. In humans, the expression of the Paneth cell products such as HD5, lysozyme and *s*PLA_2 has been analysed by *in situ* hybridisation and immunohistochemistry, and these observations do not suggest an obvious role for Paneth cells in the pathogenesis of Crohn's disease.

1.3.4.1 Alpha defensin expression

The alpha defensins 5 (HD5) and 6 (HD6) are potent antimicrobials peptides which are likely to confer resistance to infection by intestinal pathogens (Bevins 2004). In normal and Crohn's disease-affected terminal ileum, expression of HD5 peptides is restricted to Paneth cells (Porter 1997, Cunliffe 2001). In Crohn's

disease-affected terminal ileal tissue, HD5 immunohistochemical staining is strongest in Paneth cells, although staining is observed in isolated epithelial cells located near the villous tip in terminal ileal sections (Cunliffe 2001). In Crohn's and ulcerative colitis, metaplastic Paneth cells express HD5 (Cunliffe 2001). By *in situ* hybridisation, HD5 and HD6 mRNA expression is highly restricted to Paneth cells in histologically normal small intestinal tissue (Salzman 1998), although mRNA expression has not been analysed in inflammatory bowel disease. HD6 peptide expression has not been quantitated by immunoblot analysis in normal and Crohn's disease-affected intestinal tissue, and there is no suitable antibody for immunohistochemical analysis of HD6.

Measurement of HD5 and HD6 mRNA expression in intestinal tissue, using quantitative real-time RT-PCR and microarray gene profiles, suggest that HD5 and HD6 mRNA levels are not significantly different in histologically normal and Crohn's disease-affected small intestinal tissue (Fahlgren 2003, Lawrance 2001). These studies, however, show that HD5 and HD6 mRNA expression is significantly increased in Crohn's and ulcerative colitis (Lawrance 2001, Fahlgren 2003), which is most likely accounted for by the presence of metaplastic Paneth cells. Interestingly, microarray gene profile shows that HD5 mRNA expression is increased approximately 40-fold in Crohn's colitis, higher than any other gene on the microarray gene profile (Lawrance 2001). It should be noted that mRNA quantitation using microarray gene profiling is not absolutely quantitative and often dependant on the quality of the high-density oligonucleotide 'chip'. As murine defensins have the ability to modulate inflammatory responses in enterocytes (Lin 2004), there is a possibility that HD5 and HD6 may influence inflammatory responses in humans, but these assumptions are untested. Deficient expression of HD5 and HD6 may predispose to intestinal infection and inflammation but overall, these observations show that expression of these antimicrobial peptides is not lowered, and may be increased.

1.3.4.2 Secretory phospholipase A_2 Group IIA ($sPLA_2$) expression

Secretory phospholipase A_2 Group IIA ($sPLA_2$) is an antimicrobial enzyme that also plays a role in the modulation of inflammatory responses (Nevalainen 1997,

Harwig 1995, Qu 1996, Six 2000). In Crohn's disease, Paneth cells are the most prominent cell types that express *s*PLA_2 mRNA and protein at the site of inflammation although this enzyme is also expressed, albeit more weakly, in intestinal columnar cells (Haapamäki 1999). Other immunohistochemical studies report similar findings (Minami 1994, Lilja 1995), and *s*PLA_2 enzyme activity is increased in Crohn's disease (Olaison 1988, Lilja 1995). More recently, Lawrance and colleagues (2001), using microarray gene profiling of intestinal tissue, showed increased *s*PLA_2 expression in inflammatory bowel disease.

The role of *s*PLA_2 in the pathogenesis of Crohn's disease is uncertain, given that this enzyme, which has antibacterial properties, may prolong the inflammatory reaction in the intestinal mucosa. In animal studies, *s*PLA_2 activity is increased in PAF or LPS-induced small intestinal injury (Rozenfeld 2001). These effects, however, are mediated by intestinal bacteria, and it is unclear whether increased enzyme activity reflects an appropriate host response to bacterial infection or proinflammatory activity. Intriguingly, in dextran sulphate sodium-induced colitis, Tomita and colleagues (2003) have shown that specific inhibition of *s*PLA_2 reduced the size of mucosal erosions and decreased colonic inflammation *in vivo*, suggesting that *s*PLA_2 has a dominant pro-inflammatory role in this model of colitis. Whether inhibition of *s*PLA_2 activity in Crohn's disease reduces intestinal inflammation is unclear and requires further investigation.

1.3.4.3 Lysozyme expression

Lysozyme, a bacteriolytic enzyme, is expressed by various cells in inflamed small intestinal tissue (Stamp 1992, Cappello 1992, Cunliffe 2002, Fahlgren 2003). By *in situ* hybridisation, however, Paneth cells label more intensely for lysozyme mRNA than other cell types (Stamp 1992), suggesting that Paneth cells contribute significantly to lysozyme production within the intestine. Lysozyme mRNA is detected in other epithelial cells such as the ulceration-associated cell lineage (UACL) or pseudopyloric metaplastic cells, although the staining intensity in these cells is weak (Stamp 1992). In inflamed colonic tissue, lysozyme is detected in metaplastic Paneth cells in colonic crypts (Stamp 1992, Fahlgren 2003). In leukocytes, lysozyme mRNA is detected in lamina propria mononuclear cells and

granulomas. Immunohistochemical detection confirms lysozyme expression in epithelial cells and monocytes, and also shows expression in neutrophils (Stamp 1992, Cappello 1992, Cunliffe 2002, Fahlgren 2003) and epithelial cells located near the villous tip (Cunliffe 2002).

Lysozyme mRNA expression, as determined by quantitative real time RT-PCR analysis, is not significantly different in small intestinal villous and crypt epithelial cells obtained from Crohn's disease-affected patients and controls (Fahlgren 2003). In ulcerative colitis, however, lysozyme expression is increased in epithelial cells (Fahlgren 2003), confirming earlier microarray gene profiles which report enhanced lysozyme expression in ulcerative rather than Crohn's colitis (Lawrance 2001). It is assumed that metaplastic Paneth cells, which stain positively for lysozyme mRNA and protein, account for the increased expression in colonic epithelium. Taken together, these results suggest that Paneth cell lysozyme expression is not significantly altered in Crohn's ileitis, and the increased expression seen in ulcerative colitis is likely to be due to Paneth cell metaplasia.

1.3.4.4 Tumour necrosis factor alpha (TNFα) expression

TNFα is a potent pro-inflammatory cytokine that is postulated to play a key role in the pathogenesis of Crohn's disease (Beutler 1999). TNFα production is thought to be increased in patients with Crohn's disease and anti-TNFα therapy is used successfully to treat relapses in Crohn's disease-affected patients (van Dullemen 1995, Stack 1997, Ghosh 2004). Keshav and colleagues (1990) showed that TNFα mRNA is very prominent in Paneth cells, as well as in lamina propria leukocytes, in murine small intestinal tissue. Tan and colleagues (1993) have shown that Paneth cells express TNFα mRNA in necrotising enterocolitis. Beil and colleagues (1995), using electron microscopy to identify immunohistochemical localisation of TNFα protein, have shown that TNFα protein localises to metaplastic Paneth cell granules in Crohn's disease-affected colonic tissue. TNFα protein also localised to several types of leukocytes, such as macrophages and eosinophils, and colonic epithelial cells (Beil 1995). In this study, the intensity of staining was highest in leukocytes and lowest in epithelial

cells. The lack of a suitable antibody, however, has limited an analysis of TNFα protein in control and inflamed intestinal tissue using more conventional immunohistochemical techniques.

Conflicting results have been reported in studies that have quantitated TNFα mRNA expression in intestinal tissue by RT-PCR. In paediatric IBD patients, Dionne and colleagues (1997) have shown that TNFα mRNA expression is increased in Crohn's colitis compared to controls although other studies do not show an increase in TNFα production in intestinal samples from patients with IBD (Stevens 1992, Isaacs 1992). It is postulated that local overproduction of TNFα by Paneth cells, which constitutively express this cytokine, may initiate intestinal inflammation. The cellular sources of TNFα protein, however, have not been identified as yet and it remains uncertain whether Paneth cells contribute significantly to TNFα production in intestinal inflammation.

Overall, these results suggest that the expression of Paneth cell products may be regulated in inflammatory disease, although the functional consequences of this are unknown. In Crohn's disease, Paneth cells numbers are increased and metaplastic Paneth cells are a feature of Crohn's colitis. There is evidence to suggest that lysozyme and TNFα expression is regulated in IBD, although it is unclear if expression of these products is specifically regulated in Paneth cells. In Crohn's disease, current data suggests that there is increased expression of defensin and sPLA$_2$, which are antimicrobial peptides predominantly expressed by Paneth cells. The increased expression of these antimicrobial peptides in Paneth cells most likely occurs in response to bacterial infection that may be present in Crohn's disease although some of these secreted antimicrobial peptides may play a role in inflammation.

1.4 Study aims and Hypothesis

Crohn's disease can affect the entire gastrointestinal tract, but most commonly affects the terminal ileum and colon. Mutations in the newly described NOD2 gene predispose patients to Crohn's disease although these patients usually develop inflammation of the terminal ileum or ileitis. The reasons for this are unknown as NOD2 is expressed in circulating monocytes, which are ubiquitously distributed in the body. The NOD2 gene encodes for a protein that mediates cellular activation in response to stimulation with muramyl dipeptide (MDP). Paneth cells, on the other hand, are most numerous in the terminal ileum and secrete antibacterial peptides in response to bacterial antigens, including MDP. In addition, Paneth cells may also play a role in the development of intestinal inflammation. I therefore hypothesised that Paneth cells, which are specialised for intestinal defence, express the NOD2 gene and that mutations of NOD2 affect Paneth cell function which predisposes to the development of intestinal inflammation.

The aims of this study are:

1. To analyse the expression of NOD2 in normal and Crohn's disease-affected intestinal tissue.
2. To quantitate NOD2 gene expression in intestinal epithelial cells and to identify factors that regulates NOD2 gene expression in intestinal epithelial cells and monocytes.
3. To analyse Paneth cell antimicrobial gene expression in patients with NOD2-related Crohn's disease.
4. To analyse NOD2 and Paneth cell antimicrobial gene expression in other intestinal inflammatory conditions such as necrotizing enterocolitis.
1. To determine whether intestinal epithelial cell lines can be used to assess Paneth cell function.

Chapter Two

2. Materials and Methods

2.1 Materials

A list of reagents and suppliers is attached as Appendix C.

2.2 Molecular biology Techniques

2.2.1. Bacterial Growth media

2.2.1.1 2X YT Medium

16 g tryptone, 10 g yeast extract and 5 g sodium chloride (NaCl) were dissolved in 900 mL distilled water. The pH of this solution was adjusted to 7.0 using sodium hydroxide (NaOH) pellets, and the volume of the solution adjusted to 1000 mL using distilled water. This solution was sterilised by autoclaving for 20 minutes at 15 psi (1.05 kg/cm^2) on liquid cycle.

2.2.1.2 LB Medium (Luria-Bertani Medium)

10 g tryptone, 5 g yeast extract and 10 g NaCl were dissolved in 900 mL distilled water. The pH of this solution was adjusted to 7.0 using NaOH pellets, and the volume of the solution adjusted to 1000 mL using distilled water. This solution was sterilised by autoclaving for 20 minutes at 15 psi (1.05 kg/cm^2) on liquid cycle.

2.2.1.3 Preparation of solid medium plates

Bacto-agar (Difco) was added to 2X YT media so that the final solution contained 1.5% agar. This solution was autoclaved and then cooled to 42.0°C in a water bath. Using aseptic technique, approximately 15 mL of medium were poured into sterile, 90 mm bacterial culture plates. After allowing for the medium to solidify, the plates (with theirs lids slightly ajar) were incubated in a warm room to reduce condensation. Thereafter, the plates were wrapped in plastic and stored, in an inverted position, at 4.0°C.

For the preparation of ampicillin-containing plates, ampicillin was added to medium, using aseptic technique, just before the medium was poured into the plates. The final concentration of ampicillin in the agar plates was 100 μg/ mL.

2.2.1.4 Preparation of IPTG (isopropylthio-β-D-galactoside) and X-gal (5-bromo-4-chloro-3-indoyl-β-D-galactoside)

IPTG: A 20% (w/v) solution of IPTG (0.8M) was prepared by dissolving IPTG in distilled water. The solution was sterilised by passing it through a 0.22 μm disposable filter. The solution was dispensed in aliquots and stored at -20°C.

X-gal: A 2% (w/v) solution of X-gal was prepared by dissolving X-gal in dimethyl formamide in a glass tube. The glass tube containing the solution was wrapped with aluminium foil and stored at -20.0°C.

100 μL of the IPTG and X-gal solutions were pipetted on the centre of the agar plates and spread using a sterile spreader. The plates were then incubated at 37.0°C until the solutions were absorbed into the agar.

2.2.2 Preparation of competent cells

Reagents:

1. *Escherichia coli* DH5alpha bacteria
2. 2X YT media
3. $CaCl_2$ solution [60mM calcium chloride ($CaCl_2$), 15% glycerol, 10mM PIPES buffer pH 7)

Method:

Frozen stocks of the bacterial *Escherichia coli* strain DH5alpha (a gift from Dr G MacColl, Royal Free and University College Medical School, London) were revived by streaking a sample of the stock on 2X YT solid medium plates which were then incubated at 37.0°C for 16 hours. A single bacterial colony, picked from the plate with a sterile toothpick, was propagated in 50 mL 2X YT medium that was agitated at 37.0°C for 16 hours. 200 mL of pre-warmed (to 37°C) 2X YT

media, contained in a baffled flask (1000 mL capacity), was inoculated with 2 mL of the overnight *E. coli* DH5α culture and agitated at 37.0°C for 2 hours. The optical density of this culture, checked at a wavelength of 590 nm, was 0.670.

This culture was aliquoted into chilled polypropylene centrifuge tubes (50 mL capacity), which were cooled on ice for 15 minutes. Thereafter, the bacterial culture was centrifuged at 1600*g* at 4.0°C for 7 minutes. After centrifugation, the culture supernatant was carefully aspirated and discarded, and the bacterial pellet gently resuspended in 10 mL pre-chilled $CaCl_2$ solution. The resuspended pellets were chilled on ice for a further 30 minutes, and centrifuged at 1100*g* at 4.0°C for 5 minutes. After centrifugation, the supernatant was discarded, and the bacterial pellet was gently, but thoroughly, resuspended in 2 mL pre-chilled $CaCl_2$ solution. These cells were aliquoted into pre-chilled microfuge tubes, frozen on dry ice, and stored at -80.0°C.

The transformation efficiency was tested by transfecting the competent cells with pUC18 plasmid DNA (Fermentas). The transformation efficiency of the competent cells was 9.25×10^6 transformed colonies per μg plasmid DNA.

2.2.3 Transformation of competent cells

Reagents:

1. Competent cells
2. 2X YT media
3. Ampicillin-containing 2X YT agar plates
4. X-gal
5. IPTG

Method:

Competent cells were thawed on ice and aliquoted into pre-chilled, sterile microfuge tubes so that each tube contained 50 μL competent cells. One μL of plasmid DNA (either recombinant or control pUC18 plasmids), containing less than 50 ng of DNA, were added to the competent cells. As a control, no DNA was

added to some competent cells. The microfuge were gently swirled to mix the contents and stored on ice for 30 minutes. The tubes were transferred to a non-shaking heating block, preheated to 42.0°C, and heated for 90 seconds exactly ('heat-shock' treatment). Immediately thereafter, the tubes were cooled on ice for 2 minutes. 450 μL of pre-warmed (37.0°C) 2X YT media were added to the tubes, which were incubated at 37.0°C for 60 minutes in a shaking heating block. Thereafter, either 20 μL or 200 μL of the transformed competent cells were spread on ampicillin-containing 2X YT agar that were plated with X-gal and IPTG 30 minutes beforehand. These plates were incubated at 37.0°C for 16 hours, and thereafter stored at 4.0°C for 4 hours to permit blue colour development.

Using a sterile toothpick, white colonies, containing recombinant plasmids, were picked from the agar plates, and inoculated into fresh 2X YT media containing ampicillin. Blue colonies were picked from plates containing competent cells transfected with control pUC18 plasmids. There was no growth on the agar plates that contained competent cells without plasmid DNA.

2.2.4 Preparation of bacterial stocks

Reagents:

60% glycerol (sterilised)

Method:

1.35 mL of bacterial culture was added to sterile storage tube containing 450 μL sterile 60% glycerol [sterilised by autoclaving for 20 minutes at 15 psi (1.05 kg/cm^2) on liquid cycle]. This solution was mixed, using a vortex mixer, to evenly disperse the glycerol, and the culture was frozen in dry ice or liquid nitrogen, and stored at -80.0°C. Bacteria were recovered by scraping the frozen surface of the culture with a sterile inoculating loop which was streaked across an LB or 2X YT agar plate containing the appropriate antibiotic. The plate was incubated overnight at 37.0°C.

2.2.5 Phenol extraction and ethanol precipitation of nucleic acids

Phenol extraction was performed to remove contaminating proteins from DNA and RNA preparations.

Reagents:

1. Solvent resistant 1.5 mL microfuge tubes
2. Phenol [C_6H_6O]: Chloroform [$CHCl_3$]: Isoamyl Alcohol [$(CH_3)_2CHCH_2CH_2OH$] 25:24:1 saturated with 10 mM Tris, pH 8.0, 1 mM EDTA
3. Chloroform: isoamyl alcohol (24:1)
4. 100% ethanol (CH_3CH_2OH), chilled on ice.
5. 70% ethanol, chilled on ice.
6. 3 M sodium acetate ($C_2H_3NaO_2$) (pH 5.2)
7. Dry ice

Method:

DNA or RNA preparations, in a 300 µL volume, were transferred to a sterile polypropylene tube containing 300 µL phenol: chloroform: isoamyl alcohol. Using a vortex mixer, the contents of the tube were mixed until an emulsion formed. The microfuge tube was centrifuged at 13 000 rpm (16 100 *g*) for 5 minutes at room temperature. Following centrifugation to enact phase separation, the upper aqueous layer was carefully aspirated, avoiding the protein and phenol interface. To further purify DNA, the aqueous phase was transferred to a sterile polypropylene tube containing 300 µL phenol: chloroform: isoamyl alcohol. The contents were mixed using a vortex mixer. The microfuge tube was centrifuged at 13 000 rpm (16 100 *g*) for 5 minutes at room temperature. At this stage, no protein was visible at the interface of the aqueous and organic phases, and the aqueous phase was transferred to a fresh tube containing 300 µL chloroform. After mixing the contents, the tube was centrifuged at 13 000 rpm (16 100 *g*) for 5 minutes at room temperature. Following centrifugation, the aqueous phase (300 µL) was transferred to a fresh tube where the nucleic acids were concentrated by ethanol precipitation.

30 µL of 3M sodium acetate was added to the nucleic acids, and the contents mixed using a vortex shaker. Next, 750 µL of ice-cold 100% ethanol was added to the tube, and the contents were mixed using a vortex mixer. The nucleic acids were precipitated at -80°C for 60 minutes. Following precipitation, the microfuge tube was centrifuged at 13 000 rpm (16 100 *g*) for 10 minutes at 4°C. The supernatant was carefully removed by aspiration and the nucleic acid pellet washed with 750 µL 70% ice-cold ethanol. The tube was centrifuged at 13 000 rpm (16 100 *g*) for 10 minutes at 4°C and, after carefully discarding the supernatant, the nucleic pellet suspended in 50 µL nuclease-free water and stored at -20°C.

2.2.6 Preparation of plasmid DNA by alkaline lysis with sodium dodecyl sulphate (SDS): Minipreparation

Plasmid DNA was isolated from bacterial cultures by treatment with alkali and SDS, and the resulting DNA preparations analysed by restriction endonuclease digestion and electrophoresis.

Reagents:

1. 2X YT medium
2. Ampicillin (100 mg/mL)
3. STE Buffer: 10 mM Tris-Cl (pH 8.0), 0.1 M NaCl, 1 mM EDTA (pH 8.0). Solution was sterilised by autoclaving and stored at 4.0°C
4. Lysis Buffer: 25 mM Tris (pH 8.0), 10 mM EDTA (pH 8.0), 50 mM glucose. Solution was filter sterilised and stored at 4.0°C
5. 0.2 M NaOH, 1% SDS. This solution was freshly prepared before use.
6. 3M sodium acetate solution ($C_2H_3NaO_2$) (pH 5.2)
7. Isopropanol [$(CH_3)_2CHOH$]
8. 70% ethanol
9. 10 mM Tris-HCl (pH 7.4)
10. RNase A (10 mg/mL)
11. Phenol: chloroform: isoamyl alcohol (50:49:1)
12. Chloroform: isoamyl alcohol (49:1)

13. 100% ethanol
14. Nuclease free water

Method:

A single bacterial colony, transformed with plasmid vectors, was picked from an agar plate with a sterile toothpick and cultured at 37.0°C for 16 hours in a sterile container containing 10 mL of 2X YT culture medium and ampicillin (100 μg/ mL). Following overnight culture, the culture medium was transferred to a 50 mL-centrifuge tube and centrifuged at 2000 rcf (836 *g*) for 10 minutes at 4°C. After discarding the supernatant, the bacterial pellet was washed in ice-cold 1 mL STE buffer to remove any residual culture medium; this suspension was transferred to a microfuge tube and centrifuged at 13 000 rpm (16 100 *g*) for 2 minutes at room temperature. After discarding the supernatant, the bacterial pellet was suspended in 150 μL lysis buffer by vigorous shaking. 200 μL of freshly prepared 0.2 M NaOH, 1% SDS solution was added to the microfuge tube, which was immediately inverted several times to gently mix the contents, and the microfuge tube was placed in ice for 10 minutes. 300 μL ice-cold 3M sodium acetate solution (pH 5.2) was added to the microfuge tube, which was immediately inverted several times to gently mix the contents. Next, the tube was placed in ice for a further 30 minutes. The microfuge tube was centrifuged at 13 000 rpm (16 100 *g*) for 10 minutes at room temperature, and the supernatant (approximately 700 μL) transferred to a fresh microfuge tube and centrifuged at 13 000 rpm (16 100 *g*) for 10 minutes at room temperature. The supernatant was transferred to a fresh microfuge tube containing 700 μL isopropanol, and the contents mixed by inverting the tube. The tube was stored at -80.0°C for 15 minutes to allow for precipitation of DNA and centrifuged at 13 000 rpm (16 100 *g*) for 10 minutes at room temperature. After discarding the supernatant, the DNA pellet was washed in 1 mL 70% ethanol and the microfuge tube centrifuged at 13 000 rpm (16 100 *g*) for 10 minutes at room temperature. After removing the supernatant by aspiration, the pellet was dissolved in 300 μL 10 mM Tris-HCl (pH 7.4). RNA was removed from the preparation by adding 5 μL RNase A (10 mg/mL) and incubating the microfuge tube at 37.0 °C for 60 minutes in a heating block. Following incubation, 300 μL phenol: chloroform: isoamyl alcohol (50:49:1) was added to

the microfuge tube. After thoroughly mixing the contents, the microfuge tube was centrifuged at 13 000 rpm (16 100 *g*) for 5 minutes. The supernatant (approximately 300 µL) was carefully aspirated from the tube and transferred to a fresh tube containing 300 µL phenol: chloroform: isoamyl alcohol (50:49:1); after mixing the contents, the tube was centrifuged at 13 000 rpm (16 100 *g*) for 5 minutes. The supernatant (approximately 300 µL) was carefully aspirated from the tube and transferred to a fresh tube containing 300 µL chloroform: isoamyl alcohol (49:1). After mixing the contents, the microfuge tube was centrifuged at 13 000 rpm (16 100 *g*) for 5 minutes and the supernatant (approximately 300 µL) was carefully aspirated and transferred to a fresh tube. 30 µL 3M sodium acetate and 750 µL 100% ethanol were added to the solution, which was shaken to mix the contents, and the tube stored at -80.0°C for 15 minutes to allow for precipitation of DNA. A DNA pellet was obtained by centrifuging the tube at 13 000 rpm (16 100 *g*) for 10 minutes. After discarding the supernatant, the pellet was washed in 1 mL 70% ethanol. The tube was centrifuged at 13 000 rpm (16 100 *g*) for 10 minutes and, after discarding the supernatant, the DNA pellet was dissolved in 200 µL nuclease free water and stored at -20.0°C.

The yield from this minipreparation was approximately 30 µg plasmid DNA.

2.2.7 DNA minipreparation with QIAprep® Spin Miniprep kit

QIAprep® Spin Miniprep kits use silica-gel-membrane technology to obtain plasmid DNA. Following alkaline lysis of bacterial cells, plasmid DNA is selectively adsorped onto silica in the presence of high salts, and eluted into a low-salt buffer. The silica-gel-membrane adsorps DNA, while RNA and cellular proteins are not retained by the membrane. The procedure consists of three main steps: preparation and clearing of a bacterial lysate, adsorption of DNA onto the QIAprep membrane, and washing and elution of plasmid DNA.

Reagents:

1. QIAprep® Spin Miniprep kit
2. 100% ethanol
3. Nuclease-free water

Method:

Alkaline lysis of bacteria: Bacteria are lysed under alkaline conditions, and the lysate neutralised and adjusted to high-salt binding conditions in one step.

A bacterial pellet was obtained by centrifuging 7.5 mL of liquid bacterial culture at 4000 rpm (345 *g*) for 15 minutes at 4°C. This pellet was resuspended in 250 µL of Buffer P1 (containing RNase A) and transferred to a microfuge tube. 250 µL of Buffer P2 (containing NaOH) was added to the tube, which was gently inverted five times to mix the contents. After 5 minutes, 350 µL Buffer N3 (containing guanidine hydrochloride and acetic acid) was added to the tube, which was gently inverted to mix the contents.

Lysate clearing: Lysates were cleared by centrifugation at 13 000 rpm (16 100 *g*) for 10 minutes at room temperature, and the supernatants were applied to the QIAprep® spin columns.

DNA adsorption to the QIAprep membrane: The QIAprep® spin column was centrifuged at 13 000 rpm (16 100 *g*) for 60 seconds, and the flow-through discarded.

Washing and elution of plasmid DNA: The membrane was washed with 500 µL Buffer PB, which was removed by centrifuging the spin column at 13 000 rpm (16 100 *g*) for 60 seconds. Next, the membrane was washed with 750 µL Buffer PE, which was removed by centrifuging the spin column at 13 000 rpm (16 100 *g*) for 60 seconds. After discarding the flow-through, the residual wash buffer was removed by centrifuging the spin column at 13 000 rpm (16 100 *g*) for 60 seconds. After washing, the QIAprep® column was placed in a clean microfuge tube, and 50 µL of nuclease-free water was added to the centre of the membrane. Following a short incubation lasting 1 minute, the DNA was collected by centrifugation at 13 000 rpm (16 100 *g*) for 1 minute. The eluted DNA was stored at -20°C.

2.2.8 Digestion of DNA by restriction endonucleases

Reagents:

1. Restriction enzymes and buffers (see Table 2.1)
2. Nuclease-free water

Table 2.1. Restriction endonucleases and buffers

Enzyme	**Buffer** (Supplied as 10× concentration)	**Supplier**
Ecl136II	Buffer Ecl136II	Fermentas
EcoRI	React 3	Invitrogen
HindIII	React 2	Invitrogen
PstI	React 2	Invitrogen
PvuII	React 4	Invitrogen
SmaI	React 4	Invitrogen
SstI	React 2	Invitrogen
The following buffers were used for DNA digestion using two restriction endonucleases:		
Enzymes	**Buffer**	
Ecl136II and EcoRI	React 2	
EcoRI and HindIII	React 2	
PstI and HindIII	React 2	
SstI and Hind III	React 2	

Restriction enzyme digestion of DNA was performed in sterile 1.5 mL microfuge tubes using commercially available restriction enzymes and appropriate buffers (Table 2.1). Analytic digests were performed in a 20 µL reaction volume, and preparative digests were performed in a 50 µL volume. All buffers were supplied in 10x concentration, and the enzymes stocks contained 10 U of enzyme in each µL: One unit of enzyme is defined as the amount needed to digest 1 µg of DNA to completion in 1 hour, in the recommended buffer, and at the recommended temperature in a 20 µL reaction volume.

For analytic digests, 0.5 to 1.0 μg of DNA were digested for 1 hour at 37.0°C in a sterile microfuge tube according to the following protocol:

DNA (0.5-1.0 μg)	x μL*
10x buffer	2 μL
Nuclease-free water	x μL*
Restriction enzyme	1 μL
Reaction volume	20 μL

*The volume of DNA and nuclease-free water was adjusted so that the total reaction volume was 20 μL.

For preparative digests, the following recipe was used to digest 10 μg to 20 μg of DNA (in a sterile microfuge tube) for 2 hours at 37.0°C:

DNA (10-20 μg)	x μL*
10x buffer	5 μL
Nuclease-free water	x μL*
Restriction enzyme	5 μL
Reaction volume	50 μL

*The volume of DNA and nuclease-free water was adjusted so that the total reaction volume was 50 μL.

After completion of the reaction, the digested DNA fragments were visualised by agarose gel electrophoresis and ethidium bromide staining. The digested DNA fragments from preparative reactions were purified by phenol extraction and ethanol precipitation.

2.2.9 Reverse Transciptase Polymerase Chain Reaction (RT-PCR)

2.1.9.1 Primers

All oligonucleotide DNA primers were synthesised and purified by reverse-phase High Pressure Liquid Chromatography (HPLC) by Thermo Electron GmbH, Germany. Primers were synthesised to a scale of 0.02 μmoles, and shipped in a dry or lyophilised form. The oligonucleotide primers were reconstituted in nuclease-free water to 100 μM concentration, and stored at -20 °C. These oligonucleotide primers were diluted to a final concentration of 10 μM for use in PCR amplification reactions, and all primers were designed to anneal at 60 °C during PCR amplification. I designed the primers after visually examining the nucleotide sequences that are accessible on PubMed, a service provided by the United States National Library of Medicine (http://www.ncbi.nlm.nih.gov/entrez/query.fcgi). Primer lengths were usually 20 nucleotide bases in length. All primer pairs were designed to span an intron to distinguish mRNA from contaminating genomic DNA amplicons. Table 2.2 lists the oligonucleotide primers used in RT-PCR, nested RT-PCR and quantitative RT-PCR reactions.

Table 2.2 Oligonucleotide primers

Primer	5' – 3' sequence	Expected size (base pairs)	Accession number
IL-8 2878F	CTT TCT GAT GGA AGA GAG CTC	RNA 676	M28130
IL-8 3968R	GT CCT CAC AAC ATC ACT GTG	DNA 1090	
HD5(i) 1454F	CTG AGT CAC TCC AGG AAA G	RNA 204	M97925
HD5(i) 2636R	GGC CAC TGA TTT CAC ACA C	DNA 1196	
HD5(e) 1412F	CCA TCC TTG CTG CCA TTC TC	RNA 268	
HD5(e) 2658R	CGA CAG CAG AGT CTG TAG AG	DNA 1247	
HD6(i) 1493F	CAC TGC AGG CAA AAG CTT ATG	RNA 241	U33317
HD6(i) 2644R	CTC TCT GTT CTC ATC CCT C	DNA 1151	
HD6(e) 1471F	CCA CTC CAA GCT GAG GAT G	RNA 314	
HD6(e) 2697R	TAG GAC ACA CGA CAG TTT CC	DNA 1226	
NOD2 115520F (e)	GCG CGA TAA CAA TAT CTC AGA	RNA 402	AJ303140
NOD2 122313R (e)	CAG AGT TCT TCT AGC ATG ACG	DNA 6794	
NOD2 115545F (i)	GGC ATC TGC AAG CTC ATT G	RNA 336	
NOD2 122258R (i)	CCA CAC TGC CAA TGT TGT TC	DNA 6714	
GAPDH 3608F (i)	CTT CAC CAC CAT GGA GAA G	RNA 488	J04038
GAPDH 4470R (i)	GC TTC ACC ACC TTC TTG ATG	DNA 863	
GAPDH 3543F (e)	CGA GAT CCC TCC AAA ATC AAG	RNA 693	
GAPDH 4610R (e)	G AGC TTG ACA AAG TGG TCG	DNA 1068	
Lysozyme 4353F (e)	GCT GCA AGA TAA CAT CGC TG	RNA 210	X14008
Lysozyme 5417R (e)	ACC TTT CAC TTA ATT CCT ACT CCC	DNA 1060	
*s*PLA$_2$ 1422F	GCT GTG TCA CTC ATG ACT G	RNA 188	M22431
*s*PLA$_2$ 3770R	GTA GGT CGT CTT GTT TCT AGC	DNA 2348	J04704
TLR4 8055F	GCC CTA AAC CAC ACA GAA G	RNA 270	AF177765
TLR4 8580R	CT GGA TAA ATC CAG CAC CTG	DNA 526	
TNFα 1814F	GAG TGA CAA GCC TGT AGC CC	RNA 265	AY066019
TNFα 2380R	TGG CAG AGA GGA GGT TGA CC	DNA 566	

F: forward primer; R: reverse primer. All primers pairs were designed to span introns, and the expected genomic DNA and mRNA sizes (number of nucleotide base pairs) is indicated. (i) indicates the internal and (e) the external primer set used for nested RT-PCR reactions. All numbers indicate the starting nucleotide position of the primer, listed according to the GenBank accession number.

Reagents:

1. 10 μM sense and anti-sense primers (Primers synthesised by Thermo Electron GmbH, Germany)
2. 25 mM $MgCl_2$
3. 10 mM deoxynucleotide triphosphate (dNTP) mix (containing 10 mM dATP, 10 mM dTTP, 10 mM dCTP and 10 mM dGTP)
4. 10X Qiagen PCR Buffer (Contains Tris-Cl, KCl, $(NH_4)_2SO_4$, 15 mM $MgCl_2$; pH 8.7. Manufacturer does not disclose information regarding concentrations)
5. 5X Q-Solution (Qiagen; manufacturer does not disclose details of composition)
6. *Taq* polymerase (5U/ μL; Qiagen)
7. DEPC-treated water

Method:

PCR was performed using the Eppendorf Mastercycler® Gradient thermocycler (Eppendorf Scientific). Each 20 μl PCR reaction contained 2 μl of cDNA, 1 μM of sense and anti-sense primer, 1.5 mM $MgCl_2$, 5 mM each of dATP, dTTP, dCTP and dGTP, 2μl PCR buffer (Qiagen, Crawley, UK), 4μl of Q-solution (Qiagen) and 0.25U Taq polymerase (Qiagen). Intron-spanning primer pairs were used to amplify each cDNA. RT-PCR was performed, in a 20 μL reaction volume, according to the following protocol:

cDNA	2 μL
10 μM primers (sense + anti-sense)	2 μL
25 mM MgCl	1.5 μL
10 mM d NTP mix	1 μL
Taq polymerase (5U/ μL)	0.25 μL
PCR Buffer solution	2 μL
5X Q-Solution	4 μL
DEPC-treated water	7.25 μL
Reaction volume	20.0 μL

RT-PCR was performed using the Eppendorf Mastercycler® Gradient thermocycler (Eppendorf Scientific). Synthesised cDNA was initially denatured at 94 °C for 3 minutes, and amplified using 40 cycles of denaturation at 94 °C, annealing at 60 °C for 30 seconds, and extension at 72 °C for 60 seconds. The amplified products were visualised on 1.2% agarose gel stained with ethidium bromide and photographed under UV light.

2.2.9.2 Nested RT-PCR

Nested RT-PCR was used to amplify cDNA synthesised from laser capture microdissection (LCM)-acquired cells. The genes of interest, as well as non-DNA control templates, were amplified by two rounds of PCR. The first-stage amplification was performed as described above. Afterwards, 2 μL of PCR product and non-template control were amplified in the second-stage PCR using the same cycling conditions.

NOD2, HD6 and GAPDH mRNA expression in LCM-derived tissue were determined by nested RT-PCR using the following internal intron-spanning primer sets for the second-stage PCR: NOD2: 5'-GGCATCTGCAAGCTCATTG-3' and 5'-CACACTGCCAATGTTGTTC-3'; HD6: 5'-CACTGCAGGCAAAAGCTTATG-3' and 5'-CTCTCTGTTCTCATCCCTC-3'; and GAPDH: 5'-CTTCACCACCATGGAGAAG-3' and 5'-GCTTCACCACCTTCTTGATG-3'.

2.2.9.3 Quantitative RT-PCR: creation of standards

Quantitative real-time PCR was performed using the Rotor-Gene amplification system (Biogene, Kimbolton, UK). Each 20μl PCR reaction contained 2μl of cDNA, 1μM of sense and anti-sense primer, 1.5mM MgCl2, 5mM each of dATP, dTTP, dCTP and dGTP, 1 μL SYBR green (Biogene; final concentration 1:60 000), 2μl PCR buffer (Qiagen, Crawley, UK), 4μl of Q-solution (Qiagen) and 0.25U Taq polymerase (Qiagen). Intron-spanning primer pairs were used to amplify each cDNA.

Relative levels of GAPDH, NOD2, and defensin 6 PCR products were calculated according to the threshold cycle (C_T) value, normalized using the value of the sample with the lowest level of each product, and the data expressed as the ratio of NOD2 to GAPDH. Specificity of the desired PCR products was determined by melting curve analysis and confirmed by agarose gel electrophoresis and ethidium bromide staining.

The threshold cycle (C_T) was defined as the cycle number at which fluorescence emission exceeds the fixed threshold. At the end of each reaction, the recorded fluorescence intensity (Rn) is used for the following calculations by the Rotor-Gene thermocycler software: Rn^+ is the Rn value of a reaction containing all components (the sample of interest); Rn^- is the Rn value detected in NTC (baseline value). ΔRn is the difference between Rn^+ and Rn^-, and indicates the magnitude of the signal generated by the PCR. ΔRn plotted against cycle numbers produces the amplification curves from which the C_T values are derived.

The size of all PCR products was verified by agarose gel electrophoresis and UV transillumination. To further confirm the specificity of the real-time RT-PCR reaction, the PCR products were screened by melt curve analysis. The melting point of a DNA fragment depends on its individual length and guanine-cytosine (G/C) content. Thus, the determination of the individual melting temperature for a DNA fragment can be used to characterize the amplification products. The melt curve is derived by plotting the first negative derivative (-dF/dT) against the temperature. Typically, small amplitude peaks, corresponding to primer dimers, melt at a lower temperature due to their shorter length, whereas peaks from the specific amplification product are of larger amplitude and occur at higher melting temperatures.

2.2.9.4 The comparative C_T method ($\Delta\Delta C_T$) for relative quantitation of gene expression

Gene expression was quantitated by comparing the C_T values of the samples of interest with a control sample, using the comparative C_T method. The C_T values of

both the control and samples of interest were normalised to an endogenous housekeeping gene, glyceraldehyde-3-phosphate dehydrogenase (GAPDH).

The comparative C_T method is also known as the $2^{-\Delta\Delta CT}$ method, where

$\Delta\Delta C_T = \Delta C_T$, sample – ΔC_T, reference

Here, ΔC_T, sample is the C_T for any sample normalised to the endogenous housekeeping gene (GAPDH) and ΔC_T, reference is the CT value for the control also normalised to the endogenous housekeeping gene (GAPDH).

The amplification efficiencies of the endogenous reference and target genes were approximately equal, thus ensuring that the $\Delta\Delta C_T$ calculations were valid. Using serial dilutions of GAPDH and NOD2 cDNA, the amplification efficiencies for GAPDH and NOD2 were 99% and 96% respectively.

2.2.10 Quantification of NOD2 RNA by quantitative real-time PCR

An absolute standard curve method, using serial dilutions of NOD2, was used to determine the sensitivity of NOD2 detection by PCR. Using RT-PCR, NOD2 cDNA sequences were amplified from PBMC-derived cDNA. These sequences, visualised by ethidium bromide staining after agarose gel electrophoresis, were extracted from the gel using a commercial kit and then quantitated by fluorometry.

2.2.10.1 NOD2 DNA quantitation by fluorometry

DNA concentrations were determined by fluorometry using the fluorescent dye bisBenzimide (Hoechst 33258). This dye binds to AT sequences in double stranded DNA, and is specific for the quantitation of nanogram amounts of DNA (range 10 ng/mL – 10 μg/mL). When excited with 360 nm light, the fluorescence emission of the dye at 460 nm increases significantly in the presence of DNA. A DNA standard calibration curve was constructed after measuring known amounts of calf DNA dissolved in a solution containing bisBenzimide. The least squares

regression equation derived from this standard curve was used to calculate the concentration of NOD2 cDNA.

Reagents:

1. DNA standard (product number D48100) containing 1 mg/mL solution of calf thymus DNA in 10 mM Tris HCl, 1 mM EDTA, pH 7.4
2. bisBenzimide (Hoechst 33258; product number B1302) containing 1 mg/mL bisBenzimide in deionised water
3. 10X Fluorescent Assay Buffer (product number F7171) comprising 100 mM Tris HCl, 10 mM EDTA, 2M NaCl, pH 7.4

Method:

The bisBenzimide and Fluorescent Assay Buffer were dissolved in deionised water to prepare a solution containing 2 μg/mL bisBenzimide, 10 mM Tris HCl, 1 mM EDTA and 200 mM NaCl, pH 7.4. DNA standards were prepared by thoroughly dissolving 10, 20, 50, 100, 200, 500 and 1000 ng calf thymus DNA in 200 μL freshly prepared bisBenzimide solution. These solutions, including one not containing DNA ('blank'), were added to separate wells in a 96-well plate, which was placed in a fluorometer with the following settings: excitation wavelength 360 nm and emission wavelength 460 nm. The emissions were read at ambient temperature, and a calibration curve was drawn by plotting total DNA concentration versus relative fluorescent units (RFU) (Figure 2.1).

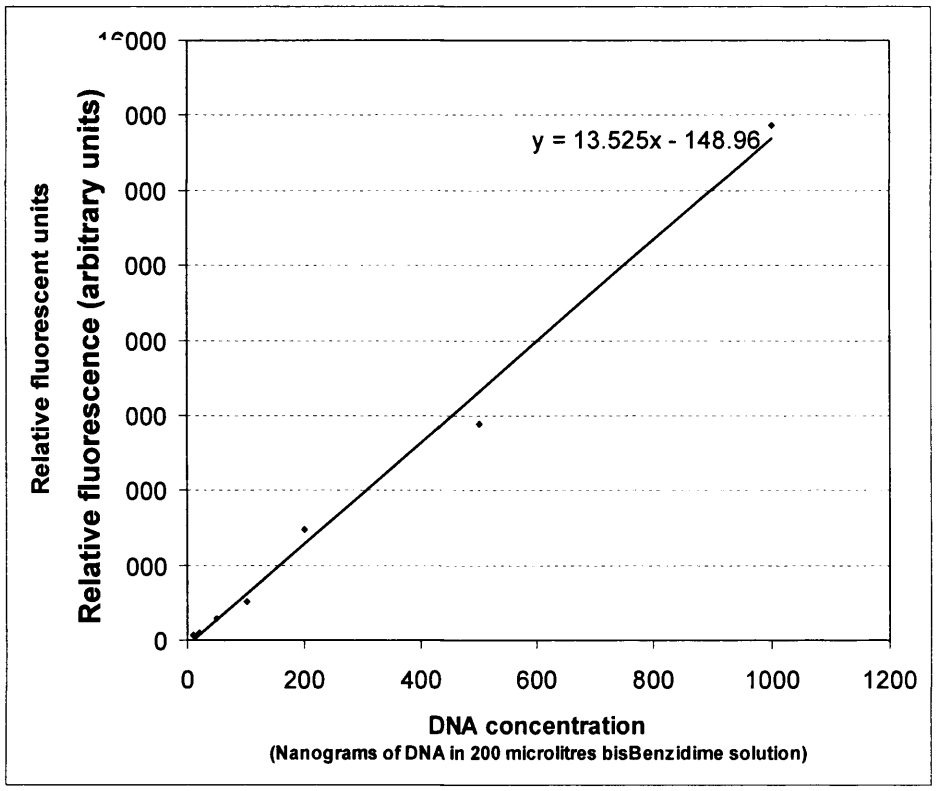

Figure 2.1. Standard curve to determine DNA concentrations using fluorometry.

The least squares regression equation for the line generated by the standard samples was y = 13,53x-148.96 where y is the emission expressed in relative fluorescent units (RFU) and x is the DNA concentration. The emission reading from 5 µl of NOD2 PCR product dissolved in 200 µL bisBenzimide solution was 2077 RFU; this meant that each µL of the undiluted NOD2 PCR product solution contained approximately 32.92 ng or 8.10 x 10^{10} molecules. Next, these NOD2 molecules were diluted in 100 µL aliquots; the initial aliquot contained 10 µL of the undiluted NOD2 PCR product solution and 90 µL water. This and subsequent aliquots were diluted ten-fold, so that 8.10 x 10^{3} NOD2 cDNA molecules were present in 100 µL of solution diluted by a factor of 10^{8}.

2.3 Collection of cells and tissues for RNA extraction

2.3.1 Collection of intestinal tissue and PBMC

Intestinal tissue and PBMC were collected from patients undergoing treatment at the Royal Free Hospital, London. Crohn's disease-affected tissue was collected from patients undergoing surgical resection, and normal small intestinal tissue was obtained from the surgical resection margins of specimens from patients with intestinal carcinoma or benign intestinal obstruction, and no clinical or histological evidence of IBD. Intestinal tissues were placed in containers containing ice-cold PBS, which were placed in a container filled with ice, and transported to the laboratory. PBMC were harvested, using Ficoll density gradient centrifugation, from peripheral blood obtained from healthy volunteers, or from otherwise healthy patients with polycythaemia undergoing venesection (described on page 102). The project was approved by the joint Ethics Committee of the Royal Free Hampstead NHS Trust and Royal Free and University College Medical School (London, UK).

Intestinal tissue sections, from infants that were treated for necrotizing enterocolitis and intestinal atresia at the Chris Hani-Baragwanath Hospital, Johannesburg, South Africa, were obtained from archived wax-embedded tissue blocks. Ethical permission for this study was obtained from the Ethics Committee of the University of the Witwatersrand, Johannesburg.

2.3.2 Isolation of crypt and villus epithelial cells

The mucosa was dissected from surgically resected segments of terminal ileum, rinsed in 10mM dithiothreitol in PBS for 10 minutes and then incubated in 30mM EDTA for 10 minutes at room temperature to detach the epithelium from the basement membrane. Mucosal segments were pinned onto a corkboard and attached to a mechanical shaker, and shaken in aliquots of ice-cold PBS for 1-minute periods. Shaking initially detached epithelial cells from the villi, and subsequently from crypts, with intervening fractions containing mixed populations, and the composition of each fraction was evaluated microscopically. Relative expression of defensin 6 mRNA, determined by quantitative real-time RT-PCR, was subsequently used to confirm that the villus-derived fractions did

not contain Paneth cells, while crypt-derived fractions were greatly enriched for this marker. Epithelial cells were collected by centrifugation at 400g for 5 minutes, and lysed in Trizol reagent to extract cellular RNA.

2.3.3 Laser capture microdissection

Terminal ileal tissue was embedded in OCT compound (Tissue-Tek, Sakura Finetechnical, Tokyo, Japan) and stored at –70°C. 8μm-thick sections were mounted on uncoated and uncharged slides, then fixed in 70% ethanol for 5 minutes, rinsed in water, and stained with haematoxylin and eosin. Sections were dehydrated in graded ethanol baths followed by xylene, and allowed to air-dry completely. Approximately 250 Paneth cells and villus epithelial cells, separately microdissected from the same section, were captured on LCM Transfer Film caps (Arcturus Engineering, Mountain View, California, USA) using the PixCell II LCM system (Arcturus Engineering). The dissected cells were treated with tissue lysis solution (20mM Tris-HCl pH 8.0, 20 mM EDTA, 2% sodium dodecyl sulphate) for 2 minutes, and lysed in Trizol reagent (Life Technologies) to extract cellular RNA.

2.3.4 RNA extraction

Reagents:

1. Trizol® reagent
2. Isopropanol
3. 70% ethanol
4. Nuclease-free water

Method:

RNA extraction from human intestinal tissue, intestinal epithelial cells, peripheral blood mononuclear cells (PBMC) and hepatic leukocytes was performed using Trizol® reagent. Surgically resected intestinal tissue samples were transferred in sterile tubes, chilled on ice, from the operating theatre to the laboratory, where samples were stored at -80°C. For RNA extraction, these tissues were removed from storage and crushed using a pestle and mortar filled with liquid nitrogen.

Alternatively, the frozen tissue was homogenised using a power homogeniser. 100 mg of crushed or homogenised tissue was lysed using 1 mL Trizol reagent.

For RNA extraction from intestinal epithelial cells grown in monolayer, the culture medium was removed from the culture flasks, and the cells were twice washed with PBS. After removing the PBS, the cells were lysed with Trizol reagent: 1 mL Trizol was added per $10cm^2$ surface area of the culture dish. As an example, for intestinal epithelial cells cultured in 6-well plates (surface area 9.6 cm^2 per well), 1 mL Trizol was added to each well. The Trizol-filled culture dishes were left on ice for 1 minute, to allow for cell lysis, and the lysate was transferred to clean microfuge tubes, and stored at -20°C.

For RNA extraction from PBMC cultured in 6-well plates, the culture medium containing non-adherent lymphocytes was transferred to clean microfuge tubes and centrifuged at 13 000 rpm (16 100 *g*) for 5 minutes at 4°C. After discarding the supernatant, the lymphocyte pellet was lysed using 400 µL Trizol reagent. The remaining adherent mononuclear cells in the 6-well culture plates were lysed using 600 µL Trizol, and this solution was transferred to the microfuge tubes containing the lysed lymphocytes so that the entire cell lysate was present in 1 mL Trizol reagent.

For RNA extraction, microfuge tubes containing cell and tissue samples, in 1 mL Trizol reagent, were incubated at room temperature (typically 22 °C) for 5 minutes. Next, 400 µL chloroform was added to each tube, and mixed for 15 seconds using a vortex mixer. The samples were then incubated at room temperature for 2 minutes, and centrifuged at 14 000 rpm (20 817 *g*) for 10 minutes at 4 °C to allow for phase separation. The upper or RNA-containing aqueous phase was removed by careful aspiration, taking care to avoid the protein interface, and transferred to fresh tubes containing 600 µL isopropanol. After mixing the contents, the sample was incubated at room temperature for 10 minutes to allow for RNA precipitation. Next, the tubes were centrifuged at 14 000 rpm (20 817 *g*) for 10 minutes at 4 °C to collect the RNA pellet. After discarding the supernatant, the RNA pellet was washed in 750 µL 70% ethanol

and the tubes were centrifuged at 14 000 rpm (20 817 *g*) for 10 minutes at 4 °C. After discarding the supernatant, the RNA pellet was air dried and resuspended in 22 µL nuclease-free water. 20 µL of RNA solution was used for cDNA synthesis, and 2 µL of solution used to quantify and assess RNA integrity by spectrophotometry and agarose gel electrophoresis.

2.3.5 Synthesis of cDNA

Reagents:

1. Oligo(dT)$_{12-18}$ primer (0.5 µg/µL; Invitrogen Life Technologies)
2. 10 mM dNTP
3. 5X First Strand Buffer [250 mM Tris-HCl (pH 8.30, 375 mM KCl, 15 mM $MgCl_2$; Invitrogen Life Technologies]
4. Moloney Murine Leukemia Virus Reverse Transcriptase (M-MLV RT) (200 units/µL; Invitrogen Life Technologies)
5. Nuclease-free water

Method:

For cDNA synthesis, 2 µg of total RNA, in 20 µl of nuclease-free water, and 0.5 µg oligo(dT) primer (Life Technologies Ltd), were heated to 65° C for 5 minutes and rapidly cooled on ice. Reverse transcription was performed at 37.0°C for 2 hours, in a 50 µl volume comprising 50 mM Tris-HCl pH 8.3, 75 mM KCl, 3 mM $MgCl_2$, 0.5 mM each of dATP, dTTP, dCTP and dGTP, and 800 U Moloney murine leukemia virus reverse transcriptase (MMLV-RT; Life Technologies Ltd). cDNA synthesis was performed, in a 50 µL reaction volume, according to the following protocol:

RNA (2 µg)	20 µL
Oligo(dT) primer	1 µL
10 mM dNTP	2.5 µL
5X First Strand buffer	10 µL
MMLV-RT	4 µL
Nuclease-free water	12.5 µL
Reaction volume	50.0 µL

Synthesised cDNA was stored at -20°C.

2.3.6. *In situ* hybridisation

2.3.6.1 Ligation of cDNA into plasmid vectors

Reagents:

T4 DNA Ligase (5 U/ μL; Fermentas)

10X Ligation buffer: 400 mM Tris-HCl, 100 mM $MgCl_2$, 100 mM DTT, 5 mM ATP (pH 7.8)

Method:

A 234 base pair sequence of the human TNFα gene, obtained by digestion of human TNFα cDNA sequence with the restriction enzyme PvuII (nucleotide position 452 to 686; NCBI accession number M10988), was ligated into the multiple cloning site of the pPCR Script Amp SK(+) vector (Stratagene). The TNFα cDNA sequence was obtained from Dr. Satish Keshav. The pPCR Script Amp vector was initially linearised by digestion with the restriction endonuclease, SmaI. Both plasmid and TNFα DNA were purified by phenol extraction and ethanol precipitation prior to use in the ligation reactions.

The ligation reactions were performed in a 10 μL reaction volume comprising 10ng pPCR-Script Amp plasmid DNA (pre-digested with SmaI), 20 ng 234 base pair-TNFα cDNA, 40 mM Tris-HCl, 10 mM $MgCl_2$, 10 mM DTT, 0.5 mM ATP, 5 U T4 DNA ligase. The reaction mixture was incubated at 16.0°C for 16 hours, and the ligation products transformed into competent cells.

HD-5 and HD-6 cDNA sequences were synthesised by RT-PCR amplification of terminal ileal RNA. Restriction sites for the enzymes HindIII and PstI were incorporated into the oligonucleotide primer designs. The following primers were used for HD-5 amplification: 5'-GAAG AAGCTT CTG AGT CAC TCC AGG AAA G-3' (sense strand primer) and 5'-GAAG CTGCAG GGC CAC TGA TTT CAC ACA C-3' (anti-sense strand primer). The following primers were used for HD-6 amplification: 5'- GAAG AAGCTT CCA CTC CAA GCT GAG GAT G-3' (sense strand primer) and 5'- GAAG CTGCAG GGA CAC ACG ACA GTT TCC TT-3' (anti-sense strand primer).

After amplification of HD-5 and HD-6 cDNA by RT-PCR, the PCR products were extracted from agarose gels and purified. The HD-5 and HD-6 cDNA sequences were digested with restriction enzymes HindIII and Pst, and then purified. 30 ng of HD-5 and HD-6 cDNA and 10 ng of pPCR-Script Amp plasmid DNA (pre-digested with HindIII and PstI, and purified) were used for ligation reactions (described above).

DH5α competent cells were transformed with ligation products, and plasmid containing-strains were selected for ampicillin sensitivity and X-gal/ IPTG colour selection. DNA minipreparations of plasmid DNA was performed, and the identity of the cloned DNA sequences verified by restriction mapping and DNA sequencing.

The following vectors were previously constructed by my supervisor, Dr Satish Keshav: the plasmid vector, pGEM-3 (Promega), containing the subcloned lysozyme sequence (Chung 1988, Keshav 1991); the plasmid vector, pBluescript II KS + (Stratagene), containing the subcloned secretory phospholipase A2 Group IIA (sPLA$_2$) sequence (Keshav 1997). The NOD2 sequence was cloned into the pPCR-Script Amp (Stratagene) vector.

Plasmids, containing the subcloned sequences in the multiple cloning sites, were linearised by restriction enzyme digestion. Restriction nucleases were chosen to cleave DNA so that subcloned sequences remained in continuity with RNA polymerase transcription start sites. The linearised plasmids were visualised by agarose gel electrophoresis and UV transillumination to verify complete digestion by restriction nucleases. The linearised plasmids were purified by phenol: chloroform extraction and ethanol precipitation. A list of restriction nucleases and corresponding RNA polymerases used initiate transcription, is shown in Table 2.3.

Table 2.3. Vector constructs for *in vitro* riboprobe transcription

Construct (Parent vector/ subcloned cDNA sequence)	Probe Length (base pairs)	Restriction endonuclease	RNA polymerase
pGEM-LYZ (pGEM-3/ Lysozyme)	738 (corresponding to nucleotide positions 1 to 738; NCBI accession number J03801)	EcoRI	Sp6
		HindIII	T7
pBS-PLA2 IIA (pBluescript II KS +/ sPLA2 IIA)	402 (corresponding to nucleotide positions 525 to 927; NCBI accession number NM_000300)	SstI	T3
		HindIII	T7
pPCR-TNFα (pPCR-Script Amp/ TNFα)	234 (corresponding to nucleotide positions 452 to 686; NCBI accession number M10988)	Ecl136II	T7
		EcoRI	T3
pPCR-NOD2 (pPCR-Script Amp /NOD2)	220 (corresponding to nucleotide positions 4117 to 4337; NCBI accession number NM_022162)	Ecl136II	T7
		EcoRI	T3
pPCR-HD-5 (pPCR-Script Amp /HD-5)	204 (corresponding to nucleotide positions 94 to 997; NCBI accession number BC069690)	PstI	T7
		HindIII	T3
pPCR-HD-6 (pPCR-Script Amp /HD-6)	278 (corresponding to nucleotide positions 136 to 413; NCBI accession number BC069728)	PstI	T7
		HindIII	T3

2.3.6.2 Transcription of digoxigenin-labelled riboprobes

Reagents:

1. DIG RNA labelling Kit (Roche) comprising:
    a. 10X labelling mix (Roche): 10 mM ATP, 10 mM CTP, 10 mM GTP, 6.5 mM UTP, 3.5 mM digoxigenin-11-2'-deoxy-uridine-5'-triphosphate (DIG-11-UTP); pH 7.5
    b. 10X transcription buffer (Roche): 400 mM Tris-HCl pH 8.0; 60 mM MgCl2, 100 mM DTT, 20 mM spermidine
    c. RNA polymerases (Sp6, T3 and T7)
2. Nuclease-free water
3. DNase 1 (10 U/μL; RNase-free)
4. 0.2 M EDTA (pH 8.0)
5. 3M sodium acetate (pH 5.2)
6. 100% ethanol

Method:

Digoxigenin-labelled riboprobes were transcribed in a 50 μL reaction volume containing 1 to 5 μg linearised DNA, 1 mM ATP, 1 mM CTP, 1 mM GTP, 0.65 mM UTP, 0.35 mM DIG-11-UTP, 40 mM Tris-HCl (pH 8.0), 6 mM $MgCl_2$, 10 mM DTT, 2 mM spermidine, and 40 U RNA polymerase (either Sp6, T3, or T7). The following protocol was used for *in vitro* transcription of digoxigenin-labelled riboprobes:

Linearised plasmid DNA (1 -5 μg)	μL*
Nuclease-free water	μL*
10X labelling mix	5 μL
10X transcription buffer	5 μL
Sp6/ T3/ T7 (20 U/ μL)	2 μL
Final volume	50 μL

*Adjusted to ensure a final reaction volume of 50 μL.

The reaction mixture was set-up in a nuclease-free microfuge tube placed in ice, and then incubated at 37 °C. After 60 minutes of incubation, 20U of polymerase

(1 μL) was added to the reaction mixture, and reaction mixture incubated for a further 60 minutes. After removing 2 μL of sample volume for analysis (to visualise the DNA template), the DNA template was removed by adding 20 U DNase 1 (10 U/μL; RNase-free) to the reaction volume, which was then incubated at 37°C for 15 minutes. A further 4 μL of the reaction volume was removed (2 μL to assess probe integrity using gel electrophoresis and UV transillumination; 2 μL for dot-blot quantitation). Thereafter, 2 μL of 0.2M EDTA was added to the tube to stop the reaction. The contents of the tube were collected by brief centrifugation and 51 μL of nuclease-free water was added to the reaction mixture to adjust the volume to 100 μL. The riboprobes were stored, as an ethanol precipitate, at -20°C after adding 10 μL 3M sodium acetate (pH 5.2) and 250 μL 100% ethanol to the reaction mixture. Riboprobes were stably stored at -20 °C for 12 months. For *in situ* hybridization, the riboprobes were re-suspended in nuclease-free water and then added to the hybridization mixture.

2.3.6.3 Quantitation of digoxigenin-labelled riboprobes

Following transcription, the integrity of the riboprobes and the DNA template (before and after DNase I digestion) was verified by agarose gel electrophoresis, and the digoxigenin-labelled riboprobes were quantified by 'dot-blot' analysis, an immunologic detection of riboprobes blotted onto a neutral nylon membrane (Hybond^{TM}-NX, Amersham). The concentration of the transcribed riboprobes was also estimated by agarose gel electrophoresis.

Reagents:

1. Neutral nylon membrane (Hybond^{TM}-NX, Amersham)
2. RNA standards (100 ng/ mL; Roche)
3. Washing buffer (pH 7.5): 0.1 M Maleic acid, 0.15 M NaCl, 0.3% (v/v) Tween 20; pH 7.5. pH adjusted with NaOH pellets and solution stored at room temperature.
4. Maleic acid buffer: 0.1 M Maleic acid, 0.15 M NaCl; pH 7.5. pH adjusted with NaOH pellets and solution stored at room temperature.

5. Detection buffer: 0.1M Tris-HCl, 0.1M NaCl; pH 9.5. pH adjusted with NaOH pellets and solution stored at room temperature.
6. 10X Blocking solution: Blocking reagent (Roche; composition not disclosed by manufacturer) was dissolved in maleic acid buffer to a final concentration of 10% (w/v). This solution was autoclaved and stored at 4°C. 1X Blocking solution was freshly prepared by diluting 10X blocking reagent ten-fold in maleic acid buffer.
7. Antibody solution: An antibody solution was freshly prepared by diluting an alkaline phosphatase conjugated anti-digoxigenin antibody (150 U/ 200 µL; Roche) 5 000-fold in blocking solution to achieve a final antibody concentration of 150 mU/mL.
8. Colour substrate solution: This solution, which was protected from light, was freshly prepared by dissolving 200µL of NBT/BCIP stock solution in 10mL of detection buffer. NBT/BCIP stock solution (Roche) contains 18.75 mg/mL NBT (Nitro blue tetrazolium chloride) and 9.4 mg/mL BCIP (5-Bromo-4-chloro-3-indolyl phosphate, toludine salt) in 67% DMSO (v/v).

Procedure:

Known concentrations of RNA solutions, or RNA standards, ranging from 1.5 pg/µL to 1 ng/µL, were prepared by dissolving control RNA (100 ng/mL; Roche) in DEPC-treated water. Similar dilution series were prepared for the transcribed riboprobes and RNA standards, and are shown in Table 2.4.

Table 2.4. Riboprobe dilution series for dot-blot quantitation

Aliquot number	Dilution factor	
		RNA concentration
i	1:100	1 ng/mL
A	1:1000	100 pg/mL
B	1:2000	50 pg/mL
C	1: 4000	25 pg/mL
D	1: 8000	12.5 pg/mL
E	1: 16000	6.25 pg/mL
F	1: 32000	3.13 pg/mL
G	1: 64000	1.56 pg/mL

One μL from each dilution sample was blotted onto a neutral nylon membrane and allowed to dry. The RNA was cross-linked to the membrane by UV irradiation at 245 nm for 2 minutes at 1.5 J/cm^2.

Using a plastic box and shaking platform, the nylon membrane (8 cm by 8 cm) was twice rinsed with washing buffer for 2 minutes. The membrane was then incubated with 20 mL blocking solution for 30 minutes, and then with 20 mL antibody solution for 30 minutes. The membrane was then twice washed with 50 mL washing buffer and left to soak in 20 mL detection buffer for 5 minutes. Finally, the membrane was covered with 10 mL colour substrate solution and the plastic box was removed from the shaking platform and covered with foil to protect the membrane from light. The membrane was incubated with the colour substrate solution for 16 hours and the reaction was stopped by rinsing the membrane in distilled water.

The quantity of transcribed riboprobe was estimated by visual colorimetric analysis, and an example is shown below (Figure 2.2):

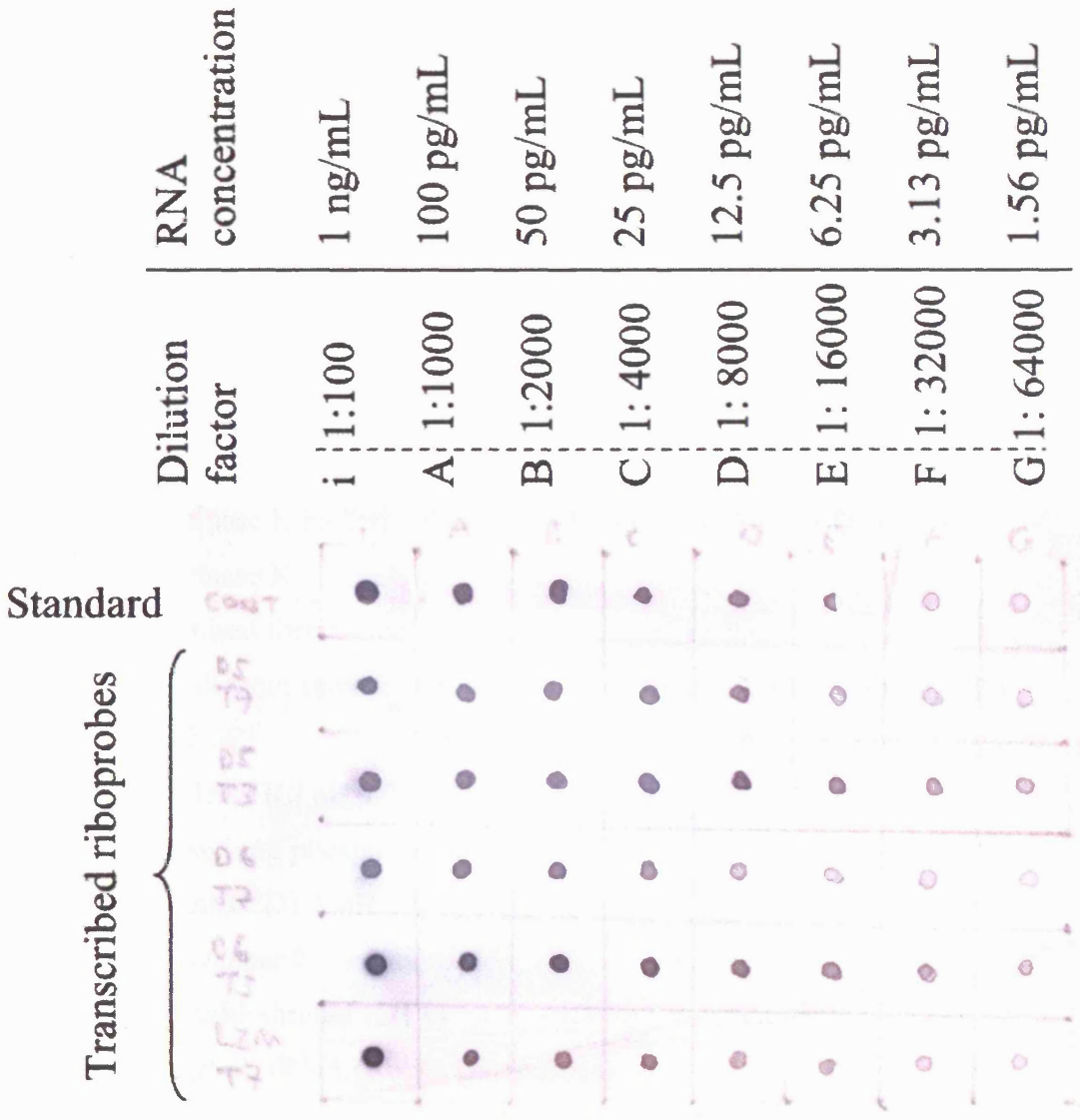

Figure 2.2. Dot blot quantitation of digoxigenin-labelled riboprobes. *A dot blot used for the quantitation of digoxigenin-labelled riboprobes shows decreasing intensity of staining of standard quantities of digoxigenin-labelled RNA in the top row. The concentration of transcribed riboprobes is determined by matching the intensity of staining of the transcribed riboprobes to the staining intensity of the standards, and adjusting for the dilution factor.*

2.3.6.4 *In situ* hybridisation

Reagents:

1. 10% neutral buffered formalin
2. Poly-l-lysine-coated slides
3. Xylene
4. 100% ethanol; also diluted with DEPC-treated water to prepare 95%, 80%, 70%, 60%, 40%, and 20% ethanol solutions
5. 4% paraformaldehyde in phosphate buffered saline (PBS)
6. Phosphate buffered saline (PBS)
7. 0.2 M hydrochloric acid (HCl)
8. Proteinase K buffer: 100mM Tris-HCl pH 7.4, 5mM EDTA
9. Proteinase K
10. Deionised formamide
11. 50% dextran sulphate (Amersham Biosciences, Little Chalfont, UK))
12. 5 M NaCl
13. 1 M Tris-HCl pH 7.2
14. 1 M sodium phosphate buffer pH 6.8
15. 500 mM EDTA pH 8.0
16. 50X Denhardt's solution:
17. 1 M dithiothreitol (DTT)
18. 10 mg/mL tRNA (Roche Diagnostics)
19. 20X saline-sodium citrate (SSC) solution: 175.3g NaCl and 88.2g Sodium Citrate were dissolved in distilled water, and the solution pH adjusted to 7.0 with NaOH. The final volume was adjusted to 1 L, and the solution sterilised by autoclaving
20. NTE solution: 500 mM NaCl, 1 mM EDTA, 10 mM Tris-HCl pH 7.4
21. 20 mg/ mL RNase A
22. Human, horse and rabbit serum
23. Mouse anti-digoxigenin monoclonal antibody (Roche Diagnostics)
24. Biotinylated anti-mouse antibody (Vector Laboratories, Burlingame, CA, USA)
25. avidin-biotin peroxidase complex (ABC) reagent (Vector Laboratories)

Method:

Preparation of slides and fixation of material:

Resected surgical tissues were fixed overnight in 10% neutral buffered formalin, and embedded in paraffin wax blocks. Tissue sections, of 8 micron thickness, were cut using a microtome, and placed on Poly-L-Lysine coated slides (VWR). These slides were either dried at 37°C for 4-8 hours or air-dried for 16 hours at room temperature, and stored at room temperature until further use.

Pre-treatments of materials on slides:

Tissue sections were dewaxed with fresh xylene by placing the slides in a Schieferdecker jar that filled with xylene. Three washes, with fresh xylene, lasting 20 minutes each, were performed using a rocking platform. The sections were then rehydrated to water through graded ethanol baths by twice washing them in 100% ethanol for 5 minutes, in 95% ethanol for 5 minutes, in 70% ethanol for 5 minutes, and finally, twice in DEPC-treated water for 5 minutes. The tissue sections were fixed using 4% paraformaldehyde in phosphate buffered saline (PBS) for 20 minutes at room temperature. The sections were twice rinsed in PBS for 5 minutes, treated with 0.2M HCl for 20 minutes and rinsed in DEPC-treated water. The sections were soaked in 100mM Tris-HCl pH 7.4, 5mM EDTA (Proteinase K buffer) for 5 minutes, and treated with Proteinase K (40μg/ml) in the same solution at 37°C for 15 minutes precisely. The sections were rinsed with Proteinase K buffer, and twice washed in PBS for 5 minutes. Next, tissue sections were dehydrated through a series of graded ethanol baths by washing, for 2 minutes each, in 20%, 40%, 60%, 80% and 100% ethanol solutions.

In situ hybridisation:

The slides were removed from the Schieferdecker jar, allowed to air dry briefly, and placed in an airtight, humidified incubation box. Each section was coated with 50-150 μL of hybridisation mixture, depending on the size of the tissue section. Hybridization mixture containing eitherNOD2 (1.0 ng/μl), TNFα (2.0 ng/μl), lysozyme (1.4 ng/μl), *s*PLA_2 (0.7 ng/μL), HD5 (1.0 ng/μl), or HD6 (1.0 ng/μl), riboprobes were pipetted directly onto the sections. Both anti-sense and sense (control) strand riboprobes were used for hybridisation. These probe

concentrations were determined empirically beforehand. The hybridization mixture comprised 50% deionised formamide, 10% dextran sulphate (Amersham Biosciences), 300mM NaCl, 10mM Tris-HCl pH 7.2, 10mM sodium phosphate buffer pH 6.8, 5mM EDTA pH 8.0, 1X Denhardt's solution, 50mM dithiothreitol and 1mg/mL tRNA (Roche Diagnostics). Slides were hybridized at 42°C for 16 hours in an airtight, humidified container.

Post-hybridisation washes:

Following hybridisation, the slides were removed from the incubation box and placed in a Schieferdecker jar. These hybridized sections were twice washed, with constant agitation for 15 minutes in a shaking water bath, in 2X saline-sodium citrate (SSC) solution and rinsed in 500mM NaCl, 10mM Tris-HCl pH 7.4, 1mM EDTA (NTE solution) at 37°C. The sections were then treated with 20 μg/mL RNase A in NTE solution for 30 minutes at 37°C, and rinsed in NTE buffer. Stringency washes were performed by rinsing the sections, with constant agitation in a shaking water bath, in 0.2X SSC at 37°C for 30 minutes, followed by two washes in 0.2X SSC at 42°C for 30 minutes.

Immunohistochemistry:

Following the stringency washes, the sections were washed in PBS for 10 minutes. The slides were removed from the Schieferdecker jar and mounted on Sequenza Coverplates^{TM} that were placed in Sequenza slide racks (Thermo Electron, Hemel Hempstead, United Kingdom). Sections were covered with 1% human and 1% horse serum in PBS (blocking solution) for 30 minutes, rinsed with PBS and then incubated with a mouse anti-digoxigenin monoclonal antibody (Roche Diagnostics) for 90 minutes at room temperature. Sections were then rinsed in PBS, covered with blocking solution for 30 minutes, and rinsed again in PBS before incubation with a biotinylated anti-mouse antibody (Vector Laboratories, Burlingame, CA, USA) for 30 minutes. Sections were then rinsed PBS, and covered with blocking solution for 30 minutes, rinsed again in PBS and incubated with the avidin-biotin peroxidase complex (ABC) reagent (Vector Laboratories) for 30 minutes, and then rinsed in PBS. The slides were removed from the Sequenza Coverplates and the sections were covered with a solution

containing 0.7mg/ml diaminobenzidine (DAB) and 0.02% hydrogen peroxide. The sections were periodically examined under the microscope to monitor the development of the brown precipitate. The reaction was terminated at the same time for all slides in a single experiment, by rinsing the slides in PBS. Sections were counterstained with haematoxylin for 5 seconds and mounted under coverslips with DPX.

All glassware used for in situ hybridization was baked at 200°C for 14 hours beforehand, and RNase-free chemicals were obtained from Sigma Chemical Company, Poole, UK, except where otherwise indicated. All water used in these experiments was treated with diethyl-pyrocarbonate to eliminate RNase contamination.

2.3.7 Northern blotting/ hybridisation

Northern hybridisation is used to measure the amount and size of RNA's transcribed from eukaryotic genes and to estimate their abundance.

Reagents:

1. 50X Denhardt's solution: 2 g Ficoll 400 (Sigma), 2 g polyvinyl pyrrolidone, and 2 g bovine serum albumin were dissolved in 200 mL DEPC-treated water using a heat-sterilised magnetic stirrer-bar. The solution was filter-sterilised and stored in aliquots at -20.0°C.
2. Ethidium bromide (200 μg/ml)
3. 37 % Formaldehyde
4. Formamide
5. 10X Formaldehyde gel-loading dye: 50% glycerol, 10 mM EDTA (pH 8.0), 0.25% (w/v) bromophenol blue, and 0.25% (w/v) xylene cyanol FF. The following protocol was used to prepare 1 mL of 10X formaldehyde gel-loading buffer:

Glycerol	500 μL
0.5M EDTA (pH8.0)	20 μL
2.5% (w/v) bromophenol blue	100 μL
2.5% (w/v) xylene cyanol	100 μL
Nuclease-free water	280 μL
Final volume	1000 μL

6. 10X MOPS electrophoresis buffer: 0.2 M MOPS (pH 7.0), 20 mM sodium acetate, 10 mM EDTA (pH 8.0). 10X MOPS buffer was prepared by dissolving 41.8 g of MOPS in 700 mL DEPC-treated water, and the solution pH adjusted to 7.0 with 2N NaOH. 20 mL 1M sodium acetate and 20 mL 0.5M EDTA (pH 8.0) were added to the solution, and the final volume adjusted to 1000 mL with DEPC-treated water. The solution was passed through a 0.45 μm filter, and stored at room temperature protected from light.
7. 0.05 M NaOH
8. 0.5 M Tris (pH 7.4)

9. DEPC-treated water
10. Neutral nylon membrane (Hybond^{TM}-NX; Amersham Biosciences)
11. 20X, 6X and 2X SSC buffer

2.3.7.1 Separation of RNA through a denaturing gel

A 1.5% agarose gel, containing 2.0 M formaldehyde, was prepared by dissolving 1.5 g agarose in 85 mL water. This solution was heated, using a microwave oven (for 3 minutes using the low power setting), and cooled to 50 °C. 10 mL 10X MOPS buffer and 5.4 mL formaldehyde (37%) was added to the solution, which was cast in a horizontal electrophoresis box that was specifically used for RNA analysis. The gel was allowed to set at room temperature and, once polymerised, was covered with 1X MOPS solution to a depth of 5 mm. The gel was run for 5 minutes at 65 V (5 V/ cm) prior to loading the RNA samples.

The RNA samples were denatured in nuclease-free microfuge tubes in the following manner. 40 μg RNA, dissolved in 8 μL nuclease-free water, was added to a nuclease-free microfuge tube containing 6 μL 10X MOPS buffer, 10 μL formaldehyde and 30 μL formamide (37%). This mixture was heated to 65 °C for 5 minutes and briefly cooled on ice. After brief centrifugation (16 100 *g* for 15 seconds) to collect the contents, 6 μL of 10X formaldehyde gel-loading dye was added to the reaction mixture. Next, 30 μL (containing 20 μg total RNA) of the reaction mixture was loaded into each well. The gel was run at 65 V (5 V/ cm) for five hours, at which stage the dye front had migrated approximately 10 cm. Electrophoresis was stopped and the gel rinsed in DEPC-treated water for 5 minutes. Next, the gel was denatured in 0.05 M NaOH for 30 minutes, and then washed in DEPC-treated water for 5 minutes. The gel was then neutralised in 0.5 M Tris (pH 7.4) for 1 minute, washed briefly in DEPC-treated water, and then soaked in 2X SSC for 30 minutes. The gel was briefly illuminated under UV light to visualise the RNA.

2.3.7.2 Transfer of RNA to a solid support

A neutral nylon membrane (Hybond^{TM}-NX), cut to match the size of the gel, was briefly rinsed in DEPC-treated water and soaked in 2X SSC buffer for 5 minutes. The RNA was transferred from the gel to the nylon membrane using an upward capillary transfer system, which was assembled as described below. Absorbent, but firm, sponge sheets were placed in a glass reservoir containing 20X SSC. The gel was placed on filter paper sheets, pre-wet with 2X SSC solution, which were placed on the sponge supports. The nylon membrane was carefully aligned over the gel, and filter paper sheets, pre-wet with 2X SSC solution, were placed on the gel. Next, dry paper towels were placed over the sheets of filter paper, and a glass plate, supporting a weight, was placed over the dry paper towels. The nylon membrane, filter sheets and paper towels were all cut to match the size of the gel, and no air bubbles were present between the sheets of filter paper, between the filter paper and the gel, and between the gel and nylon membrane. The assembly was carefully constructed to ensure the filter paper and dry towels placed on top of the gel did not droop over the edges of the gel and touch the solution in the glass reservoir. The assembly schema for upward capillary transfer system is shown in Figure 2.3.

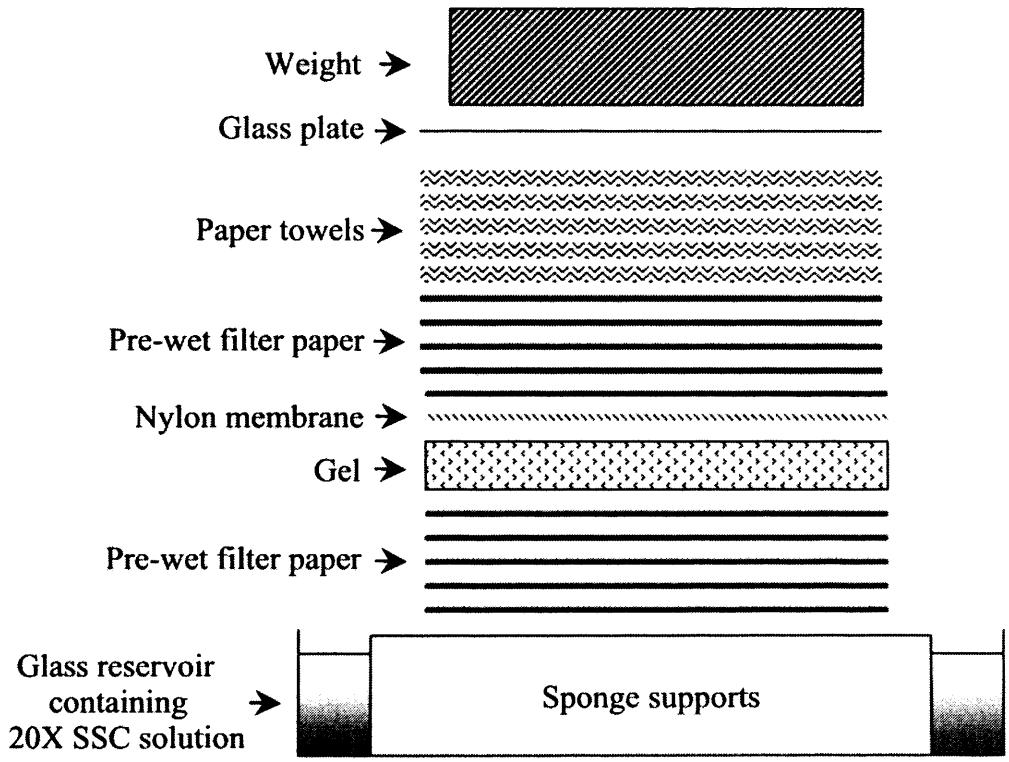

Figure 2.3. Assembly schema for upward capillary transfer system.

The RNA was transferred (for 16 hours) from the gel to the membrane by upward capillary transfer using SSC as a transfer buffer.

2.3.7.3 Fixation of RNA to the solid matrix

After transfer, the capillary assembly was disassembled, and the nylon membrane was rinsed in 6X SSC buffer for 5 minutes. The RNA was cross-linked to the membrane by UV irradiation at 245 nm for 2 minutes at 1.5 J/cm^2. The formaldehyde gel was visualised under UV light to verify that the RNA had transferred from the gel.

2.3.7.4 Hybridisation of the immobilized RNA to probes complementary to the sequence of interest

Reagents:

1. 5X OLB Buffer: 5 mM dATP, 5 mM dTTP, 5 mM dGTP, 1M HEPES, 250 mM Tris HCl (pH 8.0), 25 mM $MgCl_2$, 100 mM NaCl, 10 mM DTT
2. ^{32}P dCTP (10 mCi/mL) (Redivue deoxycylidine 5' [α ^{32}P] triphosphate, triethylammonium salt; 11TBq/mmol, ~3000 Ci/mmol)
3. BSA (10 mg/mL; Sigma)
4. Klenow Fragment of DNA polymerase (2 U/μL)
5. Random hexamers (132 ng/μL)
6. Nuclease free water
7. tRNA (10 mg/mL)
8. 5M ammonium acetate (CH_3COONH_4)
9. 100% ethanol
10. TE buffer (pH 7.6)
11. Pre-hybridisation solution: 50% deionised formamide, 1M NaCl, 0.02% (v/v) SDS, 5X Denhardt's solution, 8 mg salmon sperm DNA, 10% (w/v) dextran sulphate. The pre-hybridisation buffer was mixed by boiling, and then cooled on ice. The following protocol was used to prepare 40 mLs of pre-hybridisation buffer:

NaCl	2.34 g
50X Denhardt's solution	4 mL
Formamide	20 mL
50% Dextran sulphate	8 mL
10% SDS	400 μL
Salmon sperm DNA (10 mg/mL)	600 μL
DEPC-treated water	7 mL

12. 2X SSC, 0.1% SDS and 0.2X SSC, 0.1% SDS solutions

Methods:

The nylon membranes were hybridised with probes to locate GAPDH and NOD2 RNA. The ^{32}P-labelled DNA probes were prepared in a dedicated laboratory

reserved for the handling of radioactive reagents, and appropriate precautions were taken when handling ^{32}P.

GAPDH and NOD2 PCR products, gel-extracted and purified, were used as DNA templates for random primed DNA labelling. A microfuge tube, containing 50 ng of DNA and 1 μL random hexamers (132 ng/ μL, Invitrogen) dissolved in 13.5 μL nuclease-free water, was heated at 95°C for 5 minutes and then rapidly cooled on ice. Next, ^{32}P-labelled GAPDH and NOD2 DNA probes were synthesised in 25 μL reaction volume containing 10 μg bovine serum albumin, 5 μL 5X OLB buffer, 2 U Klenow fragment and 25 μCi ^{32}P-dCTP (1.3×10^8 cpm/ μg) were synthesised using random hexamers. The reaction mixture was incubated at room temperature for 16 hours. The following protocol was used to synthesise the probes:

Random hexamers	1 μL (132 ng/μL)
DNA (50 ng)	x μL*
Nuclease free water	x μL*
BSA (10 mg/mL)	1 μL
5X OLB Buffer	5 μL
Klenow (2 U/ μL)	1 μL
^{32}P dCTP (10 mCi/mL)	2.5 μL
Final volume	25 μL

*Adjusted to 25 μL final reaction volume.

Following random priming, transfer RNA was added to the reaction mixture, and the labelled probes were precipitated using ammonium acetate. 6 μL transfer RNA (10 mg/mL) and 269 μL nuclease-free water were added to the microfuge tube which was gently shaken to mix the contents. Next, 30 μL 5 M ammonium acetate and 750 μL 100% ethanol were added to the microfuge tube and probe was precipitated on dry ice for 60 minutes. The microfuge tube was centrifuged at 13 000 rpm (16 100 *g*) for 10 minutes, and the supernatant carefully transferred to a separate microfuge tube. The pellet was washed in 500 μL 70% ethanol, and the microfuge tube was centrifuged at 13 000 rpm (16 100 *g*) for 10 minutes. After

carefully aspirating the supernatant, the pellet was briefly air-dried and re-suspended in 100 μL TE buffer (pH 7.6).

Using a scintillation counter, the radioactivity counts of the probe and ethanol wash supernatants were measured, and approximately 35-60% of the ^{32}P dCTP were incorporated into the probes.

2.3.7.5 Northern hybridisation

Using a commercial rotating wheel, the nylon membrane was incubated with pre-hybridisation solution for 5 hours at 50.0°C. The ^{32}P-labelled probe was denaturated by heating at 95°C for 5 minutes, and then rapidly chilled on ice. The probe was added the hybridisation solution so that the final concentration of probe in the hybridisation solution was 5 X 10^5 cpm/mL. The nylon membrane was incubated with the probe-containing hybridisation solution at 42°C for 16 hours.

After hybridisation, the membrane was removed from the rotating wheel and placed in a plastic box containing 1000 mL pre-warmed (42°C) 2X SSC, 0.1% SDS. The membrane washed for 10 minutes in a shaking water bath heated to 42°C. After refilling the plastic box with fresh 2X SSC, 0.1% SDS solution, the membrane was washed in this manner two more times. Next, the membrane was washed with 1000 mL 0.2X SSC, 0.1% SDS solution for 30 minutes at 60 °C. After refilling the plastic box with fresh 0.2X SSC, 0.1% SDS solution, the membrane was washed in this manner two more times.

Following the stringency washes, the membrane was dried and wrapped in cling film. An autoradiograph was established by exposing the membrane to X-ray film (Kodak) at -70°C for 24 hours.

2.4 Protein detection and expression

2.4.1 Protein immunoblot (Western Blot Procedure)

Reagents:

The following solutions were prepared for use in SDS polyacrylamide gel electrophoresis (SDS-PAGE):

1. Acrylamide: 30% acrylamide/ bis solution
2. 10% SDS (w/v): 10g SDS was dissolved in 100 mL distilled water
3. Separating buffer: 27.23 g Tris base was dissolved in 80 mL distilled water, and adjusted to pH 8.8 with 6 M HCl. Distilled water was added to adjust the final volume of the solution to 150 mL.
4. Stacking Buffer: 6 g Tris base was dissolved in 60 mL distilled water, and adjusted to pH 6.8 with 6 M HCl. Distilled water was added to adjust the final volume of the solution to 100 mL.
5. Sample buffer: 0.06 M Tris-HCl (pH 6.8), 25% glycerol, 2% SDS, 0.01% (w/v) bromophenol blue, and 5% (v/v) β-mercaptoethanol. 10 mLs of sample buffer was prepared by adding 3.55 mL distilled water, 1.25 mL 0.5 M Tris-HCl (pH 6.8), 2.5 mL glycerol, 2.0 mL 10% SDS, 0.2 mL 0.5% (w/v) bromophenol blue (0.001g/0.2 mL), and 0.5 mL β-mercaptoethanol.
6. 10X running buffer: 6.06 g Tris base, 72 g glycine, and 5 g SDS were dissolved in 500 mL distilled water and stored at 4°C. For electrophoresis, the running buffer was used at 1X concentration by adding 50 mL 10X running buffer to 450 mL distilled water.
7. 10% Ammonium Persulfate (APS) Solution: 100 mg ammonium persulfate dissolved in 1 mL distilled water; solutions were stored at 4 °C for no longer than 7 days.
8. Lysis Buffer: 0.5% SDS, 10 mM Tris, pH 7.4, and 0.1% Protease inhibitor (Sigma)
9. Coomassie Stain solution: Prepared by mixing 0.5 g Coomassie Blue, 200 mL distilled water, 50 mL acetic acid, and 250 mL methanol

10. De-stain solution: Prepared by mixing 200 mL distilled water, 50 mL acetic acid, and 250 mL methanol

An 8%, 10 mL-volume, separating gel was prepared according to the following protocol:

Distilled water	4.7 mL
Acrylamide	2.7 mL
Separating buffer	2.5 mL
10% SDS	0.1 mL
10% APS (fresh)*	50 µL
TEMED*	5 µL
Final volume	10.06 mL

An 8%, 5 mL-volume, stacking gel was prepared according to the following protocol:

Distilled water	2.35 mL
Acrylamide	1.35 mL
Separating buffer	1.25 mL
10% SDS	50 µL
10% APS (fresh)*	25 µL
TEMED*	2.5 µL
Final volume	5.03 mL

*These reagents were added last into the mixtures.

2.4.2 Preparation of samples

2.4.2.1 Lysis of cells

PBMC (1 x 10^8 cells), and Caco-2 (2 x 10^7 cells) and HT29 (6 x 10^7 cells) intestinal epithelial cells (cultured to 90-100% confluence) were concentrated by centrifugation in microfuge tubes, thoroughly resuspended in 1 mL ice-cold lysis buffer and kept on ice for 1 hour. Frozen intestinal tissue samples (100 mg), which were obtained from macroscopically normal regions of resected surgical tissue, were crushed, under liquid nitrogen, using a mortar and pestle and transferred to pre-chilled microfuge tubes. Lysis buffer (1 mL) was added to the

tissue fragments after the liquid nitrogen had completely evaporated from the microfuge tubes. The lysate was further homogenised using a 22G needle and syringe and kept on ice for a further 60 minutes. All lysates were then centrifuged at 14000 rpm (20 817 *g*) for 5 minutes at 4°C. Following centrifugation, the protein-rich supernatant was transferred to sterile pre-chilled microfuge tubes and stored at -20°C.

2.4.2.2 Quantification of protein

Extracted proteins were quantitated using a Coomassie® Protein Assay Reagent Kit (Pierce Biotechnology, Perbio Science UK Ltd, Tattenhall, UK). Protein standards and test samples were diluted 5-fold using lysis buffer solution (diluted 5-fold) as the diluent. The dilute lysis buffer solution was prepared by a 5-fold dilution: these dilutions were necessary as high SDS concentrations interfere with the assay. Five µL of lysis buffer diluent ('blank'), BSA protein standards and test samples were pipetted into individual wells (in a 96-well microplate) containing 250 µL Coomassie reagent and mixed by shaking for 30 seconds. The plate was incubated at room temperature for 10 minutes, and the absorbance of the diluent, BSA standards and samples measured at 595 nm. A standard curve was derived by plotting the absorbance readings obtained from BSA standards against absorbance at 595 nm (Figure 2.4), which was used to determine the protein concentrations in the test samples.

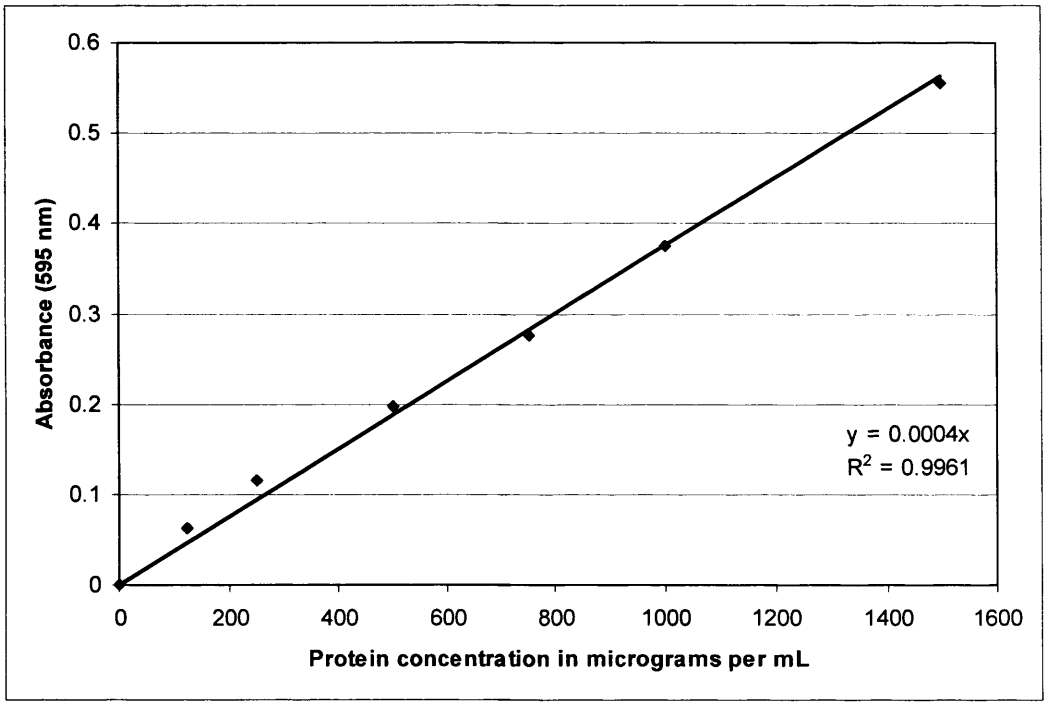

Figure 2.4. Standard curve to determine protein concentrations using spectrophotometry.

2.4.2.3 Preparation of the gels

The sample proteins were resolved using SDS-polyacrylamide (SDS-PAGE) gel electrophoresis, according to the method described by Laemmli (1970). Protein electrophoresis was performed using the Mini-PROTEAN® 3 Cell tank (BioRad Laboratories Ltd, Hemel Hempstead, UK). After assembling a glass cassette in the casting stand, an 8% separating gel was cast to a level approximately 1 cm below the comb teeth. 250 μL of isopropanol was carefully poured on top of the separating gel to degas and level the top edge of the gel. After the separating gel had set, the isopropanol was removed from the glass cassette and the area above the polymerised gel was thoroughly washed with distilled water and dried using tissue paper. An 8% stacking gel was cast above the separating gel and allowed to set with a moulding comb in place. After gently removing the comb from the polymerised gel, the wells were washed with running buffer. The glass cassette was removed from the casting stand and placed in the electrode assembly; this assembly was then placed into the clamping frame thus forming the inner chamber assembly. The inner chamber was filled with 125 mL running buffer and transferred to a tank that was prefilled with 200 mL running buffer. At this stage, the protein samples, each containing 15 μg protein, were mixed with an equal

volume of 2X sample buffer in a microfuge tube, heated at 95 °C for 5 minutes and allowed to cool to room temperature. The protein samples were then carefully loaded into the wells using a pipette. Electrophoretic separation was performed at 100 V for approximately 90 minutes, or when the protein standard ladder dye front was visible near the bottom of the resolving gel.

After completion of the electrophoretic separation, the gel was carefully removed from the glass cassette and equilibrated in blotting buffer for 10 minutes. A piece of polyvinylidene difluoride (PVDF) membrane (Hybond™ P membrane, Amersham Biosciences UK Limited, Little Chalfont, UK), cut to match the size of the gel, was briefly soaked in 100% methanol for 10 seconds, and then soaked in distilled water for 5 minutes, and equilibrated in blotting buffer for 10 minutes. Protein transfer from the gel to the PVDF membrane was performed using a semi-dry electrophorectic transfer cell (Trans-Blot® SD blotter, BioRad Laboratories Ltd, Hemel Hempstead, UK). The gel and PVDF membrane were sandwiched between saturated sheets of buffer-soaked filter paper (also cut to match the size of the gel and PVDF membrane) in the following way. Pre-soaked filter paper was gently layered onto the platinum anode. The PVDF membrane was placed over the filter papers and rolled with a glass rod to extrude air bubbles. The gel was placed on top of the PVDF membrane, and a glass rod was rolled over the surface of the gel to extrude air bubbles. Pre-soaked filter paper was carefully layer onto the gel, and rolled with a glass rod to extrude air bubbles. The cathode plate was placed over the gel- PVDF membrane-filter paper assembly and the protein was transferred from the gel to the membrane at 20 V for 90 minutes.

Following transfer of protein, the membrane was carefully removed from the gel and soaked overnight, at 4°C, in blocking buffer (5% w/v non-fat dried milk in TPBS). The gel was Coomassie-stained to confirm that protein transfer had occurred.

The membrane was then washed, three times, in PBS-Tween solution (0.01%). The membrane was incubated in a solution containing the primary antibody (either Polyclonal Rabbit Anti-Human Lysozyme or NOD2) in 10% goat serum in

PBS-Tween for 90 minutes on a shaking mechanical platform. The final concentrations of the primary antibodies were as follows: lysozyme 35.5 μg/mL, NOD2 2.15 μg/mL. Thereafter the membrane was thrice washed in PBS-Tween solution and incubated for 60 minutes in 15 mL 10% goat serum in PBS-Tween containing the secondary antibody at 1:10 000 dilution. For the lysozyme immunoblotting, a peroxidase labelled anti-rabbit antibody was used whereas a peroxidase labelled anti-mouse antibody was used for NOD2 immunoblotting. The membrane was thrice washed in PBS-Tween and placed on filter paper to remove the excess PBS-Tween. Next, the entire membrane surface was covered with 2 mL of ECL reagent, which was left on the membrane for 1 minute. The excess ECL fluid was drained from the membrane using filter paper, and the membrane was wrapped in Clingfilm and placed in an X-ray cassette. The membrane was exposed to Kodak ® Biomax XAR Scientific Imaging film (Anachem) for 20 seconds and developed.

2.4.3 Immunohistochemistry

Reagents:

1. Xylene
2. Ethanol (100%, 95%, and 70% solutions)
3. DEPC-treated water
4. PBS
5. 0.3% H_2O_2 in methanol
6. Blocking solution: 20% goat or horse serum in PBS
7. Biotinylated anti-rabbit and anti-mouse immunoglobulin antibody
8. ABC reagent
9. DAB/ 0.02% hydrogen peroxide
10. DPX mountant

Method:

Tissue sections, 8 microns thick, were cut from wax-embedded tissue blocks using a microtome. These sections were placed on clean glass slides, and allowed to air dry for 16 hours. To dewax the sections, the slides were thrice washed for 20 minutes in fresh xylene. The sections were rehydrated through a series of graded ethanol baths: twice in 100% ethanol for 5 minutes, then 95% ethanol for 5 minutes, then 70% ethanol for 5 minutes, and finally in DEPC-treated water for 5 minutes. After soaking the sections in PBS for 10 minutes, the slides were placed in 0.3% H_2O_2 in methanol for 30 minutes and rinsed in PBS. The slides were removed from the Schieferdecker jar and mounted on Shandon Coverplates™ (Thermo Electron), and placed in Sequenza slide racks (Thermo Electron). The sections were rinsed with PBS, and covered with 20% goat or horse serum in PBS (blocking solution) for 30 minutes. After rinsing in PBS, sections were incubated for 90 minutes with the primary antibody. The concentrations of primary antibodies are listed in Table 2.5. Sections were rinsed with PBS, incubated with a biotinylated anti-rabbit or anti-mouse immunoglobulin antibody (Vector Laboratories) in PBS containing 1% goat or horse serum, for 30 minutes, and then rinsed with PBS. Sections were incubated with ABC reagent for 30 minutes, rinsed with PBS, covered with a solution containing 0.7 mg/ml DAB and 0.02% hydrogen peroxide, and monitored for the development of brown precipitate.

Developed slides were rinsed in PBS to stop the reaction, counterstained with haematoxylin, and mounted under coverslips with DPX. Separate controls sections were incubated without the primary antibody and with an unrelated primary antibody.

2.4.4 Cytospins for CD68 immunocytochemistry

Reagents:

Shandon pre-made cuvettes Cat n° 5991040 (box of 50).

Method:

For immunocytochemistry, cytospin cell preparation was used to create a monolayer of PBMC on poly-l-lysine-coated glass slides. PBMC, 5×10^4 cells suspended in 100 µL HBSS, were loaded into Shandon pre-made cuvettes (Thermo Electron) attached to glass slides. The cuvettes were spun at 1000 rpm for 3 minutes in a Shandon Cytospin 3 cytocentrifuge (Thermo Electron). The glass slides, which were carefully separated from the cuvettes, were air dried for 1 minute, and fixed in 95% ethanol for 5 minutes at room temperature. The slides were stored at -20 °C. For immunocytochemistry, the slides were placed in a Schieferdecker jar and briefly warmed to room temperature for 10 minutes. The slides were fixed in acetone for 10 minutes, washed in PBS for 5 minutes, and incubated in PBS containing 0.3% H_2O_2 for 30 minutes. The slides were washed in PBS for 5 minutes, and mounted on Shandon Coverplates™ (Thermo Electron) and placed in Sequenza slide racks (Thermo Electron). The PBMC monolayer was rinsed with PBS, and covered with 20% horse serum in PBS (blocking solution) for 30 minutes. After rinsing in PBS, the PBMC monolayer was incubated for 90 minutes with monoclonal anti-human CD68 antibody. The slides were rinsed with PBS, incubated with a biotinylated anti-mouse immunoglobulin antibody (Vector Laboratories) in PBS containing 1% horse serum, for 30 minutes, and then rinsed with PBS. Sections were incubated with ABC reagent for 30 minutes, rinsed with PBS, covered with a solution containing 0.7 mg/ml DAB and 0.02% hydrogen peroxide, and monitored for the development of brown precipitate. Developed slides were rinsed in PBS to stop the reaction, counterstained with hematoxylin, and mounted under coverslips with DPX. Separate controls sections were incubated without the primary antibody.

Table 2.5. Primary and secondary antibodies used for immunohistochemistry

Primary antibody		Secondary antibody	
Description and supplier	Final concentration	Description	Final concentration
NOD2 (108 μg/ mL); anti-human rabbit polyclonal, Dr Gabriel Nunez, University of Michigan, USA	2.15 μg/mL in PBS containing 1% goat serum	Biotinylated anti-rabbit antibody (1.5 mg anti-IgG + 0.5 mg anti-IgM/ mL), made in goat	10 μg/ mL (7.5 μg mL anti-IgG + 2.5 μg anti-IgM/ mL) in PBS containing 1% goat serum
NOD2 (2D9; 100 μg/ mL); monoclonal anti-human NOD2, Dr Gabriel Nunez, University of Michigan, USA	2 μg/ mL in PBS containing 1% horse serum	Biotinylated anti-mouse antibody (1.5 mg anti-IgG + 0.5 mg anti-IgM/ mL), made in horse	10 μg/ mL (7.5 μg mL anti-IgG + 2.5 μg anti-IgM/ mL) in PBS containing 1% horse serum
monoclonal anti-human CD68 antibody (15.5 mg/ mL) (Clone PG-M1; DakoCytomation, Ely, Cambridgeshire, UK)	62 μg/ mL in PBS containing 1% horse serum in.	Biotinylated anti-mouse antibody (1.5 mg anti-IgG + 0.5 mg anti-IgM/ mL), made in horse	10 μg/ mL (7.5 μg mL anti-IgG + 2.5 μg anti-IgM/ mL) in PBS containing 1% horse serum
Lysozyme (7.1 mg/ mL); anti-human rabbit polyclonal antibody, DakoCytomation, Ely, Cambridgeshire, UK)	35.5 μg/ mL in PBS containing 1% goat serum	Biotinylated anti-rabbit antibody (1.5 mg anti-IgG + 0.5 mg anti-IgM/ mL), made in goat	10 μg/ mL (7.5 μg mL anti-IgG + 2.5 μg anti-IgM/ mL) in PBS containing 1% goat serum
sPLA_2 (2.5 mg/ mL); anti-human rabbit polyclonal antibody (Dr T Nevalainen, Department of Pathology, University of Turku, Finland)	25 μg/ mL in PBS containing 1% goat serum	Biotinylated anti-rabbit antibody (1.5 mg anti-IgG + 0.5 mg anti-IgM/ mL), made in goat	10 μg/ mL (7.5 μg mL anti-IgG + 2.5 μg anti-IgM/ mL) in PBS containing 1% goat serum

2.5 Cell culture

2.5.1 Isolation of peripheral blood mononuclear cells (PBMC)

Reagents:

1. Histopaque® 1077: A solution containing polysucrose and sodium diatrizoate, adjusted to a density of 1.077 g/mL.
2. Hanks' balanced salt solutions (HBSS)
3. Roswell Park Memorial Institute (RPMI)-1640 Medium
4. 10% pooled human AB serum
5. Phytohaemagglutinin PHA-P (Lectin from Phaseolus vulgaris)

Method:

Blood was collected from human healthy volunteers or from patients with polycythaemia, who were otherwise well, into anti-coagulant tubes containing K_3EDTA (BD Diagnostics). 25 mL whole blood was carefully layered onto 15 mL Histopaque® 1077 in a 50 mL-centrifuge tube, and centrifuged at 1400 rpm (409 *g*) for 20 minutes at room temperature. Following centrifugation, mononuclear cells form a distinct layer at the plasma- Histopaque® interface, and neutrophils and red blood cells form a pellet at the tube base. The layer of mononuclear cells was carefully aspirated and placed in fresh 50 mL-centrifuge tubes. HBSS was added to adjust the final volume to 40 mL, and the tubes centrifuged at 1400 rpm (409 *g*) for 7 minutes at room temperature. After discarding the supernatant containing contaminating platelets, the PBMC pellet was suspended in 30 mL HBSS, and centrifuged at 1200 rpm (301 *g*) for 7 minutes at room temperature. This wash was repeated, twice more, to remove contaminating platelets. Following the final wash, the PBMC were suspended in RPMI-1640 medium and counted using an improved Neubauer counting chamber. The monocytes were seeded in T25 culture flasks, at a concentration of 10^5 cells/cm^2, and maintained in RPMI 1640 medium supplemented with 10% pooled human AB serum, 100U/ml penicillin and 1mg/ml streptomycin, at 37°C in a 95% air/ 5% CO2 atmosphere.

To determine the effect of *in vitro* culture on NOD2 expression, PBMC were incubated for 24, 48 and 72 hours, and recovered by aspiration and mechanical

scraping to ensure that both adherent and non-adherent cells were obtained. PBMC and cultured cells were cytocentrifuged onto slides, air-dried, fixed in 95% ethanol for 5 minutes, and stored at -20°C. Before immunodetection, slides were warmed to room temperature, fixed in acetone for 10 minutes, rinsed in PBS and placed in 0.3% H2O2 in methanol for 30 minutes, and rinsed again in PBS. Slides were stained with a monoclonal anti-human CD68 antibody (DakoCytomation), as described above. For RNA extraction, the recovered PBMC were lysed in Trizol® reagent.

2.5.2 Lymphokine preparation and cell stimulation

A lymphokine (soluble cytokines secreted by lymphocytes) preparation was obtained by stimulating PBMC with phytohaemagglutinin (PHA). PBMC, in RPMI 1640 medium supplemented with 10% pooled human AB serum, 100U/ml penicillin and 1mg/ml streptomycin (Sigma), were seeded at a concentration of 10^5 cells/cm^2 in T25 culture flasks and incubated at 37°C in a 95% air/ 5% CO2 atmosphere for 1 hour. The cells were stimulated with PHA (5 μg/ml) for 48 hours, and lymphocyte clumping was noted during microscopic examination of the cells. Thereafter, the supernatant was collected from the culture flasks and placed in sterile centrifuge tubes which were centrifuged at 1400 rpm for 5 minutes at 4 °C. The cell-free supernatant, containing lymphokine, was used to stimulate Caco-2 and HT-29 intestinal epithelial cells (at 50% confluence) *in vitro* for 48 hours. DMEM culture medium containing 50% lymphokine solution was used to stimulate the intestinal epithelial cells for 48 hours at 37 °C.

2.5.3 Cell culture

Reagents:

1. 100x Antibiotic antimycotic solution: 10 000 U penicillin, 10 mg streptomycin, and 25 μg amphotericin B per mL)
2. 10x Trypsin-EDTA solution: 5.0 g porcine trypsin, 2.0 g EDTA·4 Na in 0.9% NaCl; cell culture tested

3. Trypsin solution: 1 mL 10x Trypsin-EDTA solution and 9 ml Dulbecco PBS
4. Dulbecco PBS
5. Dulbecco's modified Eagle medium (DMEM)
6. DMEM/F12 medium
7. 10% foetal calf serum
8. 200 mM L-Glutamine
9. Caco-2 intestinal epithelial cells (ATCC Number HTB-37)
10. HT-29 intestinal epithelial cells (ATCC Number HTB-38)
11. SW480 intestinal epithelial cells (ATCC Number CCL-228)

Caco-2 and HT29 intestinal epithelial cells were obtained from Dr. K. Srai and Dr. C. Osborne (Departments of Medicine and Biochemistry, Royal Free and University College Medical School, London). These investigators had originally purchased the cells from LCG Promochem, the European distribution partner for American Type Culture Collection (ATCC) products. SW480 cells were purchased directly from LCG Promochem.

2.5.3.1 Propagation of intestinal epithelial cell lines

Human colon cancer cell lines Caco-2 and HT29 (American Type Culture Collection, Manassas, USA) were cultured in Dulbecco's modified Eagle medium (DMEM) supplemented with 10% foetal calf serum, 2mM L-Glutamine, 1 U/mL penicillin, 1 μg/mL streptomycin and 2.5 ng/mL amphotericin B, at 37°C in a 95% air/ 5% CO2 atmosphere. SW480 cells were cultured in DMEM/F12 medium supplemented with 10% foetal calf serum, 1 U/mL penicillin, 1 μg/ml streptomycin and 2.5 ng/mL amphotericin B, at 37°C in a 95% air/ 5% CO2 atmosphere. All reagents used for cell culture were purchased from Sigma Chemical Company, Poole, UK.

Cell lines were propagated after reaching 80-90% confluence in T75 flasks (usually after one week of culture). The growth medium was poured from the flask, and the cells were twice washed with 10 mL Dulbecco PBS. After pouring out the PBS, 5 mL of trypsin solution was added to the flask. After 1 minute,

approximately 4.5 mL of the trypsin solution was removed from the flask, and the flask was incubated at 37.0°C for 12 to 15 minutes. Following trypinisation, the cells were visualised under an inverted microscope to confirm cell detachment from the plastic walls of the flask. The detached cells were thoroughly suspended in 8 mL of appropriate culture medium. After calculating the cell count, using an improved Neubauer counting chamber, cells were seeded into fresh T75 culture flasks according to the following concentrations: 2-4 x 10^4 cells/ cm^2 for Caco-2 and HT-29 cells, and 10^4 cells/ cm^2 for SW480 cells. Fresh culture medium was added to the T75 flask so that cells were allowed to propagate in 10 mL growth medium; the growth medium was replenished twice weekly. All cell lines were checked and found to be free from mycoplasma infection by Ms Demetra Mavri (Research assistant, Centre for Hepatology, Royal Free and University College Medical School, London).

Table 2.6. Seeding concentrations used to propagate intestinal epithelial cells.

Cell type	Seeding concentration (cells/ cm^2)	Cell yield from trypsin-treated confluent cells cultured in T75 flasks
Caco-2	2-4 x 10^4	1-2 x 10^7
HT-29	2-4 x 10^4	2-3 x 10^7
SW480	1 x 10^4	2-3 x 10^7

2.6 Secretory Phospholipase Assay

Caco-2 intestinal epithelial cells express secretory phospholipase A2 Group IIA (sPLA$_2$), an antibacterial enzyme secreted by Paneth cells. There were no suitable commercially available antibodies to detect secreted sPLA$_2$ protein, and this assay was performed to detect sPLA$_2$ enzymatic activity in Caco-2 cell culture supernatants.

2.6.1 Enzymes

Porcine pancreas PLA$_2$ (Group IB) was obtained from the Sigma Chemical Company, Poole, UK. Human pancreatic PLA$_2$ is not commercially available, although the porcine enzyme is virtually identical in structure and activity (Kudo 1993). Duodenal secretions containing pancreatic PLA$_2$ were obtained from patients undergoing oesophagogastroduodenoscopy. Secretions were centrifuged to remove cellular debris and food particles, and the supernatants stored at -20°C. Ethical approval for the collection of duodenal secretions had been obtained from the Royal Free Hampstead NHS Trust local ethics committee.

Bee venom PLA$_2$ was obtained from Sigma Chemical Company. This enzyme is closely related to human pro-inflammatory sPLA$_2$, which is not available commercially and cannot be readily isolated from human clinical material. The circulating sPLA$_2$ in rabbit serum is also virtually identical to human pro-inflammatory sPLA$_2$, and was also used in the assays.

2.6.2 Enzyme assay

Pancreatic sPLA$_2$ (Group IB) preferentially hydrolyses phosphatidylethanolamine and phosphatidylserine (Kudo 2002), however, it also hydrolyses phosphatidylcholine in the presence of low concentrations of detergent such as deoxycholate (Hanasaki 1999, Kudo 1993). Furthermore, the digestion of phospholipids in the diet by pancreatic sPLA$_2$ (Group IB) occurs in the presence of bile acids in the digestive tract. I therefore performed the control enzyme assay using phosphatidylcholine micelles suspended in a solution containing deoxycholate.

Pro-inflammatory *s*PLA_2 (Group IIA) preferentially hydrolyses phospholipids substrates incorporated into bacterial cell membranes, although it is also active against micellar and vesicular substrates. It has no acyl-chain or polar head group preference.

Reagents:

1. Dipalmitoyl phosphatidylcholine stock solution: 120 mM dipalmitoyl L-α-phosphatidylcholine (1, 2-dipalmitoyl-sn-glycero-3-phosphocholine), [dissolved in chloroform: methanol 9:1(v/v)].
2. 1-palmitoyl-2-[1-^{14}C]palmitoyl L-3-phosphaditylcholine (925 kBq/ml, 1.85-2.29 GBq/mmol)
3. Chloroform: methanol 3:1 (v/v)
4. Glycine buffer: 20 mM glycine, pH 8.0; 6 mM sodium deoxycholate; 0.1% Triton X-100
5. 200 mM $CaCl_2$
6. 20 mM EDTA
7. Lipid extraction solution [Chloroform: methanol 1:1 (v/v)]
8. Hexane: diethyl ether: acetic acid 90:20:10 (v/v/v)
9. Ecoscint A scintillation fluid

2.6.2.1 Preparation of the dipalmitoyl phosphatidylcholine substrate solution

6 μmoles dipalmitoyl L-α-phosphatidylcholine (final concentration 12mM), and 10 nmoles 1-palmitoyl-2-[1-^{14}C]palmitoyl L-3-phosphaditylcholine was dissolved in chloroform: methanol 3:1. Dipalmitoyl phosphatidylcholine substrate solution was prepared as follows:

50 μl dipalmitoyl phosphatidylcholine stock solution

22 μl 1-palmitoyl-2-[1-^{14}C] palmitoyl phosphatidylcholine

438 μl chloroform: methanol 3:1

Substrate solutions were dried at 40°C under a stream of nitrogen, and the residue reconstituted in 1000 µl glycine buffer, heated to 60°C for 2 minutes and cooled. After cooling, 20 µl $CaCl_2$ (200 mM) was added to the reconstituted substrate, until a clear solution was obtained.

2.6.2.2 Enzymatic hydrolysis of substrate

50 µl of the enzyme solution (duodenal juice/serum/commercial enzyme/cell culture supernatant) was added to 100 µl substrate solution and incubated at 37°C for 1 hour. The enzyme reaction was stopped by adding 150 µl EDTA (20 mM) to the reaction mixture. Commercial enzyme solutions contained 400 U/ml bee venom *s*PLA_2 and 1330 U/ml porcine pancreas *s*PLA_2.

2.6.2.3 Extraction of hydrolysis products

300 µl of the enzyme reaction mixture was added to 4ml chloroform: methanol 1:1 (v/v) in flat-bottomed glass tubes. Thereafter 1.2 ml distilled water was added to the lipid extraction solution and mixed well. After phase separation by centrifugation, 1 ml of the organic phase was dried at 40°C under a stream of nitrogen, redissolved in 30 µl chloroform and placed on glass-backed TLC plates.

2.6.2.4 Thin Layer Chromatography (TLC)

Glass-backed TLC plates were placed in solvent chambers containing hexane: diethyl ether: acetic acid 90:20:10 (v/v/v). Relevant fractions scrapped from the TLC plates were placed in scintillation vials containing 8 ml Ecoscint A fluid and radioactivity counts measured in an automated scintillation counter.

2.7 Statistical analysis

Values in the text and figures are expressed as the mean ± S.E.M. (Standard error of the mean). Statistical differences between means were determined using Student's t-test and considered significant if $P<0.05$. All analyses were performed using GraphPad Prism version 3.02 (25 April 2000).

Chapter Three

3. Localisation of NOD2 gene expression in Crohn's disease

3.1 Introduction

Crohn's disease is a chronic inflammatory disease that can affect the entire gastrointestinal tract although the terminal ileum, colon or anorectum are most commonly affected. Many studies, however, have shown that in NOD2-associated Crohn's disease, the terminal ileum is most commonly affected region although the reason for this association is unclear (Ahmad 2002, Cuthbert 2002, Lesage 2002).

NOD2, an intracellular protein that is postulated to function as a pathogen recognition receptor (PAMP) and play a role in innate defences, is mainly expressed in circulating monocytes that are ubiquitously distributed throughout the body (Ogura 2001a). Monocytes, which are key elements of the innate defences, can respond to pathogens irrespective of the site of infection. There is therefore no satisfactory explanation to account for the disease localisation, i.e. terminal ileitis that is a feature of NOD2-related Crohn's disease, and NOD2 expression has not been analysed in intestinal tissue from patients. It is possible therefore, that NOD2 may also be expressed in other cells involved in innate defences, including specialised intestinal epithelial cells, such as Paneth cells.

In mice, Paneth cells secrete antimicrobial peptides in response to stimulation by bacterial antigens, including the bacterial antigen muramyl dipeptide (MDP) (Ayabe 2000). In addition, these cells are most numerous in the terminal ileum and also express pro-inflammatory molecules such as secretory phospholipase A_2 Group IIA (sPLA$_2$) and TNFα and may play a role in intestinal inflammation (Porter 2002). I therefore hypothesised that NOD2 is also expressed in Paneth cells, and analysed NOD2 expression in intestinal tissue.

To test this hypothesis, I used reverse transcriptase PCR (RT-PCR) and immunoblotting to determine whether NOD2 mRNA and protein expression is detected in intestinal tissue. Then, I used *in situ* hybridisation and immunohistochemistry to detect the cellular sources of NOD2 expression in terminal ileal tissue obtained from patients with Crohn's disease and in histologically normal terminal ileal sections obtained from patients with colorectal cancer. In addition, I also determined whether metaplastic Paneth cells, which are found in inflamed colonic tissue, expressed NOD2.

3.2 Results

3.2.1 Reverse transcriptase polymerase chain reaction (RT-PCR) amplification of NOD2 mRNA in intestinal tissue and peripheral blood mononuclear cells

To determine whether NOD2 is expressed in intestinal tissue, I used RT-PCR to amplify NOD2 and human alpha defensin 6 (HD6) sequences in terminal ileal tissue and PBMC. Using reverse transcriptase PCR (RT-PCR), NOD2 mRNA could not be amplified in the terminal ileum, where Paneth cells are most abundantly found although NOD2 mRNA expression was more readily detected in peripheral blood mononuclear cells. Expression of a house-keeping gene, GAPDH, was easily detected in terminal ileal tissue and PMBC, and expression of HD6 was detected in terminal ileal tissue (Figure 3.1).

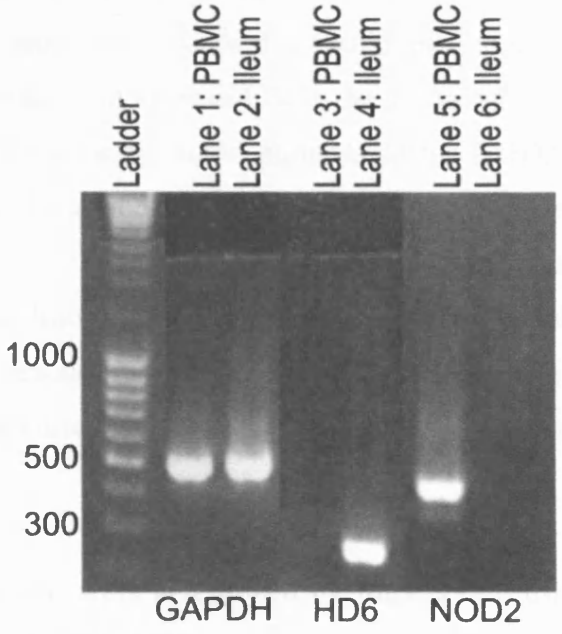

Figure 3.1. NOD2 and HD6 mRNA expression in terminal ileum and PBMC. *Using RT-PCR, NOD2 mRNA is detected in PBMC (Lane 5), but not in the terminal ileum (Lane 6). GAPDH mRNA is amplified in both tissues (Lanes 1 and 2), and HD-6 mRNA is easily amplified in terminal ileal tissue (Lane 4) but not in PBMC (Lane 3). PCR products were separated using agarose gel electrophoresis and visualised using ethidium bromide staining. The expected PCR amplicon size (in base pairs) was used to confirm the identity of the PCR products: GAPDH 488; HD6 241; NOD2 402.*

The lack of NOD2 expression in intestinal tissue by the RT-PCR assay I used, which is a sensitive method for detecting gene expression, was surprising as terminal ileal tissue sections contain tissue macrophages and, most probably, circulating monocytes in the intestinal blood vessels. RNA degradation in the resected terminal ileal tissue specimens may account for the lack of NOD2 amplification, but GAPDH and HD6 mRNA were easily detected by RT-PCR. These genes, however, are abundantly expressed in intestinal tissues and it is possible that NOD2 is not abundantly expressed. I hypothesised, therefore, that the dynamic range of the RT-PCR reaction used did not permit detection of low copy numbers of NOD2 mRNA. Therefore, I used quantitative real-time RT-PCT to determine the minimum number of NOD2 molecules that could be amplified by RT-PCR to determine the sensitivity of this technique.

Using RT-PCR, NOD2 cDNA sequences were amplified from PBMC-derived cDNA. These sequences, visualised by ethidium bromide staining after agarose gel electrophoresis, were extracted from the gel using a commercial kit and then quantitated by fluorometry. Serial dilutions of the NOD2 cDNA were prepared, which were then amplified by real-time PCR to determine the minimum number of NOD2 molecules that could be amplified using the present PCR amplification conditions. In addition, the starting concentration of NOD2 cDNA used in the real-time PCR reactions were correlated with the cycle number where linear amplification occurred in order to gauge the accuracy of real-time PCR quantitation.

DNA concentrations were determined by fluorometry using the fluorescent dye bisBenzimide (Hoechst 33258) as described in section 2.1.10 of Chapter 2. 2 μL of each dilution solution were then amplified by real-time PCR in a 20 μL reaction volume, using intron-spanning NOD2 primers. This analysis showed that at least 1.62×10^3 NOD2 molecules are required in a 20 μL reaction volume for successful amplification by PCR, so that the amplification products could be reliably identified by melt curve analysis and visualised by ethidium bromide staining after electrophoretic separation on an agarose gel (Figure 3.2).

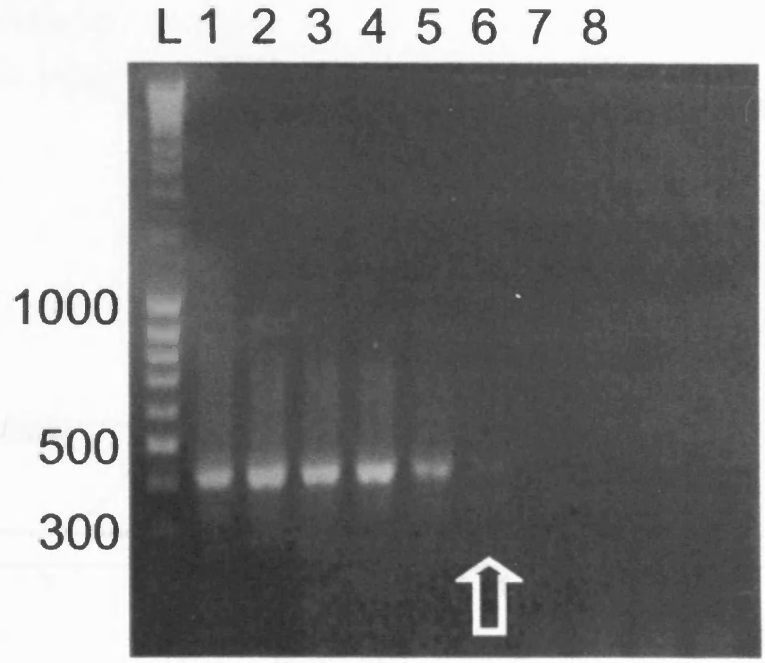

Figure 3.2. Visualisation of NOD2 amplicons by ethidium bromide staining. *Using quantitative real-time RT-PCR, approximately 1.62 × 10^3 NOD2 molecules (Lane 6) are required to be present in a 20 μL reaction volume for successful visualisation by ethidium bromide staining on an agarose gel (arrow). PCR products were separated using agarose gel electrophoresis and visualised using ethidium bromide staining. The expected PCR amplicon size (in base pairs) was used to confirm the identity of the PCR products: NOD2 402. (L: ladder)*

These PCR reactions were also analysed to assess the accuracy of the real-time PCR reactions by comparing the starting concentration of NOD2 cDNA molecules with the cycle number where linear amplification occurred. This take-off value, or C_T value, denotes the starting cycle at which product fluorescence is detectable and can be directly related to the starting copy number of the sample (Figure 3.3). A standard curve, constructed by plotting the C_T values against known concentrations of NOD2 cDNA (Figure 3.3), showed a strong correlation between the Ct value and starting concentration of NOD2 cDNA (r=0.99968).

A:

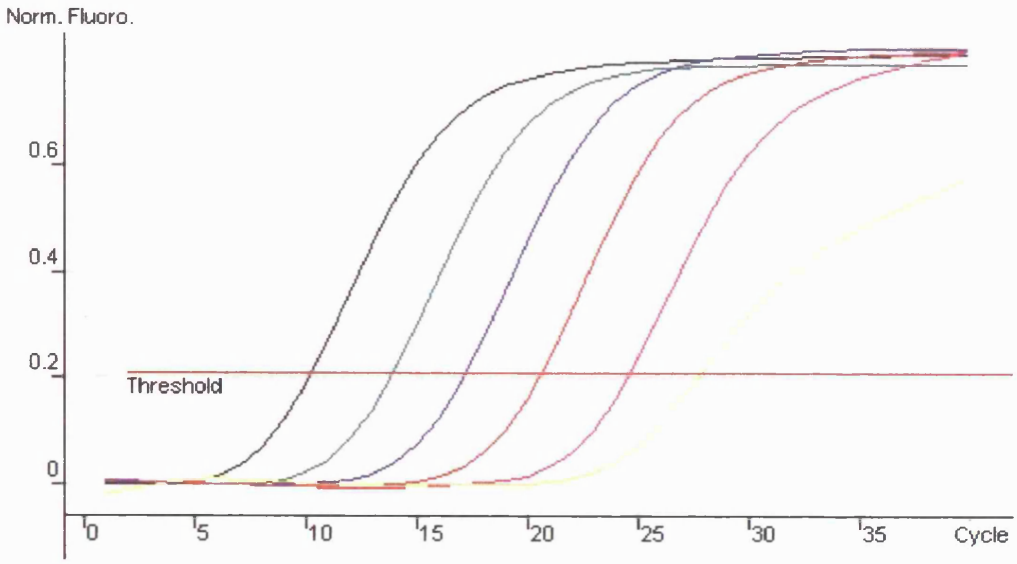

B:

Colour	Given Concentration (ng/μL)	Ct value
	3.29×10^{-1}	10.30
	3.29×10^{-2}	13.98
	3.29×10^{-3}	17.26
	3.29×10^{-4}	20.68
	3.29×10^{-5}	24.68
	3.29×10^{-6}	27.96

Figure 3.3. Real-time PCR analysis of NOD2 cDNA standards. *A: Background-corrected fluorescence data for NOD2 cDNA standards, ranging in concentration from 3.29 x 10^{-1} to 3.29 x 10^{-6} ng/μL, which show parallel curves passing a threshold (arbitrarily set within the exponential growth of fluorescence with respect to cycle number) at equally spaced intervals of approximately 3.5 cycles/10-fold change in concentration. B: Table showing the starting concentrations of NOD2 cDNA and corresponding Ct values, colour-matched to the fluorescence curves shown in A.*

These analyses verified the accuracy of real-time RT-PCR analysis to quantitate NOD2 gene expression, as the C_T value strongly correlated with the starting

cDNA concentrations (Figure 3.4). The accuracy of real-time PCR analysis using other primers, such as GAPDH, was also verified in this way.

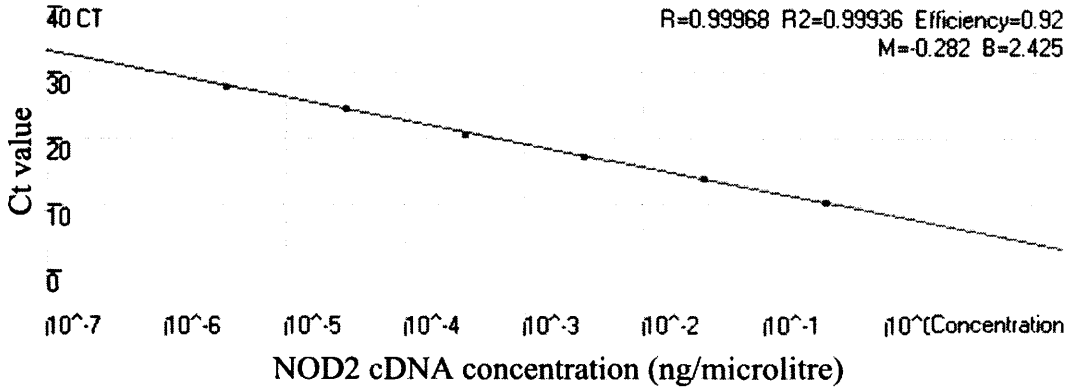

Figure 3.4. Standard curve of threshold cycle number (C_T) versus log concentration of NOD2 cDNA. *The line represents a best logarithmic fit to the data (cDNA concentration = $10^{(-0.282*CT + 2.425)}$; $r = 0.99968$, $r^2 = 0.99936$).*

For successful NOD2 detection by RT-PCR, at least 4 fg of the targeted NOD2 cDNA sequences are needed in each microlitre (μL) of the PCR reaction volume for successful amplification. This is the equivalent to approximately 81 molecules of NOD2 cDNA per μL of the reaction volume. The RT-PCR reaction mixtures containing PBMC cDNA contained at least 1.92×10^4 NOD2 cDNA molecules per μL, and NOD2 sequences were easily amplified. It is likely that the number of NOD2 molecules in terminal ileal cDNA preparations is considerably less, and that the lower limit of RT-PCR dynamic range is not sensitive for the detection of small copy numbers.

These results did not exclude the possibility that Paneth cells express NOD2, as the cDNA sequences synthesised from terminal ileal mRNA are derived from various cellular sources, and as Paneth cells constitute a small fraction of the total intestinal cell population. Low copy Paneth cell-mRNA sequences may therefore not be easily detected by RT-PCR. Therefore, I next determined whether NOD2 expression could be analysed using alternative methods such as immunoblotting, *in situ* hybridisation, and immunohistochemistry.

3.2.2 NOD2 protein detection in the terminal ileum and peripheral blood mononuclear cells by immunoblotting

The NOD2 protein was not detected in cellular lysates obtained from PBMC, inflamed and non-inflamed terminal ileal tissue, and colonic epithelium by immunoblotting. In contrast, lysozyme, which is abundantly produced by Paneth cells and PBMC, was easily detected in these samples by immunoblotting (Figure 3.5).

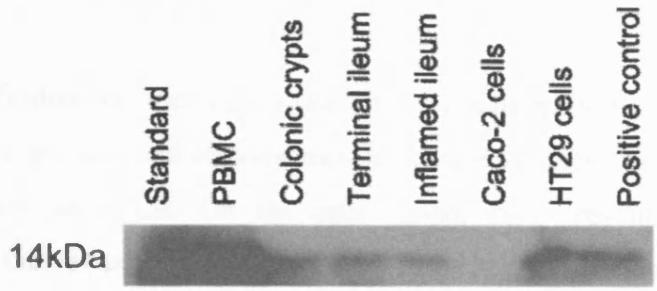

Figure 3.5. Lysozyme protein expression in PBMC, intestinal tissue and epithelial cell lines. *Lysozyme protein (14 kDa) is easily detected in cellular lysates obtained from PBMC, inflamed and non-inflamed terminal ileal tissue, colonic epithelium and HT29 intestinal cells. The protein is also detected in the standard sample, which contains hen egg lysozyme and the positive control (also terminal ileal tissue).*

Paneth cell-derived antimicrobial enzymes, such as HD6 and lysozyme, could be easily detected by RT-PCR or immunoblotting although NOD2 expression could not be detected. These results suggest that NOD2 is either absent in intestinal tissue or, more likely, expressed at low levels that do not permit detection by these techniques. Next, I used *in situ* hybridisation and immunohistochemistry, which are also sensitive techniques to detect mRNA and protein expression, to determine whether NOD2 is expressed in Paneth cells.

3.2.3 Determination of NOD2 mRNA expression in the terminal ileum by *in situ* hybridisation

3.2.3.1 Optimising tissue permeability for *in situ* hybridisation

In situ hybridisation (ISH) is a method of localising and detecting specific mRNA sequences in morphologically preserved tissues sections by hybridising the complimentary strand of a nucleotide probe to the sequence of interest. The sensitivity of the technique is such that threshold levels of detection are in the region of 10-20 copies of mRNA per cell (Harper 1986).

Standard hybridisation techniques require the electrophoretic separation of DNA or RNA on a gel, and subsequent transfer to membranes that are probed with a complimentary sequence. On the other hand, ISH presents a unique set of problems as the sequence to be detected will be at a lower concentration, may be masked because of associated proteins, or protected within a cell or cellular structure. To overcome this, tissues are treated with a protease, usually Proteinase K, to increase tissue permeability and the visibility of the nucleotide sequence to the probe without destroying the structural integrity of the cell or tissue. Prior tissue fixation is an important factor that governs the amount of digestion needed for adequate tissue permeabilisation, and initial experiments, to empirically determine the optimal Proteinase K concentrations, were performed on frozen sections that were fixed in paraformaldehyde. Thereafter, Proteinase K concentrations required for tissue permeabilisation were optimised for wax-embedded duodenal biopsies. These biopsies were fixed in formalin overnight, as the archived tissue blocks that would be used for subsequent ISH experiments would most likely have been fixed in this way in our histopathology department.

Previously, using ISH with radiolabelled probes, Chung (1988) and Keshav (1991) have demonstrated that Paneth cells express lysozyme mRNA abundantly. Based on these observations, I determined the concentrations of Proteinase K required for digestion of frozen and wax-embedded tissue sections that allowed lysozyme mRNA detection by digoxigenin-labelled probes. Thereafter, subsequent ISH would be performed using Proteinase K concentrations that

produced an intense lysozyme hybridisation signal whilst maintaining the integrity of the tissue section.

The following concentrations of Proteinase K were used to permeabilise frozen sections: 30, 60 and 90 μg/mL. Wax-embedded sections were treated with 20 and 40 μg/mL Proteinase K. All tissue sections were treated with Proteinase K for 15 minutes at 37.0°C.

For frozen sections hybridised with the lysozyme antisense riboprobe, positive signal was noted in those sections treated with 30, 60 and 90 μg/mL Proteinase K. Lysozyme mRNA staining was most intense in those sections treated with 60 μg/mL Proteinase K, compared with those sections treated with 30 and 90 μg/ mL Proteinase K. The tissue morphology was preserved in those sections treated with 30 and 60 μg/mL Proteinase K, although excessive tissue digestion was noted in sections treated with 90 μg/mL Proteinase K (Figure 3.6). For wax-embedded sections, lysozyme mRNA staining was most intense in sections treated with 40 μg/mL Proteinase K, with good preservation of tissue morphology (Figure 3.7). For all Proteinase K concentrations tested, parallel sections were treated with control lysozyme sense-strand riboprobes. These sections did not show positive staining, thus confirming the specificity of detection.

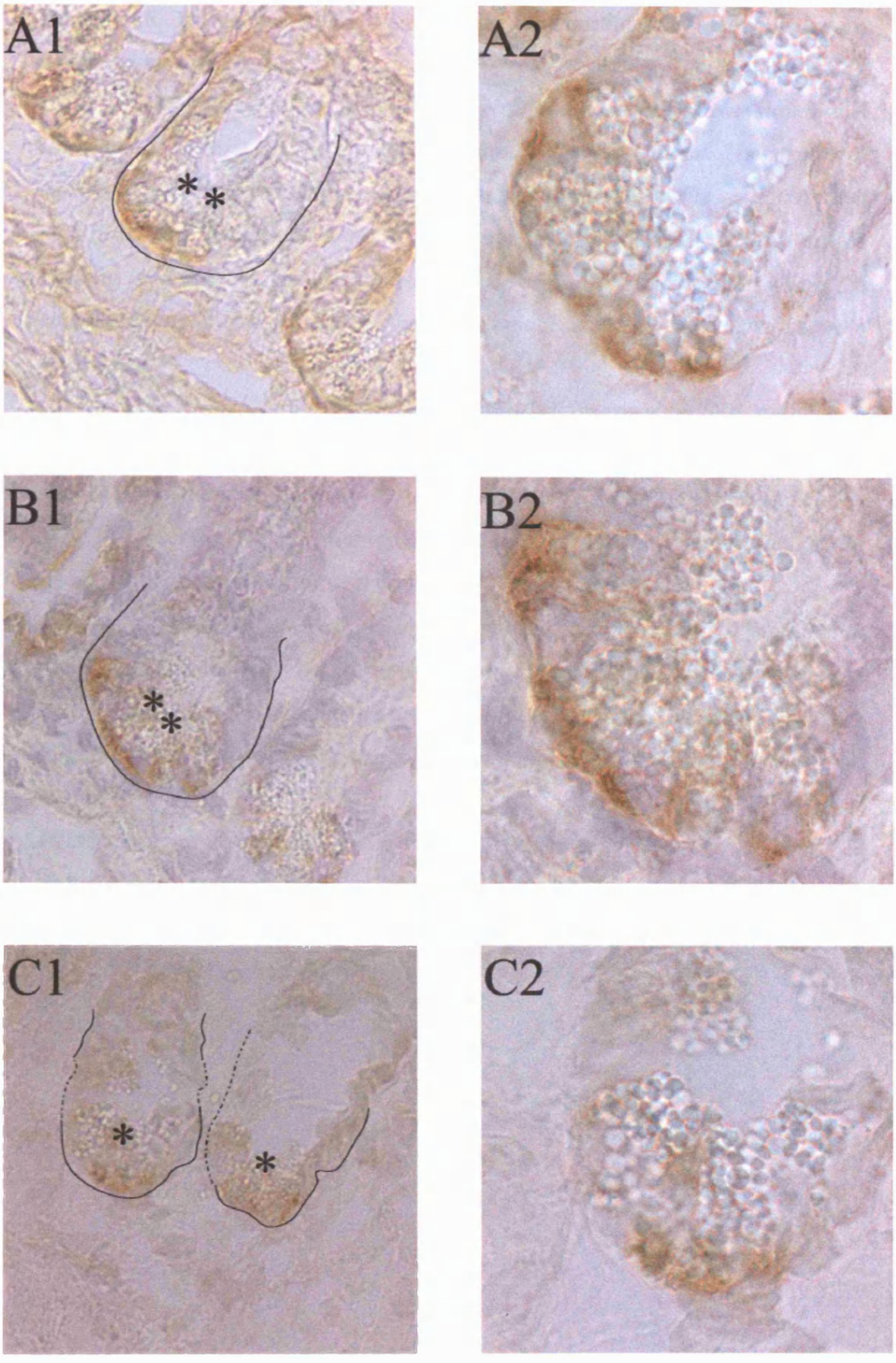
A1
A2
B1
B2
C1
C2

Figure 3.6. Lysozyme mRNA expression in Proteinase K-treated frozen duodenal sections (page 119).

(A1). In situ hybridisation demonstrates positive lysozyme mRNA staining in Paneth cells (asterisks) in histologically normal duodenal tissue. The structural morphology of the intestinal crypt (solid line) is preserved in this section treated with 30 μg/mL Proteinase K. At higher magnification (A2), the positive mRNA staining is located in the infranuclear nuclear region of Paneth cells, where the endoplasmic reticulum is located. Numerous apical secretory granules are seen in Paneth cells.

(B1). In situ hybridisation demonstrates positive lysozyme mRNA staining in Paneth cells (asterisks), with structural preservation of the intestinal crypt (solid line) in this section treated with 60 μg/mL Proteinase K. At higher magnification (B2), the lysozyme mRNA staining is more intense compared to section A (30 μg/mL Proteinase K) and section B (90 μg/mL Proteinase K.

(C1). In situ hybridisation demonstrates positive lysozyme mRNA staining in Paneth cells (asterisks), but the structural integrity of intestinal crypts (broken lines) are disrupted in this section treated with 90 μg/mL Proteinase K. At higher magnification (C2), the lysozyme mRNA staining is of a weaker intensity than section B2.

All sections were hybridised with the digoxigenin-labelled lysozyme antisense strand riboprobe, and viewed under the 40x objective (A1, B1 and C1), or the 100x objective (A2, B2 and C2).

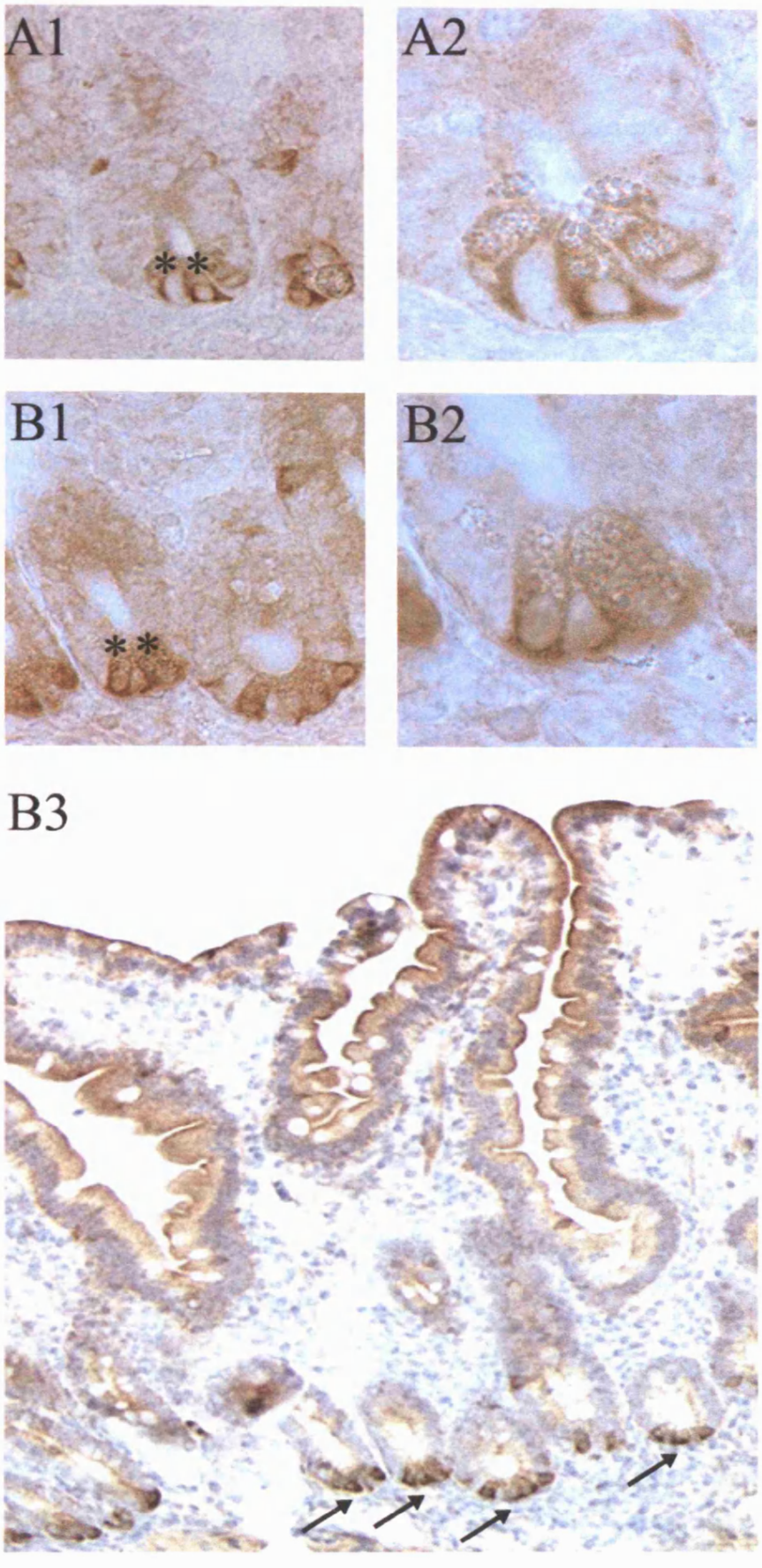
A1
A2
B1
B2
B3

Figure 3.7. Lysozyme mRNA expression in Proteinase K-treated wax-embedded duodenal sections (page 121).

(A1). In situ hybridisation demonstrates positive lysozyme mRNA staining in Paneth cells (asterisks) in histologically normal duodenal tissue. The structural morphology of the intestinal crypt is preserved in this section treated with 20 μg/mL Proteinase K. At higher magnification (A2), the positive mRNA staining is located in the infranuclear nuclear region of Paneth cells, and the overall cellular morphology is better preserved compared to frozen sections.

(B1). In situ hybridisation demonstrates positive lysozyme mRNA staining in Paneth cells (asterisks), with structural preservation of the intestinal crypt in this section treated with 40 μg/mL Proteinase K. At higher magnification (B2), the lysozyme mRNA staining is slightly more intense compared to section A. At lower magnification (B3), lysozyme mRNA staining is most prominent in Paneth cells in the intestinal crypts (arrows). The brown staining on the edges of the tissue section is an artefact: this stain, which is not intense, was very distinguishable from the intense mRNA staining in Paneth cells.

All sections were hybridised with the digoxigenin-labelled lysozyme antisense strand riboprobe, and viewed under the 10x objective (B3), 40x objective (A1 and B1) or the 100x objective (A2 and B2).

These results indicate that for tissues fixed in formalin overnight and embedded in paraffin-wax, tissue permeabilisation using 40 μg/mL Proteinase K is likely to produce strong intensity mRNA hybridisation signals with preservation of tissue morphology. Next, tissue sections from patients with Crohn's disease and controls were permeabilised with 40 μg/mL Proteinase K prior to hybridisation using digoxigen-labelled riboprobes to detect NOD2 mRNA expression.

3.2.3.2 NOD2 mRNA is expressed by Paneth cells and lamina propria leukocytes

To analyse NOD2 expression in intestinal tissue, I obtained archived tissue sections from eight patients with Crohn's disease and five patients with colorectal carcinoma from the Department of Histopathology at the Royal Free Hampstead

NHS Trust. Ethical permission for the use of this material was obtained from the local ethics committee.

In Crohn's disease-affected terminal ileum tissue sections hybridised with the digoxigenin-labelled antisense riboprobes, NOD2 mRNA was clearly detected in intestinal epithelial cells and lamina propria leukocytes by *in situ* hybridisation. Specifically, NOD2 mRNA was localised to epithelial cells located at the bases of the crypts of Lieberkühn. These cells contained a large number of secretory granules in their apical cytoplasm and were morphologically typical of Paneth cells (Figure 3.8). In adjacent sections, the NOD2 expressing cells also stained positively for secretory phospholipase A_2 Group IIA (sPLA$_2$) and lysozyme mRNA that are highly restricted markers of Paneth cells *in vivo* (Keshav 1991, Keshav 1997), which further confirmed their identity. NOD2 mRNA staining in Paneth cells was most apparent in Crohn's disease-affected terminal ileum, although a weaker signal could be detected in histologically normal terminal ileum, both from patients with Crohn's disease and those without IBD.

Ulcer associated cell lineages (UACL) are a feature of Crohn's disease, and represent newly regenerated epithelial cells. These cells stain positively for lysozyme mRNA, although NOD2 mRNA staining was not visible in these cells. Leukocytes infiltrating the lamina propria that stained for positively for NOD2 mRNA contained large bean-shaped nuclei and were morphologically typical of monocytes. These cells also stained positively for the CD68 antigen by immunostaining, thus confirming their identity as monocytes.

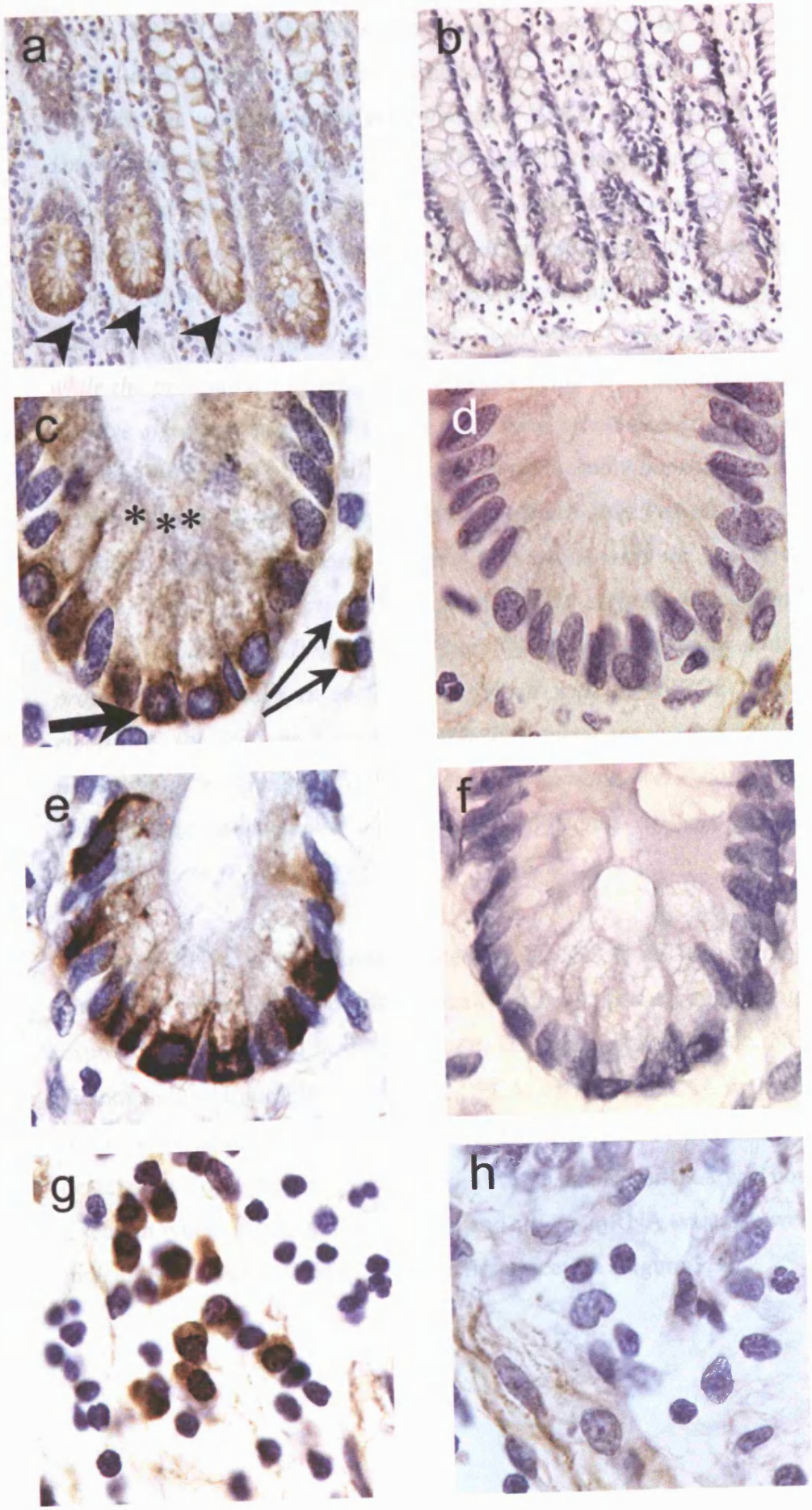
a
b
c
***
d
e
f
g
h

Figure 3.8. NOD2 mRNA is expressed by Paneth cells in small intestinal crypts and lamina propria mononuclear cells (page 124). *(a) In situ hybridization with the digoxigenin-labelled NOD2 antisense strand riboprobe demonstrates positive brown staining in small intestinal crypts (arrowheads) in Crohn's disease-affected terminal ileum. (b) Hybridization with the control sense strand riboprobe shows no signal, confirming specificity of detection. (c) Within crypts, positive staining is present mainly in the infra-nuclear region of Paneth cells (thick arrows), where mRNA and rough endoplasmic reticulum is localized, while the protein-rich granules in the apical cytoplasm (asterisks) are unstained. Positive signal is also noted in lamina propria mononuclear cells (thin arrows). (d) Sections hybridized with the control sense strand riboprobe show no positive staining. (e) NOD2-positive crypt cells are identified as Paneth cells by localizing lysozyme mRNA in adjacent sections hybridized with the lysozyme antisense strand riboprobe. (f) Sections hybridized with the control sense strand riboprobe show no staining. (g) Positive NOD2 mRNA staining is seen in scattered lamina propria mononuclear in sections hybridised with the NOD2 antisense strand riboprobe. (h) Sections hybridized with the control sense strand riboprobe show no staining in lamina propria cells. All sections were counterstained with haematoxylin, and viewed under the 20x objective (a) and (b), or the 100x objective (c) to (h).*

Although ISH is not a quantitative technique, NOD2 mRNA staining was more intense in inflamed than histologically normal tissue, suggesting that gene expression is increased in inflammation. Using an arbitrary scale, NOD2 mRNA did not stain as intensely as lysozyme, sPLA$_2$ or TNFα mRNA within Paneth cells in Crohn's disease-affected terminal ileal tissue (Figure 3.10). NOD2 mRNA was detected in 7 of 8 patients with Crohn's disease. NOD2 mRNA was not detected in a section where staining for lysozyme and sPLA$_2$ mRNA was also weak, possibly indicative of RNA degradation in this tissue section (Figure 3.9).

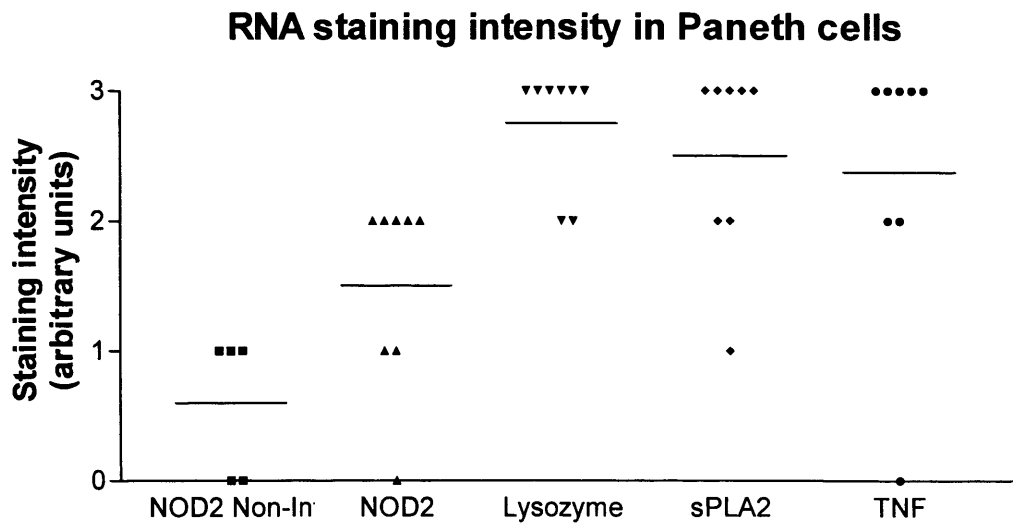

Figure 3.9. NOD2, lysozyme, $sPLA_2$, and TNFα mRNA staining intensity in Paneth cells. *Paneth cell NOD2, lysozyme, $sPLA_2$, and TNFα mRNA staining intensity were determined in parallel sections from 8 patients with Crohn's disease and compared to NOD2 mRNA staining in 5 control patients. The intensity of mRNA staining in Paneth cells was graded as follows: +: weak staining - staining confined to the infranuclear region of the cell; ++: moderate staining - staining extending beyond the infranuclear region of the cell, but not completely surrounding the nucleus; +++: strong staining - dense staining that completely surrounding the cell nucleus. (Non-In.: Non-inflamed tissue)*

3.2.4 NOD2 protein is expressed by Paneth cells and lamina propria leukocytes

To confirm NOD2 expression in Paneth cells, I used immunohistochemistry to detect NOD2 protein. In terminal ileal sections, the NOD2 protein was detected by immunohistochemical staining using a purified rabbit polyclonal antibody raised against the N-terminal CARD domains of a recombinant NOD2 protein. In Crohn's disease-affected terminal ileum sections, positive immunoreactivity was observed in Paneth cells in the crypt bases and in adjacent lamina propria mononuclear cells. NOD2 protein was also easily detected in Paneth cells in histologically normal small intestine, although expression in mononuclear cells was observed in inflamed tissue only. Within the gastrointestinal tract, NOD2 protein was expressed in duodenal, jejunal and terminal ileal sections, although the greatest staining was noted in the terminal ileal crypts where Paneth cells are most numerous. Immunohistochemistry with an unrelated rabbit antibody, and without primary antibody, gave no signal, confirming the specificity of detection (Figure 3.10).

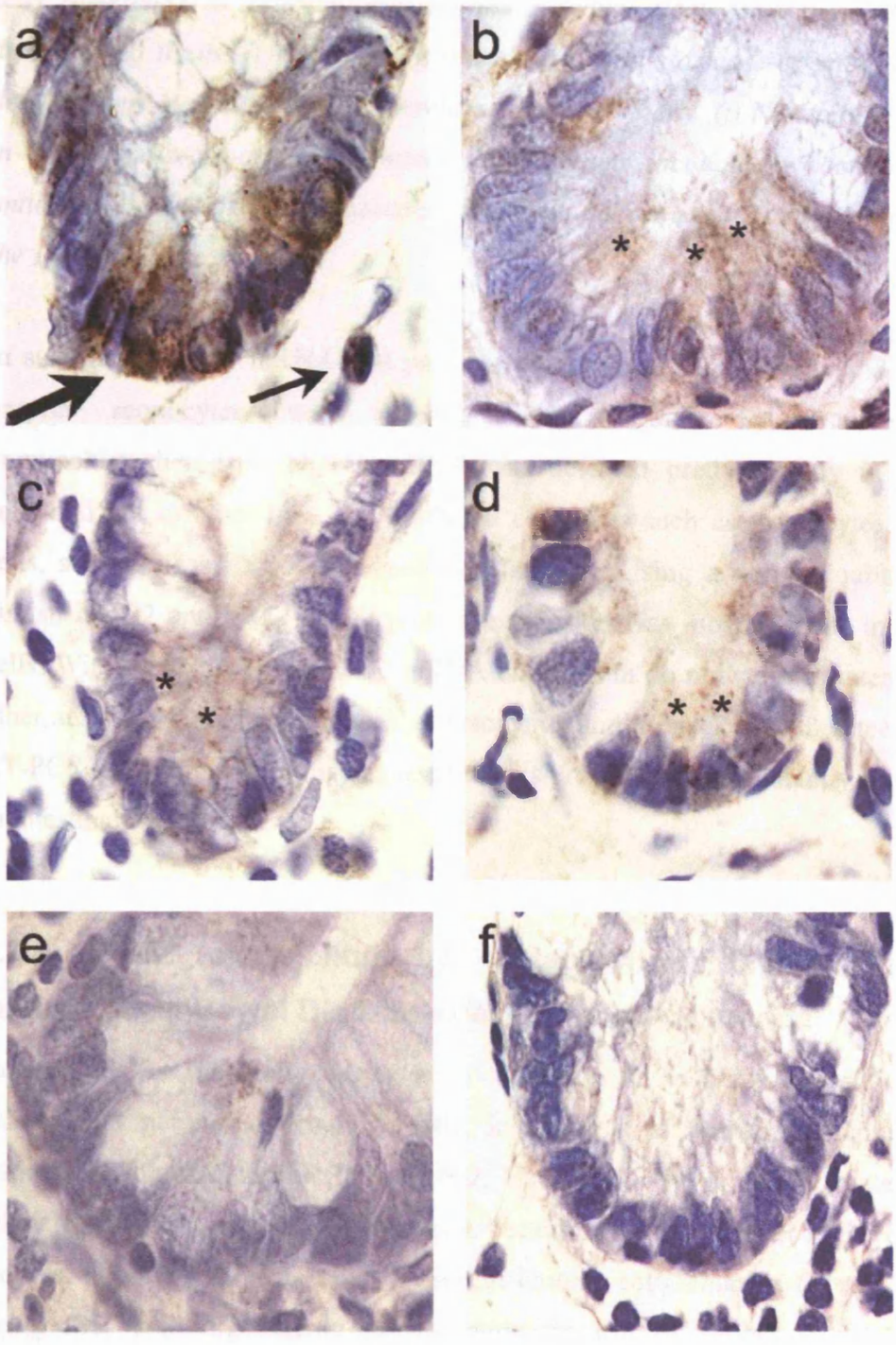

Figure 3.10. NOD2 protein is expressed by Paneth cells in small intestinal crypts. *(a) In Crohn's disease-affected terminal ileum, positive immunohistochemical staining, using a purified rabbit antibody raised against recombinant NOD2 protein, is seen in the basal and apical cytoplasm in Paneth cells (thick arrow) and in a monocyte in the lamina propria (thin arrow). (b-d) Positive immunohistochemical staining of a weaker intensity is seen in Paneth*

cells (asterisks) in histologically normal terminal ileal (b), jejunal (c) and duodenal (d) tissue. (e) No staining is seen in Crohn's disease-affected terminal ileal sections incubated with an unrelated rabbit antibody. (f) No staining is seen in Crohn's disease-affected terminal ileal sections incubated without primary antibody. All sections were counterstained with haematoxylin, and viewed under the 100x objective.

In summary, NOD2 mRNA and protein expression in Paneth cells and lamina propria monocytes was detected by *in situ* hybridisation and immunohistochemistry. NOD2 mRNA was detected predominantly in Paneth cells and not in other intestinal epithelial cell types such as enterocytes, goblet cells, stem cells or ulcer-associated cell lineages. Using a purified rabbit anti-human NOD2 antibody, NOD2 protein expression was most obvious in Paneth cells. Within Paneth cells, NOD2 mRNA and protein do not stain as intensely as other antimicrobial enzymes, such as lysozyme, and the lack NOD2 detection by RT-PCR and immunoblotting suggest that this protein is not abundantly expressed in intestinal tissue.

3.2.5 NOD2 expression by metaplastic Paneth cells in Inflammatory Bowel Disease-affected colonic mucosa

Paneth cells are generally absent from the colon in health; however, colonic Paneth cell metaplasia occurs in IBD, in which it is thought to represent a response to chronic injury (Porter 2002, Haapamaki 1997). These metaplastic cells are unlikely to initiate inflammation because they appear later in the disease process, although they may play a role in chronic inflammation (Porter 2002). Using ISH with digoxigenin-labelled antisense mRNA probes, I determined whether NOD2 was also expressed in metaplastic Paneth cells. I localised NOD2 mRNA to metaplastic Paneth cells in Crohn's disease-affected colonic crypt epithelium, as well as in ulcerative colitis-affected colon. The positive NOD2 ISH signal co-localised in adjacent sections with lysozyme mRNA, confirming the identity of metaplastic Paneth cells. The intensity of staining of metaplastic Paneth cells was comparable with that of Paneth cells in the inflamed terminal

ileum, although there were fewer Paneth cells in each crypt, and most crypts did not contain any detectable NOD2 mRNA or protein.

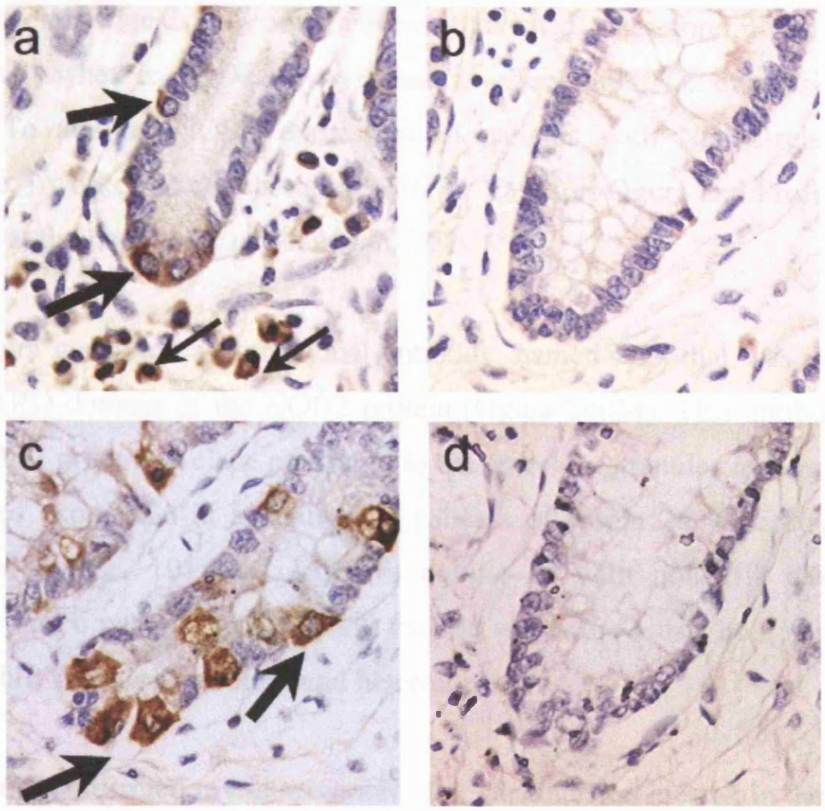

Figure 3.11. NOD2 mRNA is expressed by metaplastic Paneth cells in Crohn's disease-affected colonic mucosa. *(a) In situ hybridization with the digoxigenin-labelled NOD2 antisense strand riboprobe demonstrates positive brown staining in metaplastic Paneth cells (thick arrows) present in the crypt epithelium in Crohn's disease-affected colon, and a positive signal is also seen in lamina propria mononuclear cells (thin arrows). (b) Sections hybridized with the control sense strand riboprobe show no staining. (c) NOD2-positive colonic epithelial cells are identified as metaplastic Paneth cells (thick arrows) by localizing lysozyme mRNA in adjacent sections hybridized with the lysozyme antisense strand riboprobe. (d) Sections hybridized with the control sense strand riboprobe show no staining. Lysozyme mRNA is more abundantly expressed than NOD2 mRNA, and lysozyme mRNA staining is more intense. All sections were counterstained with haematoxylin, and viewed under the 40x objective.*

3.2.6 NOD2 protein expression in Crohn's disease-affected patients carrying the NOD2 mutations

The NOD2 genotype status of the cases that I used to demonstrate NOD2 expression in Paneth cells could not be established. Therefore, it was important to determine whether NOD2 genotype had an effect on NOD2 expression in Paneth cells. To analyse NOD2 expression in patients with NOD2-related Crohn's disease, I worked in collaboration with Dr Yasunori Ogura and Professor Gabriel Nunez at the University of Michigan, USA.

Dr Ogura generated a monoclonal antibody, named 2D9 that was raised against the CARD domain of the NOD2 protein (Ogura 2003a). This antibody localised the NOD2 protein in close proximity to the secretory granules in Paneth cells. We analysed expression in a total of 52 patients of whom 26 were diagnosed with Crohn's disease, 10 with ulcerative colitis, 10 with non-IBD gastrointestinal disease and 6 patients with Crohn's disease who were either homozygous for the frameshift mutation or compound heterozygotes.

This work confirmed my observations that Paneth cells, located in the normal and inflamed regions of terminal ileum, as well as metaplastic Paneth cells present in the colonic mucosa in patients with IBD express the NOD2 protein (Figure 3.12). NOD2 was expressed in Paneth cells irrespective of the NOD2 genotype. NOD2 expression in mononuclear cells was seen in inflamed tissue only.

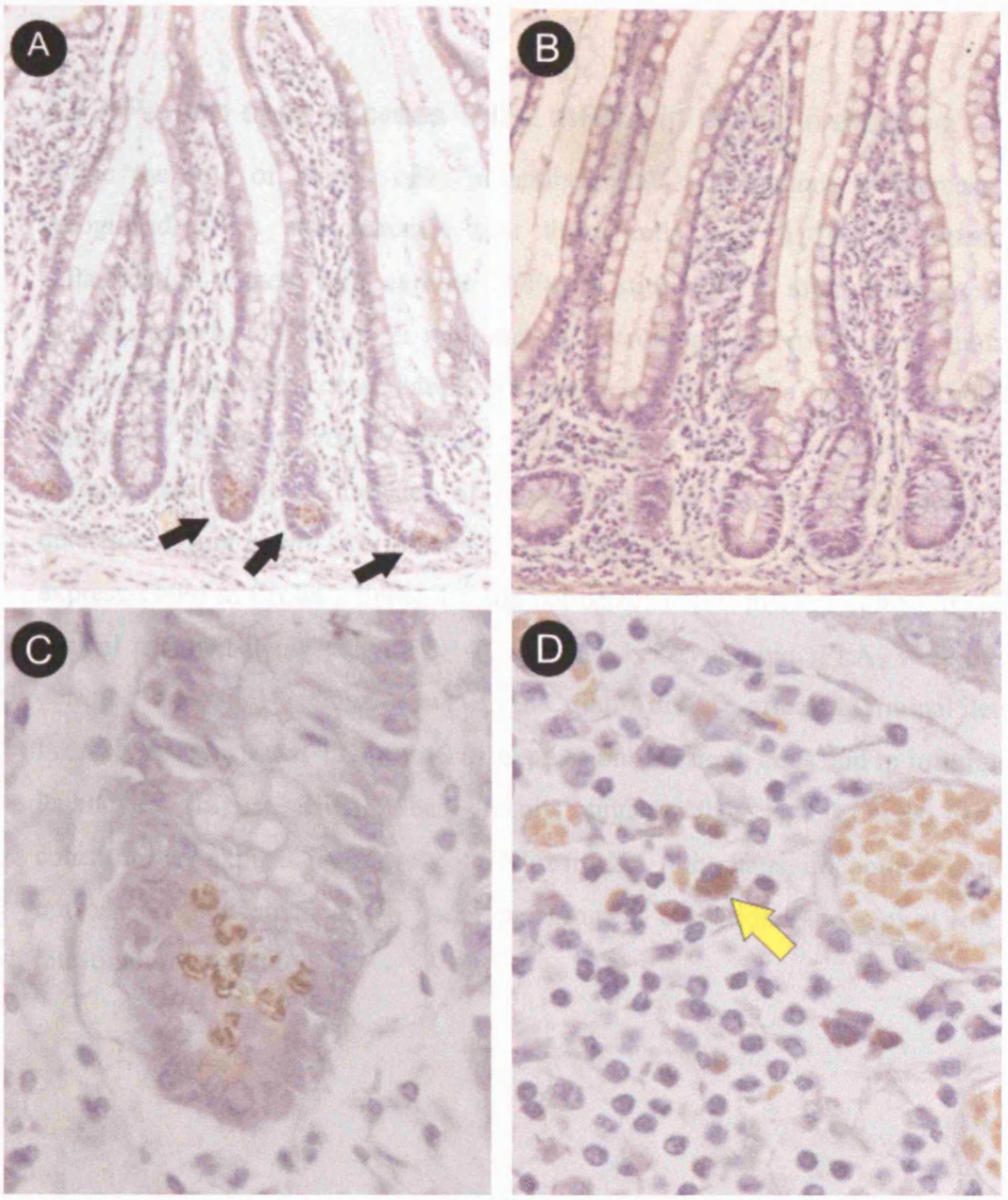

Figure 3.12. NOD2 protein expression in Crohn's disease. (A) *Using the monoclonal 2D9 antibody, NOD2 is protein is detected in Paneth cells in the intestinal crypts in Crohn's disease-affected terminal ileal section (arrows). (B) No staining is seen in Crohn's disease-affected terminal ileal sections incubated with no primary antibody. (C) NOD2 protein staining is prominent in the apical region of Paneth cells. (D) NOD2 protein is also detected by immunohistochemical staining within the cytoplasm of lamina propria mononuclear leukocytes (yellow arrow). All sections are counterstained with haematoxylin, and viewed under the 20x objective (A and B) or 100x objective (C and D).*

3.2.7 Paneth cells express TNFα mRNA in Crohn's disease

While the role of Paneth cells in antibacterial host defence is increasingly recognized, it is also possible that these cells play a role in intestinal inflammation. Paneth cells express TNFα constitutively in mice, in response to hypoxia-reperfusion injury in rats, and in necrotizing enterocolitis in humans. Despite the clinical success of anti-TNF treatment for Crohn's disease, the cellular sources of TNFα in Crohn's disease-affected tissue have so far remained poorly defined, partly due to the lack of suitable reagents for immunohistochemical detection. Using *in situ* hybridization, I therefore determined whether Paneth cells express TNFα in Crohn's ileitis. I could not detect TNFα mRNA in histologically normal terminal ileum (Figure 3.14), although lysozyme and sPLA$_2$ were easily detected in parallel sections. However, in Crohn's disease-affected terminal ileum, I readily demonstrated TNFα mRNA expression in Paneth cells and in infiltrating leukocytes (Figure 3.13). These results suggest that Paneth cells do not constitutively express high levels of TNFα mRNA in humans, in contrast to mice, but can be induced to do so under pathological conditions and play a role in intestinal inflammation.

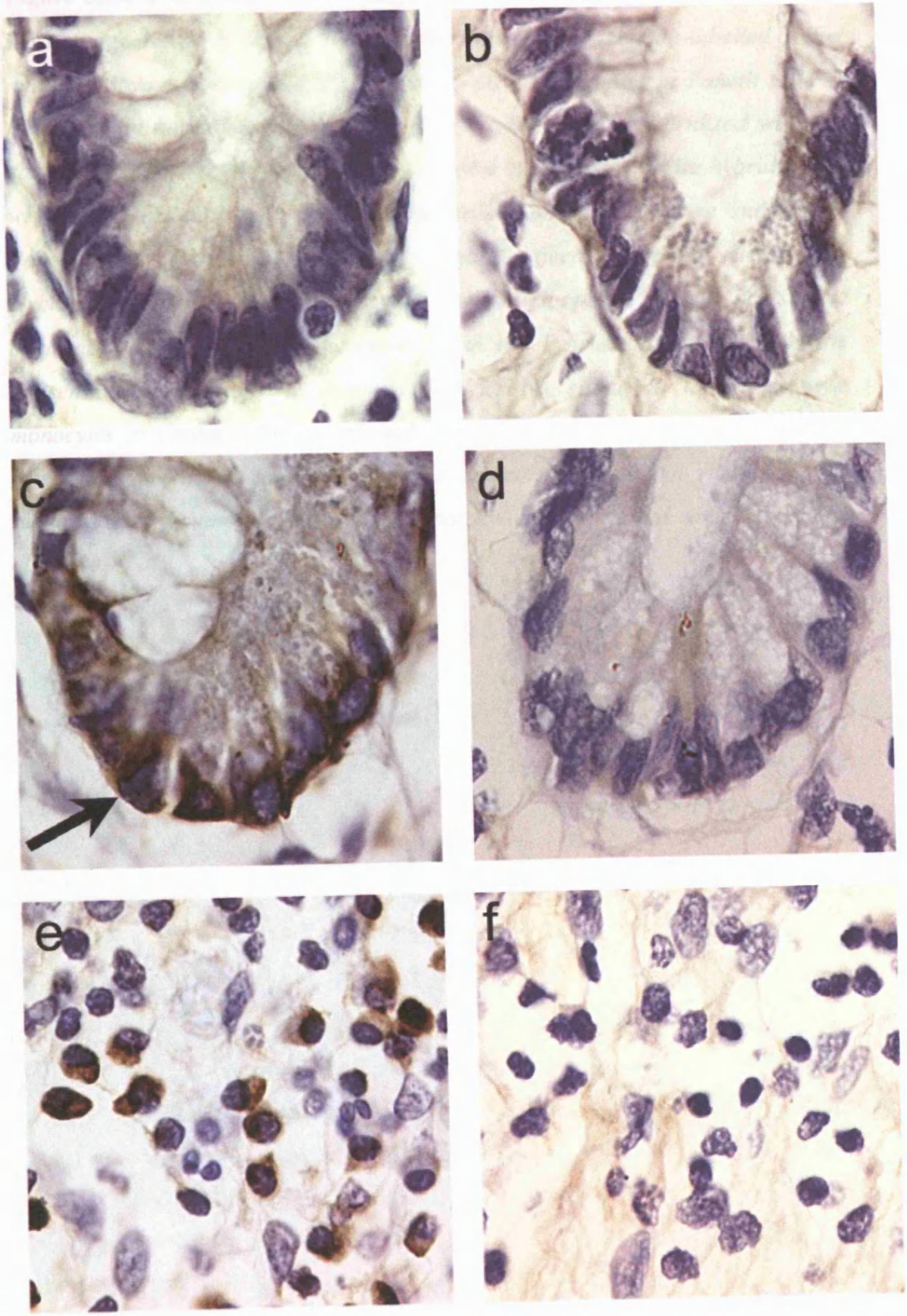
a
b
c
d
e
f

Figure 3.13. TNFα mRNA is strongly expressed in Paneth cells in Crohn's ileitis (page 134). *(a) In situ hybridization with the digoxigenin-labelled TNFα antisense strand riboprobe demonstrates no positive staining in Paneth cells in histologically normal terminal ileum. (b) Parallel sections hybridized with the control sense strand riboprobe show no positive staining. (c) In situ hybridization with the TNFα antisense strand riboprobe demonstrates positive staining in Paneth cells (arrowed) in Crohn's disease-affected terminal ileum. (d) Hybridization with the control sense strand riboprobe shows no signal, confirming the specificity of detection. (e) In situ hybridization with the TNFα antisense strand riboprobe demonstrates positive signal in lamina propria monocytes in Crohn's disease-affected terminal ileum. (f) No positive signal is detected in sections hybridized with the control sense strand riboprobe. All sections were counterstained with haematoxylin, and viewed under the 100x objective.*

3.3 Discussion

These results confirm my hypothesis, and show that Paneth cells, located at the base of the intestinal crypt, express NOD2. NOD2 expression was also demonstrated in mononuclear cells. I was able to demonstrate expression of NOD2 mRNA, using *in situ* hybridisation, and protein, using immunohistochemistry with both a purified rabbit polyclonal antibody and the 2D9 monoclonal antibody, in Paneth cells. In addition, metaplastic Paneth cells, present in IBD-affected colonic mucosa, also expressed NOD2.

My results also show that Paneth cells also express the pro-inflammatory cytokine TNFα, which is implicated in the pathogenesis of Crohn's disease. There is increasing evidence that Paneth cells are involved in intestinal inflammation. Paneth cell hyperplasia occurs in response to signals derived from activated T cells in models of enteric infection (Kamal 2001), and in IBD, Paneth cell metaplasia is seen in the colon. In mice, Paneth cells constitutively express TNFα mRNA that is apparently not translated into protein, probably because of regulation by the AU-rich element in the 3' untranslated region of the TNFα gene (Keshav 1990). Interestingly, deletion of this regulatory region in transgenic mice causes terminal ileitis, but not generalized intestinal inflammation, suggesting that local overproduction of TNFα, potentially in Paneth cells, is important (Kontoyiannis 1999).

These results, which analysed NOD2 expression in intestinal tissue is important as they have identified, for the first time, specific cells in the intestine that express NOD2. It is likely, therefore, that understanding the physiological role of NOD2 in these cells may yield insights into the pathophysiology of NOD2-related Crohn's disease. These results do not indicate the level of expression in these cells types as *in situ* hybridisation and immunohistochemistry are not quantitative techniques. Nonetheless, my results show that NOD2 mRNA and protein stains most intensely in Paneth cells, which may indicate a prominent role for these cells in the pathophysiology of Crohn's disease.

Berrebi and colleagues (2003), using immunohistochemistry and *in situ* hybridisation, also show that NOD2 is expressed in mononuclear cells and epithelial cells in inflamed colonic mucosa in patients with Crohn's disease. These investigators, however, did not analyse NOD2 expression in terminal ileal tissue, which is most commonly affected in patients with NOD2-related Crohn's disease. It is possible that the NOD2-expressing epithelial cells identified by these investigators may, speculatively, represent metaplastic Paneth cells (J-P Cezard, personal communication).

Although NOD2 expression in Paneth cells could be detected by *in situ* hybridisation and immunohistochemistry, I was surprised that NOD2 expression in terminal ileal tissue could not be detected by RT-PCR. A possible explanation for this discrepancy is that the dynamic ranges of PCR reactions are insensitive for the detection of low copy numbers of NOD2 mRNA molecules. The mRNA sequences that are extracted from terminal ileal tissue are derived from a variety of cellular sources, and as Paneth cells constitute a small fraction of the total intestinal cellular population, Paneth cell-mRNA sequences will be present in small quantities in terminal ileum-RNA extracts. Furthermore, RNA extracted from surgically resected tissue showed RNA degradation, as determined by UV transillumination of ethidium bromide-stained agarose gels, which may also account for the poor detection of NOD2 by PCR.

As far as I am aware, RT-PCR amplification of NOD2 in intestinal epithelial cells has only been demonstrated in intestinal epithelial cell lines (Gutierrez 2002) or in mechanically isolated epithelial cells (Hisamatsu 2003). In addition, NOD2 is not easily detected in terminal ileal tissue by immunoblotting. Rosenstiel and colleagues (2003) have successfully detected the NOD2 protein in intestinal biopsies by immunoblotting, and this experiment was technically very difficult to perform (Philip Rosenstiel, personal communication). Most other investigators have not detected NOD2 protein in intestinal tissue by immunoblotting and we, in collaboration with Professor G Nunez, could not detect NOD2 protein in isolated intestinal crypts, which are enriched with Paneth cells. Even after concentrating the crypt proteins by immunoprecipitation, I have been unable to detect NOD2 using either purified rabbit polyclonal or monoclonal 2D9 antibodies (Gabriel

Nunez, personal communication). Overall, these observations suggest that NOD2 is expressed at low levels in Paneth cells and its expression is difficult to detect in intestinal tissue.

Although conventional methods of mRNA and protein expression i.e. RT-PCR and immunoblotting suggest that NOD2 is not abundantly expressed in intestinal tissue, my results identify Paneth cells and mononuclear cells as the most prominent NOD2-expressing cells in intestinal tissue. These results may therefore indicate that Paneth cells and monocytes play an important role in the pathophysiology of NOD2 related-Crohn's disease.

In the next section, I determined the level of NOD2 gene expression in Paneth cells and peripheral blood mononuclear cells. Presently, there is no Paneth cell-like cell line and I therefore determined whether intestinal epithelial cell lines express NOD2 and also investigated whether NOD2 expression can be regulated in cell lines and PBMC.

Chapter four

4. Regulation of NOD2 gene expression by microbial and pro-inflammatory mediators

4.1 Introduction

Previously, in intestinal sections obtained from patients with Crohn's disease, I have shown that Paneth cells and lamina propria mononuclear cells express the NOD2 gene product. NOD2 expression was not only confined to Paneth cells present in the terminal ileum, where they are most numerous, but was also evident in metaplastic Paneth cells that are found in IBD-affected colonic tissue. Using non-quantitative techniques such as *in situ* hybridisation and immunohistochemistry, my observations extend the work of other studies that describe NOD2 expression in monocytes and myelomonocytic cells (Ogura 2001a, Gutierrez 2002). The purpose of this chapter was to investigate further the expression of NOD2 in Paneth cells and peripheral blood mononuclear cells (PBMC). Therefore, I quantitated NOD2 gene expression in Paneth cells that were obtained by laser capture microdissection from terminal ileal tissue sections. In addition, I quantitated NOD2 expression in intestinal epithelial cells obtained from surgically resected terminal ileal segments.

Within primary cells, NOD2 is most abundantly expressed in PBMC (Gutierrez 2002) although there are no reports quantitating NOD2 mRNA expression in primary epithelial cells. As NOD2 is most likely to be functionally important in those cells that express the gene at the highest levels, I therefore determined whether Paneth cells express the NOD2 gene at levels comparable to mononuclear cells. It is likely that NOD2 is likely to be expressed at low levels by epithelial cells and monocytes as expression in intestinal tissue is not easily detected by conventional techniques, such as RT-PCR and immunoblotting - NOD2 mRNA molecules are likely to be classified as scarce or intermediate, i.e. less than 300 molecules per cell (Alberts 1994). To facilitate quantitation, I isolated Paneth cells from terminal ileal tissue sections by laser capture microdissection, and intestinal crypts from terminal ileal tissue by mechanical dissociation and compared NOD2

mRNA expression, using real-time RT-PCR, in crypt and villus epithelial cells, and PBMC.

In haematopoietic cells, I determined if NOD2 expression was regulated in PBMC as NOD2 expression increases as precursor cells of the myelomonocytic lineage differentiate into mature monocytes (Gutierrez 2002). To determine whether there are further changes in NOD2 expression as mononuclear cells differentiate into tissue macrophages, I analysed NOD2 expression in tissue granulomata, which contain mature macrophages and newly recruited mononuclear cells and determined NOD2 expression in PBMC as monocytes differentiate into macrophages *in vitro*.

Previously, using *in situ* hybridisation, I showed that NOD2 RNA stained more intensely in Paneth cells in inflamed terminal ileal tissue sections compared to controls, suggesting that NOD2 expression may be regulated in Crohn's disease. Ideally, I would assess NOD2 regulation in primary cells obtained from patients with NOD2-related Crohn's disease and controls. However, this was not practically feasible as it would take a considerable length of time to identify patients with the NOD2 mutations by genotyping. Furthermore, intestinal tissue could only be obtained from patients undergoing surgical treatment. For these reasons, I used intestinal epithelial cells and PBMC to analyse NOD2 expression.

In inflammatory bowel disease, intestinal epithelial cells are exposed to various inflammatory mediators that are produced by activated leukocytes, and I speculated that these mediators may also regulate NOD2 expression in these cells. T helper 1 (T_H1) lymphocytes, which produce pro-inflammatory cytokines such as IFNγ and TNFα, are thought to mediate mucosal inflammation in Crohn's disease, and mucosal T-cells that are isolated from patients with Crohn's disease secrete increased amounts of IFNγ (Bouma 2003). I therefore determined whether NOD2 expression could be regulated in intestinal epithelial cells by lymphokine-containing medium. Thereafter, I determined whether the pro-inflammatory cytokines TNFα and IFNγ specifically regulate NOD2 expression in intestinal epithelial cells and PBMC.

In animal models of IBD, the presence of bacteria is essential for the development of intestinal inflammation (Bouma 2003). As it is postulated that NOD2 mediates cellular inflammation after interacting with bacteria or bacterial products, I determined whether bacterial products could regulate NOD2 expression and cellular inflammation in intestinal epithelial cells.

4.2 Results

4.2.1 NOD2 quantitation in Paneth cells and PBMC

To quantitate NOD2 expression, I isolated Paneth cells and villus epithelial cells by laser capture microdissection from tissue sections. In surgically resected small intestinal tissue, I isolated intestinal crypts and villus epithelial cells by detaching the epithelium from the basement membrane using calcium chelation and mechanical shaking.

4.2.1.1 Laser capture microdissection

Laser capture microdissection (LCM) is a technique that allows specific cells to be isolated from a tissue section, which is usually stained with haematoxylin and eosin and mounted on adhesive-free glass slides. In LCM, targeted cells adhere to a thermoplastic membrane that has been activated by a low energy infrared laser pulse. The thermoplastic membrane, made of ethylene vinyl acetate, has a diameter of 6 mm and is mounted on an optically clear cap, which fits on standard 0.5 mL microfuge tubes, thus facilitating the transfer of cellular contents from the adherent cells to microfuge tubes containing appropriate buffer solutions. The analysis of mRNA expression in microdissected cells, using reverse transcription PCR (RT-PCR), is a relatively newly described technique, which I used to analyse NOD2 expression in LCM-acquired Paneth cells.

Gene profiling and quantitation has been successfully performed in LCM-acquired cells although there are several factors that may limit gene expression in LCM-acquired Paneth cells. Firstly, in archived human sections, approximately 200-300 Paneth cells can be extracted by LCM from a section of terminal ileal tissue. In general, several thousand LCM-acquired cells are required for gene quantitation or profiling (Stappenbeck 2002a), and gene quantitation in human tissue may be limited by the small number of LCM-acquired Paneth cells. Secondly, cells from frozen tissue sections, which yield better quality RNA, are more difficult to dissect by LCM as ethanol, which is used as a tissue fixative, increases the adherence of the tissue to glass slides. Thirdly, eosin inhibits PCR reactions (Fend 2000, Eltoum 2002) and the mRNA molecules in Paneth cells,

which contain numerous intensely-staining apical eosinophilic granules, may not amplify easily by RT-PCR. Finally, small amounts of non-dissected cells adhere non-specifically to thermoplastic membrane, contaminating LCM-acquired cell preparations. Although gene quantitation in Paneth cells present in archived human tissue may be technically difficult, this technique nonetheless provides an independent method to confirm that Paneth cells express the NOD2 gene.

To determine whether Paneth cell-derived mRNA could be amplified by RT-PCR, I extracted total cellular RNA from haematoxylin and eosin-stained frozen terminal ileal sections that were fixed on glass slides with ethanol. Frozen sections were manually scraped off the glass slide, using a sterile surgical blade, and collected in microfuge tubes. Similarly, haematoxylin and eosin-stained wax sections were manually scrapped off glass slides, and collected in microfuge tubes. After using xylene washes to de-wax the paraffin-embedded sections, I used oligodT primers to synthesise cDNA from total cellular RNA extracted from both frozen and wax sections. These cDNA sequences were subsequently amplified by PCR, so that a single 40-cycle PCR amplification reaction could amplify GAPDH and defensin 6 mRNA in frozen but not wax sections (Figure 4.1). NOD2 mRNA, however, could not be amplified in frozen sections by this method. These results suggested that NOD2 quantitation in LCM acquired cells would be difficult, considering that each tissue section contained approximately 2500 Paneth cells – 10-times as many that are likely to be acquired by LCM.

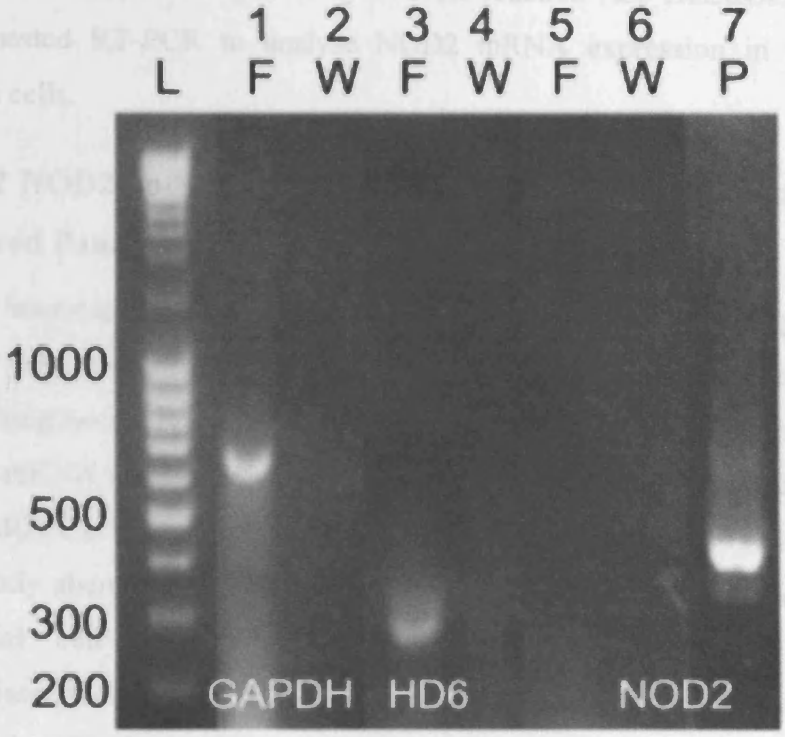

Figure 4.1. GAPDH and defensin 6 mRNA expression in a frozen terminal ileal section. *Using RT-PCR, GAPDH (Lane 1) and HD6 mRNA (Lane 3) were amplified from a single frozen section of terminal ileal tissue. Prior staining of this section with haematoxylin and eosin did not inhibit PCR amplification of GAPDH and HD6 mRNA, which is abundantly expressed in Paneth cells. NOD2 mRNA can be amplified from PBMC (Lane 7) but not from this frozen section (Lane 5). PCR products were separated using agarose gel electrophoresis and visualised using ethidium bromide staining. The expected PCR amplicon size (in base pairs) was used to confirm the identity of the PCR products: GAPDH 693; HD6 241; NOD2 402. (L: ladder; F: frozen section; W: water; P: PBMC)*

In LCM-acquired cells, I was unable to analyse gene expression using RT-PCR. After a 40-cycle PCR reaction, I could detect expression of a gene that is highly expressed in Paneth cells, such as lysozyme, but these results could not be consistently replicated. I used a number of different strategies to optimise RT-PCR amplification of mRNA obtained from LCM-acquired Paneth cells, including pooling LCM-acquired cells from many sections, but could not amplify

Paneth cell-mRNA using a 40-cycle PCR reaction (see Discussion). I therefore used nested RT-PCR to analyse NOD2 mRNA expression in LCM-acquired Paneth cells.

4.2.1.2 NOD2 and alpha defensin 6 (HD6) mRNA expression in LCM-acquired Paneth cells

Using laser-capture microdissection, I obtained relatively pure populations of Paneth cells and villus epithelial cells from terminal ileal tissue sections (Figure 4.2). Using nested RT-PCR, I confirmed that human alpha defensin 6 (HD6) and NOD2 mRNA were most abundantly expressed in the Paneth cell fraction. Some HD6 mRNA is amplified in the villus epithelial cell fraction (Figure 4.2), and this apparently aberrant expression is probably caused by contamination of the villus epithelial cell samples with Paneth cell-fragments during laser-capture microdissection. Greater NOD2 and HD6 mRNA expression were demonstrated in Paneth cells obtained from both frozen and wax-embedded sections, although gene expression could not quantified by real-time RT-PCR.

To eliminate the possibility of false positive results using nested PCR, which is an extremely sensitive technique, I used nuclease-free water as a non-template negative control that was also re-amplified in the second stage PCR reaction. Nested PCR reactions are extremely sensitive for the detection of low copy numbers of cDNA, which undergo two cycles of amplification. As the PCR amplification efficiency of small numbers of cDNA molecules is variable, minor differences in amplification efficiency are therefore artificially exaggerated in the second round of amplification using nested PCT. Although I could not quantitate NOD2 gene expression using nested PCR, the results obtained using this method are very specific, and support the previous findings, which show that Paneth cells specifically express the NOD2 gene.

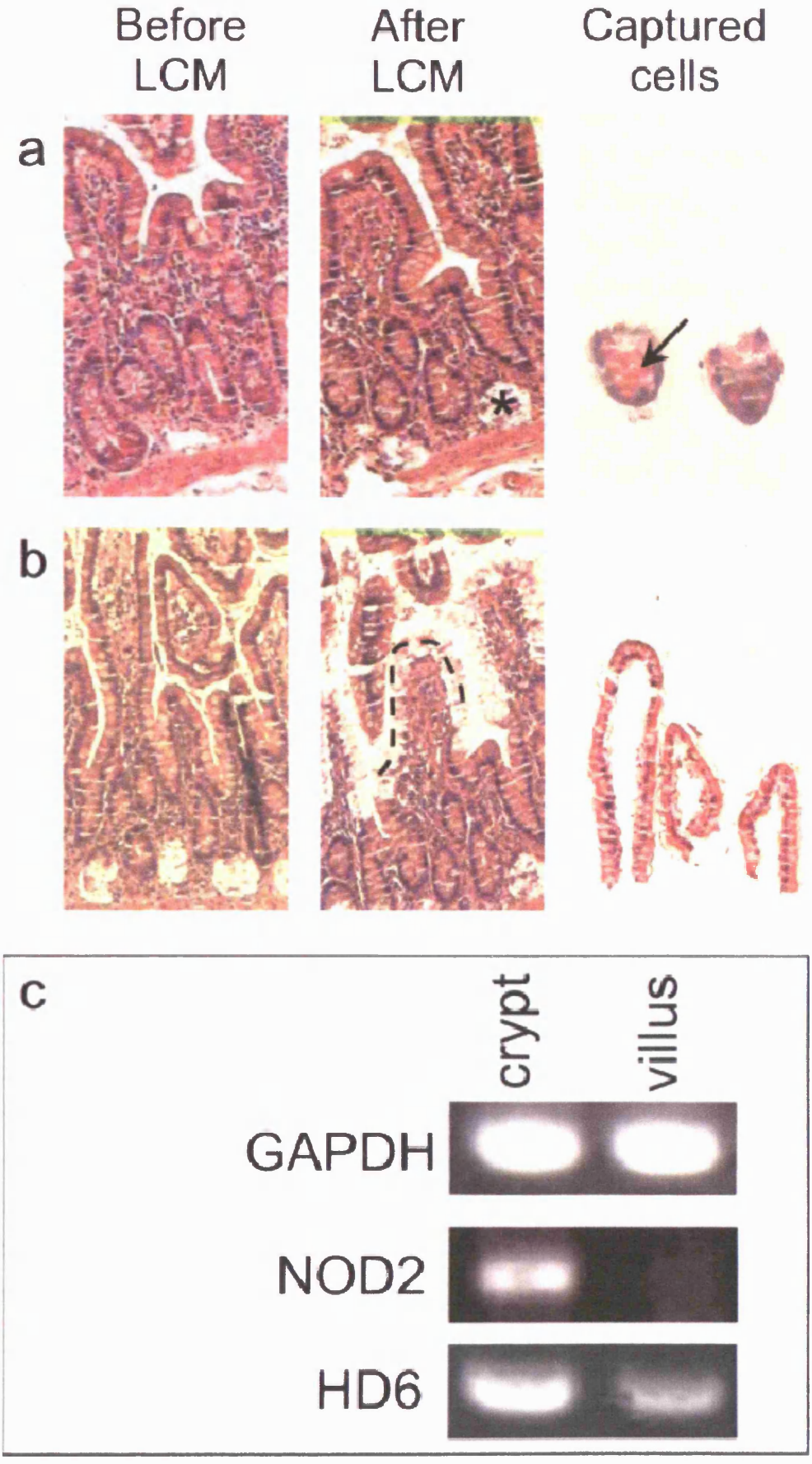
Before LCM
After LCM
Captured cells
a
b
c
crypt
villus
GAPDH
NOD2
HD6

Figure 4.2. Expression of NOD2 mRNA in microdissected Paneth cells (page 146). *Sections of small intestine before and after laser-capture microdissection of Paneth cells (a) and villus epithelial cells (b) are shown stained with haematoxylin and eosin and viewed under the 10x objective. The upper panels show Paneth cells and the lower panels show villus epithelial cells, before microdissection (left-most panels) and after microdissection (middle panels). Microdissected cells captured on membranes are shown in the right-most panels. (c) NOD2, HD6 and GAPDH mRNA were analyzed by nested RT-PCR using intron-spanning primer pairs, in samples of LCM-acquired Paneth cells and villus epithelial cells. For samples with equivalent GAPDH expression, NOD2 mRNA expression is readily detected in crypt Paneth cells but not in villus epithelial cells. HD6 is detected in both Paneth cells and villus epithelial cells, with much lower levels in the villus epithelial fraction. PCR products were separated by agarose gel electrophoresis and visualized by ethidium bromide staining. The expected PCR amplicon size (base pairs) was used to confirm the identity of the PCR products: GAPDH 693; HD6 314; NOD2 402.*

4.2.1.3 Quantification of NOD2 mRNA expression in villus and crypt epithelial cells

To quantify NOD2 gene expression in epithelial cells, I extracted RNA from larger numbers of epithelial cells that were obtained from surgically resected terminal ileal tissue. Large numbers of cells were obtained by calcium chelation and mechanical shaking of fresh ileal tissue, which separates epithelial cells from the underlying basement membrane. Using this technique, I collected cells comprising mainly of villous epithelial cells after the initial periods of mechanical shaking, and collected mainly crypt epithelial cells after further periods of mechanical shaking (Figure 4.3). This technique, which allowed me to obtain a purer population of Paneth cells, optimised the detection of NOD2 in intestinal epithelial cells by RT-PCR. In addition, I extracted RNA from a larger number of cells (in aliquots containing either >90% villus epithelial cells or >90% intestinal crypts) which allowed me to obtain sufficient numbers of intact sheets of villus-epithelium and intestinal crypts to perform quantitative real-time RT-PCR, without the need for nested PCR cycles.

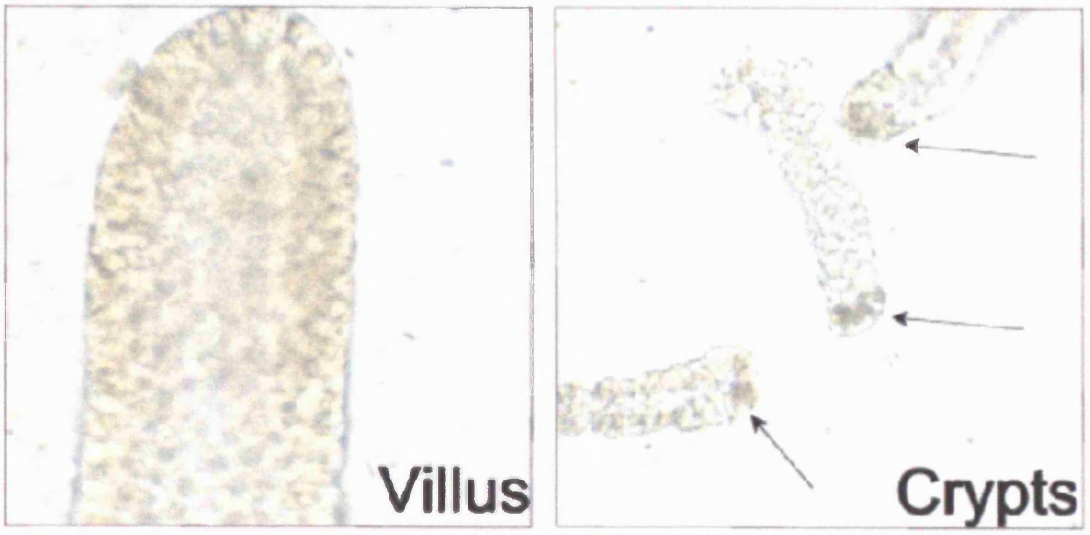

Figure 4.3. Villus and crypts isolated from surgically resected intestinal tissue. *Whole villi and crypts containing Paneth cells (arrows) were obtained by calcium chelation and mechanical shaking of mucosal tissue dissected from surgically resected small intestinal segments, and viewed under the 20x objective in an inverted phase microscope.*

By real-time RT-PCR analysis, NOD2 mRNA expression is approximately 85 fold enriched in crypt epithelial cells as compared to villous epithelial cells (Figure 4.4). The current technique used to separate epithelial cells does not yield exclusive crypt and villous epithelial cells populations, and a minor level of NOD2 mRNA expression seen in the villus epithelial cell fraction. This is most likely due to the presence of a small percentage of crypt epithelial cells in the villous cell fraction, or may reflect a lower level of NOD2 expression in villous epithelial cells, which is less likely to be the case. HD6 mRNA, which is much more abundantly expressed than NOD2 in Paneth cells, was enriched approximately 100 fold in crypts, confirming the successful separation of crypts and villi (Figure 4.4).

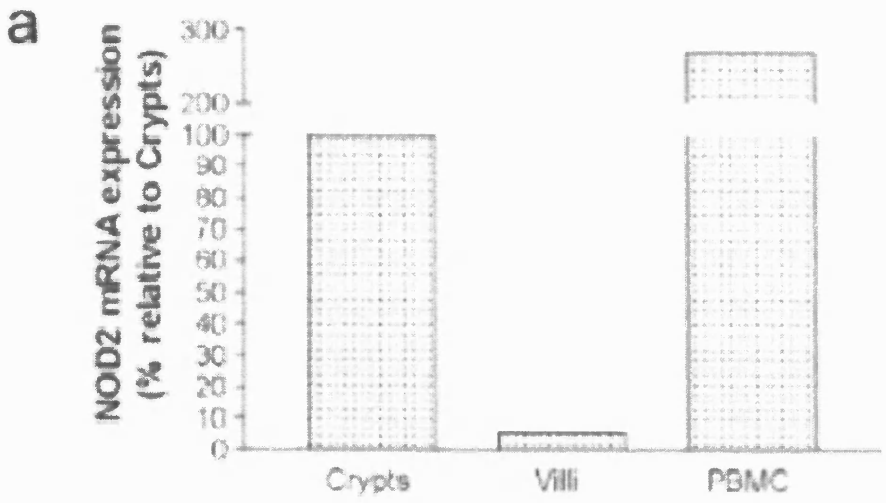
a
NOD2 mRNA expression
(% relative to Crypts)
300
200
100
90
80
70
60
50
40
30
20
10
0
Crypts
Villi
PBMC

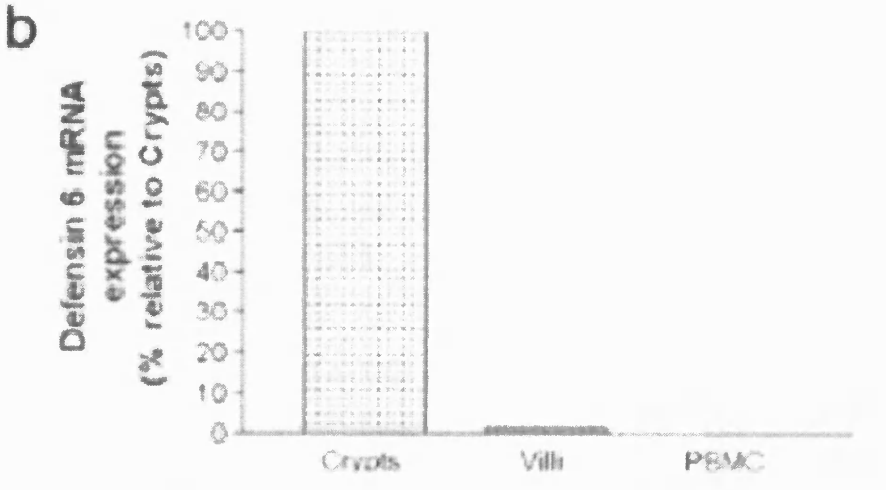
b
Defensin 6 mRNA
expression
(% relative to Crypts)
100
90
80
70
60
50
40
30
20
10
0
Crypts
Villi
PBMC

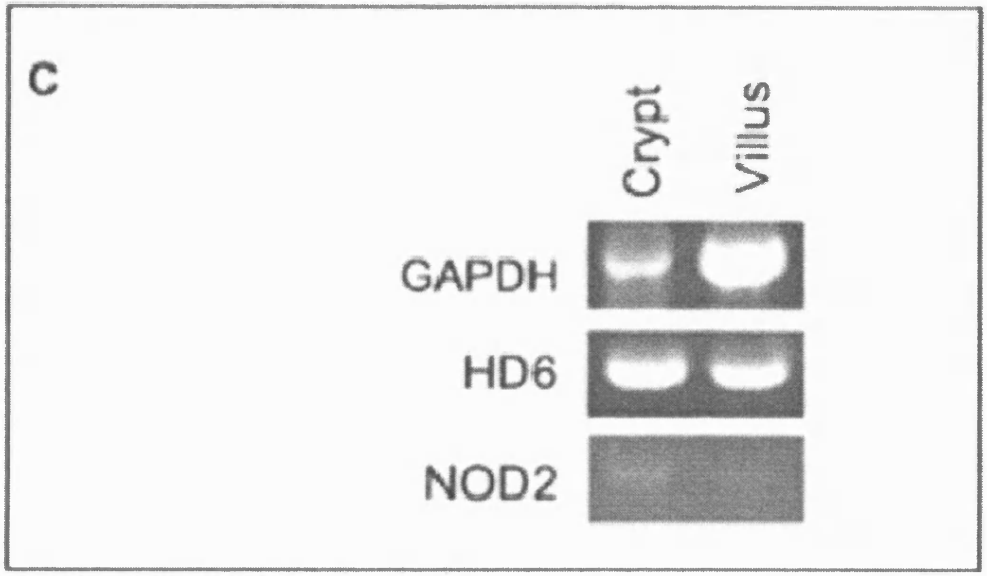
c
Crypt
Villus
GAPDH
HD6
NOD2

Figure 4.4. Expression and quantification of NOD2 mRNA in crypt epithelial cells and PBMC (page 149). *Quantitative real-time RT-PCR analysis of crypt and villus epithelium shows enrichment of (a) NOD2 and (b) HD6 mRNA expression in crypts compared to villi. For comparison, NOD2 expression in freshly isolated peripheral blood mononuclear cells (PBMC) is also shown, and this is approximately 2.7-fold greater than in crypts. The relative expression of NOD2, HD6 and GAPDH mRNA were determined by real-time RT-PCR, using intron-spanning primers, and the NOD2: GAPDH and HD6: GAPDH ratios calculated for each sample. Results are shown as the relative expression compared to the level in crypts. The data are representative of three experiments. PCR products were separated using agarose gel electrophoresis and visualised using ethidium bromide staining. The expected PCR amplicon sizes (base pairs) were used to confirm the identity of the PCR products: GAPDH 693; HD6 241; NOD2 402.*

To determine the significance of NOD2 expression in Paneth cells, I compared NOD2 mRNA expression in crypt and villous epithelial cells and PBMC. This quantitative analysis of NOD2 mRNA expression showed that expression was highest in freshly isolated PBMC and that Paneth cells expressed NOD2 at approximately 30-40% of the levels in PBMC. As Paneth cells comprise approximately 10% of the crypt cell number, and monocytes comprise 10% of PBMC, NOD2 mRNA levels in Paneth cells are calculated to be approximately 30%-40% of the level in monocytes (Figure 4.4).

To confirm that NOD2 is mainly expressed by Paneth cells in the small intestinal epithelium, I isolated intestinal crypts and villus epithelial cells from ileal tissue, and isolated colonic crypts, which normally do not contain Paneth cells, from patients without IBD. Real-time RT-PCR quantitation confirmed that NOD2 mRNA is predominantly expressed in small intestinal crypts, which contain Paneth cells. In contrast, minimal NOD2 mRNA expression could be detected in villus epithelial cells or colonic crypts (Figure 4.5).

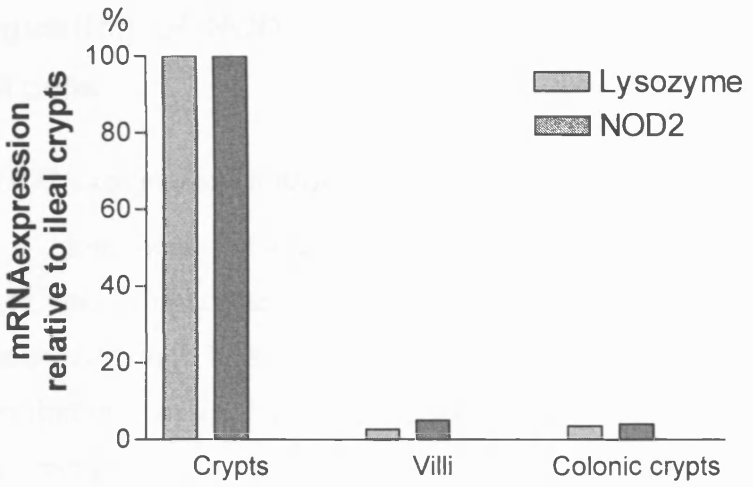

Figure 4.5. Expression of NOD2 mRNA in crypt and villus epithelial cells isolated from ileal tissue. *Quantitative real-time RT-PCR analysis of crypt and villus epithelium shows enrichment of lysozyme and NOD2 mRNA expression in crypts. Lysozyme expression is enriched approximately 40-fold in crypts and NOD2 expression is enriched approximately 20-fold crypts from the ileum compared to villi or colonic crypts. Relative expression of NOD2 and lysozyme mRNA was determined by real-time RT-PCR, using intron-spanning primers, and the NOD2: GAPDH and lysozyme: GAPDH ratios calculated for each sample. Results are shown as the relative expression compared to the level in small intestinal crypts. The data are representative of three experiments.*

Overall, these results show that NOD2 is most prominently expressed by Paneth cells in intestinal epithelial tissue, and that the level of expression is approximately 30% of the level of expression in PBMC.

4.2.2 Regulation of NOD2 expression in PBMC and intestinal epithelial cells

4.2.2.1 NOD2 expression in mononuclear cells in Crohn's disease

There is a prominent inflammatory infiltrate composed of monocytes, macrophages, and lymphocytes within the lamina propria of Crohn's disease-affected tissue. Although NOD2 is most abundantly expressed in PBMC, I was surprised to find that, by *in situ* hybridisation and immunohistochemistry, NOD2 expression is not prominent in tissue macrophages. NOD2 RNA and protein were readily detected in scattered mononuclear cells, which were characterised by indented nuclei and moderate amounts of cytoplasm. These cells with these typical morphologic characteristics also expressed the CD68 antigen, thereby confirming their identity as monocytes (Figure 4.6). I did not observe NOD2 expression in the majority of resident tissue macrophages, which also express CD68. In Crohn's disease-affected tissue, most cells strongly expressed the CD68 marker for mononuclear phagocytes in granulomata. NOD2-positive cells, however, were found on the periphery of granulomas whereas mature macrophages at the centre did not express NOD2 RNA or protein (Figure 4.6). Overall, these observations suggest that NOD2 expression by mononuclear phagocytes is most abundant in circulating monocytes, and in tissues, in newly recruited monocytes, rather than in mature macrophages.

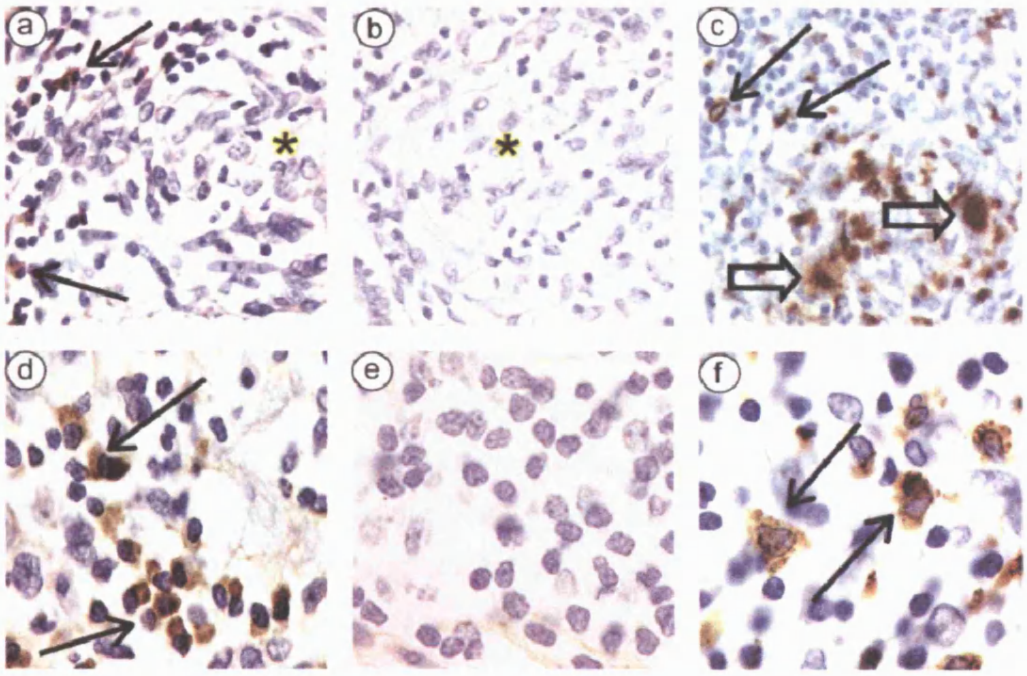

Figure 4.6. NOD2 expression in mononuclear cells in inflamed intestinal tissue. *(a) In situ hybridization with the digoxigenin-labelled NOD2 antisense strand riboprobe demonstrates NOD2 RNA in newly recruited monocytes (arrows) located on the periphery of a granuloma, and not in centrally located histiocytes and epitheloid macrophages (asterisk) in Crohn's disease-affected terminal ileum. (b) Hybridization with the control sense strand riboprobe shows no signal, confirming specificity of detection. The asterisk indicates the central region of the granuloma. (c) Immunohistochemical staining using an anti-CD68 antibody positively identifies newly recruited monocytes (arrows) located on the periphery of a granuloma, and mature macrophages (open arrows) located centrally within a granuloma. (d) In situ hybridization with the NOD2 antisense strand riboprobe demonstrates positive signal in lamina propria monocytes (arrows), which are identified by their nuclear morphology, but not in other leukocytes. (e) No positive signal is detected in sections hybridized with the control sense strand riboprobe. (f) Immunohistochemical staining using an anti-CD68 antibody verifies the identity of lamina propria monocytes (arrowed). All sections were counterstained with haematoxylin, and viewed under the 40x objective (a) to (c), or the 100x objective (d) to (f).*

4.2.2.2 NOD2 expression is regulated in mononuclear cells *in vitro*

My observations on NOD2 expression in tissue granulomata add to the evidence that NOD2 expression in mononuclear cells changes as these cells undergo maturation and differentiation. Gutierrez and colleagues (2002) have shown that in myelomonocytic cells, NOD2 expression is much lower in the immature cell precursors and that NOD2 expression in these cells increases as they mature and differentiate towards monocytes. In addition, other studies have shown that NOD2 mRNA expression, as determined by Northern blot analysis, was easily detected in peripheral blood mononuclear cells (PBMC), whereas little or no expression was detected in macrophage-rich organs such as the liver and spleen (Ogura 2001a). I therefore investigated the regulation of NOD2 expression in PBMC, obtained from healthy volunteers, which were maintained in culture to allow monocytes to differentiate into macrophages. Using quantitative real-time RT-PCR, I showed that NOD2 expression decreases with time in PBMC maintained in tissue culture (figure 4.7). NOD2 mRNA levels declined steeply initially, and were approximately 10% of the starting level after 24 hours of culture. Thereafter, the decline was more gradual but could still be detected in PBMC that were maintained in culture for 5 days. This decline in NOD2 expression was not due to a decrease in the relative number of monocytes or macrophages, which remained constant as determined by immunocytochemical detection of CD68 antigen in cytospin preparations (figure 4.8).

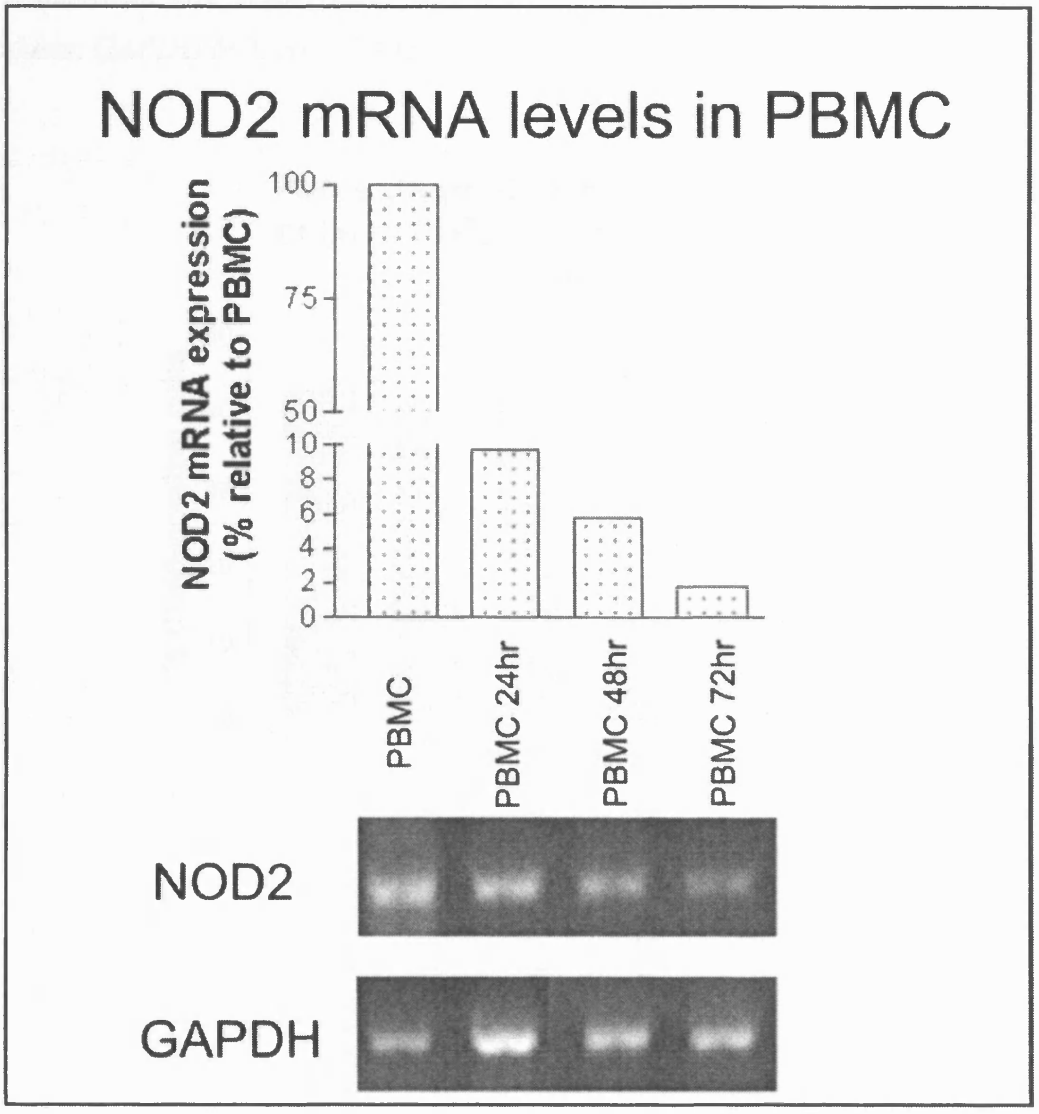

Figure 4.7. NOD2 mRNA expression in peripheral blood mononuclear cells. *NOD2 mRNA expression was quantified in freshly isolated PBMC and in cells maintained in culture for 24, 48 and 72 hours, using real-time RT-PCR with intron-spanning primers. Results were normalized using GAPDH mRNA as an internal standard. NOD2 mRNA levels are shown as a percent relative to the level in freshly isolated PBMC. The lower panel shows NOD2 and GAPDH amplification products from mRNA extracted from freshly isolated PBMC, and cells maintained in culture for 24, 48 and 72 hours, using RT-PCR with intron-spanning primers. PCR products were separated using agarose gel electrophoresis and visualized using ethidium bromide staining. The expected*

PCR amplicon size (base pairs) was used to confirm the identity of the PCR products: GAPDH 693; NOD2 402.

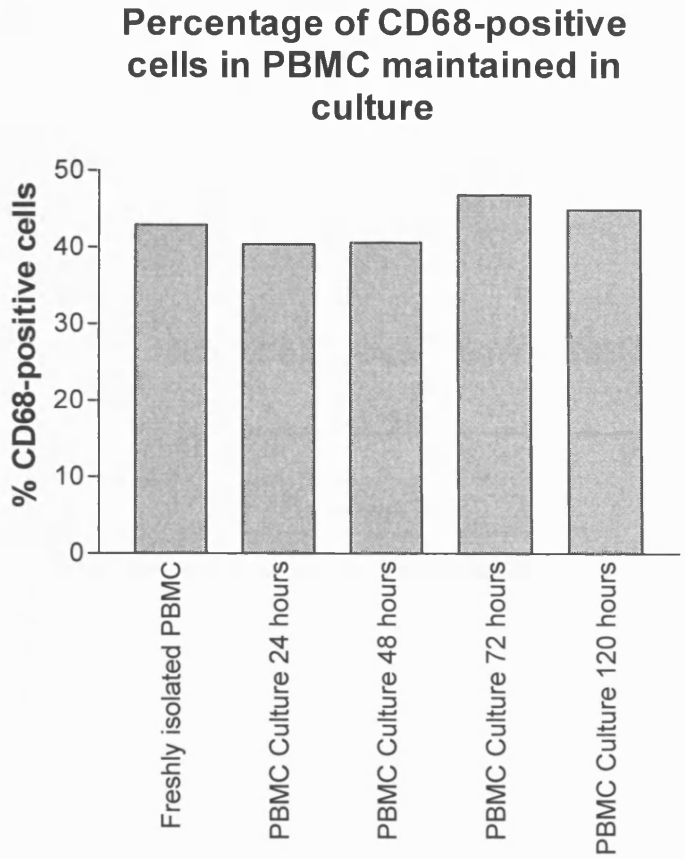

Figure 4.8. Percentage of CD68 positive cells in primary PBMC maintained in culture. *Cytospin preparations of freshly-isolated PBMC and those that were maintained in culture for 24, 48, 72 and 120 hours were stained for the CD68 antigen. The percentage of CD68-positive cells in these preparations was: 42.9 % in freshly isolated PBMC, 40.4% in PBMC cultured for 24 hours, 40.6 in PBMC cultured for 48 hours, 46.8% in PBMC cultured for 72 hours, and 44.9% in PBMC cultured for 120 hours.*

To confirm that NOD2 expression decreases as PBMC are maintained in culture, I extracted PBMC from blood that had been removed by venesection from polycythaemic patients who were otherwise healthy. Using quantitative real-time RT-PCR, NOD2 expression decreased to 67% of the starting levels after 24 hours

of culture. After 48 hours of culture, NOD2 expression decreased by 50% in PBMC and after 72 hours of culture, expression decreased by 56% (Figure 4.9). Although NOD2 mRNA expression did not decrease as dramatically in PBMC extracted from polycythaemic patients compared to PBMC extracted from healthy volunteers for reasons that are unclear, these results confirm an association between NOD2 mRNA expression levels and the length of time of PBMC culture. These results suggest that NOD2 expression decreases in monocytes as they differentiate into macrophages *in vitro*.

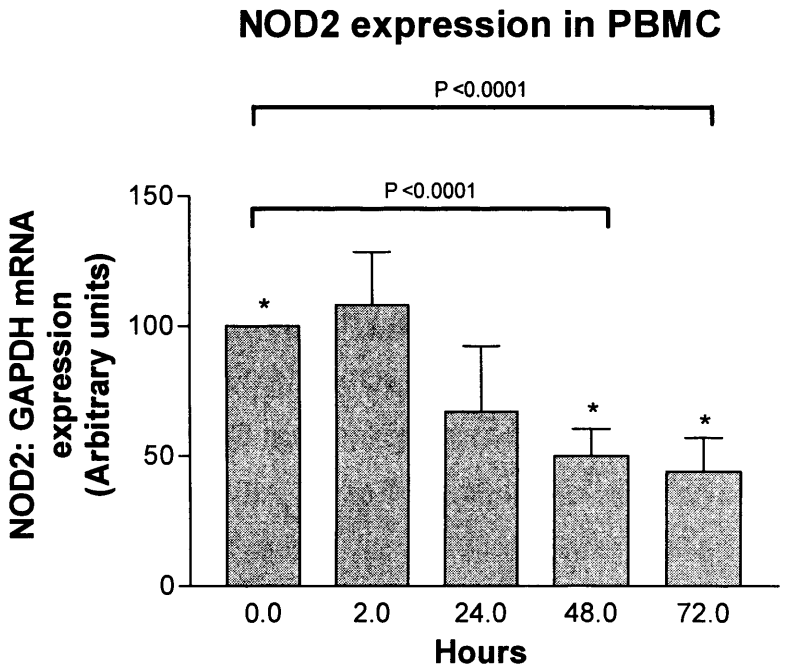

Figure 4.9. NOD2 mRNA expression in PBMC extracted from polycythaemic patients. *NOD2 mRNA expression was quantified in freshly isolated PBMC and in cells maintained in culture for 24, 48 and 72 hours, using real-time RT-PCR with intron-spanning primers. Results were normalized using GAPDH mRNA as an internal standard. NOD2 mRNA levels are shown as a percent relative to the level in freshly isolated PBMC which is set as 100%. Values in the figure are expressed as the mean ± SEM (Standard error of the mean). Experiments were performed seven times (n=7), and differences between stimulated and control cells were analyzed by two-tailed, non-paired t test, with a P value <0.05 indicative of statistical significance.*

4.2.2.3 Regulation of NOD2 expression in PBMC

Next, I determined whether it is possible to regulate NOD2 expression in PBMC that were stimulated with pro-inflammatory cytokines and bacterial antigens. In PBMC obtained from healthy volunteers, NOD2 expression was generally difficult to detect in these cells that were maintained in culture for at least 24 hours. To facilitate detection of NOD2 expression in PBMC maintained in culture, I obtained a larger number of PBMC from otherwise healthy polycythaemic patients undergoing venesection.

4.2.2.4 NOD2 mRNA expression in PBMC stimulated with TNFα and dexamethasone

Treatment with steroids and anti-TNFα antibodies often induce remission in Crohn's disease-affected patients suffering from acute relapses. I therefore determined whether TNFα and dexamethasone could regulate NOD2 mRNA expression in PBMC. NOD2 mRNA expression was increased in PBMC stimulated with TNFα (100 ng/mL) compared to control cells. By real-time RT-PCR analysis, NOD2 mRNA levels were approximately 25% and 60% higher after 24 and 72 hours of culture in TNFα-stimulated PBMC as compared to control cells. Dexamethasone treatment (1 μg/mL), on the other hand, appeared to decrease NOD2 expression. In dexamethasone-treated PBMC, NOD2 mRNA levels could not be quantitated and NOD2 PCR products could not be visualised by gel electrophoresis in PBMC maintained in culture for at least 24 hours (Figure 4.10).

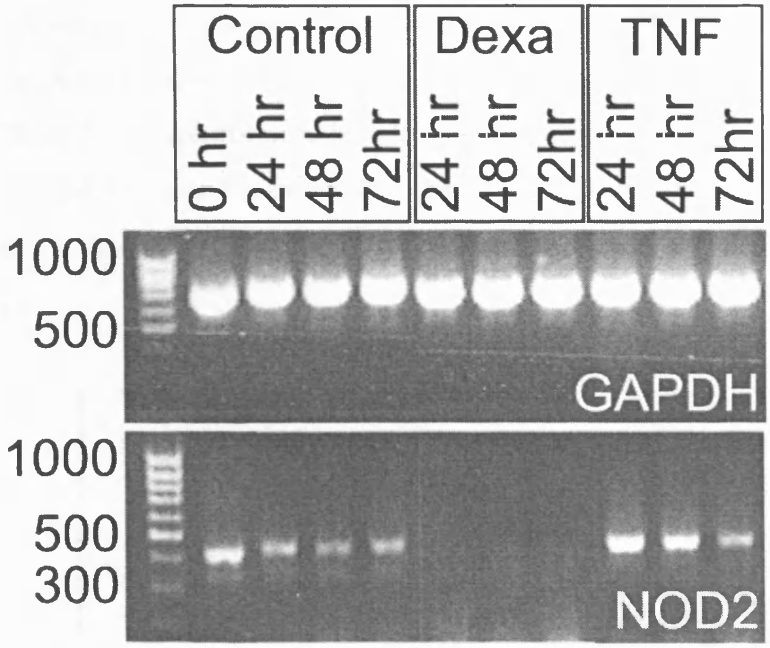

Figure 4.10. TNFα and dexamethasone regulate NOD2 expression in PBMC. *RT-PCR analysis of GAPDH and NOD2 expression in PBMC maintained in culture shows that NOD2 expression is decreased in PBMC stimulated with dexamethasone and increased in cells stimulated with TNFα. PCR products were separated using agarose gel electrophoresis and visualised using ethidium bromide staining. The expected PCR amplicon size (base pairs) was used to confirm the identity of the PCR products: GAPDH 693; NOD2 402. (0 hr: freshly isolated PBMC; Dexa: dexamethasone; TNF: TNFα).*

4.2.2.5 NOD2 mRNA expression in PBMC after stimulation with LPS and muramyl dipeptide (MDP)

The precise function of NOD2 remains undefined at present. It is postulated that NOD2 functions as an intracellular receptor or 'sensor' for the bacterial product muramyl dipeptide (MDP) although it was originally proposed that NOD2 facilitated the detection of LPS. I therefore determined whether these ligands had an effect of NOD2 expression in PBMC that were maintained in culture.

There was no apparent difference in NOD2 expression in PBMC that were stimulated with LPS (10 ng/mL) for 48 hours (Figure 4.11). In PBMC that were stimulated with MDP (20 μg/mL), NOD2 expression was increased after 2 hours of stimulation, but expression levels decreased thereafter. The decline in NOD2

expression, however, was more gradual in MDP-stimulated PBMC. NOD2 mRNA levels declined rapidly so that expression could not be detected by real-time RT-PCR in 2 of 3 control samples after 24 hours and 48 hours of culture. In MDP-stimulated PBMC, on the other hand, NOD2 mRNA could be detected in all samples after 24 hours of culture, and in 1 of 3 samples after 48 hours of culture (Figure 4.12).

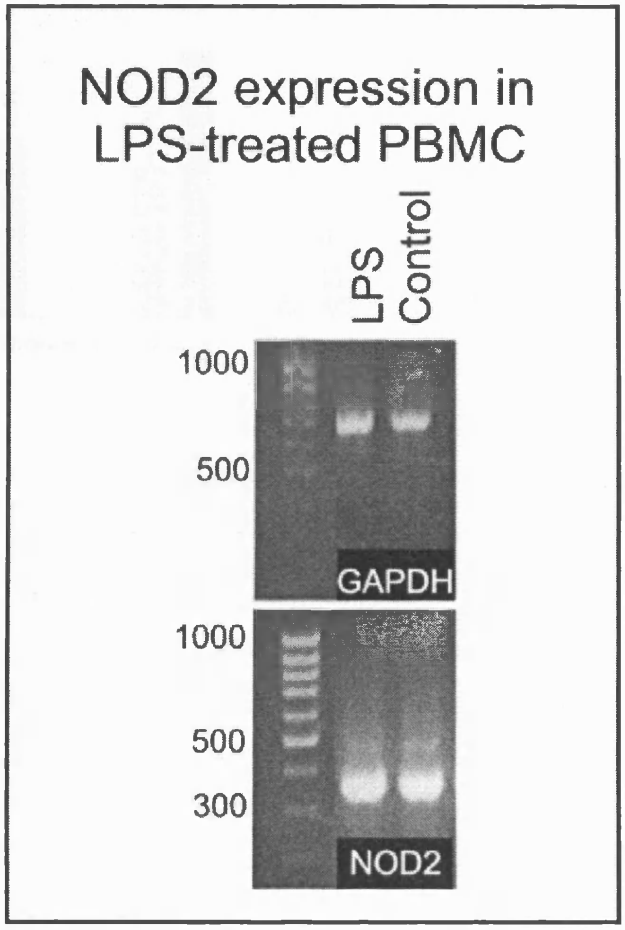

Figure 4.11. NOD2 mRNA expression in LPS stimulated-PBMC. *RT-PCR analysis of GAPDH and NOD2 expression in control PBMC and PBMC stimulated with LPS (10 ng/mL) for 48 hours shows no apparent difference in NOD2 expression. PCR products were separated using agarose gel electrophoresis and visualised using ethidium bromide staining. The expected PCR amplicon size (base pairs) was used to confirm the identity of the PCR products: GAPDH 693; NOD2 336.*

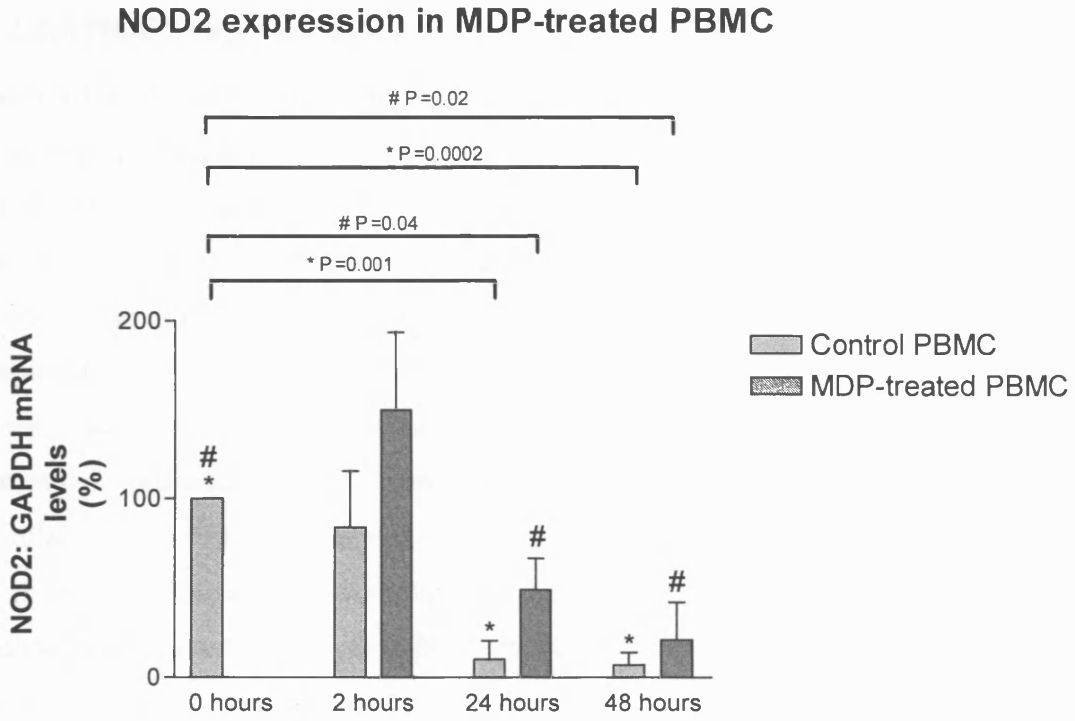

Figure 4.12. NOD2 mRNA expression in PBMC stimulated with MDP. *In PBMC maintained in culture for 2 hours, NOD2 mRNA expression was slightly lower in unstimulated cells as compared to MDP stimulated cells. After 24 and 48 hours of culture, NOD2 mRNA levels were expressed at relatively higher levels in MDP-treated PBMC although the difference between untreated and MDP-treated cells at each time point was not significant. NOD2 expression levels were significantly reduced in control and MDP stimulated cells maintained in culture for 24 and 48 hours compared to the levels in freshly isolated PBMC. The relative expression of NOD2 and GAPDH mRNA were determined using intron-spanning primers, and the NOD2: GAPDH ratios calculated for each sample. Results are shown relative to the expression in freshly isolated PBMC where NOD2 expression has been defined as 100%. Values in the figure are expressed as the mean ± SEM (Standard error of the mean). Experiments were performed three times (n=3), and differences between stimulated and control cells were analysed by two-tailed, non-paired t test, with a P value <0.05 indicative of statistical significance.*

4.2.2.6 NOD2 expression in intestinal epithelial cells

Within the intestinal epithelium, I have shown that NOD2 is most prominently expressed in Paneth cells. There is, however, no suitable *in vitro* or *ex vivo* model to assess gene regulation in Paneth cells and I therefore determined whether NOD2 is expressed in intestinal epithelial cell lines as they might make a useful model to investigate the regulation of NOD2 expression. I showed that NOD2 expression can be detected by RT-PCR in immortalised intestinal epithelial cell lines. Caco-2 intestinal epithelial cells, which display some features of small intestinal epithelial differentiation, constitutively expressed the NOD2 gene at similar levels to PBMC cultured for 24 hours. These Caco-2 cells also expressed high levels of secretory phospholipase A_2 ($sPLA_2$) and lysozyme mRNA that are normally restricted to Paneth cells in small intestinal crypts. In contrast, HT29 cells expressed low levels of NOD2 mRNA that could be demonstrated only by quantitative real-time RT-PCR (Figure 4.13).

I then used both Caco-2 and HT29 cells [and SW480 cells after Hisamatsu and colleagues (2003) reported NOD2 expression in these cells] to investigate NOD2 regulation in intestinal epithelial cells.

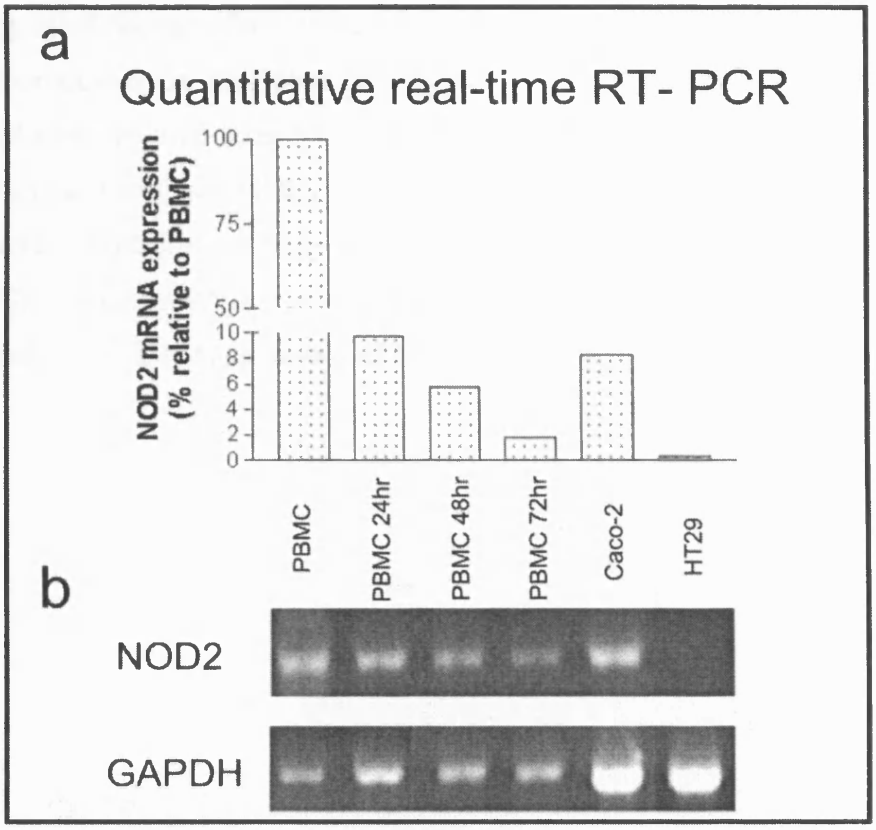

Figure 4.13. NOD2 mRNA expression in intestinal epithelial cells. *NOD2 mRNA expression was quantified in freshly isolated PBMC and in cells maintained in culture for 24, 48 and 72 hours, and Caco-2 and HT29 cells, using real-time RT-PCR with intron-spanning primers. Results were normalized using GAPDH mRNA as an internal standard. NOD2 mRNA levels are shown as a percent relative to the level in freshly isolated PBMC. The lower panel shows NOD2 and GAPDH amplification products from mRNA extracted from PBMC and Caco-2 and HT29 cells, using RT-PCR with intron-spanning primers. PCR products were separated using agarose gel electrophoresis and visualized using ethidium bromide staining. The expected PCR amplicon size (base pairs) was used to confirm the identity of the PCR products: GAPDH 693; NOD2 402.*

4.2.2.7 Regulation of NOD2 expression in intestinal epithelial cells

Previously, using *in situ* hybridisation and immunohistochemistry, I observed that NOD2 RNA and protein appeared to stain more intensely in Crohn's disease-

affected tissue as compared to controls, which suggested that NOD2 expression may be regulated during inflammation. To potentially mimic the *in vivo* effect of activated leukocytes on the intestinal epithelium, I treated Caco-2 cells with conditioned medium containing lymphokine, which are soluble cytokines secreted by lymphocytes. I analysed NOD2 mRNA expression in Caco-2 cells, cultured in growth medium containing 50% lymphokine, by northern blotting (RNA blotting) and RT-PCR. NOD2 mRNA expression was not easily detected by northern blot analysis, indicating low basal levels of NOD2 expression in Caco-2 cells (Figure 4.14).

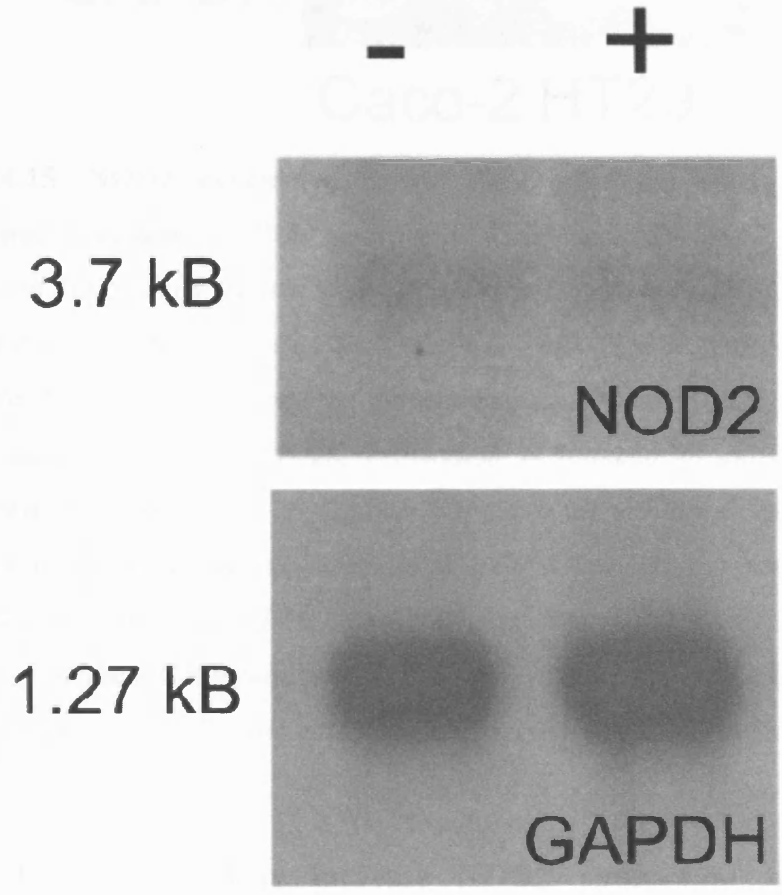

Figure 4.14. Northern blot analysis of NOD2 and GAPDH expression in Caco-2 cells. *NOD2 mRNA expression is not easily detected in Caco-2 cells, including cells stimulated with conditioned medium from PHA-stimulated lymphocytes. GAPDH mRNA expression, in contrast, is easily detected in Caco-2 cells by northern blotting.*

As the low levels of NOD2 mRNA expression in Caco-2 cells were not easily detected by northern blotting, I used RT-PCR to analyse NOD2 expression in intestinal epithelial cells stimulated by lymphokine. By RT-PCR, NOD2 expression was increased in Caco-2 cells and induced in HT29 cells that were treated with conditioned medium from PHA stimulated lymphocytes (Figure 4.15).

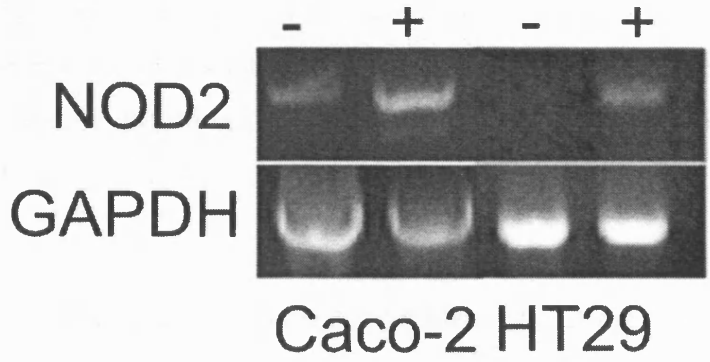

Figure 4.15. NOD2 expression is intestinal epithelial cells treated with conditioned medium. *RT-PCR analysis of GAPDH and NOD2 expression in Caco-2 and HT29 cells treated with lymphokine-conditioned medium (+) shows an increase in NOD2 expression in Caco-2 cells that constitutively express NOD2. In HT29 cells, which do not express detectable NOD2 mRNA under normal culture conditions, NOD2 expression is induced in cells treated with conditioned medium. PCR products, stained with ethidium bromide, were separated by agarose gel electrophoresis and visualised by transillumination under UV light. The expected PCR amplicon size (base pairs) was used to confirm the identity of the PCR products: GAPDH 693; NOD2 402. (- indicates control cells and + indicates cells cultured in lymphokine-containing growth medium)*

4.2.2.8 TNFα and IFNγ increase NOD2 expression in intestinal epithelial cells

In vitro, PHA-stimulated lymphocytes secrete various cytokines, such as IFNγ, TNFα, IL-4 and GM-CSF. To identify whether these cytokines regulate NOD2 expression in intestinal epithelial cells, I quantitated NOD2 expression, using real-time RT-PCR, in intestinal epithelial cells that were stimulated with recombinant

human IFNγ (10^3 U/mL), TNFα (100 ng/mL), IL-4 (10 ng/mL) and GM-CSF (10 ng/mL) proteins.

In intestinal epithelial cell lines, NOD2 expression is increased in cells that had been treated with recombinant TNFα and IFNγ. In Caco-2 cells, which constitutively express NOD2, TNFα stimulation increased NOD2 mRNA expression 2.5-fold whilst IFNγ stimulation induced a smaller (1.7-fold) increase in NOD2 expression. Stimulation with both TNFα and IFNγ increased NOD2 mRNA expression 3.5-fold in Caco-2 cells (Figure 4.16). There was no change in NOD2 expression in Caco-2 cells that were treated with IL-4 and GM-CSF.

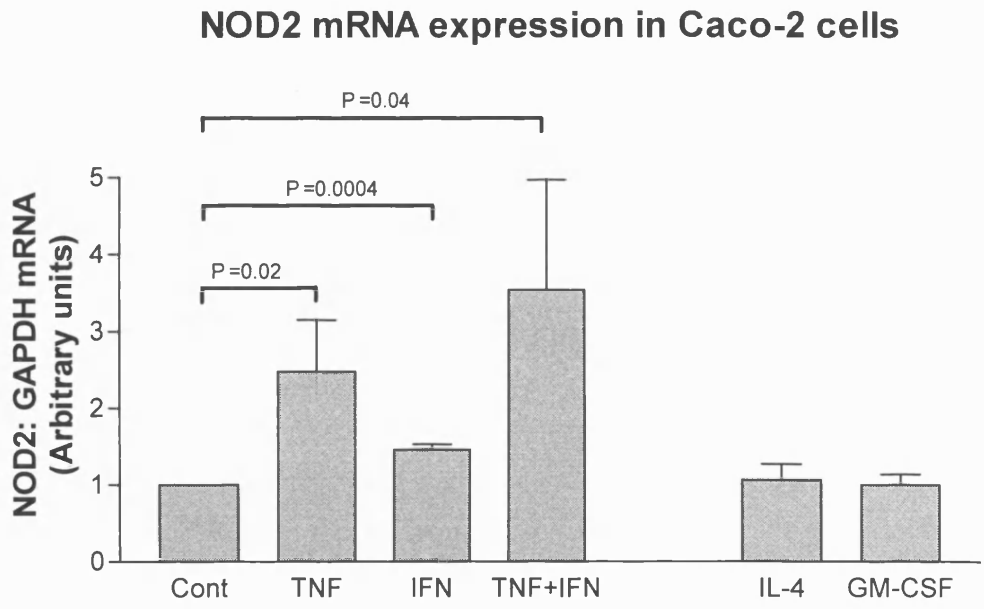

Figure 4.16. Regulation of NOD2 expression in Caco-2 cells. *Using quantitative real-time RT-PCR, NOD2 mRNA expression was increased in Caco-2 cells stimulated by TNFα (P=0.0185) and IFNγ (P=0.0004). Co-stimulation with TNFα and IFNγ also increased NOD2 expression (P=0.0373) although NOD2 expression was not regulated by IL-4 or GM-CSF stimulation. The relative expression of NOD2 and GAPDH mRNA were determined using intron-spanning primers, and the NOD2: GAPDH ratios calculated for each sample. Results are shown as the relative expression compared to the level in unstimulated (control) Caco-2 cells, which was arbitrarily set as 1 unit. Values in the figure are expressed as the mean ± SEM (Standard error of the mean). Experiments were*

performed three times, and differences between stimulated and control cells were analysed by two-tailed, non-paired t test, with a P value <0.05 indicative of statistical significance.

TNFα also induced NOD2 expression in HT29 cells, which do not constitutively express the gene (Figure 4.17). In HT29 cells, IFNγ also induced NOD2 expression, albeit to a weaker extent (Figure 4.17). In HT29 cells, TNFα induced a 2.6-fold greater increase in NOD2 expression than IFNγ, although the relative increase in NOD2 expression could not be quantified as there is no constitutive NOD2 expression in HT29 cells.

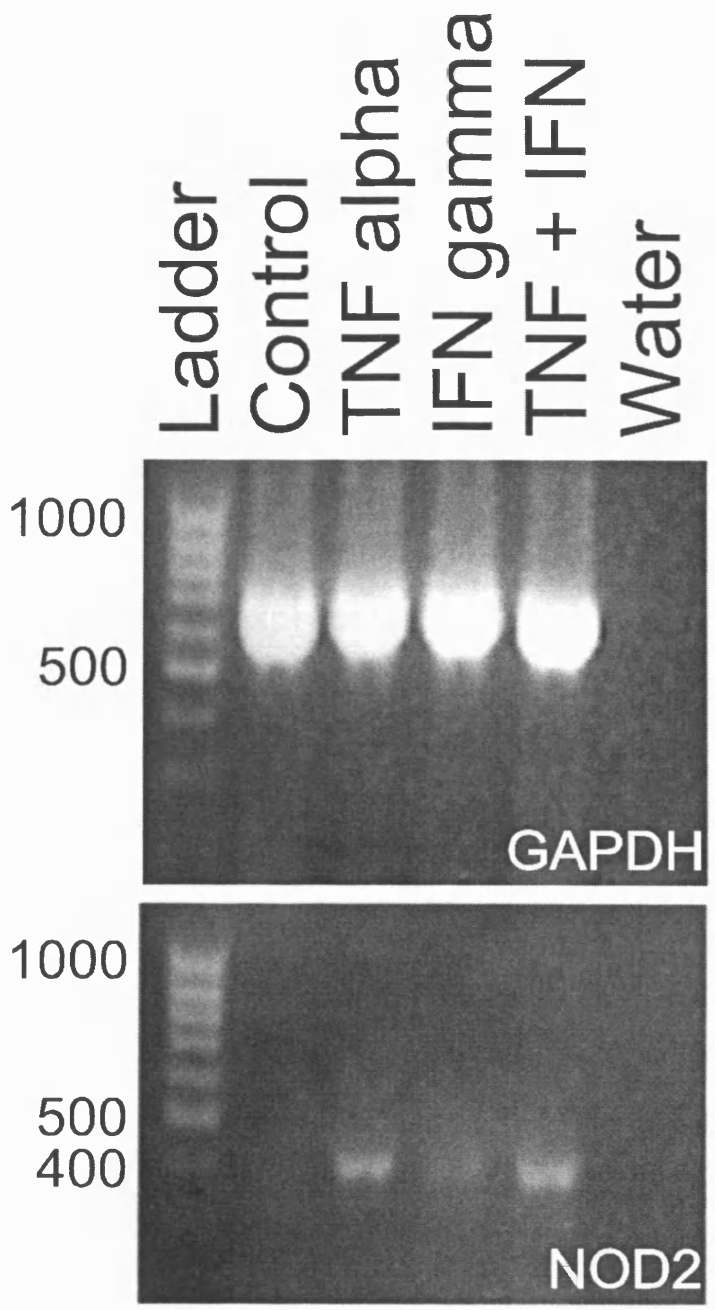

Figure 4.17. NOD2 expression in HT29 cells. *RT-PCR analysis of GAPDH and NOD2 expression in HT29 cells treated with TNFα (100 ng/mL) and IFNγ (10^3 U/mL) shows that NOD2 expression is induced in cells treated with TNFα, IFNγ, or both cytokines. PCR products, stained with ethidium bromide, were separated by agarose gel electrophoresis and visualised by transillumination under UV light. The expected PCR amplicon size (base pairs) was used to confirm the identity of the PCR products: GAPDH 693; NOD2 402.*

At the time of performing these experiments, Hisamatsu and colleagues (2003) reported that NOD2 mRNA is constitutively expressed at higher levels in SW480 cells in comparison to other intestinal epithelial cell lines.

I therefore investigated NOD2 mRNA expression in the SW480 intestinal epithelial cell line. In SW480 cells, TNFα stimulation increased NOD2 expression 1.8-fold although, surprisingly, IFNγ stimulation did not increase NOD2 expression (Figure 4.18). NOD2 expression was increased 2-fold in cells treated with both TNFα and IFNγ.

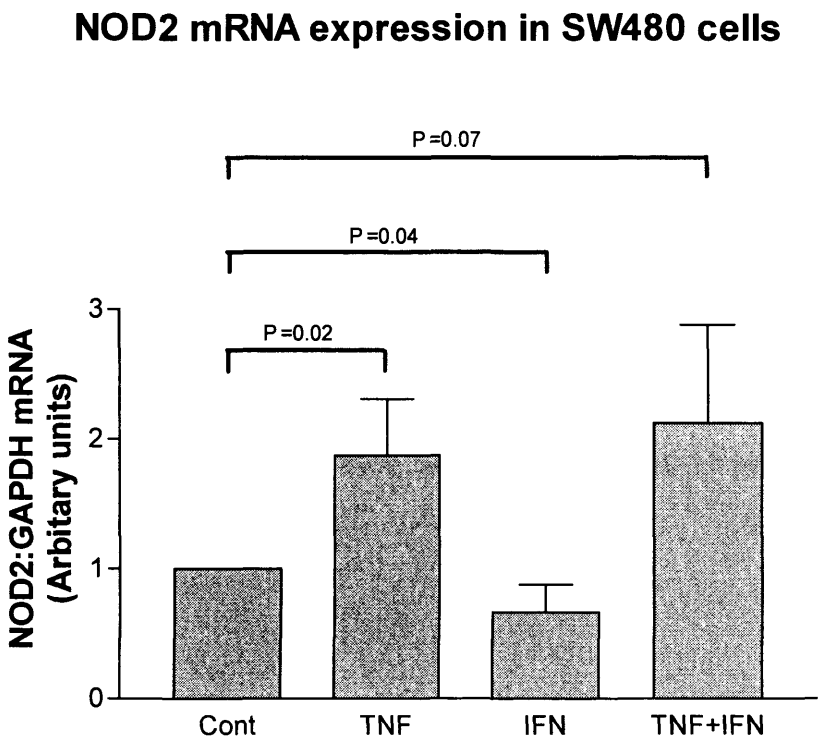

Figure 4.18. Regulation of NOD2 expression in SW480 cells. *Using quantitative real-time RT-PCR, NOD2 mRNA expression was increased in SW480cells stimulated by TNFα (P=0.0178). Stimulation of these cells with IFNγ alone did not increase NOD2 expression (a significant decrease in expression was observed) and co-stimulation with TNFα and IFNγ increased NOD2 expression, which was not significant. The relative expression of NOD2 and GAPDH mRNA was determined using intron-spanning primers, and the NOD2: GAPDH ratios calculated for each sample. Results are shown as the relative expression*

compared to the level in unstimulated SW480 cells, which was arbitrarily set as 1 unit. Values in the figure are expressed as the mean ± SEM (Standard error of the mean). Experiments were performed three times, and differences between stimulated and control cells were analysed by two-tailed, non-paired t test, with a P value <0.05 indicative of statistical significance.

Overall, these results show that TNFα increases NOD2 expression in intestinal epithelial cells. These increases, however, appear modest in comparison to the increases in IL-8 mRNA measured in intestinal epithelial cells stimulated with TNFα. In Caco-2 cells, stimulation with either TNFα or IFNγ increased IL-8 mRNA expression 5.8-fold and 1.9-fold respectively. Stimulation with both these cytokines increased IL-8 expression 5.9-fold in Caco-2 cells (Figure 4.19). In HT29 cells, much larger increases in IL-8 mRNA expression were noted after stimulation with TNFα and IFNγ (Figure 4.20). In these cells, TNFα stimulation induced a 43.5-fold increase in IL-8 expression, and IFNγ stimulation increased IL-8 expression approximately 5-fold. Treating HT29 cells with both TNFα and IFN synergistically increased IL-8 expression 200-fold. In SW480 cells, TNFα increased IL-8 mRNA expression 5.9-fold whereas IFNγ increases expression modestly (1.3-fold). IL-8 expression was increased 13-fold in cells stimulated with both cytokines (Figure 4.21).

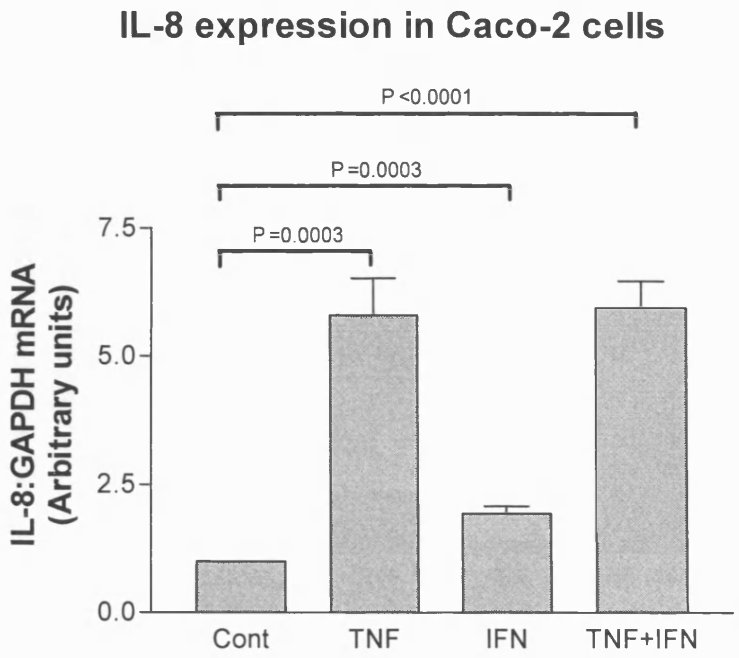

Figure 4.19. IL-8 expression in Caco-2 cells. *Using quantitative real-time RT-PCR, IL-8 mRNA expression was significantly increased in Caco-2 cells stimulated by TNFα (P=0.0003). A smaller but significant increase was seen in cells stimulated with IFNγ and TNFα and IFNγ also synergistically increase IL-8 mRNA in these cells (P=<0.0001). The relative expression of IL-8 and GAPDH mRNA were determined using intron-spanning primers, and the IL-8: GAPDH ratios calculated for each sample. Results are shown as the relative expression compared to the level in unstimulated Caco-2 cells, which was arbitrarily set as 1 unit. Values in the figure are expressed as the mean ± SEM (Standard error of the mean). Experiments were performed three times, and differences between stimulated and control cells were analysed by two-tailed, non-paired t test, with a P value <0.05 indicative of statistical significance.*

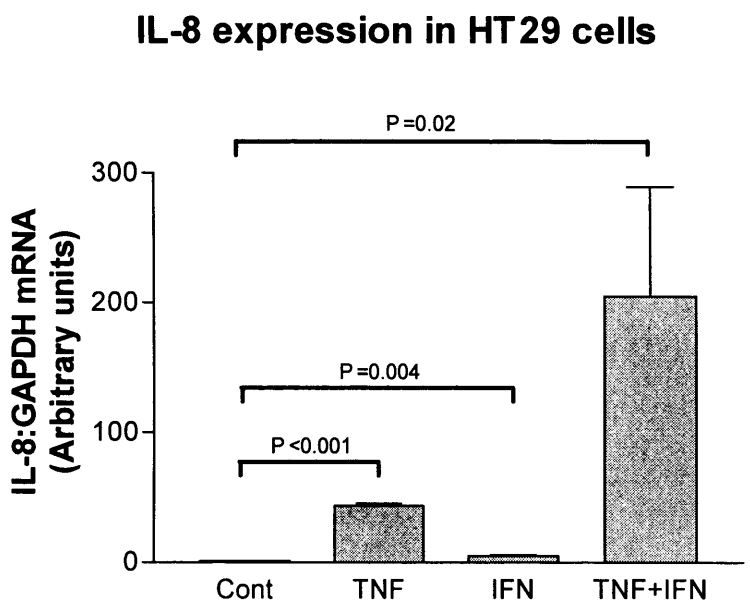

Figure 4.20. IL-8 expression in HT29 cells. *Using quantitative real-time RT-PCR, IL-8 mRNA expression is significantly increased in HT29 cells stimulated by TNFα (P<0.001). A smaller but significant increase is seen in cells stimulated with IFNγ alone (P=0.004) and TNFα and IFNγ also synergistically increase IL-8 mRNA in these cells (P=0.020). The relative expression of IL-8 and GAPDH mRNA were determined using intron-spanning primers, and the IL-8: GAPDH ratios calculated for each sample. Results are shown as the relative expression compared to the level in unstimulated HT29 cells, which was arbitrarily set as 1 unit. Values in the figure are expressed as the mean ± SEM (Standard error of the mean). Experiments were performed three times, and differences between stimulated and control cells were analysed by two-tailed, non-paired t test, with a P value <0.05 indicative of statistical significance.*

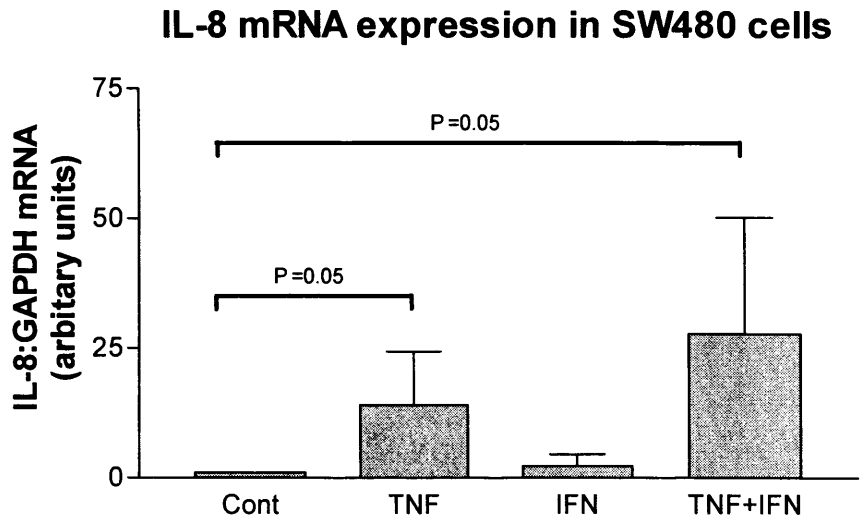

Figure 4.21. Regulation of IL-8 expression in SW480 cells. *Using quantitative real-time RT-PCR, IL-8 mRNA expression is significantly increased in SW480 cells stimulated by TNFα (P=0.05) and a smaller non-significant increase is seen in cells stimulated with IFNγ . Stimulation with both TNFα and IFNγ synergistically increase IL-8 expression (P=0.05). The relative expression of IL-8 and GAPDH mRNA were determined using intron-spanning primers, and the IL-8: GAPDH ratios calculated for each sample. Results are shown as the relative expression compared to the level in unstimulated SW480 cells, which was arbitrarily set as 1 unit. Values in the figure are expressed as the mean ± SEM (Standard error of the mean). Experiments were performed three times, and differences between stimulated and control cells were analysed by two-tailed, non-paired t test, with a P value <0.05 indicative of statistical significance.*

In PBMC, NOD2 expression appears to be regulated by dexamethasone treatment, which decreases NOD2 expression. I therefore determined whether dexamethasone treatment could regulate NOD2 expression in intestinal epithelial cells. In Caco-2 cells, dexamethasone treatment decreased NOD2 expression by approximately 35% whereas TNFα stimulation increases NOD2 expression by approximately 2.5 fold (Figure 4.22). Dexamethasone did not induce NOD2 expression in HT29 cells, which do not constitutively express the gene.

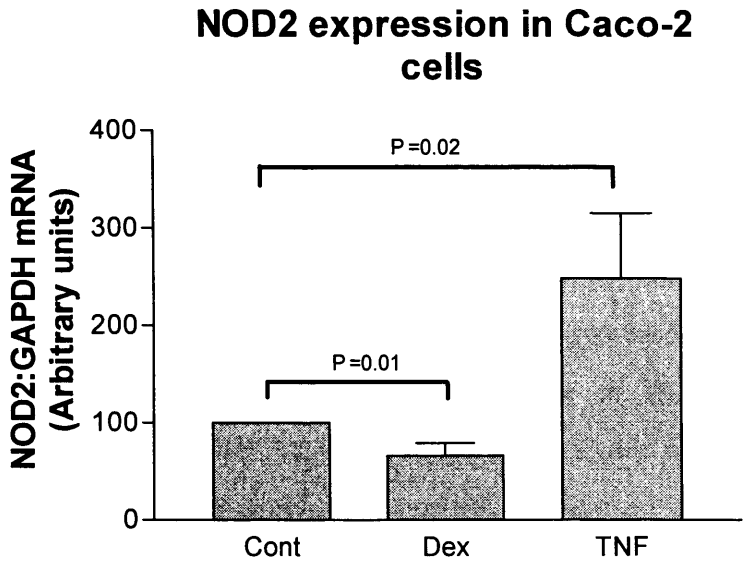

Figure 4.22. Regulation of NOD2 expression in Caco-2 cells by dexamethasone. *Using quantitative real-time RT-PCR, NOD2 mRNA expression is significantly decreased in Caco-2 cells stimulated by dexamethasone (P=0.01), and significantly increased in cells stimulated with TNFα (P=0.02). The relative expression of NOD2 and GAPDH mRNA were determined using intron-spanning primers, and the NOD2: GAPDH ratios calculated for each sample. Results are shown as the relative percentage of expression in unstimulated Caco-2 cells, which was defined as 100%. Values in the figure are expressed as the mean ± SEM (Standard error of the mean). Experiments were performed three times, and differences between stimulated and control cells were analysed by two-tailed, non-paired t test, with a P value <0.05 indicative of statistical significance.*

4.2.2.9 NOD2 mRNA expression in intestinal epithelial cells stimulated with lipopolysaccharide (LPS)

Previous investigators that have demonstrated NOD2 expression in intestinal epithelial cells have postulated that NOD2 function as an intracellular bacterial 'sensor' (Inohara 2003a). Although controversial, some investigators describe the expression of toll-like receptors (TLRs) in intestinal epithelial cells and speculate that intestinal epithelial cells may respond to stimulation by bacterial antigens (Cario 2000). I therefore determined whether NOD2 mRNA changes in intestinal epithelial cells that were stimulated with the bacterial products LPS and MDP.

Initially, using real-time RT-PCR, I could not demonstrate any change in NOD2 and IL-8 mRNA expression in Caco-2 and HT29 cells that were stimulated with LPS. Next, I pre-treated Caco-2 and HT29 cells with TNFα and IFNγ for 48 hours, which is reported to increase TLR4 and MD-2 expression and LPS responsiveness in intestinal epithelial cells (Abreu 2002), before stimulation with LPS. After taking into account the increase in NOD2 expression induced by TNFα and IFNγ treatment, there was no further change in NOD2 expression, as measured by real-time RT-PCR, in these pre-treated cells that were stimulated with LPS. IL-8 mRNA expression increased in response to TNFα and IFNγ stimulation but there was no change in expression in pre-treated cells that were stimulated with LPS. In addition, Caco-2 and HT29 cells were grown to confluence in transwell plates and I pre-treated these cells in a basal direction with TNFα and IFNγ. These pre-treated cells were then apically stimulated with LPS. Using RT-PCR, NOD2 mRNA expression was increased after pre-treatment with TNFα and IFNγ, and additional LPS stimulation did not appear to markedly influence NOD2 expression (Figure 4.23). Overall, these results indicate that Caco-2 and HT29 cells are generally unresponsive to stimulation with LPS, and a potential role for LPS in NOD2 regulation in intestinal epithelial cells cannot be analysed in the system that I used.

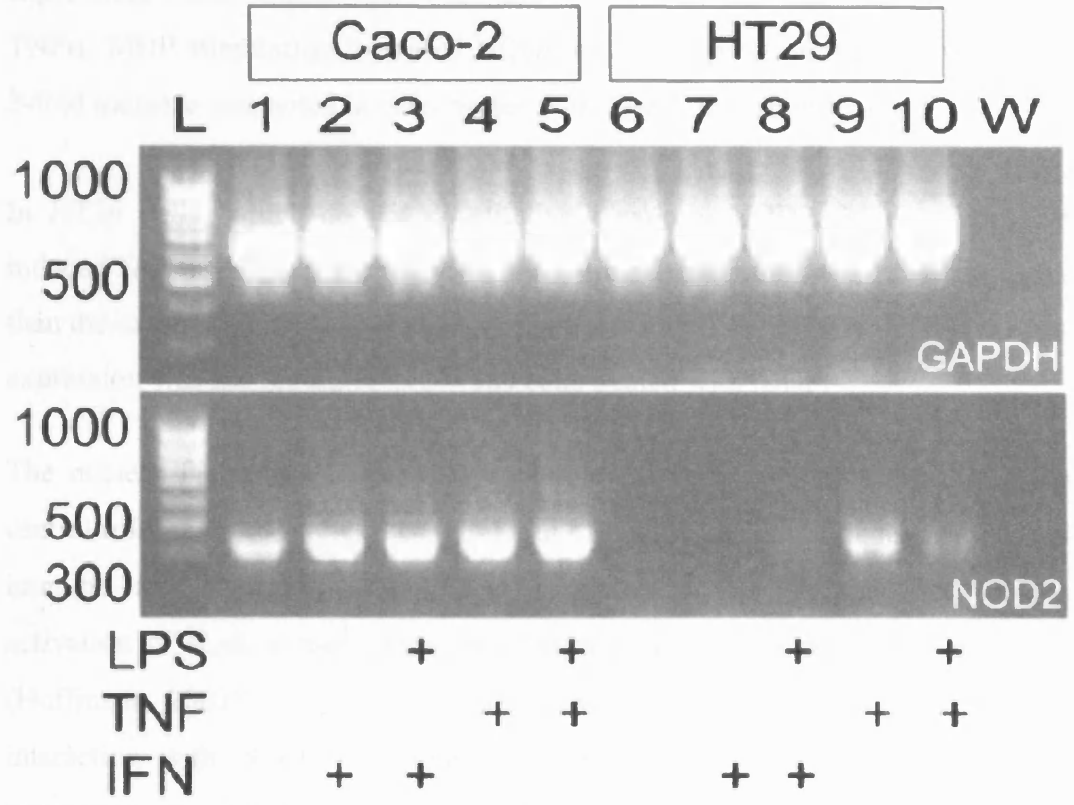

Figure 4.23. NOD2 expression in intestinal epithelial cells stimulated with LPS. *RT-PCR analysis of GAPDH and NOD2 expression Caco-2 and HT29 cells treated with IFNγ (10^3 U/mL) (Lanes 2 and 7) and TNFα (100 ng/mL) (Lanes 4 and 9); and in LPS-stimulated cells that were pre-treated with IFNγ (Lanes 3 and 8) or TNFα (Lanes 5 and 10). Untreated control cells are shown in Lanes 1 and 6. PCR products, stained with ethidium bromide, were separated by agarose gel electrophoresis and visualised by transillumination under UV light. The expected PCR amplicon size (base pairs) was used to confirm the identity of the PCR products: GAPDH 693; NOD2 402.*

4.2.2.10 NOD2 mRNA expression in intestinal epithelial cells stimulated with muramyl dipeptide (MDP)

Next, I determined whether MDP could regulate NOD2 expression in intestinal epithelial cells. By real-time RT-PCR analysis, a modest (2-fold) increase in NOD2 mRNA expression was noted in Caco-2 cells stimulated with MDP (Figure 4.24). Next, I pre-treated Caco-2 and HT29 cells with TNFα, to increase NOD2

expression, before stimulation with MDP. In Caco-2 cells that were treated with TNFα, MDP stimulation increased NOD2 mRNA expression 3.3-fold whereas a 2-fold increase was noted in cells treated with TNFα only (Figure 4.24).

In HT29 cells, which do not constitutively express NOD2, MDP stimulation induced NOD2 mRNA expression in TNFα-treated cells that was 1.5-fold greater than the level of NOD2 expression in cells treated with TNFα only. NOD2 mRNA expression was not regulated in SW480 cells treated with MDP.

The nuclear factor κB (NF-κB) is an important transcription factor that has a central role in coordinating the expression of a wide variety of genes that control immune responses (Li 2002). For example, NF-κB induces transcription activation of IL-8, a chemokine that functions as a neutrophil chemoattractant (Hoffmann 2002). As MDP is postulated to induce NF-κB activation after interacting with NOD2 (Girardin 2003), I therefore quantitated IL-8 mRNA expression in intestinal epithelial cells stimulated with MDP. In Caco-2 cells stimulated with MDP, IL-8 mRNA expression increases modestly (1.6-fold) in comparison to a 5-fold increase seen in cells stimulated with TNFα. In Caco-2 cells that were pre-conditioned with TNFα, MDP stimulation increased IL-8 mRNA expression 17-fold (Figure 4.25). SW480 cells were unresponsive to stimulation with MDP and showed no increases in NOD2 or IL-8 mRNA expression.

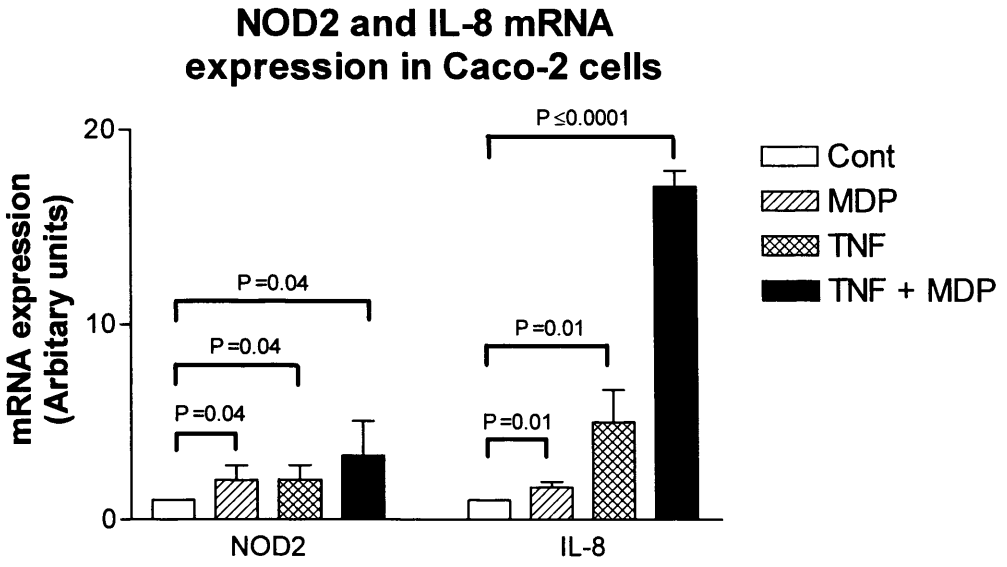

Figure 4.24. Regulation of NOD2 and IL-8 expression in Caco-2 cells by MDP. *Using quantitative real-time RT-PCR, NOD2 mRNA expression is increased in Caco-2 cells stimulated by TNFα and MDP although the increase in expression was not statistically significant. TNFα induced a larger increase in IL-8 expression than MDP, which also increased IL-8 expression. The increases in IL-8 expression induced by MDP and TNFα are statistically significant. A synergistic increase, which is statistically significant, was seen in cells stimulated with TNFα and MDP. The relative expression of NOD, IL-8 and GAPDH mRNA was determined using intron-spanning primers, and the NOD2: GAPDH and IL-8: GAPDH ratios calculated for each sample. Results are shown as the relative expression compared to the level in unstimulated Caco-2 cells, which was arbitrarily set as 1 unit. Values in the figure are expressed as the mean ± SEM (Standard error of the mean). Experiments were performed three times, and differences between stimulated and control cells were analysed by two-tailed, non-paired t test, with a P value <0.05 indicative of statistical significance.*

Overall, these results show that MDP stimulation induces modest responses in NOD2 and IL-8 mRNA expression in intestinal epithelial cells. Also, NOD2 regulation appears to be regulated to a greater degree by TNFα in intestinal epithelial cells (although the overall response to TNFα stimulation is also modest). Stimulation with the bacterial antigens LPS and MDP does not increase IL-8 mRNA transcription in intestinal epithelial cells to the same level does TNFα

stimulation. MDP, however, appears to cause a synergistic increase in IL-8 mRNA in Caco-2 pretreated with TNFα (which increases baseline NOD2 expression), suggesting that NOD2 may play a role in mediating MDP-induced cellular responses. This hypothesis, however, can be more accurately tested in cells expressing wild-type and mutant NOD2 proteins.

4.3 Discussion

4.3.1 NOD2 gene quantitation in Paneth cells

Paneth cells express the NOD2 gene at levels that are approximately a third of the levels in circulating monocytes, which express NOD2 most abundantly. By *in situ* hybridisation and immunohistochemistry, NOD2 is most prominently expressed in Paneth cells and lamina propria mononuclear cells. NOD2 gene quantitation in primary intestinal epithelial cells was difficult to determine as NOD2 is not readily detected in intestinal tissue by RT-PCR. Gene quantitation by real-time RT-PCR was only ascertained after obtaining large numbers of intestinal epithelial cells, using calcium chelation and mechanical dissociation, from resected intestinal tissue. NOD2 is most prominently expressed in intestinal crypts, and the level of expression in Paneth cells are approximately 30-40% of levels measured in freshly isolated PBMC.

NOD2 expression could not be quantitated in LCM-acquired epithelial cells although I was able to confirm that NOD2 is specifically expressed in Paneth cells by nested RT-PCR. It is likely that insufficient amounts of RNA were extracted from LCM-captured Paneth cells in tissue sections to permit accurate quantitation using real-time RT-PCR. For gene quantitation in LCM-acquired cells, sufficient amounts of RNA should be obtained from captured cell populations. Stappenbeck and colleagues (2002a) estimate that, in murine intestinal tissue, approximately 500 cell equivalents, with each cell yielding 10-30 pg of RNA, are required for real-time RT-PCR gene quantitation in LCM-acquired cells. In human tissue sections, I was unable to dissect more than 250 Paneth cells per section and it is also likely that significant RNA degradation occurs in resected human intestinal tissue prior to tissue fixation. To optimise RNA extractions, I digested tissue sections with Proteinase K (using variable concentrations and varying time periods) and used a commercial kit (Qiagen) to extract RNA from LCM-acquired cells but these methods did not increase the RNA yield. I used several methods to optimise gene quantitation in LCM-acquired cells without success. These methods include performing reverse transcription with a highly thermostable, cloned avian RNase H- reverse transcriptase enzyme (ThermoScript® RT, Invitrogen), and

priming with random hexamers or gene-specific primers. PCR amplification was performed with different sets of oligo-primers but gene products could not be amplified without using nested PCR. Newer techniques, which amplify extracted RNA sequences by *in vitro* transcription prior to quantitation using real-time PCR may permit gene quantitation in Paneth cells acquired by LCM from paraffin-embedded tissue sections. Presently, the commercial kits available for gene quantitation in paraffin-embedded tissue (Paradise kit, Arcturus) are very expensive.

Although I was able to quantitate NOD2 mRNA expression in Paneth cells by isolating large numbers of intestinal crypts from surgically resected tissue, I was unable to quantitate protein expression in these cells by immunoblotting. NOD2 protein is difficult to detect in primary cells, even in PBMC that abundantly express NOD2, and other laboratories report similar difficulties (G Nunez, personal communication 2003). NOD2 protein has been detected by immunoblotting in primary colonic epithelial cells from patients with Crohn's disease but not in healthy controls (Rosenstiel 2003) but these immunoblots have been very difficult to perform (Philip Rosenstiel, personal communication, 2003). Thus, NOD2 gene quantitation in patients with NOD2-related Crohn's disease appears to be only really feasible in resected tissue.

Unexpectedly, I found that NOD2 expression was not prominent in tissue macrophages. NOD2 mRNA was not directly measured in macrophages isolated from intestinal tissue although, by *in situ* hybridisation, NOD2 expression was most prominent in monocytes located in the lamina propria and on the periphery of granulomata in comparison to mature macrophages located in the centre of granulomata. Further evidence to suggest that NOD2 expression is regulated in monocytic cells was obtained from *in vitro* studies, which showed a decline in NOD2 mRNA levels in PBMC that were maintained in culture to allow monocytes to differentiate towards macrophages. It is unclear whether this decline in NOD2 levels is a programmed feature of monocyte maturation and terminal differentiation or is consequent on adhesion of cells to a substrate, which requires further investigation.

4.3.2 NOD2 regulation in PBMC and intestinal epithelial cells

Overall, the highest levels of NOD2 expression in Crohn's disease-affected terminal ileal tissue are seen in Paneth cells and lamina propria mononuclear cells, which suggest that these cells play a role in the pathogenesis of NOD2-related Crohn's disease. However, although the NOD2 gene is prominently expressed by Paneth cells, there are no suitable *in vitro* models to assess gene regulation in these cells. I determined that intestinal epithelial cell lines also express NOD2, and I therefore used these cells to investigate the regulation of NOD2 gene expression. NOD2 expression is more prominent in immortalised intestinal epithelial cells treated with a solution containing lymphokine, and using recombinant cytokines, I determined that TNFα regulates NOD2 expression, albeit weakly, in Caco-2, HT29 and SW480 cells. IFNγ is a major constituent of lymphokine but NOD2 expression is not significantly enhanced or increased after treatment with IFNγ. IFNγ may, however, act synergistically with TNFα to increase NOD2 expression in intestinal cells, and may account for the increased NOD2 expression observed in Crohn's disease.

The results obtained in the present study are consistent with results published by other investigators. These reports, which were published at the time that I performed my experiments, also show that TNFα stimulation increases NOD2 expression in intestinal epithelial cells (Gutierrez 2002, Rosenstiel 2003, Hisamatsu 2003). Hisamatsu and colleagues (2003) demonstrated, by Northern blot analysis, that TNFα increased NOD2 mRNA expression in a time- and concentration-dependent manner in SW480 cells. NOD2 mRNA expression was not increased after stimulation with IFNγ, IL-1β, IL-4 or TGFβ. Rosenstiel and colleagues (2003) showed that TNFα induced an increase in NOD2 mRNA and protein expression in various colon cancer cell lines. IFNγ did not induce NOD2 expression although co-stimulation with TNFα and IFNγ induced a synergistic increase in NOD2 expression. These investigators also demonstrated NOD2 protein expression in primary colonic epithelial cells isolated from patients with Crohn's disease but not in cells isolated from healthy controls.

The results from the present study also show that TNFα increases NOD2 expression in PBMC maintained in culture. TNFα also induces NOD2 expression in myeloblastic HL-60 cells (Gutierrez 2002) although, surprisingly, I am not aware of other studies analysing NOD2 regulation in PBMC stimulated with TNFα. As NOD2 levels decrease in PBMC maintained in culture, I found that PBMC need to be extracted from a considerable volume of blood (200 – 250 mL) to allow for NOD2 quantitation in cells maintained in culture for at least 24 hours. I analysed responses in PBMC obtained from otherwise healthy polycythaemic patients, which may be different to responses seen in PBMC obtained from healthy volunteers.

The reason that TNFα increases NOD2 expression in intestinal epithelial cells is not known, but it is likely that TNFα increases NOD2 expression by activating NF-κB. The NOD2 promoter contains three DNA elements with high homology to the NF-κB-binding consensus sequence that are located at position -674 (5'-GGGGAAGCCC-3', κB1), -301 (5'-GGGCCTCCCC-3', κB2) and -26 (5'-GGGAATTTCC-3', κB3) (Rosenstiel 2003). Rosenstiel and colleagues (2003), using cell transfectants expressing mutant forms of the NOD2 promoter, showed that deletion of the κB3 site markedly reduced TNFα or TNFα/IFNγ induced NF-κB activation. A similar, but reduced, effect was noted when κB2 was deleted from the NOD2-promoter sequence. Site-directed mutagenesis of the κB1 site did not affect TNFα or TNFα/IFNγ-induced NF-κB activation, indicating that this sequence is not a functional NF-κB-binding site. Earlier, Gutierrez and colleagues (2003) had also shown that the κB3 sequence, which is only responsive to the p65 subunit of NF-κB, mediates TNFα-induced NOD2 expression in cell transfectants (Gutierrez 2003). In this study, overexpression of a dominant negative IκBα mutant also leads to a loss of induced NOD2 promoter activity, suggesting that NF-κB is involved in the regulation of the NOD2 gene by TNFα.

In the present study, stimulation with dexamethasone, which inhibits NF-κB activity (Carlsen 2002), decreases NOD2 expression in PBMC and Caco-2 intestinal epithelial cells. Although there are no other studies to confirm this observation, these results suggest that NOD2 expression may be regulated by NF-

κB in PBMC and intestinal epithelial cells. In intestinal inflammation, NOD2 expression may be increased in intestinal epithelial cells in response to NF-κB activation, and it is possible that mutant NOD2 proteins may abrogate NF-κB activation induced by cytokines such as TNFα.

In the present study, MDP stimulation enhances IL-8 and NOD2 expression in PBMC maintained in culture for at least 24 hours. Interestingly, although enhanced NOD2 expression may occur secondarily to NF-κB activation, there was no enhancement of NOD2 expression in PBMC stimulated with LPS (in the present study), which is known to activate NF-κB (Palsson-McDermott 2004). These results, however, do not confirm a role for NOD2 in mediating cellular responses to MDP as I could not assess responses in PBMC that express mutant NOD2 proteins.

MDP is generally regarded as a putative intracellular 'ligand' for NOD2 although there is no direct evidence for this. Girardin and colleagues (2003) showed that microinjection of MDP caused NF-κB activation in RAW cells, but not in HeLa epithelial cells. There was no NF-κB activation in RAW or HeLa cells stimulated extracellularly with MDP and these investigators postulate that NOD2 mediates intracellular 'sensing' of MDP. However, these investigators also showed that NF-κB activation occurs in cell transfectants that abundantly express native NOD2 protein but not mutant NOD2 protein. Furthermore, Inohara and colleagues (2003) show that MDP induced NF-κB activation in human PBMC containing wild-type, but not mutant, NOD2 proteins. There is thus no clear explanation for difference in responses seen in RAW cells and human PBMC after extracellular MDP stimulation, but these differences may reflect species-specific differences in monocyte responsiveness to MDP. Overall, however, these studies do suggest a role for NOD2 in mediating cellular activation in response to MDP stimulation.

It is hypothesised that, within intestinal epithelial cells, NOD2 acts as an intracellular 'sensor' that mediates NF-κB activation in response to MDP and induces cellular activation. The experiments required to test this hypothesis, however, require microinjection and are technically difficult to perform. In the

present study, intestinal cell lines are generally unresponsive to stimulation with LPS, confirming the observations made by Gutierrez and colleagues (2002). I pre-treated intestinal epithelial cells with TNFα and IFNγ, which reportedly increases TLR4 expression (Abreu 2002), and then stimulated these cells with LPS. The pre-treatments increased NOD2 expression, which is expected, but there were no further changes in NOD2 or IL-8 expression in response to LPS stimulation. MDP induced weak increases in NOD2 and IL-8 mRNA expression in Caco-2 and HT29, but not SW480 cells, which suggests that intestinal epithelial are generally unresponsive to MDP stimulation. In the present analysis, it is possible that NF-κB activation is underestimated as protein secretion (for example IL-8 measurement by ELISA) was not measured. Nonetheless, NF-κB activation, as assessed by immunostaining of the p65 subunit of NF-κB, is not detected in cells stimulated with MDP, suggesting that intestinal epithelial are unresponsive to MDP (Girardin 2003).

Paneth cells, on the other hand, respond to stimulation with extracellular MDP by secreting antimicrobial peptides (Ayabe 2000). Importantly, MDP induces antimicrobial secretion from Paneth cells that is comparable to secretions induced by other bacterial antigens such as LPS, LTA and Lipid A. To assess the potential role of Paneth cells in NOD2-related Crohn's disease, however, is difficult as there is no suitable *in vitro* model to analyse Paneth cell function. An assay to assess antimicrobial secretion by human Paneth cells [similar to the assay (in murine Paneth cells) that was initially described by Ayabe and colleagues (2000)], is difficult to perform and it is likely that it will take a considerable length of time to collect intestinal tissue from patients with Crohn's disease and controls. The role of NOD2 in Paneth cell function may, however, be assessed in murine models in which NOD2 gene expression is disrupted: for example, the Paneth cell secretion assay may be assessed in response to MDP and LPS stimulation in wild-type mice and those lacking NOD2.

Chapter Five

5. Expression of Paneth cell-antimicrobial peptides and enzymes in NOD2-associated Crohn's disease and necrotizing enterocolitis

5.1 Introduction

Although the biology of Paneth cells is not well-defined, these cells are very likely to be integral components of the enteric innate defence and may play a role in the pathogenesis of Crohn's disease and necrotizing enterocolitis (Lala 2003, Keshav 2003).

In Crohn's disease, I have shown that Paneth cells express NOD2, an intracellular protein that mediates cellular activation in response to stimulation with the bacterial antigen muramyl dipeptide (MDP). Mutations in the *NOD2* gene predispose to the development of Crohn's disease in susceptible individuals although the reasons for this are unclear. Fellermann and colleagues (2003) have postulated that a lack of mucosal defensin peptides predispose to the development of Crohn's disease - these investigators have shown that beta defensin 2 and 3 expression is reduced in Crohn's disease but not ulcerative colitis. These investigators postulate further that abnormalities in NOD2 mediated NF-κB-transcription may cause reduced defensin expression (Fellermann 2003), and interestingly, have presented preliminary data showing that human alpha defensin 5 (HD5) and 6 (HD6) expression is reduced in NOD2-related Crohn's disease (Wehkamp 2004). Using *in situ* hybridisation, I therefore determined HD5, HD6, lysozyme and secretory phospholipase A2 Group IIA (sPLA$_2$) expression in tissue sections obtained from patients carrying two, one or no mutations in the NOD2 gene.

I also analysed Paneth cell antimicrobial enzyme expression in necrotizing enterocolitis (NEC), which is a serious and often fatal disease that most commonly affects prematurely born-newborns (Kliegman 1984). In NEC, there is

gross necrosis of the intestinal wall, often containing perforations, and the disorder is microscopically characterised by an acute inflammatory infiltrate, haemorrhage and ischaemic necrosis.

The aetiology of NEC is unknown but it is postulated that the disorder develops when enteric pathogens trigger an excessive and unregulated inflammatory response in the host (Neu 2005). Bacterial infection is common in NEC, and on microscopic examination, bacteria are often identified invading the intestinal wall (Ballance 1990). In addition, bacteria are implicated in causing pneumatosis intestinalis, large areas of gas-filled cysts within the intestinal wall, which are characteristic features of NEC (Ballance 1990).

Paneth cells may play a role in the pathophysiology of NEC as newborn infants have a lower number of Paneth cells than adults, which may predispose newborns to infection. Interestingly, in necrotizing enterocolitis (NEC), there appears to be a lack of lysozyme expression in Paneth cells, which suggests that these cells may play a role in the pathophysiology of this disorder (Coutinho 1998). Paneth cells, which express pro-inflammatory molecules such as TNFα and sPLA$_2$, may therefore also play a role in inflammation – interestingly, although NEC can affect the small and large intestine, inflammation is almost always initiated in the terminal ileum, where Paneth cells are most numerous (Kliegman 1984).

In neonates, a lack of enteric colonisation by commensal flora may predispose to infection and NEC (Fell 2005). Interestingly, in the mouse intestine, Paneth cell antimicrobials, such as angiogenin 4, have specific antimicrobial killing activity and can potentially regulate the composition of the enteric microflora by favouring the growth of commensal, instead of pathogenic, bacteria (Hooper 2003). Abnormal expression of Paneth cell antimicrobials may therefore predispose neonates to NEC, and intriguingly, there is some evidence to suggest that Paneth cell-antimicrobials are be selectively expressed in NEC: Salzman and colleagues (1998) have shown that HD5 and HD6 expression is apparently increased although lysozyme expression is apparently not detected within Paneth cells (Coutinho 1998). Expression of the antimicrobial enzyme, secretory phospholipase A2 Group IIA (sPLA$_2$) has, however, not been analysed in NEC. I

therefore determined whether *s*PLA$_2$, an antimicrobial enzyme that may also play a role in inflammation (Six 2000), is expressed in Paneth cells in NEC and analysed the expression of *s*PLA$_2$, lysozyme and TNFα in tissue sections from newborns with NEC and intestinal atresia.

I also analysed NOD2 expression in NEC and intestinal atresia tissue sections. Although patients with NEC apparently do not carry *NOD2* mutations (Habib 2005), in contrast to Crohn's disease, the level of NOD2 expression may be reduced or deficient in neonates in whom Paneth cell numbers are reduced.

In the last section of this thesis, I analysed the expression of Paneth cell antimicrobials in intestinal epithelial cell lines. Although Paneth cell function can be assessed in mice by measuring antimicrobial secretion, these assays are difficult to perform (Ouellette, personal communication). I therefore determined whether the expression of Paneth cell antimicrobials could be regulated in intestinal epithelial cell lines, which are more convenient to use.

5.2 Results

5.2.1 The expression of Paneth cell antimicrobial peptides and proteins in NOD2-related Crohn's disease

In histologically normal terminal ileal sections, *in situ* hybridisation confirmed that Paneth cells strongly expressed HD5 and HD6 (Figure 5.1).

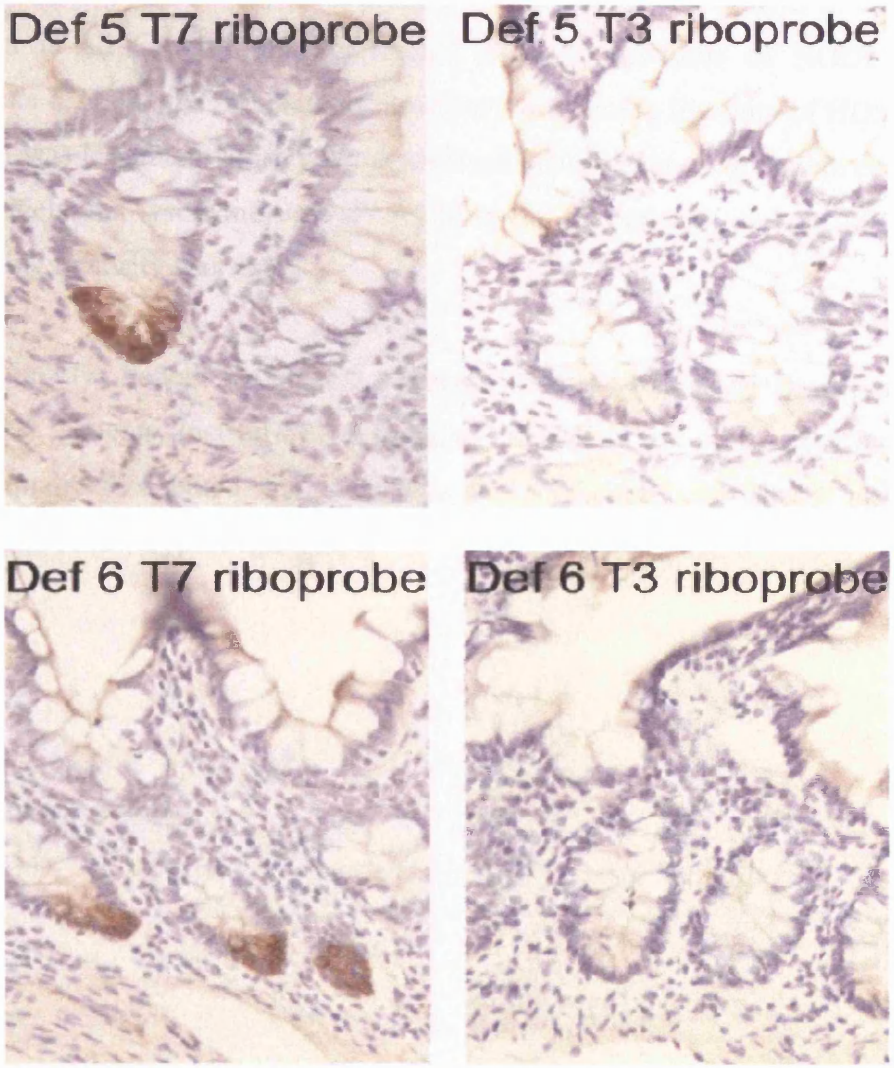

Figure 5.1. Paneth cells express HD5 and HD6 RNA. *In terminal ileal sections hybridised with the HD5 and HD6 anti-sense strand riboprobes (T7 riboprobes), positive staining is confined to Paneth cells located at the bases of the intestinal crypts. Parallel sections hybridised with HD5 and HD6 sense stand riboprobes (T3 riboprobes) show no positive staining, confirming the specificity of detection. All sections were counterstained with haematoxylin and viewed under the 20x objective.*

To analyse Paneth cell antimicrobial peptide and enzyme expression in NOD2-related Crohn's disease, I determined HD5, HD6, *s*PLA_2 and lysozyme expression in tissue sections of 4 patients who were homozygous or compound heterozygous for the NOD2 mutation ($NOD2^{-/-}$), 3 patients who were heterozygous for the NOD2 mutation ($NOD2^{+/-}$), and 3 patients with no NOD2 mutations ($NOD2^{+/+}$).

By *in situ* hybridisation, HD5 and HD6 expression was evident in the terminal ileum in all Crohn's disease-affected patients regardless of NOD2 genotype (Figure 5.2). In $NOD2^{-/-}$ patients, however, the staining intensity of HD5 and HD6 RNA was less than wild-type or control patients (Figure 5.3). Paneth cells stained positively for lysozyme and *s*PLA_2 RNA in all patients, and no difference in staining intensity was noted.

Intriguingly, Paneth cells were aberrantly distributed along the crypt axis in $NOD2^{-/-}$ patients. Instead of localising to the base of the crypt, Paneth cells were abnormally distributed and located at the crypt base and further up the mid-portions of the crypt (Figure 5.2).

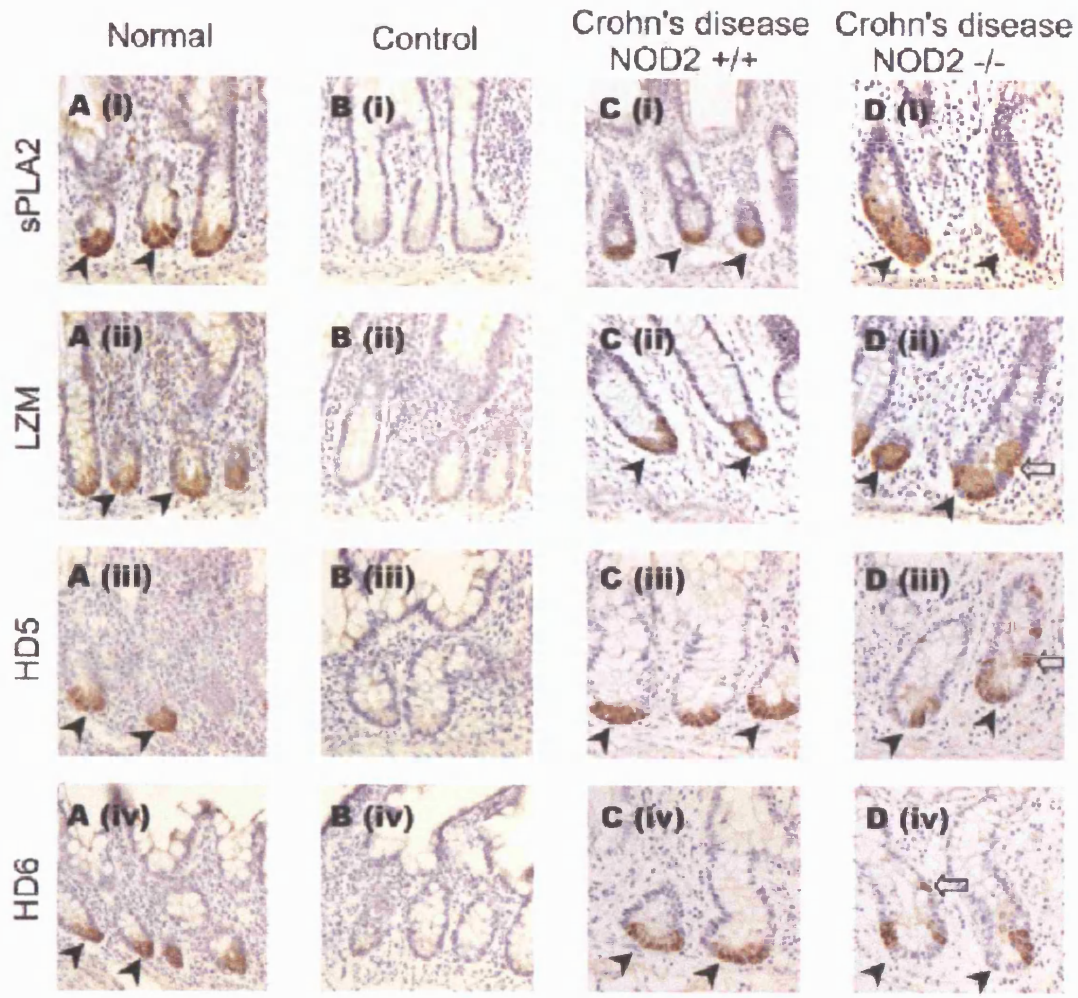

Figure 5.2. $sPLA_2$, lysozyme, and HD5 and HD6 RNA expression in NOD2-related Crohn's disease. *Column 1: (A) In situ hybridization with the digoxigenin-labelled $sPLA_2$ (i), lysozyme (ii), HD5 (iii), and HD6 (iv) antisense strand riboprobes demonstrates positive brown staining in small intestinal crypts (arrowheads) in histologically normal terminal ileum. Column B: Hybridization with the control sense strand $sPLA_2$ (i), lysozyme (ii), HD5 (iii), and HD6 (iv) riboprobes shows no signal, confirming specificity of detection. Column C: (c) In Crohn's disease patients without NOD2 mutations ($NOD2^{+/+}$), positive staining for $sPLA_2$ (i), lysozyme (ii), HD5 (iii), and HD6 (iv) RNA is present in Paneth cells located at the crypt base (arrowheads) in sections hybridized with the digoxigenin-labelled antisense strand riboprobes. Column D: Terminal ileal sections, obtained from patients who are homozygous for the NOD2 mutations ($NOD2^{-/-}$) were hybridized with digoxigenin-labelled antisense strand riboprobes. Positive staining for $sPLA_2$ (i), lysozyme (ii), HD5 (iii), and HD6 (iv) RNA is localized to Paneth cells located in the intestinal crypts (arrowheads) and further away from the crypt base, scattered among non-Paneth cell lineages (open arrows). All sections were counterstained with haematoxylin, and viewed under the 20x objective.*

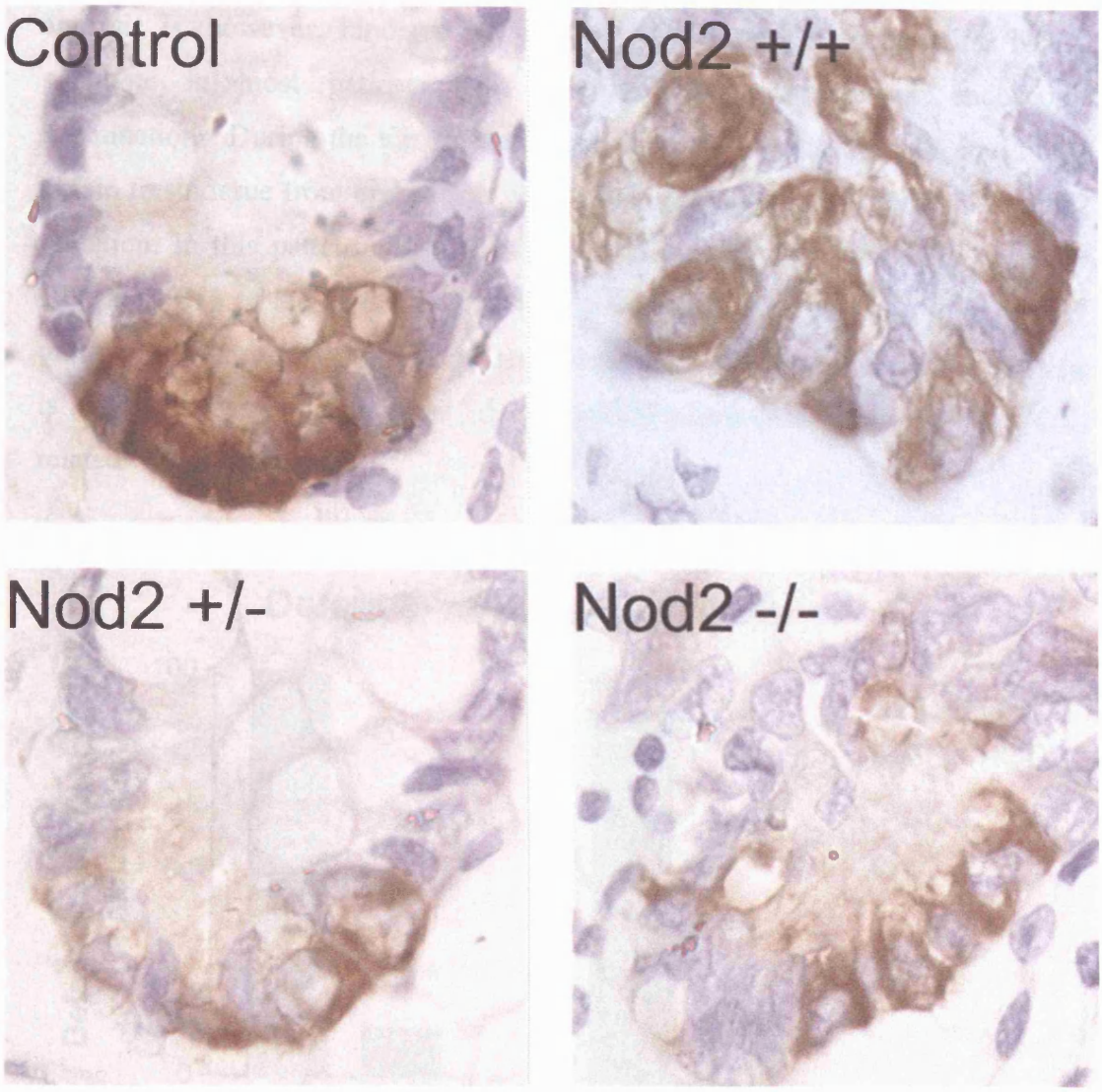

Figure 5.3. HD5 expression in Crohn's disease. *In Crohn's disease ($NOD2^{+/+}$, $NOD2^{+/-}$, $NOD2^{-/-}$), Paneth cells stain positively for HD5 RNA. The staining intensity is greatest in histologically normal tissue (Control), and weakest in $NOD2^{+/-}$ and $NOD2^{-/-}$ sections. All sections were hybridised with HD5 anti-sense strand riboprobes, and counterstained with haematoxylin and viewed under the 100x objective.*

5.2.2 Quantitating alpha defensin expression in Crohn's disease

Although the staining intensity of HD5 RNA is less in patients with NOD2-related Crohn's disease, *in situ* hybridisation is not a quantitative technique and alpha defensin expression is more accurately quantitated, using real-time RT-PCR, in tissue biopsies or specimens obtained from patients with Crohn's disease. This

analysis is, however, hindered by the lack of information concerning NOD2 genotype in most patients that have surgical treatment or endoscopic examinations. During the time taken to complete the present thesis, I could only obtain fresh tissue from one patient who is homozygous for the frameshift NOD2 mutation. In this patient, HD5 and HD6 mRNA expression was approximately 12% and 21% of the levels in a Crohn's disease-affected patient without NOD2 mutations (Figure 5.4). This preliminary observation suggests that further analysis is needed to determine whether HD5 and HD6 expression is altered in NOD2-related Crohn's disease.

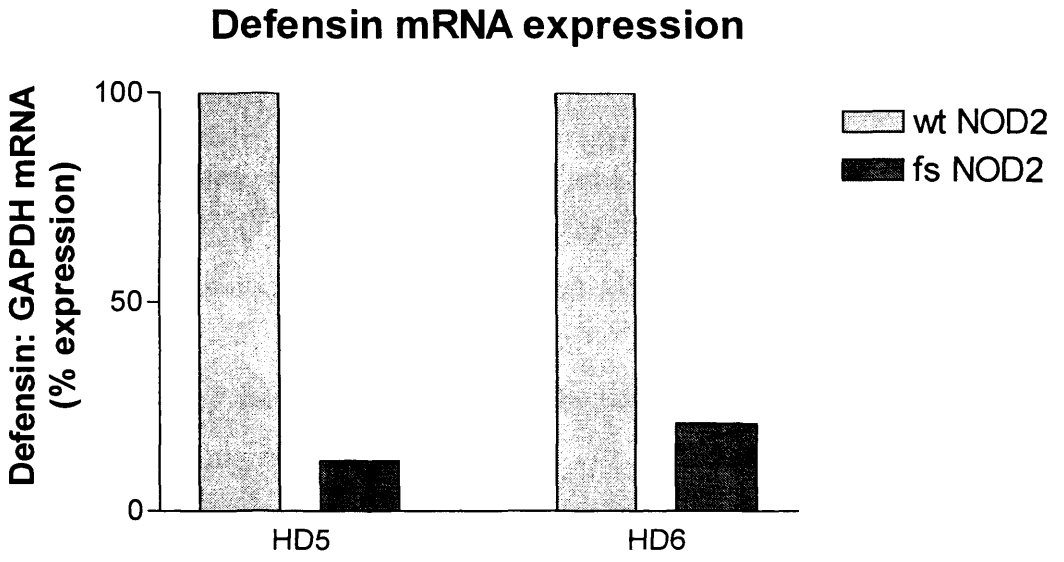

Figure 5.4. HD5 and HD6 expression in a Crohn's disease-affected patient with no NOD2 mutations and a patient homozygous for the NOD2 fs1007insC mutation. *Using quantitative real-time RT-PCR, HD5 and HD6 mRNA expression is reduced in the patient that is homozygous for the NOD2 frameshift mutation (fs NOD2) as compared to a patient carrying wild-type NOD2 gene (wt NOD2). The relative expression of NOD2 and GAPDH mRNA were determined using intron-spanning primers, and the NOD2: GAPDH ratios calculated for each sample. Results are shown as the relative expression compared to expression in the patient with no NOD2 mutations, which is set at 100%.*

5.2.3 Paneth cell antimicrobial expression in necrotizing enterocolitis

Tissue sections were obtained from paraffin embedded intestinal tissue taken from 20 neonates with NEC and 7 with intestinal atresia (representing neonatal controls), as well as 5 adult control subjects. The neonates were treated for necrotizing enterocolitis and intestinal atresia at the Chris Hani-Baragwanath Hospital, Johannesburg, South Africa, and ethical permission for use of this tissue was obtained from the Ethics Committee of the University of the Witwatersrand, Johannesburg. Histologically normal adult terminal ileal sections was obtained from 5 patients treated for colorectal cancer at the Royal Free Hospital, London, and ethical permission for use of this tissue was obtained from the Ethics Committee of the Royal Free Hampstead NHS Trust.

NEC was diagnosed according to the modified Bell criteria (Walsh 1986), which included radiological confirmation. The majority of neonates (19/20) with NEC were premature, and all had severe disease i.e. confirmed Bell Stage IIIB (Walsh 1986) at the time of surgical treatment. NEC was commonly diagnosed at an advanced stage of disease, and the mortality rate in this group was 50%. NEC most commonly involved the terminal ileum (19 of 20 cases) and proximal colon (12 of 20 cases). Most neonates with intestinal atresia were full-term (6/7) and all required curative surgical treatment within the first week of life. One patient in this group, diagnosed with jejunal atresia, died several weeks later from septicaemia.

All NEC sections were characterised by the presence of acute inflammation, haemorrhage and necrosis, which was confined by the muscularis propria in the majority of sections (19 of 20) obtained from the margins of surgically resected tissue. Transmural inflammation and necrosis was commoner in those sections obtained from areas of macroscopic necrosis (15 of 20 sections). The mucosal epithelial layer was extensively damaged by ulceration in 6 of 20 NEC sections; moreover, in all of the remaining NEC sections, a significant proportion of the epithelial layer was damaged by ulceration or necrosis, which is likely to result in an underestimation of Paneth cell-gene and protein expression.

5.2.3.1 Secretory phospholipase A_2 Group IIA ($sPLA_2$) mRNA expression in NEC

By *in situ* hybridization, $sPLA_2$ mRNA was detected in Paneth cells in 2 of 7 neonatal atresia and all histologically normal adult tissue sections. $sPLA_2$ mRNA was detected in 12 of 14 NEC sections, and the hybridisation signal was more intense compared to control neonatal sections. However, the strongest $sPLA_2$ RNA staining intensity was observed in control adult sections (Figure 5.5). By immunohistochemistry, $sPLA_2$ protein was detected in 6 of 7 neonatal atresia sections and in 12 of 14 NEC sections, and all adult sections. Although *in situ* hybridisation is not quantitative, these observations suggest that $sPLA_2$ transcription is increased in NEC as compared to control neonates (Table 5.1).

	Number of cases with positive $sPLA_2$ mRNA hybridisation signal (Percentage)	Number of cases with absent $sPLA_2$ mRNA hybridisation signal (Percentage)
NEC	12 (85.71%)	2 (14.29%)
Neonatal atresia	2* (28.57%)	5 (71.43%)

*Neonate with ileal atresia with ulceration, inflammation and perforation of the terminal ileum.

Table 5.1. $sPLA_2$ mRNA expression in NEC and neonatal atresia sections. *A positive sPLA2 mRNA hybridisation signal was more readily detected in NEC cases than control neonates ($p \leq 0.001$, Chi-squared), suggesting increased transcription in NEC. All NEC, neonatal and adult tissue sections were hybridised in parallel to control for variations in the in situ hybridisation protocol and probe concentration.*

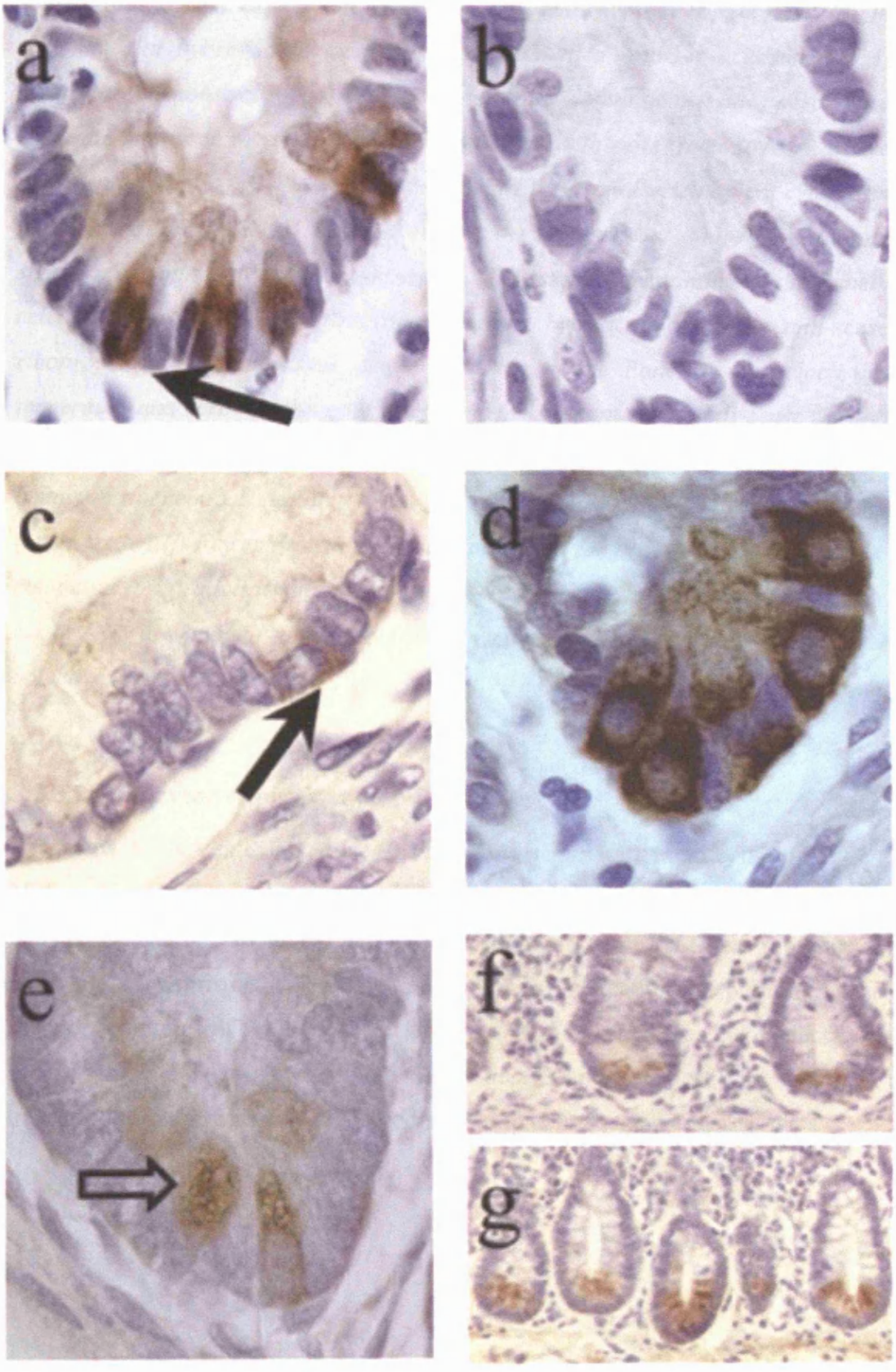
a
b
c
d
e
f
g

Figure 5.5. $sPLA_2$ expression in necrotizing enterocolitis (page 196). *(a) In NEC, in situ hybridisation with digoxigenin-labelled anti-sense strand $sPLA_2$ riboprobe demonstrates positive staining with diaminobenzidine peroxidase substrate mainly in the infra-nuclear region of Paneth cells (thick arrow), where rough endoplasmic reticulum is localised, while the granule-rich apical cytoplasm is unstained. (b) In NEC, hybridisation with the sense-strand riboprobe shows no signal, confirming specificity of detection. (c) Less intense staining in the Paneth cells is noted in neonatal intestinal sections hybridised with the anti-sense riboprobe (d) In adult tissue, intense staining of the Paneth cells, which are numerous and crowd the intestinal crypt, is seen with anti-sense strand hybridisation. (e) Using a rabbit anti- $sPLA_2$ antibody, positive immunohistochemical staining in the apical cytoplasm is seen in Paneth cells (open arrow) (f) Fewer Paneth cells stain positively for protein in neonatal tissue compared to (g) adult tissue. All sections were counterstained with haematoxylin, (a) to (e) were imaged under the 100x objective, and (f) and (g) under the 20x objective.*

5.2.3.2 Lysozyme expression in NEC

Lysozyme mRNA is detected by *in situ* hybridisation in Paneth cells in 7 of 14 NEC sections, but not in control neonatal sections. An intense hybridisation signal is noted in Paneth cells in all adult sections (Figure 5.6). In NEC, the presence of lysozyme is confirmed by immunohistochemical detection of protein in the secretory granules of the Paneth cells, and lysozyme protein was also detected in lamina propria leukocytes. (Figure 5.6) These results suggest that lysozyme transcription is increased in NEC as compared to control neonates.

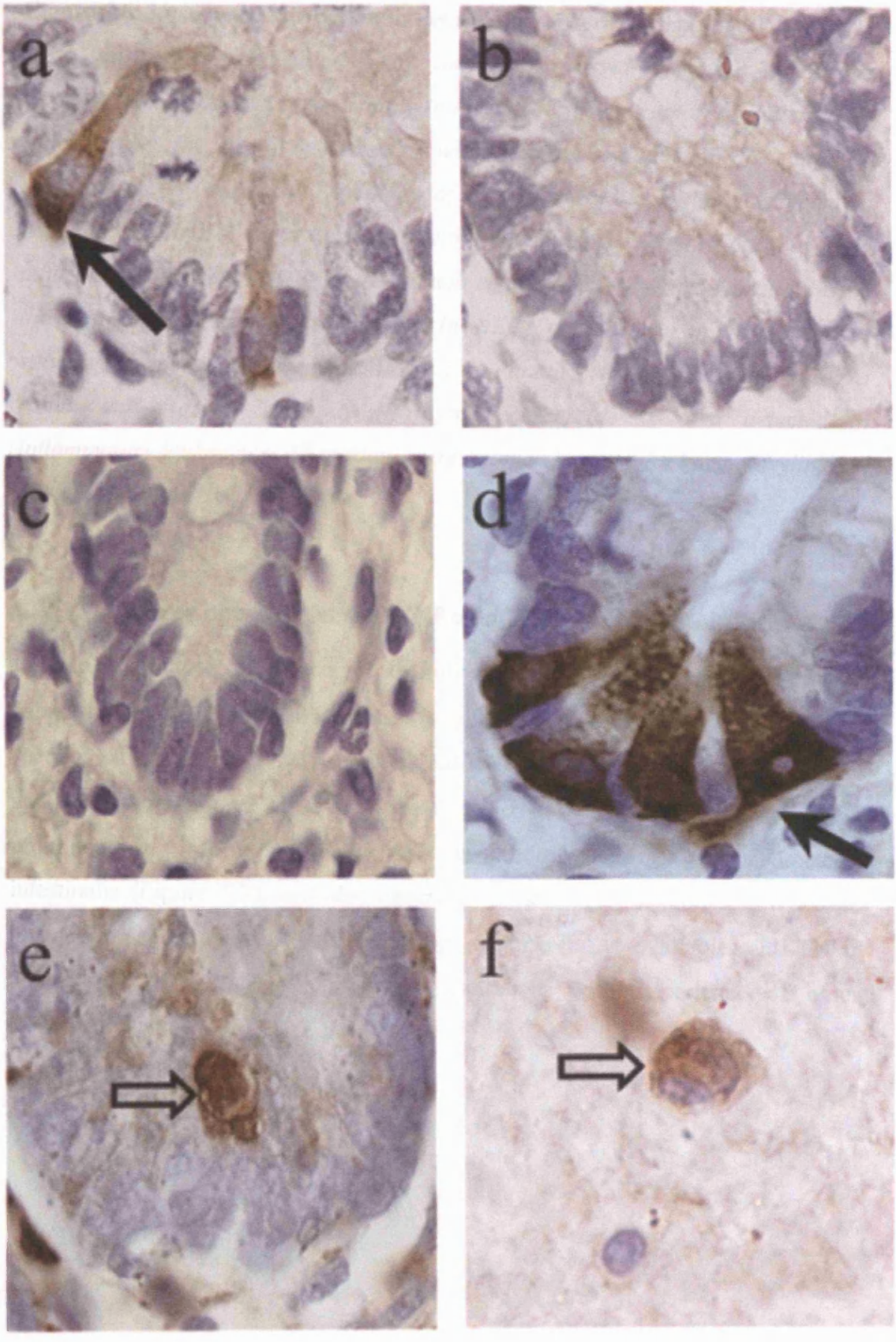
a
b
c
d
e
f

Figure 5.6. Lysozyme expression in necrotizing enterocolitis (page 198). *(a) In NEC, in situ hybridisation with anti-sense strand lysozyme riboprobe demonstrates positive staining mainly in the infra-nuclear region of Paneth cells (thick arrow). (b) control hybridisation with the sense-strand riboprobe shows no signal in NEC, confirming specificity of detection. (c) No staining is noted in neonatal intestinal sections hybridised with the anti-sense strand riboprobe. (d) In adult tissue, intense staining of the Paneth cells is seen after hybridisation using the anti-sense strand riboprobe. (e) In NEC, positive immunohistochemical staining, in the apical granules, is seen in Paneth cells (open arrow) using a rabbit anti-lysozyme antibody (f) Lysozyme peptide is also detected in inflammatory leukocytes. All sections were counterstained with haematoxylin, and imaged under the 100x objective*

5.2.3.3 Tumour necrosis factor (TNFα) mRNA expression in NEC

In neonatal sections, Paneth cells constitutively expressed TNFα mRNA in 6 of 7 cases. In NEC, TNFα mRNA expression in Paneth cells was observed in 12 of 14 sections, and a strong hybridisation signal was evident in infiltrating leukocytes and tissue macrophages (18 of 20 cases). TNFα RNA expression was especially prominent in infiltrating leukocytes surrounding regions of pneumatosis intestinalis (Figure 5.7), and also observed in circulating leukocytes. We were unable to detect TNFα protein using commercially available anti-TNFα monoclonal or polyclonal antibodies, consistent with experience of other investigators.

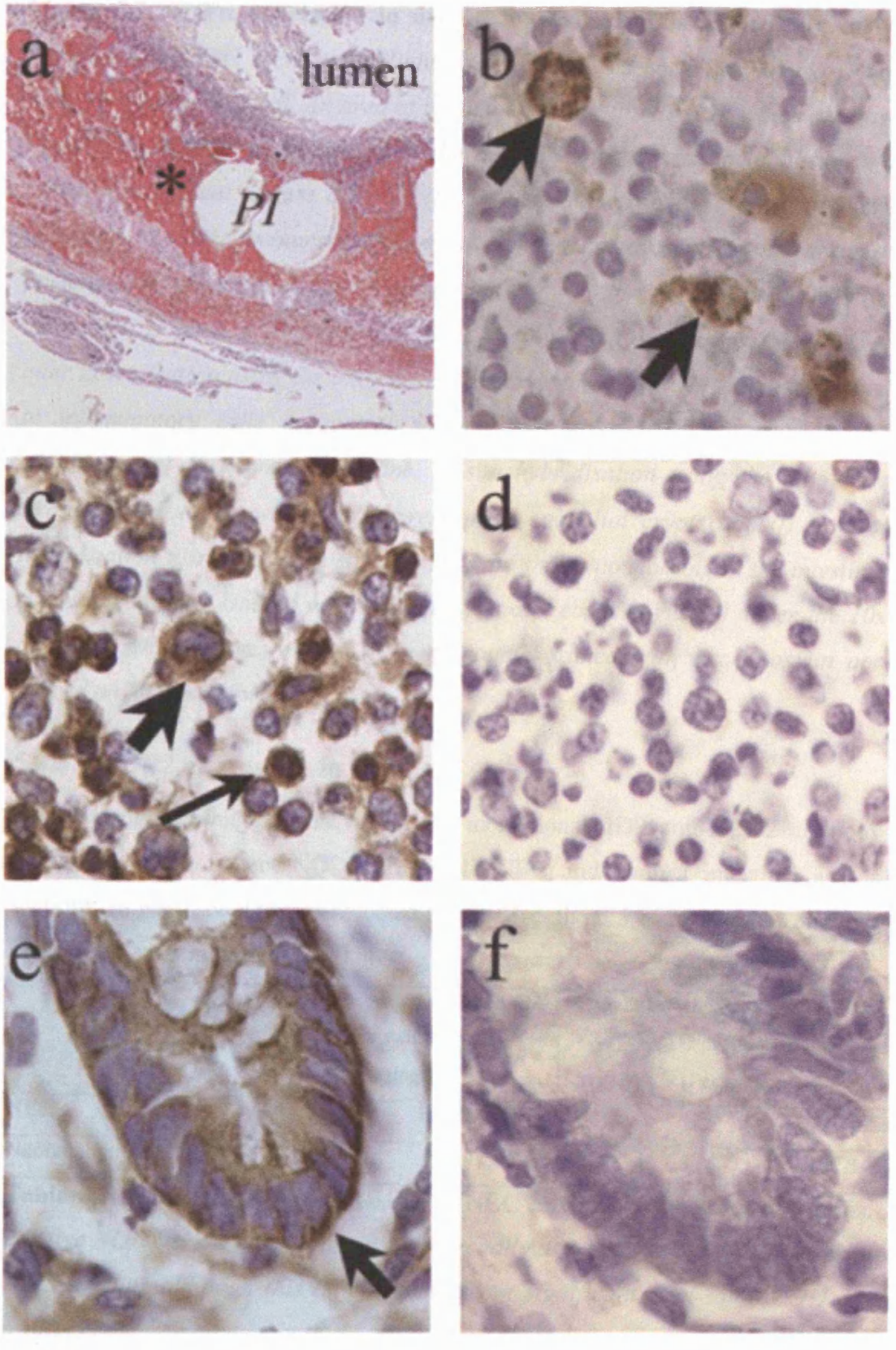
a
lumen
*
PI
b
c
d
e
f

Figure 5.7. TNFα expression in necrotizing enterocolitis (page 200). *(a) A representative NEC section, highlighting transmural necrosis and haemorrhage within the intestinal wall. An area of pneumatosis intestinalis (PI), which are gas-filled cysts thought to be caused by the products of bacterial metabolism, is a typical histological feature of NEC. (b) Numerous macrophages (thick arrows), identified by CD68 immunohistochemical staining are present around areas of pneumatosis intestinalis [see asterisk in (a)]. (c) In NEC, intense TNFα expression is seen in macrophages (thick arrow) and lymphocytes (thin arrow) after hybridisation using the anti-sense strand riboprobe. (d) No staining is noted in inflammatory cells in control sections hybridised with the sense strand riboprobe. (e) In neonatal intestine, in situ hybridisation using the anti-sense strand riboprobe shows TNFα expression in epithelial crypt cells (f) Control hybridisation using the sense strand riboprobe shows no staining in the intestinal crypts. Image (a), stained with haematoxylin and eosin is viewed under the 10x objective while images (b) to (f) were counterstained with haematoxylin and viewed under the 100x objective.*

5.2.3.4 NOD2 expression in NEC

I used immunohistochemistry, using the monoclonal 2D9 anti-NOD2 antibody (Ogura 2003), to detect NOD2 protein in NEC and control intestinal atresia sections. In NEC, NOD2 was detected in Paneth cells in 3 of 14 sections and in 3 of 7 atresia sections (Figure 5.8).

	Number of case with positive NOD2 protein staining (Percentage)	Number of cases with negative NOD2 protein staining (Percentage)
NEC	3 (21.43%)	11 (78.57%)
Neonatal atresia	3 (42.86%)	4 (57.14%)

Table 5.2. NOD2 protein expression in NEC and neonatal atresia sections. *Positive NOD2 protein staining was more readily detected in control atresia than NEC sections although this difference was not significant (Chi-squared =1.03; p=0.31).*

I expected that NOD2 protein expression would be more readily detected in cases of NEC, which is characterised by severe inflammation, than cases of atresia, but

this was not so. I also did not detect NOD2 mRNA expression in NEC or atresia sections by *in situ* hybridisation. Immunohistochemistry and *in situ* hybridisation, however, may not detect low levels of NOD2 expression in neonates and further analyses are therefore required to confirm this observation as low levels of NOD2 expression in neonatal Paneth cells may predispose neonates to enteric infection and the development of NEC.

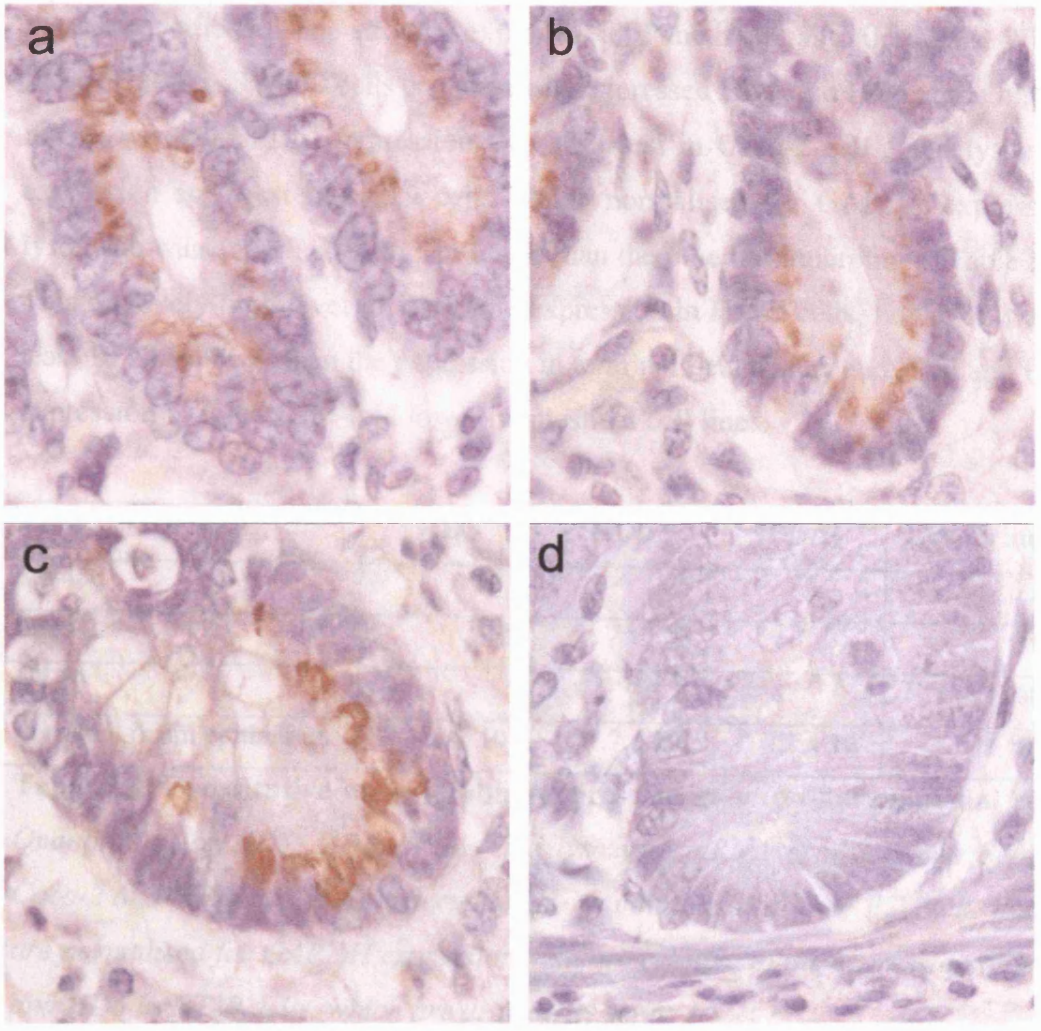

Figure 5.8. NOD2 expression in necrotizing enterocolitis. *(a) In NEC, immunohistochemical staining, using the 2D9 monoclonal antibody, localises NOD2 protein to Paneth cells within the intestinal crypts. (b) In intestinal atresia, positive NOD2 staining is noted in Paneth cells. (c) By comparison, in adult terminal ileal tissue, NOD2 protein appears to stain more intensely in Paneth cells (d) Control terminal ileal section stained with an unrelated primary antibody shows no positive immunohistochemical staining. All sections were stained with haematoxylin and viewed under the 100x objective.*

5.2.4 Expression of Paneth cell antimicrobial proteins in intestinal epithelial cells:

In the absence of an *in vitro* model to assess Paneth cell function, I determined if immortalised intestinal epithelial cells may be suitable for this purpose. I therefore determined the baseline expression of Paneth cell antimicrobial proteins, using real-time RT-PCR, in SW480, Caco-2 and HT29 cells. These analyses showed that no specific cell line strongly expressed all Paneth cell antimicrobials. Within these cell lines, SW480 cells constitutively expressed HD5 and HD6 at the highest levels, whereas *s*PLA$_2$ expression was strongest in Caco-2 cells, and lysozyme expression strongest in HT29 cells. When normalised for GAPDH expression, lysozyme was expressed at higher levels than the other antimicrobials (Table 5.3). This relatively high level of lysozyme expression in HT29 cells, however, was at least 10^4-fold lower than the expression in terminal ileal tissue, and HD5 and HD6 expression is at least 10^6-fold lower in intestinal cell lines.

	HD5	HD6	*s*PLA$_2$	Lysozyme
SW480	643	25	2	2
Caco-2	25	65	352	30
HT29	1	1	2	1268
Terminal ileum epithelium	3×10^9	1.7×10^9	2.2×10^8	1×10^8

Table 5.3. Constitutive antimicrobial expression in intestinal epithelial cells. *Quantitation of HD5, HD6, sPLA$_2$ and lysozyme mRNA expression in SW480, Caco-2 and HT29 cell lines, determined by quantitative real-time RT-PCR. Values are normalised for GAPDH expression, and are relative to the expression of HD5 and HD6 in HT29 cells, which are arbitrarily set as 1.*

5.2.4.1 Regulation of Paneth cell-antimicrobial expression in intestinal epithelial cells

To determine whether Paneth cell-antimicrobial expression could be enhanced in intestinal epithelial cells, I stimulated these cells with nutrients, cytokines and hormones such as zinc, GM-CSF and IL-4. *In vivo*, Paneth cells contain large amounts of zinc (Kobayashi 1983), and have recently been shown to contain GM-CSF (Fukuzawa 2003). I also stimulated intestinal epithelial cells with serotonin

as Paneth cells express receptors for this hormone (Fiorica-Howells 2002). Dexamethasone and IL-4 were used as stimulants as these substances are postulated to influence maturation of the intestinal epithelial barrier and improve host resistance to enteric infection (Madsen 1997). Thyroid hormone (T3) and retinoic acid were also used as T3 is thought to regulate protein synthesis and secretion in cells that contain large amounts of endoplasmic reticulum (Glantschnig 1996) - such as Paneth cells. All cells were harvested after 48 hours of stimulation with nutrients, cytokines and hormones.

Zinc supplementation caused a small increase (1.6-fold) in HD6 mRNA expression in Caco-2 cells, as assessed by quantitative real-time RT-PCR, and did not induce or enhance HD5 expression in any cell line tested. Serotonin and GM-CSF did not enhance HD5 or HD6 expression in any cell line. Stimulation with dexamethasone increased HD6 expression 6.5-fold (Figure 5.9) in Caco-2 cells and induced expression in HT29 cells. In Caco-2 cells, co-stimulation with dexamethasone and zinc did not cause a synergistic increase in HD6 expression. Dexamethasone did not enhance HD6 expression in SW480 cells and did not enhance or induce the expression of HD5 expression in any of the cell lines. Serotonin, IL-4, GM-CSF and retinoic acid did not significantly alter HD5 or HD6 expression in any cell line.

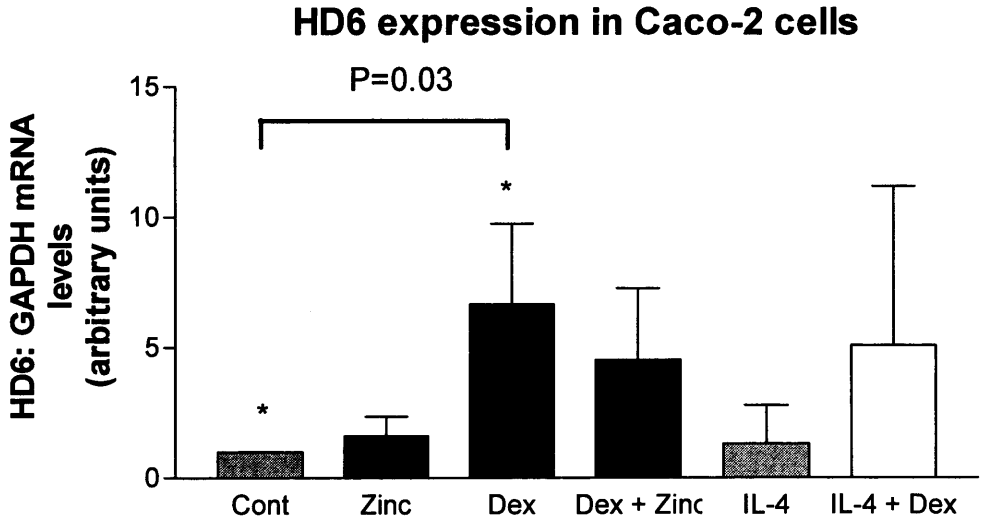

Figure 5.9. HD6 expression in Caco-2 cells. *Using quantitative real-time RT-PCR, HD6 mRNA expression was enhanced in Caco-2 cells after 48 hours of*

dexamethasone and zinc stimulation. The increase in HD6 expression induced by dexamethasone was statistically significant (P=0.03). The relative expression of HD6 and GAPDH mRNA were determined using intron-spanning primers, and the HD6: GAPDH ratios calculated for each sample. Results are shown as the relative expression compared to the level in unstimulated (control) Caco-2 cells, which was arbitrarily set as 1 unit. Values in the figure are expressed as the mean ± SEM (Standard error of the mean). Experiments were performed three times, and differences between stimulated and control cells were analysed by two-tailed, non-paired t test, with a P value <0.05 indicative of statistical significance.

Thyroid hormone (T3) stimulation enhanced HD5 expression 3-fold in SW480 cells (Figure 5.10), but did not enhance HD6 expression.

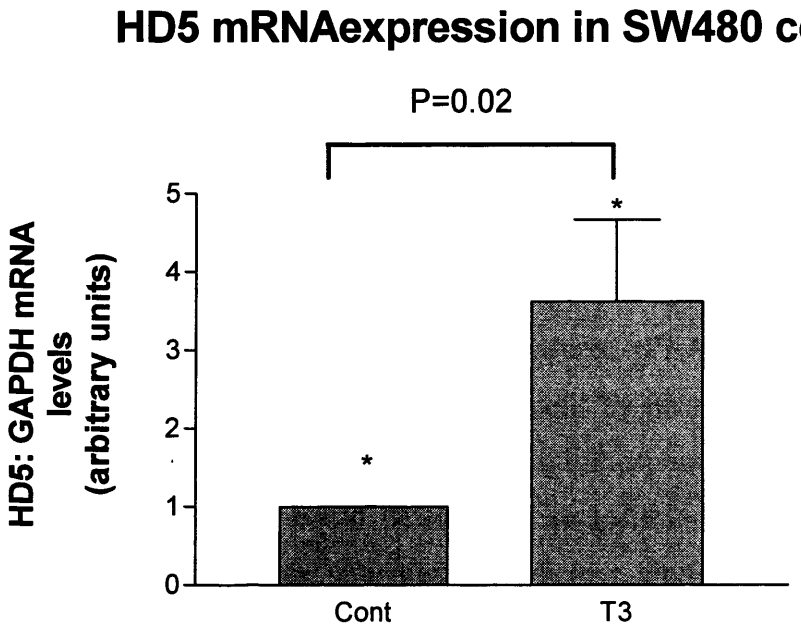

Figure 5.10. HD5 expression in SW480 cells. *Using quantitative real-time RT-PCR, HD5 mRNA expression was enhanced in SW480 cells after 48 hours of thyroid hormone (T3) stimulation. The increase in HD5 expression induced by T3 was statistically significant (P=0.02). The relative expression of HD5 and GAPDH mRNA were determined using intron-spanning primers, and the HD5: GAPDH ratios calculated for each sample. Results are shown as the relative expression compared to the level in unstimulated (control) SW480 cells, which was arbitrarily set as 1 unit. Values in the figure are expressed as the mean ±*

SEM (Standard error of the mean). Experiments were performed three times, and differences between stimulated and control cells were analysed by two-tailed, non-paired t test, with a P value <0.05 indicative of statistical significance.

There were small but significant increases in HD6 and HD5 mRNA after dexamethasone and T3 stimulation in Caco-2 and SW480 cells respectively. Overall, in intestinal epithelial cell lines, I did not find that HD5 and HD6 expression was dramatically regulated by stimulation with various agents.

5.2.4.2 Responses of intestinal epithelial cells to bacterial products

Paneth cells secrete antimicrobial peptides in response to bacteria and bacterial products including lipopolysaccharide (LPS) and muramyl dipeptide (MDP). By RT-PCR, I have shown that intestinal epithelial cells express Paneth cell antimicrobials, albeit weakly. If these intestinal epithelial cell lines are to be used to assess Paneth cell function, these cells should secrete antimicrobial proteins in response to bacteria or bacterial products. I therefore assessed if there was evidence of such a secretory pathway in Caco-2 and HT29 cells.

In Caco-2 cells that were stimulated with LPS, I was unable to detect *s*PLA_2 protein secretion by immunoblotting. I also measured *s*PLA_2 enzyme activity in the culture supernatants of LPS-treated Caco-2 cells by measuring the amount of radiolabelled palmitate released from a dipalmitoyl phosphatidylcholine (lecithin) substrate. No free palmitate could be detected in lecithin substrates that were incubated with the cell culture supernatants, whereas almost all of the lecithin substrate (98.85%) was hydrolysed in control preparations containing bee venom *s*PLA_2 (This enzyme was used because it is closely related to human *s*PLA_2, which is not available commercially and cannot be readily isolated from human clinical material). These results suggest that *s*PLA_2 secretion by Caco-2 cells is minimal, and cannot be induced by LPS stimulation. RT-PCR analysis confirmed that *s*PLA_2 expression was not increased in Caco-2 cells treated with LPS.

In HT29 cells, which secrete lysozyme into the culture supernatant, MDP-treatment did not alter the amount of lysozyme secretion, as determined by

immunoblotting (I acknowledge the assistance of my colleague, Dr Annabel Bromfield, who performed the immunoblot analysis). Using quantitative real-time RT-PCR, lysozyme mRNA expression was not significantly different in the control and MDP-stimulated HT29 cells.

I did not assess HD5 and HD6 secretion by SW480 cells, using immunoblotting, as there are no suitable commercial antibodies. Overall, these results suggest that intestinal epithelial cell lines cannot be used to assess Paneth cell function *in vitro*.

5.3 Discussion

5.3.1 Paneth cell antimicrobial peptide and enzyme expression in NOD2-related Crohn's disease

The mechanisms that predispose patients with NOD2 mutations to develop ileitis are unknown although it has been postulated that alpha defensin expression is reduced in Crohn's disease-affected carrying *NOD2* mutations (Fellermann 2003). In the present study, my results indicate that Paneth cells express antimicrobials, irrespective of NOD2 gene status. These observations were made using *in situ* hybridisation which is not a quantitative technique although HD5 and HD6 RNA staining appeared to be less prominent in patients carrying two *NOD2* mutations. A preliminary observation also suggests that HD5 and HD6 expression is reduced in a patient homozygous for the NOD2 mutations, and my observation appears consistent with the results reported by Wehkamp and colleagues (2004), who described reduced HD5 and HD6 mRNA expression in patients with NOD2-related Crohn's disease.

These observations, however, should be interpreted with caution as gene quantitation of Paneth cell products in intestinal tissue (biopsy material or resected surgical tissue) is not without problems. In real-time RT-PCR quantitation, a housekeeping gene is used as the reference gene to normalise expression of the target gene. The level of expression of a housekeeping gene is, however, dependant on the amount of tissue analysed and Paneth cell-specific mRNA targets may be erroneously over- or underestimated by real-time RT-PCR. For example, HD5 expression may be overestimated in small-sized biopsies that containing only mucosal tissue, or underestimated in larger-sized biopsies containing a greater proportion of lamina propria tissue. Ideally, a suitable reference gene would not be regulated by inflammation or infection and would only be expressed in Paneth cells.

To ascertain that Paneth cells play a role in the pathophysiology of NOD2-related Crohn's disease will require further studies. The regulation of HD5 and HD6 expression is not well understood and it may be possible that HD5 and HD6

transcription is suppressed if abundant defensin peptides are present within Paneth cell granules. Initially, therefore, it will be important to determine the expression of HD5 and HD6 peptides in patients with ileitis. Next, the function of Paneth cells, containing wild-type and mutant NOD2 proteins, needs to be assessed in patients with Crohn's disease. Secretion assays are a method of assessing Paneth cell function and we have preliminary data showing that human Paneth cells secrete antimicrobial enzymes and peptides in response to stimulation by bacterial antigens, including LPS and MDP (A. Bromfield and S. Keshav, unpublished data). Secretion assays can therefore be performed using tissues collected from a larger number of patients, including those carrying NOD2 gene mutations, to help to clarify a potential role for Paneth cells in the pathophysiology of ileitis (This study would likely require collaboration between larger IBD centres so that tissues can be collected from sufficient number of patients undergoing surgery, including those with the NOD2 mutations).

5.3.2 Paneth cell antimicrobial peptide and enzyme expression in necrotizing enterocolitis (NEC)

An increasing body of evidence shows that, with the intestinal milieu at least, Paneth cells are important and crucial elements of the innate immune system. My findings are consistent with this view, as I showed that in NEC, the expression of sPLA$_2$ and lysozyme is enhanced in Paneth cells, most likely in response to enteric infection. In the present study, in contrast to previous reports, I could identify lysozyme RNA and protein expression in Paneth cells in NEC sections by *in situ* hybridisation and immunohistochemistry. Although the baseline levels of antimicrobial peptides appear to be lower in newborn infants than adults, in NEC, Paneth cells are capable of increased antimicrobial production.

I also analysed NOD2 expression in NEC as lower levels of NOD2 expression may predispose neonates to enteric infection and subsequent NEC. In contrast to lysozyme and sPLA$_2$ RNA expression, I did not detect NOD2 RNA expression in NEC using *in situ* hybridisation. It is unlikely, however, that NOD2 RNA expression is absent in NEC as NOD2 protein could be detected in some NEC sections. Due to the extensive epithelial destruction in NEC, it is likely that I have

underestimated gene expression in Paneth cells, including NOD2 expression. NOD2 protein could be detected more readily in neonates with intestinal atresia as compared to those with NEC although NOD2 protein was most prominently expressed in adult Paneth cells. It is probably better, however, to quantitate NOD2 expression by real-time RT-PCR in resected intestinal tissue to determine if expression is lower in neonates who develop NEC.

Paneth cells may play a role in the development of intestinal inflammation as they express TNFα (Keshav 1990). Consistent with the findings of previous investigators, my results confirm that Paneth cells express this pro-inflammatory cytokine.

My results also emphasise the difficulty of using intestinal epithelial cells to assess Paneth cell function *in vitro*. In the first instance, levels of Paneth cell-derived antimicrobials are at least $10^{4\text{-}6}$- fold lower than levels expressed by Paneth cells contained in the mucosal epithelium. I attempted to induce defensin expression in intestinal epithelial cells by maintaining them in culture medium enriched with nutrients such as zinc, but met with limited success. Further studies need to be undertaken to determine whether the modest increase in HD6 mRNA expression, induced by dexamethasone, in Caco-2 can be enhanced further. Even if alpha defensin expression is dramatically enhanced in cell lines, evidence of a secretory pathway in these cells is required if they are to be used to study Paneth cell function. I could not demonstrate that these cells secreted antimicrobial enzymes in response to stimulation with bacterial products. Cell lines cannot therefore be used to assess Paneth cell function at present as they express very low levels of HD5 and HD6. Nonetheless, if it is true that alpha defensin deficiency is important in the pathogenesis of NOD2-related Crohn's disease, intestinal epithelial cell lines could be used to identify agents that enhance HD5 and HD6 expression.

In the foreseeable future, studies evaluating the role of NOD2 in Paneth cells would have to be performed in isolated Paneth cells or crypt epithelial cells obtained from patients that are wild-type and homozygous for the NOD2

genotype. These studies would probably involve several centres, taking into account the frequency of the NOD2 mutations in Crohn's disease, and the proportion of patients that require surgical resection after failing medical treatment. The effects of NOD2 mutations on antimicrobial secretion could be assessed by stimulating these cells with various bacterial products, although to test the hypothesis that NOD2 functions as an intracellular receptor for MDP who require specialised technical expertise as Paneth cells normally respond to extracellular MDP stimulation. Also for accurate quantitation, antimicrobial expression should be quantified in isolated Paneth cells or crypt epithelial cells, rather than in whole-tissue intestinal segments.

Chapter six

6. General discussion

Until very recently, the function of Paneth cells, first described over 100 years ago, has remained obscure. Recently, however, the biological significance of these cells appears to be much more clearly defined – Paneth cells play a critical role in the innate intestinal defences by affording protection against potentially lethal bacterial pathogens (Salzman 2003). In addition, recent reports suggest that these cells play a role in the pathogenesis of intestinal inflammation (Keshav 1990, Kamal 2001), and Paneth cells may play a role in the pathogenesis of Crohn's disease, necrotising enterocolitis and cystic fibrosis (Lala 2003, Coutinho 1998, Clarke 2004).

There are several hypothetical possibilities in which Paneth cells may play a role in the pathogenesis of intestinal inflammation (Keshav 2003). Firstly, Paneth cells secrete antimicrobials that may regulate the composition of the intestinal microflora and prevent infection by pathogenic bacteria. These cells also produce pro-inflammatory mediators, such as sPLA$_2$ and TNFα, which may interact with the surrounding epithelial cells and lamina propria mononuclear cells. In addition, Paneth cell products may also regulate stem cell and precursor cell differentiation and function, thus altering the characteristics of the crypt and villus epithelium (Figure 6.1).

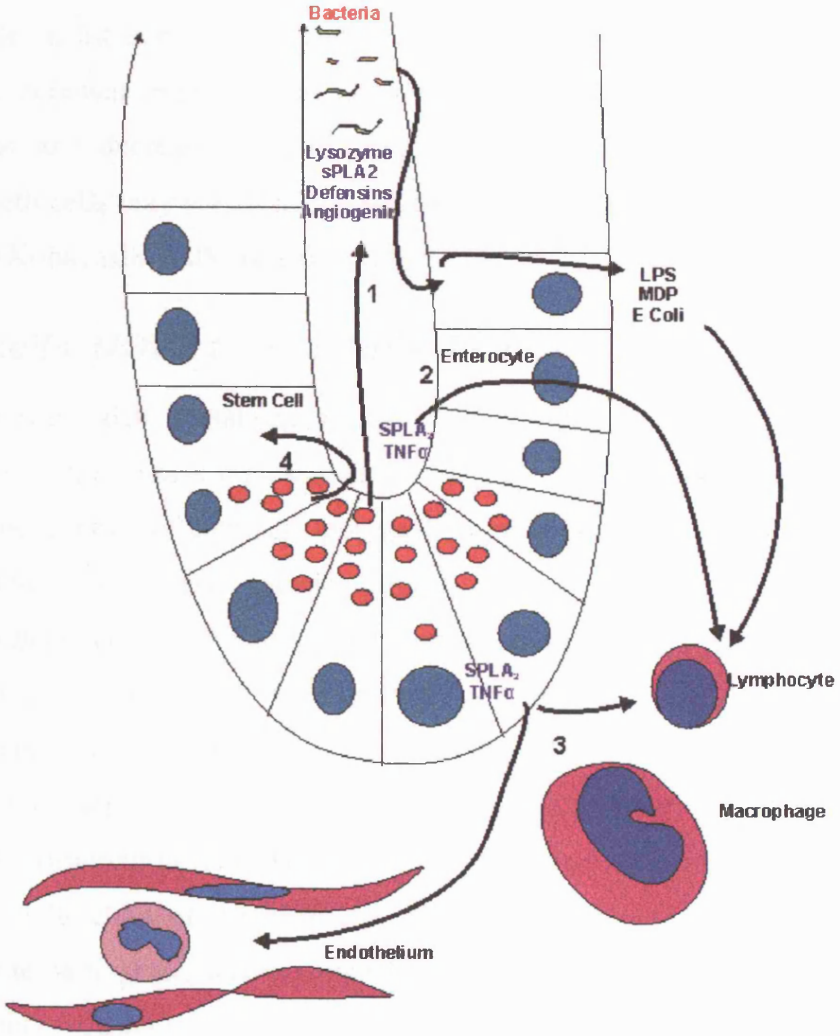

Figure 6.1. *Paneth cells potentially play a role in the development of intestinal inflammation in the following ways: By producing and secreting pro-inflammatory molecules such as TNFα, $sPLA_2$ and defensins which may interact with epithelial cells (1) or lamina propria leukocytes after reabsorption across the epithelium (2); by direct secretion of pro-inflammatory molecules into the basolateral space (3); and by regulating stem cell and precursor cell differentiation and function, thus altering the characteristics of the crypt and villus epithelium(4). Bacteria and bacterial antigens (generated by the action of Paneth cell antimicrobials), such as lipopolysaccharide (LPS) and muramyl dipeptide (MDP), may also trigger inflammation. Figure adapted from Keshav (2003).*

Thus far, there is no good experimental evidence to suggest that Paneth cells play an important role in intestinal inflammation although recent data, which show decreased alpha defensin expression in Crohn's disease-affected patients with *NOD2* mutations and decreased cryptdin expression in mice lacking NOD2, suggest that Paneth cells may play a role in the pathogenesis of NOD2-associated Crohn's disease (Kobayashi 2005, Wehkamp 2004).

6.1 Paneth cells, NOD2 and Crohn's disease

The recent discovery that mutations in the *NOD2* gene predispose to the development of Crohn's disease represent an exciting breakthrough in the efforts to define the genetic basis of common, polygenic human diseases (Ogura 2001, Hugot 2001). The *NOD2* gene encodes for an intracellular protein that is postulated to regulate cellular activation after interacting with muramyl dipeptide (MDP). MDP is a component of the peptidoglycan cell wall layer of gram-positive and gram-negative bacteria (Inohara 2003, Girardin 2003). It is hypothesised that mutant NOD2 proteins do not regulate cellular activation in response to MDP stimulation, leading to the development of chronic intestinal inflammation. The function of the NOD2 protein, however, is not definitively established and the pathogenic mechanisms whereby mutant NOD2 proteins lead to the development of Crohn's disease remains to be defined (Murray 2005).

In this thesis, I showed that Paneth cells prominently express NOD2 – I had earlier hypothesised that these cells are likely to express NOD2 as Paneth cells secrete antimicrobial products, by as yet undefined mechanisms, in response to stimulation with bacteria or bacterial products including MDP. In addition, intestinal inflammation in NOD2-associated Crohn's disease localises predominantly to the terminal ileum, which was not easily accounted for by the prevailing view that NOD2 expression is restricted to circulating monocytes (Ogura 2001). Paneth cells, on the other hand, are most numerous in the terminal ileum and also prominently express NOD2 (Lala 2003, Ogura 2003). There is now evidence to suggest that Paneth cells are implicated in the pathogenesis of NOD2-associated Crohn's disease, although the mechanism by which NOD2 influences Paneth cell function requires elucidation.

Paneth cells secrete an array of potent antimicrobial proteins, such as alpha defensins 5 (HD5) and 6 (HD6), in response to stimulation by bacteria and bacterial products (Ayabe 2000). Interestingly, Wehkamp and colleagues (2004) have shown that HD5 and HD6 mRNA expression is reduced in NOD2-related Crohn's disease. These investigators analysed Paneth cell-antimicrobial expression in intestinal biopsies from patients with Crohn's disease, and showed that HD5 and HD6, but not *s*PLA_2 and lysozyme, mRNA expression was reduced in inflamed regions of the terminal ileum. Moreover, a more profound reduction in HD5 and HD6 mRNA expression was noted in patients with NOD2-related Crohn's disease. In the colon, which contains metaplastic Paneth cells, there is increased expression of HD5 and HD5 mRNA in patients carrying the wild-type *NOD2* gene, but not in patients homozygous for the *NOD2* mutations. The expression of the pro-inflammatory cytokine TNFα was similar in all patients, irrespective of *NOD2* genotype. Notwithstanding the difficulties in accurately quantitying Paneth cell gene expression, Wehkamp and colleagues (2004) results suggest that further studies are required to determine the mechanism by which alpha defensin expression might be regulated by NOD2.

Using a murine model, Kobayashi and colleagues (2005) provide further evidence that NOD2 regulates alpha defensin expression. By disrupting the central nucleotide oligomerisation domain (NOD) of the *NOD2* gene, they generated mice that do not express NOD2 protein ($Nod2^{-/-}$ mice). These $Nod2^{-/-}$ mice were outwardly healthy and displayed normal lymphoid and myeloid cellular composition in the thymus and spleen. In addition, these mice did not develop intestinal inflammation and were not more susceptible to dextran sulphate-induced colitis. In $Nod2^{-/-}$ mice, however, some Paneth cell alpha defensins were expressed at much lower levels as compared to control mice.

Kobayashi and colleagues (2005) infected $Nod2^{-/-}$ and control mice with the pathogen *Listeria monocytogenes* by intravenous or peritoneal injection and by intragastric dosing. Interestingly, $Nod2^{-/-}$ and control mice were equally susceptible to *L. monocytogenes* introduced intravenously or via peritoneal injection, but $Nod2^{-/-}$ mice showed increased susceptibility to intestinal *L.*

monocytogenes infection. In intestinal *L. monocytogenes* infection, increased rates of bacterial translocation were measured in $Nod2^{-/-}$ mice.

These investigators then used microarray analysis to identify the genes induced in intestinal infection, and showed that a subgroup of murine alpha defensin (or cryptdin) genes was induced by *L. monocytogenes* infection. Interestingly, Paneth cell defensin-related cryptdin 2 (*Defcr2*) and Defcr-related sequence 10 (*Defcr-rs 10*) expression was low in $Nod2^{-/-}$ mice, as compared to controls, prior to enteric infection. Surprisingly, in $Nod2^{-/-}$ mice, intestinal infection further lowered *Defcr2* and *Defcr-rs 10* expression. Overall, these results suggest that the expression of certain cryptdins is dependant on NOD2. It is possible, therefore, that NOD2 plays an important and specific role in protecting against intestinal bacterial infection by regulating Paneth cell defensin expression.

The potential regulation of alpha defensin expression by NOD2, however, must be more clearly defined to show that Paneth cells play a role in the pathophysiology of Crohn's disease. Presently, the regulation of alpha defensin expression is not well understood: there is evidence to suggest that specific bacterial pathogens may regulate HD5 expression (Salzman 2003b) and an analysis of HD5 expression in human diseases such as necrotising enterocolitis (Salzman 1998), inflammatory bowel disease (Cunliffe 2001), HIV-related cryptosporiodis (Kelly 2004, Dhaliwal 2003) and intestinal metaplasia of the upper gastrointestinal tract (Shen 2005) may also provide further clues.

Salzman and colleagues (2003b) have shown that specific enteric pathogens can inhibit Paneth cell alpha defensin expression in mice. These investigators determined that the human pathogen *Salmonella* serovar Typhimurium inhibits cryptdin 1 and lysozyme expression in mice that were orally inoculated with this pathogen. The reduction in cryptdin 1 expression was not due to a general dysfunction of Paneth cells, and does not occur as a generalised response to enteric or gram-negative bacterial infection. Instead, it appears that Cryptdin 1 expression is decreased in response to a specific interaction between *Salmonella* serovar Typhimurium and the intestinal epithelium. This interaction is dependant on the *Salmonella* pathogenicity island 1 (SPI1) that encodes a type III secretion

system and activates the p38 MAPK pathway in the intestinal epithelial cells. This finding therefore suggests that specific bacterial pathogens can regulate alpha defensin expression and it remains to be established if the reduction in HD5 and HD6 expression in NOD2-associated Crohn's disease occurs secondarily to infection by specific (as yet unidentified) bacterial pathogens.

In HIV-related cryptosporidiosis, Kelly and colleagues (2004) show that Paneth cells contain less secretory granules and are reduced in number. The depletion in Paneth cell granules, which contain HD5 and HD6 peptides, is associated with HIV infection, reduced body mass and decreased plasma zinc levels. The depletion of Paneth cell granules may be explained by the increased episodes of intestinal infections associated with HIV infection, malnutrition and zinc deficiency. If this were true, then I would expect that HD5 and HD6 transcription is increased (as in neonates with necrotizing enterocolitis). Instead, HD5 mRNA transcription, as assessed by *in situ* hybridisation and quantitative RT-PCR, appears unchanged compared to controls suggesting that nutritional factors, such as zinc, may regulate alpha defensin expression (Kelly 2004).

Paneth cells are zinc-containing cells and in the rat, intravenous injection of diphenylthiocarbazone (dithizone), a zinc chelator, results in Paneth cell depletion (Sawada 1991). In addition, in patients with zinc deficiency, Paneth cells demonstrate ultrastructural abnormalities (Kobayashi 1983). Zinc deficiency is common in Crohn's disease (Goh 2003, Griffin 2004) and zinc supplementation may prevent relapse in patients with Crohn's disease (Sturniola 2001). It is plausible that zinc may play a role in maintaining normal Paneth cell function and it would be interesting to determine whether reduced alpha defensin in NOD2-associated Crohn's disease is associated with zinc status.

In Crohn's disease, NOD2 may regulate HD5 and HD6 expression through direct or indirect mechanisms. For instance, it is possible that the decreases in alpha defensin expression, seen in $Nod2^{-/-}$ mice and NOD2-related Crohn's disease, are secondary to intestinal infection by pathogenic bacteria or aberrant colonisation by commensal bacteria. In mice, pathogenic bacteria decrease cryptdin 1 expression (Salzman 2003b) and commensal intestinal microflora, specifically

Bacteroides thetaiotamicron, can induce specific Paneth cell-antimicrobial proteins (Hooper 2003). In this scenario, aberrant NOD2 proteins alter the composition of the intestinal microflora or predispose to bacterial infections through mechanisms that are independent of alpha defensin production: alpha defensin expression is subsequently regulated by specific bacterial pathogens. Considering that NOD2 may mediate the killing of intracellular bacteria (Hisamatsu 2003), it is possible that the antibacterial properties of NOD2 are not mediated via alpha defensin peptides, which are secreted proteins. Furthermore, *Defcr2* and *Defcr-rs 10* expression is decreased in $NOD2^{-/-}$ mice prior to *L. monocytogenes* infection (which further depress expression) and it would be important to confirm whether any differences in *Defcr2* and *Defcr-rs 10* expression are seen in wild-type and $NOD2^{-/-}$ mice that are reared in a germ-free environment.

NOD2 may also directly regulate HD5 and HD5 expression although, at present, there is no evidence for this. One hypothesis though, based on the recent identification of transcription factor 4 (TCF4) binding sites on the *HD5* and *HD6* promoter regions, is that NOD2 may regulate defensin expression by interacting with the canonical Wnt signalling cascade (Abeya, manuscript in preparation).

Van Es and colleagues (2005) have recently shown that Paneth cell maturation in the intestinal crypt is dependant on Wnt signalling, which is mediated via β-catenin and transcription factor 4 (TCF4). Interestingly, these investigators have identified a highly conserved TCF binding site in the promoter region of the murine cryptdins and human *HD5* and *HD6* genes. In addition, Andreu and colleagues (2005) have shown that the cryptdin and alpha defensin gene family, including HD5 and HD6, are direct targets of β-catenin signalling. Using cell transfectants, these investigators show that HD5 and HD6 expression is regulated by a β-catenin/ TCF4-dependent pathway (Andreu 2005). This therefore raises the possibility that HD5 and HD6 expression may be regulated by cross-talk between NOD2 and the Wnt-β-catenin/TCF4- pathway.

Our observations showing aberrant Paneth cell distribution within the intestinal crypt in NOD2-related Crohn's disease may also suggest that NOD2 may interact with the Wnt-β-catenin/ TCF4 signalling cascade (Abeya, manuscript in preparation). Paneth cells express the TCF4 target molecule EphB3, an ephrin receptor, which is a member of the tyrosine kinase (RTK) receptor family. EphB3 is essential for the correct positioning of Paneth cells at the bases of the intestinal crypts (Batlle 2002). Batlle and colleagues (2002) have shown that mutations in the *EphB3* gene, which contains a TCF site in the promoter region, results in malpositioning of Paneth cells along the crypt-villus axis. Thus, both the reduction in HD5 and HD6 expression and the malpositioned Paneth cells seen in NOD2-associated Crohn's disease may be accounted for by an altered interaction between (mutant) NOD2 and Wnt-β-catenin/TCF4 pathways.

Finally, it remains to be determined whether the reductions in alpha defensin expression are physiologically important in NOD2-associated Crohn's disease. HD5 and HD6 are potent antimicrobials and, in murine models, Paneth cell-defensin deficiency does not result in the development of intestinal inflammation (Wilson 1999). An alternate explanation, therefore, is that mutant NOD2 may predispose to Crohn's disease by primarily affecting the functioning of monocytes rather than Paneth cells.

6.2 Mononuclear cells, NOD2 and Crohn's disease

Maeda and colleagues (2005) generated mice that expressed mutant NOD2 ($Nod2^{2939iC}$) proteins, analogous to mutant protein encoded by the Leu1007fsinsC mutation in humans. These investigators primarily analysed the effects of the frameshift NOD2 mutation on MDP-induced NF-κB activation in isolated bone marrow-derived macrophages (BMDMs), and assessed intestinal inflammation in dextran sodium sulphate (DSS)-treated $Nod2^{2939iC}$ mice.

Maeda and colleagues (2005) showed that in BMDMs isolated from control and $Nod2^{2939iC}$ mice, MDP induced greater NF-κB activation and IL-1β secretion in $Nod2^{2939iC}$ macrophages. These investigators showed enhanced NF-κB activation

and intestinal inflammation in DSS-treated $Nod2^{2939iC}$ mice in comparison to DSS-treated wild-type mice, and suggested that the increased inflammation in $Nod2^{2939iC}$ mice is mediated by the pro-inflammatory cytokine IL-1β. Perhaps surprisingly, these results suggest that the frameshift mutation is a gain-of-function allele, and are contrary to both *in vitro* studies using overexpression of the frameshift mutant (Ogura 2001, Inohara 2003, Girardin 2003, Abbott 2004), and human genetic studies that suggest that the analogous mutation in human NOD2 is a loss-of-function allele (Lesage 2002).

Earlier, Watanabe and colleagues (2004), using NOD2-deficient and control wild-type mice, showed that bacterial peptidoglycan evoked increased secretion of the T_H1 cytokines IL-12, IL-18 and IFNγ in NOD2-deficient splenocytes than in control splenocytes. In addition, NOD2-deficient splenocytes secreted greater amounts of T_H1 cytokines in response to MDP and Pam_3Cys or Pam_3CSK4 (synthetic TLR2 agonists). MDP lowered IL-12 secretion in NOD2-replete splenocytes that were stimulated with bacterial peptidoglycan or Pam_3Cys. In contrast, MDP did not regulate IL-12 secretion in NOD2-deficient splenocytes that were stimulated with bacterial peptidoglycan or Pam_3Cys. Similar observations were made *in vivo*, higher serum levels of IL-12 were measured in NOD2-deficient mice, than in controls, after intravenous administration of peptidoglycan. These results show that peptidoglycan stimulation increases IL-12 secretion in NOD2-deficient mice.

Using flow cytometry to analyse cell populations present in the splenocyte preparations, these investigators identified macrophages as the main sources of IL-12 and IL-18, and T-cells and macrophages as the main sources of IFNγ (Watanabe 2004). Leukocytes may therefore also play a key role in the pathogenesis of NOD2-related Crohn's disease.

The results from murine studies reveal the complexity of understanding NOD2 function and its role in the pathogenesis of Crohn's disease. Several of the hypotheses that have been advanced to explain the observations in the murine studies can be divided conceptually into those suggesting that mutant NOD2 is

defective in performing critical functions required for limiting inflammation ("loss-of-function"), and those proposing that mutant NOD2 proteins activate pro-inflammatory pathways ("gain-of-function"). However, these hypotheses are not mutually exclusive and may be valid in combination, particularly as the function of NOD2 is elucidated.

6.3 Elucidating NOD2 function

At present, NOD2 is postulated to play a role in intracellular pathogen recognition and in modifying signal transduction (Murray 2005). As NOD2 contains a LRR motif, similar to plant R proteins and Toll-like receptors, it is postulated to detect bacterial products. Indeed, based largely on the results of transfection studies, NOD2 is often described as an intracellular receptor for MDP. However, direct binding of MDP to the NOD2 LRR domain has never been demonstrated although it is possible that NOD2 functions as a "guard" protein. In this scenario, NOD2 detects a modified host protein, which perhaps complexes with MDP, with subsequent signal transduction that triggers cellular defence mechanisms (McDowell 2003, Murray 2005).

Candidate proteins that interact with NOD2 include GRIM-19 (Barnich 2005) and TAK1 (Chen 2004). These interactions, however, have only been demonstrated in transfected cells, which express these proteins in abundance. In epithelial cells, NOD2 interacts with GRIM-19, a subunit of the NADH:ubiquinone complex (Fearnley 2001) and a suppressor of STAT3 transcriptional activity (Zhang 2003). This interaction contributes to NOD2-dependent NF-κB activation in these cells (Barnich 2005), although suppression of STAT3 activity may augment programmed cell death, of which NF-κB is a potent inhibitor (Karin 2002). TAK1 plays a role in IL-1 and TNFα-induced IKK and NF-κB activation and NOD2 appears to inhibit the ability of TAK1 to activate NF-κB in the absence of RIP2 (Chen 2004). The precise role that NOD2 plays in cellular activation and apoptosis remains to be defined, and much remains to be learned about the physiologically relevant mechanisms of NOD2 signal transduction.

Although MDP causes a very weak response, measured relative to TLR pathway activation in primary macrophages, MDP can synergize with other TLR agonists to promote a synergistic response usually measured by cytokine secretion (Murray 2005). This MDP-TLR agonist synergy is dependent on NOD2 because macrophages from NOD2-deficient mice are refractory to MDP stimulation, either when given in high concentrations (Pauleau 2003) or with small amounts of TLR agonists (Murray 2005). Molecules other than NOD2 may, however, also 'sense' MDP. Recently, NALP3/cryopyrin, in addition to NALP1 and NALP2, has also been claimed to respond to MDP (Martinon 2004). Interestingly, macrophages isolated from a patient with Muckle-Wells syndrome, a dominant autoinflammatory disease caused by mutations in *Nalp3*, overproduce IL-1b in response to MDP stimulation (Martinon 2004). Therefore, the mechanisms that govern the NOD2–MDP interaction are likely to reveal the functions of NOD2 and potentially other proteins involved in MDP sensing. In addition, it is important to understand how NOD2 regulates the synergistic induction of cytokine release when cells are exposed to both MDP and a TLR agonist.

6.4 Paneth cells, TNFα and intestinal inflammation

Another aspect of Paneth cell function that may be important in the pathogenesis of Crohn's disease is their putative role in intestinal inflammation. Paneth cell hyperplasia occurs in response to signals derived from activated T cells in models of enteric infection (Kamal 2001), and in IBD, Paneth cell metaplasia is seen in the colon. In mice, Paneth cells constitutively express TNFα RNA that is apparently not translated into protein, probably because of regulation by the AU-rich element in the 3' untranslated region of the TNFα gene (Keshav 1990). Interestingly, deletion of this regulatory region in transgenic mice causes terminal ileitis, but not generalized intestinal inflammation, suggesting that local overproduction of TNFα, potentially in Paneth cells, is important (Kontoyiannis 1999). In addition, Lin and colleagues (2004) have recently reported that certain alpha defensin molecules exert pro-inflammatory responses in intestinal epithelial cells by activating NF-κB and p38 mitogen-activated protein kinase (MAPK). Thus, the ability of certain alpha defensins to act as a paracrine regulator of the

intestinal inflammatory response raises the possibility that dysregulation of Paneth cell function may contribute to the development of inflammatory diseases such as Crohn's disease.

Bibliography

1. Abbott, D. W., Wilkins, A., Asara, J. M., & Cantley, L. C. 2004, "The Crohn's disease protein, NOD2, requires RIP2 in order to induce ubiquitinylation of a novel site on NEMO", *Curr.Biol.*, vol. 14, no. 24, pp. 2217-2227.

2. Abreu, M. T., Arnold, E. T., Thomas, L. S., Gonsky, R., Zhou, Y., Hu, B., & Arditi, M. 2002, "TLR4 and MD-2 expression is regulated by immune-mediated signals in human intestinal epithelial cells", *J.Biol.Chem.*, vol. 277, no. 23, pp. 20431-20437.

3. Abreu, M. T., Fukata, M., & Arditi, M. 2005, "TLR signaling in the gut in health and disease", *J.Immunol.*, vol. 174, no. 8, pp. 4453-4460.

4. Ahmad, T., Armuzzi, A., Bunce, M., Mulcahy-Hawes, K., Marshall, S. E., Orchard, T. R., Crawshaw, J., Large, O., de Silva, A., Cook, J. T., Barnardo, M., Cullen, S., Welsh, K. I., & Jewell, D. P. 2002, "The molecular classification of the clinical manifestations of Crohn's disease", *Gastroenterology*, vol. 122, no. 4, pp. 854-866.

5. Ahrens, P., Kattner, E., Kohler, B., Hartel, C., Seidenberg, J., Segerer, H., Moller, J., & Gopel, W. 2004, "Mutations of genes involved in the innate immune system as predictors of sepsis in very low birth weight infants", *Pediatr.Res.*, vol. 55, no. 4, pp. 652-656.

6. Alberts, B., Bray, D., Lewis, J., Raff, M., Roberts, K., & Watson, J. D. 1994, Molecular Biology of the Cell (3rd edition). Chapter 8. The Cell Nucleus: RNA synthesis and RNA processing. p.409. New York, Garland Publishing.

7. Aldhous, M. C., Nimmo, E. R., & Satsangi, J. 2003, "NOD2/CARD15 and the Paneth cell: another piece in the genetic jigsaw of inflammatory bowel disease", *Gut*, vol. 52, no. 11, pp. 1533-1535.

8. Alhopuro, P., Ahvenainen, T., Mecklin, J. P., Juhola, M., Jarvinen, H. J., Karhu, A., & Aaltonen, L. A. 2004, "NOD2 3020insC alone is not sufficient for colorectal cancer predisposition", *Cancer Res.*, vol. 64, no. 20, pp. 7245-7247.

9. Andreu, P., Colnot, S., Godard, C., Gad, S., Chafey, P., Niwa-Kawakita, M., Laurent-Puig, P., Kahn, A., Robine, S., Perret, C., & Romagnolo, B. 2005, "Crypt-restricted proliferation and commitment to the Paneth cell lineage following Apc loss in the mouse intestine", *Development*, vol. 132, no. 6, pp. 1443-1451.

10. Andriulli, A., Annese, V., Latiano, A., Palmieri, O., Fortina, P., Ardizzone, S., Cottone, M., D'Inca, R., & Riegler, G. 2004, "The frame-shift mutation of the NOD2/CARD15 gene is significantly increased in ulcerative colitis: an *IG-IBD study", *Gastroenterology*, vol. 126, no. 2, pp. 625-627.

11. Annese, V., Latiano, A., Bovio, P., Forabosco, P., Piepoli, A., Lombardi, G., Andreoli, A., Astegiano, M., Gionchetti, P., Riegler, G., Sturniolo, G. C., Clementi, M., Rappaport, E., Fortina, P., Devoto, M., Gasparini, P., & Andriulli, A. 1999, "Genetic analysis in Italian families with inflammatory bowel disease supports linkage to the IBD1 locus--a GISC study", *Eur.J.Hum.Genet.*, vol. 7, no. 5, pp. 567-573.

12. Annese, V., Latiano, A., & Andriulli, A. 2003, "Genetics of inflammatory bowel disease: the beginning of the end or the end of the beginning?", *Dig.Liver Dis.*, vol. 35, no. 6, pp. 442-449.

13. Armuzzi, A., Ahmad, T., Ling, K. L., de Silva, A., Cullen, S., van Heel, D., Orchard, T. R., Welsh, K. I., Marshall, S. E., & Jewell, D. P. 2003, "Genotype-phenotype analysis of the Crohn's disease susceptibility haplotype on chromosome 5q31", *Gut*, vol. 52, no. 8, pp. 1133-1139.

14. Ayabe, T., Satchell, D. P., Wilson, C. L., Parks, W. C., Selsted, M. E., & Ouellette, A. J. 2000, "Secretion of microbicidal alpha-defensins by intestinal Paneth cells in response to bacteria", *Nat.Immunol.*, vol. 1, no. 2, pp. 113-118.

15. Bach, S. P., Renehan, A. G., & Potten, C. S. 2000, "Stem cells: the intestinal stem cell as a paradigm", *Carcinogenesis*, vol. 21, no. 3, pp. 469-476.

16. Ballance, W. A., Dahms, B. B., Shenker, N., & Kliegman, R. M. 1990, "Pathology of neonatal necrotizing enterocolitis: a ten-year experience", *J.Pediatr.*, vol. 117, no. 1 Pt 2, pp. S6-13.

17. Barnich, N., Hisamatsu, T., Aguirre, J. E., Xavier, R., Reinecker, H. C., & Podolsky, D. K. 2005, "GRIM-19 interacts with nucleotide oligomerization domain 2 and serves as downstream effector of anti-bacterial function in intestinal epithelial cells", *J.Biol.Chem.*, vol. 280, no. 19, pp. 19021-19026.

18. Batlle, E., Henderson, J. T., Beghtel, H., van den Born, M. M., Sancho, E., Huls, G., Meeldijk, J., Robertson, J., van de, W. M., Pawson, T., & Clevers, H. 2002, "Beta-catenin and TCF mediate cell positioning in the intestinal epithelium by controlling the expression of EphB/ephrinB", *Cell*, vol. 111, no. 2, pp. 251-263.

19. Beg, A. A., Sha, W. C., Bronson, R. T., Ghosh, S., & Baltimore, D. 1995, "Embryonic lethality and liver degeneration in mice lacking the RelA component of NF-kappa B", *Nature*, vol. 376, no. 6536, pp. 167-170.

20. Beil, W. J., Weller, P. F., Peppercorn, M. A., Galli, S. J., & Dvorak, A. M. 1995, "Ultrastructural immunogold localization of subcellular sites of TNF-alpha in colonic Crohn's disease", *J.Leukoc.Biol.*, vol. 58, no. 3, pp. 284-298.

21. Bergenfeldt, M., Nystrom, M., Bohe, M., Lindstrom, C., Polling, A., & Ohlsson, K. 1996, "Localization of immunoreactive secretory leukocyte protease inhibitor (SLPI) in intestinal mucosa", *J.Gastroenterol.*, vol. 31, no. 1, pp. 18-23.

22. Berrebi, D., Maudinas, R., Hugot, J. P., Chamaillard, M., Chareyre, F., De Lagausie, P., Yang, C., Desreumaux, P., Giovannini, M., Cezard, J. P., Zouali, H., Emilie, D., & Peuchmaur, M. 2003, "Card15 gene overexpression in mononuclear and epithelial cells of the inflamed Crohn's disease colon", *Gut*, vol. 52, no. 6, pp. 840-846.

23. Bertin, J., Nir, W. J., Fischer, C. M., Tayber, O. V., Errada, P. R., Grant, J. R., Keilty, J. J., Gosselin, M. L., Robison, K. E., Wong, G. H., Glucksmann, M. A., & DiStefano, P. S. 1999, "Human CARD4 protein is a novel CED-4/Apaf-1 cell death family member that activates NF-kappaB", *J.Biol.Chem.*, vol. 274, no. 19, pp. 12955-12958.

24. Beutler, B. 2001, "Autoimmunity and apoptosis: the Crohn's connection", *Immunity.*, vol. 15, no. 1, pp. 5-14.

25. Beutler, B. 2003, "Not "molecular patterns" but molecules", *Immunity.*, vol. 19, no. 2, pp. 155-156.

26. Beutler, B. A. 1999, "The role of tumor necrosis factor in health and disease", *J.Rheumatol.Suppl*, vol. 57, pp. 16-21.

27. Bevins, C. L. 2004, "The Paneth cell and the innate immune response", *Curr.Opin.Gastroenterol.*, vol. 20, no. 6, pp. 572-580.

28. Binder, V. 1998, "Genetic epidemiology in inflammatory bowel disease", *Dig.Dis.*, vol. 16, no. 6, pp. 351-355.

29. Boirivant, M., Fuss, I. J., Chu, A., & Strober, W. 1998, "Oxazolone colitis: A murine model of T helper cell type 2 colitis treatable with antibodies to interleukin 4", *J.Exp.Med.*, vol. 188, no. 10, pp. 1929-1939.

30. Bonen, D. K. & Cho, J. H. 2003, "The genetics of inflammatory bowel disease", *Gastroenterology*, vol. 124, no. 2, pp. 521-536.

31. Bonen, D. K., Ogura, Y., Nicolae, D. L., Inohara, N., Saab, L., Tanabe, T., Chen, F. F., Foster, S. J., Duerr, R. H., Brant, S. R., Cho, J. H., & Nunez, G. 2003a, "Crohn's disease-associated NOD2 variants share a signaling defect in response to lipopolysaccharide and peptidoglycan", *Gastroenterology*, vol. 124, no. 1, pp. 140-146.

32. Booth, C. & Potten, C. S. 2000, "Gut instincts: thoughts on intestinal epithelial stem cells", *J.Clin.Invest*, vol. 105, no. 11, pp. 1493-1499.

33. Bouma, G. & Strober, W. 2003, "The immunological and genetic basis of inflammatory bowel disease", *Nat.Rev.Immunol.*, vol. 3, no. 7, pp. 521-533.

34. Brant, S. R., Fu, Y., Fields, C. T., Baltazar, R., Ravenhill, G., Pickles, M. R., Rohal, P. M., Mann, J., Kirschner, B. S., Jabs, E. W., Bayless, T. M., Hanauer, S. B., & Cho, J. H. 1998, "American families with Crohn's disease have strong evidence for linkage to chromosome 16 but not chromosome 12", *Gastroenterology*, vol. 115, no. 5, pp. 1056-1061.

35. Brant, S. R., Picco, M. F., Achkar, J. P., Bayless, T. M., Kane, S. V., Brzezinski, A., Nouvet, F. J., Bonen, D., Karban, A., Dassopoulos, T., Karaliukas, R., Beaty, T. H., Hanauer, S. B., Duerr, R. H., & Cho, J. H. 2003, "Defining complex contributions of NOD2/CARD15 gene mutations, age at onset, and tobacco use on Crohn's disease phenotypes", *Inflamm.Bowel.Dis.*, vol. 9, no. 5, pp. 281-289.

36. Bry, L., Falk, P., Huttner, K., Ouellette, A., Midtvedt, T., & Gordon, J. I. 1994, "Paneth cell differentiation in the developing intestine of normal and transgenic mice", *Proc.Natl.Acad.Sci.U.S.A*, vol. 91, no. 22, pp. 10335-10339.

37. Calkins, B. M. 1989, "A meta-analysis of the role of smoking in inflammatory bowel disease", *Dig.Dis.Sci.*, vol. 34, no. 12, pp. 1841-1854.

38. Cappello, M., Keshav, S., Prince, C., Jewell, D. P., & Gordon, S. 1992, "Detection of mRNAs for macrophage products in inflammatory bowel disease by in situ hybridisation", *Gut*, vol. 33, no. 9, pp. 1214-1219.

39. Cario, E., Rosenberg, I. M., Brandwein, S. L., Beck, P. L., Reinecker, H. C., & Podolsky, D. K. 2000, "Lipopolysaccharide activates distinct signaling pathways in intestinal epithelial cell lines expressing Toll-like receptors", *J.Immunol.*, vol. 164, no. 2, pp. 966-972.

40. Carlsen, H., Moskaug, J. O., Fromm, S. H., & Blomhoff, R. 2002, "In vivo imaging of NF-kappa B activity", *J.Immunol.*, vol. 168, no. 3, pp. 1441-1446.

41. Cavanaugh, J. 2001, "International collaboration provides convincing linkage replication in complex disease through analysis of a large pooled data set: Crohn disease and chromosome 16", *Am.J.Hum.Genet.*, vol. 68, no. 5, pp. 1165-1171.

42. Cavanaugh, J. A., Callen, D. F., Wilson, S. R., Stanford, P. M., Sraml, M. E., Gorska, M., Crawford, J., Whitmore, S. A., Shlegel, C., Foote, S., Kohonen-Corish, M., & Pavli, P. 1998, "Analysis of Australian Crohn's disease pedigrees refines the localization for susceptibility to inflammatory bowel disease on chromosome 16", *Ann.Hum.Genet.*, vol. 62 (Pt 4), pp. 291-298.

43. Cavanaugh, J. A., Adams, K. E., Quak, E. J., Bryce, M. E., O'Callaghan, N. J., Rodgers, H. J., Magarry, G. R., Butler, W. J., Eaden, J. A., Roberts-Thomson, I. C., Pavli, P., Wilson, S. R., & Callen, D. F. 2003, "CARD15/NOD2 risk alleles in the development of Crohn's disease in the Australian population", *Ann.Hum.Genet.*, vol. 67, no. Pt 1, pp. 35-41.

44. Chen, C. M., Gong, Y., Zhang, M., & Chen, J. J. 2004, "Reciprocal cross-talk between Nod2 and TAK1 signaling pathways", *J.Biol.Chem.*, vol. 279, no. 24, pp. 25876-25882.

45. Chen, L. W., Egan, L., Li, Z. W., Greten, F. R., Kagnoff, M. F., & Karin, M. 2003, "The two faces of IKK and NF-kappaB inhibition: prevention of systemic inflammation but increased local injury following intestinal ischemia-reperfusion", *Nat.Med.*, vol. 9, no. 5, pp. 575-581.

46. Cho, J. H., Nicolae, D. L., Gold, L. H., Fields, C. T., LaBuda, M. C., Rohal, P. M., Pickles, M. R., Qin, L., Fu, Y., Mann, J. S., Kirschner, B. S., Jabs, E. W., Weber, J., Hanauer, S. B., Bayless, T. M., & Brant, S. R. 1998, "Identification of novel susceptibility loci for inflammatory bowel disease on chromosomes 1p, 3q, and 4q: evidence for epistasis between 1p and IBD1", *Proc.Natl.Acad.Sci.U.S.A*, vol. 95, no. 13, pp. 7502-7507.

47. Christa, L., Carnot, F., Simon, M. T., Levavasseur, F., Stinnakre, M. G., Lasserre, C., Thepot, D., Clement, B., Devinoy, E., & Brechot, C. 1996, "HIP/PAP is an adhesive protein expressed in hepatocarcinoma, normal Paneth, and pancreatic cells", *Am.J.Physiol*, vol. 271, no. 6 Pt 1, pp. G993-1002.

48. Chung, L. P., Keshav, S., & Gordon, S. 1988, "Cloning the human lysozyme cDNA: inverted Alu repeat in the mRNA and in situ hybridization for macrophages and Paneth cells", *Proc.Natl.Acad.Sci.U.S.A*, vol. 85, no. 17, pp. 6227-6231.

49. Clarke, L. L., Gawenis, L. R., Bradford, E. M., Judd, L. M., Boyle, K. T., Simpson, J. E., Shull, G. E., Tanabe, H., Ouellette, A. J., Franklin, C. L., & Walker, N. M. 2004, "Abnormal Paneth cell granule dissolution and compromised resistance to bacterial colonization in the intestine of CF mice", *Am.J.Physiol Gastrointest.Liver Physiol*, vol. 286, no. 6, p. G1050-G1058.

50. Coutinho, H. B., da Mota, H. C., Coutinho, V. B., Robalinho, T. I., Furtado, A. F., Walker, E., King, G., Mahida, Y. R., Sewell, H. F., & Wakelin, D. 1998, "Absence of lysozyme (muramidase) in the intestinal Paneth cells of newborn infants with necrotising enterocolitis", *J.Clin.Pathol.*, vol. 51, no. 7, pp. 512-514.

51. Crichton, DN., Arnott, I., Watts, D., Mowat, C., Hutchinson, J., Drummond, HE., & Satsangi, J. 2002, "NOD2/CARD15 mutations in a Scottish Crohn's disease population", *Gut*, vol. 50 (Suppl II), A266.

52. Cunliffe, R. N., Rose, F. R., Keyte, J., Abberley, L., Chan, W. C., & Mahida, Y. R. 2001, "Human defensin 5 is stored in precursor form in normal Paneth cells and is expressed by some villous epithelial cells and by metaplastic Paneth cells in the colon in inflammatory bowel disease", *Gut*, vol. 48, no. 2, pp. 176-185.

53. Cunliffe, R. N., Kamal, M., Rose, F. R., James, P. D., & Mahida, Y. R. 2002, "Expression of antimicrobial neutrophil defensins in epithelial cells of active inflammatory bowel disease mucosa", *J.Clin.Pathol.*, vol. 55, no. 4, pp. 298-304.

54. Curran, M. E., Lau, K. F., Hampe, J., Schreiber, S., Bridger, S., Macpherson, A. J., Cardon, L. R., Sakul, H., Harris, T. J., Stokkers, P., Van Deventer, S. J., Mirza, M., Raedler, A., Kruis, W., Meckler, U., Theuer, D., Herrmann, T., Gionchetti, P., Lee, J., Mathew, C., & Lennard-Jones, J. 1998, "Genetic analysis of inflammatory bowel disease in a large European cohort supports linkage to chromosomes 12 and 16", *Gastroenterology*, vol. 115, no. 5, pp. 1066-1071.

55. Cuthbert, A. P., Fisher, S. A., Mirza, M. M., King, K., Hampe, J., Croucher, P. J., Mascheretti, S., Sanderson, J., Forbes, A., Mansfield, J., Schreiber, S., Lewis, C. M., & Mathew, C. G. 2002, "The contribution of NOD2 gene mutations to the risk and site of disease in inflammatory bowel disease", *Gastroenterology*, vol. 122, no. 4, pp. 867-874.

56. Dangl, J. L. & Jones, J. D. 2001, "Plant pathogens and integrated defence responses to infection", *Nature*, vol. 411, no. 6839, pp. 826-833.

57. de Sauvage, F. J., Keshav, S., Kuang, W. J., Gillett, N., Henzel, W., & Goeddel, D. V. 1992, "Precursor structure, expression, and tissue distribution of human guanylin", *Proc.Natl.Acad.Sci.U.S.A*, vol. 89, no. 19, pp. 9089-9093.

58. Dhaliwal, W., Bajaj-Elliott, M., & Kelly, P. 2003, "Intestinal defensin gene expression in human populations", *Mol.Immunol.*, vol. 40, no. 7, pp. 469-475.

59. Dieckgraefe, B. K. 2005, "What does football have in common with Crohn's disease? The best "defense-in" is a good offense", *Inflamm.Bowel.Dis.*, vol. 11, no. 3, pp. 322-323.

60. Dionne, S., Hiscott, J., D'Agata, I., Duhaime, A., & Seidman, E. G. 1997, "Quantitative PCR analysis of TNF-alpha and IL-1 beta mRNA levels in pediatric IBD mucosal biopsies", *Dig.Dis.Sci.*, vol. 42, no. 7, pp. 1557-1566.

61. Duerr, R. H., Barmada, M. M., Zhang, L., Davis, S., Preston, R. A., Chensny, L. J., Brown, J. L., Ehrlich, G. D., Weeks, D. E., & Aston, C. E. 1998, "Linkage and association between inflammatory bowel disease and a locus on chromosome 12", *Am.J.Hum.Genet.*, vol. 63, no. 1, pp. 95-100.

62. Duerr, R. H., Barmada, M. M., Zhang, L., Pfutzer, R., & Weeks, D. E. 2000, "High-density genome scan in Crohn disease shows confirmed linkage to chromosome 14q11-12", *Am.J.Hum.Genet.*, vol. 66, no. 6, pp. 1857-1862.

63. Dvorak, A. M. 1980, "Electron microscopy of Paneth cells in Crohn's disease", *Arch.Pathol.Lab Med.*, vol. 104, no. 7, pp. 393-394.

64. Economou, M., Trikalinos, T. A., Loizou, K. T., Tsianos, E. V., & Ioannidis, J. P. 2004, "Differential effects of NOD2 variants on Crohn's disease risk and phenotype in diverse populations: a metaanalysis", *Am.J.Gastroenterol.*, vol. 99, no. 12, pp. 2393-2404.

65. El Shewy, K. A. & Eid, R. A. 2005, "In vivo killing of Giardia trophozoites harbouring bacterial endosymbionts by intestinal Paneth cells: an ultrastructural study", *Parasitology*, vol. 130, no. Pt 3, pp. 269-274.

66. Eltoum, I. A., Siegal, G. P., & Frost, A. R. 2002, "Microdissection of histologic sections: past, present, and future", *Adv.Anat.Pathol.*, vol. 9, no. 5, pp. 316-322.

67. Erdman, S., Fox, J. G., Dangler, C. A., Feldman, D., & Horwitz, B. H. 2001, "Typhlocolitis in NF-kappa B-deficient mice", *J.Immunol.*, vol. 166, no. 3, pp. 1443-1447.

68. Esters, N., Pierik, M., van Steen, K., Vermeire, S., Claessens, G., Joossens, S., Vlietinck, R., & Rutgeerts, P. 2004, "Transmission of CARD15 (NOD2) variants within families of patients with inflammatory bowel disease", *Am.J.Gastroenterol.*, vol. 99, no. 2, pp. 299-305.

69. Fahlgren, A., Hammarstrom, S., Danielsson, A., & Hammarstrom, M. L. 2003, "Increased expression of antimicrobial peptides and lysozyme in colonic epithelial cells of patients with ulcerative colitis", *Clin.Exp.Immunol.*, vol. 131, no. 1, pp. 90-101.

70. Farmer, R. G., Michener, W. M., & Mortimer, E. A. 1980, "Studies of family history among patients with inflammatory bowel disease", *Clin.Gastroenterol.*, vol. 9, no. 2, pp. 271-277.

71. Fearnley, I. M., Carroll, J., Shannon, R. J., Runswick, M. J., Walker, J. E., & Hirst, J. 2001, "GRIM-19, a cell death regulatory gene product, is a subunit of bovine mitochondrial NADH:ubiquinone oxidoreductase (complex I)", *J.Biol.Chem.*, vol. 276, no. 42, pp. 38345-38348.

72. Fell, J. M. 2005, "Neonatal inflammatory intestinal diseases: necrotising enterocolitis and allergic colitis", *Early Hum.Dev.*, vol. 81, no. 1, pp. 117-122.

73. Fellermann, K., Wehkamp, J., Herrlinger, K. R., & Stange, E. F. 2003, "Crohn's disease: a defensin deficiency syndrome?", *Eur.J.Gastroenterol.Hepatol.*, vol. 15, no. 6, pp. 627-634.

74. Fend, F. & Raffeld, M. 2000, "Laser capture microdissection in pathology", *J.Clin.Pathol.*, vol. 53, no. 9, pp. 666-672.

75. Ferreiros-Vidal, I., Garcia-Meijide, J., Carreira, P., Barros, F., Carracedo, A., Gomez-Reino, J. J., & Gonzalez, A. 2003, "The three most common CARD15 mutations associated with Crohn's disease and the chromosome 16 susceptibility locus for systemic lupus erythematosus", *Rheumatology.(Oxford)*, vol. 42, no. 4, pp. 570-574.

76. Ferreiros-Vidal, I., Barros, F., Pablos, J. L., Carracedo, A., Gomez-Reino, J. J., & Gonzalez, A. 2003a, "CARD15/NOD2 analysis in rheumatoid arthritis susceptibility", *Rheumatology.(Oxford)*, vol. 42, no. 11, pp. 1380-1382.

77. Ferreiros-Vidal, I., Amarelo, J., Barros, F., Carracedo, A., Gomez-Reino, J. J., & Gonzalez, A. 2003b, "Lack of association of ankylosing spondylitis with the most common NOD2 susceptibility alleles to Crohn's disease", *J.Rheumatol.*, vol. 30, no. 1, pp. 102-104.

78. Fiocchi, C. 1998, "Inflammatory bowel disease: etiology and pathogenesis", *Gastroenterology*, vol. 115, no. 1, pp. 182-205.

79. Fiorica-Howells, E., Hen, R., Gingrich, J., Li, Z., & Gershon, M. D. 2002, "5-HT(2A) receptors: location and functional analysis in intestines of wild-type and 5-HT(2A) knockout mice", *Am.J.Physiol Gastrointest.Liver Physiol*, vol. 282, no. 5, p. G877-G893.

80. Fischer, W., Puls, J., Buhrdorf, R., Gebert, B., Odenbreit, S., & Haas, R. 2001, "Systematic mutagenesis of the Helicobacter pylori cag pathogenicity island: essential genes for CagA translocation in host cells and induction of interleukin-8", *Mol.Microbiol.*, vol. 42, no. 5, pp. 1337-1348.

81. Folwaczny, M., Glas, J., Torok, H. P., Mauermann, D., & Folwaczny, C. 2004, "The 3020insC mutation of the NOD2/CARD15 gene in patients with periodontal disease", *Eur.J.Oral Sci.*, vol. 112, no. 4, pp. 316-319.

82. Fukuzawa, H., Sawada, M., Kayahara, T., Morita-Fujisawa, Y., Suzuki, K., Seno, H., Takaishi, S., & Chiba, T. 2003, "Identification of GM-CSF in Paneth cells using single-cell RT-PCR", *Biochem.Biophys.Res.Commun.*, vol. 312, no. 4, pp. 897-902.

83. Ganz, T. 2000, "Paneth cells--guardians of the gut cell hatchery", *Nat.Immunol.*, vol. 1, no. 2, pp. 99-100.

84. Garabedian, E. M., Roberts, L. J., McNevin, M. S., & Gordon, J. I. 1997, "Examining the role of Paneth cells in the small intestine by lineage ablation in transgenic mice", *J.Biol.Chem.*, vol. 272, no. 38, pp. 23729-23740.

85. Gasche, C., Scholmerich, J., Brynskov, J., D'Haens, G., Hanauer, S. B., Irvine, E. J., Jewell, D. P., Rachmilewitz, D., Sachar, D. B., Sandborn, W. J., & Sutherland, L. R. 2000, "A simple classification of Crohn's disease: report of the Working Party for the World Congresses of Gastroenterology, Vienna 1998", *Inflamm.Bowel.Dis.*, vol. 6, no. 1, pp. 8-15.

86. Ghosh, D., Porter, E., Shen, B., Lee, S. K., Wilk, D., Drazba, J., Yadav, S. P., Crabb, J. W., Ganz, T., & Bevins, C. L. 2002, "Paneth cell trypsin is the processing enzyme for human defensin-5", *Nat.Immunol.*, vol. 3, no. 6, pp. 583-590.

87. Ghosh, S. 2004, "Anti-TNF therapy in Crohn's disease", *Novartis.Found.Symp.*, vol. 263, pp. 193-205.

88. Girardin, S. E., Boneca, I. G., Viala, J., Chamaillard, M., Labigne, A., Thomas, G., Philpott, D. J., & Sansonetti, P. J. 2003, "Nod2 is a general sensor of peptidoglycan through muramyl dipeptide (MDP) detection", *J Biol.Chem.*, vol. 278, no. 11, pp. 8869-8872.

89. Girardin, S. E., Hugot, J. P., & Sansonetti, P. J. 2003a, "Lessons from Nod2 studies: towards a link between Crohn's disease and bacterial sensing", *Trends Immunol.*, vol. 24, no. 12, pp. 652-658.

90. Girardin, S. E., Boneca, I. G., Carneiro, L. A., Antignac, A., Jehanno, M., Viala, J., Tedin, K., Taha, M. K., Labigne, A., Zahringer, U., Coyle, A. J., DiStefano, P. S., Bertin, J., Sansonetti, P. J., & Philpott, D. J. 2003b, "Nod1 detects a unique muropeptide from gram-negative bacterial peptidoglycan", *Science*, vol. 300, no. 5625, pp. 1584-1587.

91. Girardin, S. E., Travassos, L. H., Herve, M., Blanot, D., Boneca, I. G., Philpott, D. J., Sansonetti, P. J., & Mengin-Lecreulx, D. 2003c, "Peptidoglycan molecular requirements allowing detection by Nod1 and Nod2", *J.Biol.Chem.*, vol. 278, no. 43, pp. 41702-41708.

92. Girardin, S. E. & Philpott, D. J. 2004, "Mini-review: the role of peptidoglycan recognition in innate immunity", *Eur.J.Immunol.*, vol. 34, no. 7, pp. 1777-1782.

93. Glantschnig, H., Varga, F., & Klaushofer, K. 1996, "Thyroid hormone and retinoic acid induce the synthesis of insulin-like growth factor-binding protein-4 in mouse osteoblastic cells", *Endocrinology*, vol. 137, no. 1, pp. 281-286.

94. Goh, J. & O'Morain, C. A. 2003, "Review article: nutrition and adult inflammatory bowel disease", *Aliment.Pharmacol.Ther.*, vol. 17, no. 3, pp. 307-320.

95. Greten, F. R., Eckmann, L., Greten, T. F., Park, J. M., Li, Z. W., Egan, L. J., Kagnoff, M. F., & Karin, M. 2004, "IKKbeta links inflammation and tumorigenesis in a mouse model of colitis-associated cancer", *Cell*, vol. 118, no. 3, pp. 285-296.

96. Griffin, I. J., Kim, S. C., Hicks, P. D., Liang, L. K., & Abrams, S. A. 2004, "Zinc metabolism in adolescents with Crohn's disease", *Pediatr.Res.*, vol. 56, no. 2, pp. 235-239.

97. Gronroos, J. O., Laine, V. J., Janssen, M. J., Egmond, M. R., & Nevalainen, T. J. 2001, "Bactericidal properties of group IIA and group V phospholipases A2", *J.Immunol.*, vol. 166, no. 6, pp. 4029-4034.

98. Guo, Q. S., Xia, B., Jiang, Y., Qu, Y., & Li, J. 2004, "NOD2 3020insC frameshift mutation is not associated with inflammatory bowel disease in Chinese patients of Han nationality", *World J.Gastroenterol.*, vol. 10, no. 7, pp. 1069-1071.

99. Gutierrez, O., Pipaon, C., Inohara, N., Fontalba, A., Ogura, Y., Prosper, F., Nunez, G., & Fernandez-Luna, J. L. 2002, "Induction of Nod2 in myelomonocytic and intestinal epithelial cells via nuclear factor-kappa B activation", *J.Biol.Chem.*, vol. 277, no. 44, pp. 41701-41705.

100. Haapamaki, M. M., Gronroos, J. M., Nurmi, H., Alanen, K., & Nevalainen, T. J. 1999, "Gene expression of group II phospholipase A2 in intestine in Crohn's disease", *Am.J.Gastroenterol.*, vol. 94, no. 3, pp. 713-720.

101. Habib, Z., Arnaud, B., Pascal, d. L., Caroline, F., Yves, A., Jean-Pierre, C., Michel, P., Jean-Pierre, H., & Dominique, B. 2005, "CARD15/NOD2 is not a predisposing factor for necrotizing enterocolitis", *Dig.Dis.Sci.*, vol. 50, no. 9, pp. 1684-1687.

102. Hahm, K. B., Im, Y. H., Parks, T. W., Park, S. H., Markowitz, S., Jung, H. Y., Green, J., & Kim, S. J. 2001, "Loss of transforming growth factor beta signalling in the intestine contributes to tissue injury in inflammatory bowel disease", *Gut*, vol. 49, no. 2, pp. 190-198.

103. Hammer, R. E., Maika, S. D., Richardson, J. A., Tang, J. P., & Taurog, J. D. 1990, "Spontaneous inflammatory disease in transgenic rats expressing HLA-B27 and human beta 2m: an animal model of HLA-B27-associated human disorders", *Cell*, vol. 63, no. 5, pp. 1099-1112.

104. Hampe, J., Cuthbert, A., Croucher, P. J., Mirza, M. M., Mascheretti, S., Fisher, S., Frenzel, H., King, K., Hasselmeyer, A., Macpherson, A. J., Bridger, S., van Deventer, S., Forbes, A., Nikolaus, S., Lennard-Jones, J. E., Foelsch, U. R., Krawczak, M., Lewis, C., Schreiber, S., & Mathew, C. G. 2001, "Association between insertion mutation in NOD2 gene and Crohn's disease in German and British populations", *Lancet*, vol. 357, no. 9272, pp. 1925-1928.

105. Hanasaki, K., Ono, T., Saiga, A., Morioka, Y., Ikeda, M., Kawamoto, K., Higashino, K., Nakano, K., Yamada, K., Ishizaki, J., & Arita, H. 1999, "Purified group X secretory phospholipase A(2) induced prominent release of arachidonic acid from human myeloid leukemia cells", *J.Biol.Chem.*, vol. 274, no. 48, pp. 34203-34211.

106. Harper, M. E. & Marselle, L. M. 1986, "In situ hybridization--application to gene localization and RNA detection", *Cancer Genet.Cytogenet.*, vol. 19, no. 1-2, pp. 73-80.

107. Harwig, S. S., Tan, L., Qu, X. D., Cho, Y., Eisenhauer, P. B., & Lehrer, R. I. 1995, "Bactericidal properties of murine intestinal phospholipase A2", *J.Clin.Invest*, vol. 95, no. 2, pp. 603-610.

108. Hauer-Jensen, M., Richter, K. K., Wang, J., Abe, E., Sung, C. C., & Hardin, J. W. 1998, "Changes in transforming growth factor beta1 gene expression and immunoreactivity levels during development of chronic radiation enteropathy", *Radiat.Res.*, vol. 150, no. 6, pp. 673-680.

109. Helio, T., Halme, L., Lappalainen, M., Fodstad, H., Paavola-Sakki, P., Turunen, U., Farkkila, M., Krusius, T., & Kontula, K. 2003, "CARD15/NOD2 gene variants are associated with

familially occurring and complicated forms of Crohn's disease", *Gut*, vol. 52, no. 4, pp. 558-562.

110. Hendrickson, B. A., Gokhale, R., & Cho, J. H. 2002, "Clinical aspects and pathophysiology of inflammatory bowel disease", *Clin.Microbiol.Rev.*, vol. 15, no. 1, pp. 79-94.

111. Hermiston, M. L. & Gordon, J. I. 1995, "Inflammatory bowel disease and adenomas in mice expressing a dominant negative N-cadherin", *Science*, vol. 270, no. 5239, pp. 1203-1207.

112. Hirschfeld, M., Ma, Y., Weis, J. H., Vogel, S. N., & Weis, J. J. 2000, "Cutting edge: repurification of lipopolysaccharide eliminates signaling through both human and murine toll-like receptor 2", *J.Immunol.*, vol. 165, no. 2, pp. 618-622.

113. Hisamatsu, T., Suzuki, M., Reinecker, H. C., Nadeau, W. J., McCormick, B. A., & Podolsky, D. K. 2003, "CARD15/NOD2 functions as an antibacterial factor in human intestinal epithelial cells", *Gastroenterology*, vol. 124, no. 4, pp. 993-1000.

114. Hoffmann, E., Dittrich-Breiholz, O., Holtmann, H., & Kracht, M. 2002, "Multiple control of interleukin-8 gene expression", *J.Leukoc.Biol.*, vol. 72, no. 5, pp. 847-855.

115. Hofmann, K., Bucher, P., & Tschopp, J. 1997, "The CARD domain: a new apoptotic signalling motif", *Trends Biochem.Sci.*, vol. 22, no. 5, pp. 155-156.

116. Hollander, G. A., Simpson, S. J., Mizoguchi, E., Nichogiannopoulou, A., She, J., Gutierrez-Ramos, J. C., Bhan, A. K., Burakoff, S. J., Wang, B., & Terhorst, C. 1995, "Severe colitis in mice with aberrant thymic selection", *Immunity.*, vol. 3, no. 1, pp. 27-38.

117. Holler, E., Rogler, G., Herfarth, H., Brenmoehl, J., Wild, P. J., Hahn, J., Eissner, G., Scholmerich, J., & Andreesen, R. 2004, "Both donor and recipient NOD2/CARD15 mutations associate with transplant-related mortality and GvHD following allogeneic stem cell transplantation", *Blood*, vol. 104, no. 3, pp. 889-894.

118. Holowachuk, E. W. & Ruhoff, M. S. 2001, "Restoration of abated T cell stimulation activity of mature dendritic cells", *Biochem.Biophys.Res.Commun.*, vol. 285, no. 3, pp. 594-597.

119. Hooper, L. V., Stappenbeck, T. S., Hong, C. V., & Gordon, J. I. 2003, "Angiogenins: a new class of microbicidal proteins involved in innate immunity", *Nat.Immunol.*, vol. 4, no. 3, pp. 269-273.

120. Hugot, J. P., Laurent-Puig, P., Gower-Rousseau, C., Olson, J. M., Lee, J. C., Beaugerie, L., Naom, I., Dupas, J. L., Van Gossum, A., Orholm, M., Bonaiti-Pellie, C., Weissenbach, J.,

Mathew, C. G., Lennard-Jones, J. E., Cortot, A., Colombel, J. F., & Thomas, G. 1996, "Mapping of a susceptibility locus for Crohn's disease on chromosome 16", *Nature*, vol. 379, no. 6568, pp. 821-823.

121. Hugot, J. P., Chamaillard, M., Zouali, H., Lesage, S., Cezard, J. P., Belaiche, J., Almer, S., Tysk, C., O'Morain, C. A., Gassull, M., Binder, V., Finkel, Y., Cortot, A., Modigliani, R., Laurent-Puig, P., Gower-Rousseau, C., Macry, J., Colombel, J. F., Sahbatou, M., & Thomas, G. 2001, "Association of NOD2 leucine-rich repeat variants with susceptibility to Crohn's disease", *Nature*, vol. 411, no. 6837, pp. 599-603.

122. Huttner, K. M. & Ouellette, A. J. 1994, "A family of defensin-like genes codes for diverse cysteine-rich peptides in mouse Paneth cells", *Genomics*, vol. 24, no. 1, pp. 99-109.

123. Huzarski, T., Lener, M., Domagala, W., Gronwald, J., Byrski, T., Kurzawski, G., Suchy, J., Chosia, M., Woyton, J., Ucinski, M., Narod, S. A., & Lubinski, J. 2005, "The 3020insC allele of NOD2 predisposes to early-onset breast cancer", *Breast Cancer Res.Treat.*, vol. 89, no. 1, pp. 91-93.

124. Inohara, Chamaillard, McDonald, C., & Nunez, G. 2005, "NOD-LRR proteins: role in host-microbial interactions and inflammatory disease", *Annu.Rev.Biochem.*, vol. 74, pp. 355-383.

125. Inohara, N., del Peso, L., Koseki, T., Chen, S., & Nunez, G. 1998, "RICK, a novel protein kinase containing a caspase recruitment domain, interacts with CLARP and regulates CD95-mediated apoptosis", *J.Biol.Chem.*, vol. 273, no. 20, pp. 12296-12300.

126. Inohara, N., Koseki, T., del Peso, L., Hu, Y., Yee, C., Chen, S., Carrio, R., Merino, J., Liu, D., Ni, J., & Nunez, G. 1999, "Nod1, an Apaf-1-like activator of caspase-9 and nuclear factor-kappaB", *J.Biol.Chem.*, vol. 274, no. 21, pp. 14560-14567.

127. Inohara, N., Koseki, T., Lin, J., del Peso, L., Lucas, P. C., Chen, F. F., Ogura, Y., & Nunez, G. 2000, "An induced proximity model for NF-kappa B activation in the Nod1/RICK and RIP signaling pathways", *J.Biol.Chem.*, vol. 275, no. 36, pp. 27823-27831.

128. Inohara, N. & Nunez, G. 2001, "The NOD: a signaling module that regulates apoptosis and host defense against pathogens", *Oncogene*, vol. 20, no. 44, pp. 6473-6481.

129. Inohara, N., Ogura, Y., Chen, F. F., Muto, A., & Nunez, G. 2001a, "Human Nod1 confers responsiveness to bacterial lipopolysaccharides", *J.Biol.Chem.*, vol. 276, no. 4, pp. 2551-2554.

130. Inohara, N., Ogura, Y., & Nunez, G. 2002, "Nods: a family of cytosolic proteins that regulate the host response to pathogens", *Curr.Opin.Microbiol.*, vol. 5, no. 1, pp. 76-80.

131. Inohara, N., Ogura, Y., Fontalba, A., Gutierrez, O., Pons, F., Crespo, J., Fukase, K., Inamura, S., Kusumoto, S., Hashimoto, M., Foster, S. J., Moran, A. P., Fernandez-Luna, J. L., & Nunez, G. 2003, "Host recognition of bacterial muramyl dipeptide mediated through NOD2. Implications for Crohn's disease", *J.Biol.Chem.*, vol. 278, no. 8, pp. 5509-5512.

132. Inohara, N. & Nunez, G. 2003a, "NODs: intracellular proteins involved in inflammation and apoptosis", *Nat.Rev.Immunol.*, vol. 3, no. 5, pp. 371-382.

133. Inoue, N., Tamura, K., Kinouchi, Y., Fukuda, Y., Takahashi, S., Ogura, Y., Inohara, N., Nunez, G., Kishi, Y., Koike, Y., Shimosegawa, T., Shimoyama, T., & Hibi, T. 2002, "Lack of common NOD2 variants in Japanese patients with Crohn's disease", *Gastroenterology*, vol. 123, no. 1, pp. 86-91.

134. Isaacs, K. L., Sartor, R. B., & Haskill, S. 1992, "Cytokine messenger RNA profiles in inflammatory bowel disease mucosa detected by polymerase chain reaction amplification", *Gastroenterology*, vol. 103, no. 5, pp. 1587-1595.

135. Kamal, M., Wakelin, D., Ouellette, A. J., Smith, A., Podolsky, D. K., & Mahida, Y. R. 2001, "Mucosal T cells regulate Paneth and intermediate cell numbers in the small intestine of T. spiralis-infected mice", *Clin.Exp.Immunol.*, vol. 126, no. 1, pp. 117-125.

136. Kamal, M., Dehlawi, M. S., Brunet, L. R., & Wakelin, D. 2002, "Paneth and intermediate cell hyperplasia induced in mice by helminth infections", *Parasitology*, vol. 125, no. Pt 3, pp. 275-281.

137. Karin, M. & Lin, A. 2002, "NF-kappaB at the crossroads of life and death", *Nat.Immunol.*, vol. 3, no. 3, pp. 221-227.

138. Kelly, P., Feakins, R., Domizio, P., Murphy, J., Bevins, C., Wilson, J., McPhail, G., Poulsom, R., & Dhaliwal, W. 2004, "Paneth cell granule depletion in the human small intestine under infective and nutritional stress", *Clin.Exp.Immunol.*, vol. 135, no. 2, pp. 303-309.

139. Kelsall, B. 2005, "Getting to the guts of NOD2", *Nat.Med.*, vol. 11, no. 4, pp. 383-384.

140. Keshav, S., Lawson, L., Chung, L. P., Stein, M., Perry, V. H., & Gordon, S. 1990, "Tumor necrosis factor mRNA localized to Paneth cells of normal murine intestinal epithelium by in situ hybridization", *J.Exp.Med.*, vol. 171, no. 1, pp. 327-332.

141. Keshav, S., Chung, P., Milon, G., & Gordon, S. 1991, "Lysozyme is an inducible marker of macrophage activation in murine tissues as demonstrated by in situ hybridization", *J.Exp.Med.*, vol. 174, no. 5, pp. 1049-1058.

142. Keshav, S., McKnight, A. J., Arora, R., & Gordon, S. 1997, "Cloning of intestinal phospholipase A2 from intestinal epithelial RNA by differential display PCR", *Cell Prolif.*, vol. 30, no. 10-12, pp. 369-383.

143. Keshav, S. & Lala, S. 2003, "The Paneth Cell in IBD - New Kid on the Block? " *IBD Monitor*, vol. 5, pp. 2-10.

144. Keshav, S. 2004, The Gastrointestinal System at a Glance. Chapter 34. Ulcerative Colitis and Crohn's disease. pp. 78-79. Oxford, UK, Blackwell Science Ltd.

145. Kirschning, C. J., Wesche, H., Merrill, A. T., & Rothe, M. 1998, "Human toll-like receptor 2 confers responsiveness to bacterial lipopolysaccharide", *J.Exp.Med.*, vol. 188, no. 11, pp. 2091-2097.

146. Kirsner, J. B. & Shorter, R. G. 1982, "Recent developments in "nonspecific" inflammatory bowel disease (first of two parts)", *N.Engl.J.Med.*, vol. 306, no. 13, pp. 775-785.

147. Kliegman, R. M. & Fanaroff, A. A. 1984, "Necrotizing enterocolitis", *N.Engl.J.Med.*, vol. 310, no. 17, pp. 1093-1103.

148. Kobayashi, K. S., Chamaillard, M., Ogura, Y., Henegariu, O., Inohara, N., Nunez, G., & Flavell, R. A. 2005, "Nod2-dependent regulation of innate and adaptive immunity in the intestinal tract", *Science*, vol. 307, no. 5710, pp. 731-734.

149. Kobayashi, Y., Suzuki, H., Konno, T., Tada, K., & Yamamoto, T. Y. 1983, "Ultrastructural alterations of Paneth cells in infants associated with gastrointestinal symptoms", *Tohoku J.Exp.Med.* , vol. 139, no. 3, pp. 225-230.

150. Kontoyiannis, D., Pasparakis, M., Pizarro, T. T., Cominelli, F., & Kollias, G. 1999, "Impaired on/off regulation of TNF biosynthesis in mice lacking TNF AU-rich elements: implications for joint and gut-associated immunopathologies", *Immunity.*, vol. 10, no. 3, pp. 387-398.

151. Kudo, I., Murakami, M., Hara, S., & Inoue, K. 1993, "Mammalian non-pancreatic phospholipases A2", *Biochim.Biophys.Acta*, vol. 1170, no. 3, pp. 217-231.

152. Kudo, I. & Murakami, M. 2002, "Phospholipase A2 enzymes", *Prostaglandins Other Lipid Mediat.*, vol. 68-69, pp. 3-58.

153. Kuhn, R., Lohler, J., Rennick, D., Rajewsky, K., & Muller, W. 1993, "Interleukin-10-deficient mice develop chronic enterocolitis", *Cell*, vol. 75, no. 2, pp. 263-274.

154. Kurata, J. H., Kantor-Fish, S., Frankl, H., Godby, P., & Vadheim, C. M. 1992, "Crohn's disease among ethnic groups in a large health maintenance organization", *Gastroenterology*, vol. 102, no. 6, pp. 1940-1948.

155. Kurokawa, T., Kikuchi, T., Ohta, K., Imai, H., & Yoshimura, N. 2003, "Ocular manifestations in Blau syndrome associated with a CARD15/Nod2 mutation", *Ophthalmology*, vol. 110, no. 10, pp. 2040-2044.

156. Kurzawski, G., Suchy, J., Kladny, J., Grabowska, E., Mierzejewski, M., Jakubowska, A., Debniak, T., Cybulski, C., Kowalska, E., Szych, Z., Domagala, W., Scott, R. J., & Lubinski, J. 2004, "The NOD2 3020insC mutation and the risk of colorectal cancer", *Cancer Res.*, vol. 64, no. 5, pp. 1604-1606.

157. Lacasse, J. & Martin, L. H. 1992, "Detection of CD1 mRNA in Paneth cells of the mouse intestine by in situ hybridization", *J.Histochem.Cytochem.*, vol. 40, no. 10, pp. 1527-1534.

158. Laemmli, U. K. 1970, "Cleavage of structural proteins during the assembly of the head of bacteriophage T4", *Nature*, vol. 227, no. 5259, pp. 680-685.

159. Laine, M. L., Murillo, L. S., Morre, S. A., Winkel, E. G., Pena, A. S., & van Winkelhoff, A. J. 2004, "CARD15 gene mutations in periodontitis", *J.Clin.Periodontol.*, vol. 31, no. 10, pp. 890-893.

160. Laine, V. J., Grass, D. S., & Nevalainen, T. J. 1999, "Protection by group II phospholipase A2 against Staphylococcus aureus", *J.Immunol.*, vol. 162, no. 12, pp. 7402-7408.

161. Laine, V. J., Grass, D. S., & Nevalainen, T. J. 2000, "Resistance of transgenic mice expressing human group II phospholipase A2 to Escherichia coli infection", *Infect.Immun.*, vol. 68, no. 1, pp. 87-92.

162. Lala, S., Ogura, Y., Osborne, C., Hor, S. Y., Bromfield, A., Davies, S., Ogunbiyi, O., Nunez, G., & Keshav, S. 2003, "Crohn's disease and the NOD2 gene: a role for paneth cells", *Gastroenterology*, vol. 125, no. 1, pp. 47-57.

163. Lawrance, I. C., Fiocchi, C., & Chakravarti, S. 2001, "Ulcerative colitis and Crohn's disease: distinctive gene expression profiles and novel susceptibility candidate genes", *Hum.Mol.Genet.*, vol. 10, no. 5, pp. 445-456.

164. Le Feuvre, R. A., Brough, D., Iwakura, Y., Takeda, K., & Rothwell, N. J. 2002, "Priming of macrophages with lipopolysaccharide potentiates P2X7-mediated cell death via a caspase-1-dependent mechanism, independently of cytokine production", *J.Biol.Chem.*, vol. 277, no. 5, pp. 3210-3218.

165. Lee, E. G., Boone, D. L., Chai, S., Libby, S. L., Chien, M., Lodolce, J. P., & Ma, A. 2000, "Failure to regulate TNF-induced NF-kappaB and cell death responses in A20-deficient mice", *Science*, vol. 289, no. 5488, pp. 2350-2354.

166. Lee, S. H., Shin, M. S., Park, W. S., Kim, S. Y., Dong, S. M., Lee, H. K., Park, J. Y., Oh, R. R., Jang, J. J., Lee, J. Y., & Yoo, N. J. 1999, "Immunohistochemical analysis of Fas ligand expression in normal human tissues", *APMIS*, vol. 107, no. 11, pp. 1013-1019.

167. Lehrer, R. I. 2004, "Paradise lost and paradigm found", *Nat.Immunol.*, vol. 5, no. 8, pp. 775-776.

168. Lencer, W. I., Cheung, G., Strohmeier, G. R., Currie, M. G., Ouellette, A. J., Selsted, M. E., & Madara, J. L. 1997, "Induction of epithelial chloride secretion by channel-forming cryptdins 2 and 3", *Proc.Natl.Acad.Sci.U.S.A*, vol. 94, no. 16, pp. 8585-8589.

169. Lendrum, A. C. 1947, "The phloxine-tartrazine method as a general histological stain and for the demonstration of inclusion bodies", *J.Pathol.Bacteriol.*, vol. 59, pp. 399-404.

170. Leong, R. W., Armuzzi, A., Ahmad, T., Wong, M. L., Tse, P., Jewell, D. P., & Sung, J. J. 2003, "NOD2/CARD15 gene polymorphisms and Crohn's disease in the Chinese population", *Aliment.Pharmacol.Ther.*, vol. 17, no. 12, pp. 1465-1470.

171. Lesage, S., Zouali, H., Cezard, J. P., Colombel, J. F., Belaiche, J., Almer, S., Tysk, C., O'Morain, C., Gassull, M., Binder, V., Finkel, Y., Modigliani, R., Gower-Rousseau, C., Macry, J., Merlin, F., Chamaillard, M., Jannot, A. S., Thomas, G., & Hugot, J. P. 2002, "CARD15/NOD2 mutational analysis and genotype-phenotype correlation in 612 patients with inflammatory bowel disease", *Am.J.Hum.Genet.*, vol. 70, no. 4, pp. 845-857.

172. Li, J., Moran, T., Swanson, E., Julian, C., Harris, J., Bonen, D. K., Hedl, M., Nicolae, D. L., Abraham, C., & Cho, J. H. 2004, "Regulation of IL-8 and IL-1beta expression in Crohn's disease associated NOD2/CARD15 mutations", *Hum.Mol.Genet.*, vol. 13, no. 16, pp. 1715-1725.

173. Li, Q. & Verma, I. M. 2002, "NF-kappaB regulation in the immune system", *Nat.Rev.Immunol.*, vol. 2, no. 10, pp. 725-734.

174. Lilja, I., Smedh, K., Olaison, G., Sjodahl, R., Tagesson, C., & Gustafson-Svard, C. 1995, "Phospholipase A2 gene expression and activity in histologically normal ileal mucosa and in Crohn's ileitis", *Gut*, vol. 37, no. 3, pp. 380-385.

175. Lin, P. W., Simon, P. O., Jr., Gewirtz, A. T., Neish, A. S., Ouellette, A. J., Madara, J. L., & Lencer, W. I. 2004, "Paneth cell cryptdins act in vitro as apical paracrine regulators of the innate inflammatory response", *J.Biol.Chem.*, vol. 279, no. 19, pp. 19902-19907.

176. Liu, Z., Colpaert, S., D'Haens, G. R., Kasran, A., de Boer, M., Rutgeerts, P., Geboes, K., & Ceuppens, J. L. 1999, "Hyperexpression of CD40 ligand (CD154) in inflammatory bowel disease and its contribution to pathogenic cytokine production", *J.Immunol.*, vol. 163, no. 7, pp. 4049-4057.

177. Louis, E., Collard, A., Oger, A. F., Degroote, E., Aboul Nasr El Yafi FA, & Belaiche, J. 2001, "Behaviour of Crohn's disease according to the Vienna classification: changing pattern over the course of the disease", *Gut*, vol. 49, no. 6, pp. 777-782.

178. Lowe, M. E. 2000, "Properties and function of pancreatic lipase related protein 2", *Biochimie*, vol. 82, no. 11, pp. 997-1004.

179. Ma, Y., Ohmen, J. D., Li, Z., Bentley, L. G., McElree, C., Pressman, S., Targan, S. R., Fischel-Ghodsian, N., Rotter, J. I., & Yang, H. 1999, "A genome-wide search identifies potential new susceptibility loci for Crohn's disease", *Inflamm.Bowel.Dis.*, vol. 5, no. 4, pp. 271-278.

180. MacPherson, B. R. & Pfeiffer, C. J. 1978, "Experimental production of diffuse colitis in rats", *Digestion*, vol. 17, no. 2, pp. 135-150.

181. Madara, J. L., Podolsky, D. K., King, N. W., Sehgal, P. K., Moore, R., & Winter, H. S. 1985, "Characterization of spontaneous colitis in cotton-top tamarins (Saguinus oedipus) and its response to sulfasalazine", *Gastroenterology*, vol. 88, no. 1 Pt 1, pp. 13-19.

182. Madsen, K. L., Lewis, S. A., Tavernini, M. M., Hibbard, J., & Fedorak, R. N. 1997, "Interleukin 10 prevents cytokine-induced disruption of T84 monolayer barrier integrity and limits chloride secretion", *Gastroenterology*, vol. 113, no. 1, pp. 151-159.

183. Maeda, S., Hsu, L. C., Liu, H., Bankston, L. A., Iimura, M., Kagnoff, M. F., Eckmann, L., & Karin, M. 2005, "Nod2 mutation in Crohn's disease potentiates NF-kappaB activity and IL-1beta processing", *Science*, vol. 307, no. 5710, pp. 734-738.

184. Mahida, Y. R., Wu, K. C., & Jewell, D. P. 1989, "Respiratory burst activity of intestinal macrophages in normal and inflammatory bowel disease", *Gut*, vol. 30, no. 10, pp. 1362-1370.

185. Mallow, E. B., Harris, A., Salzman, N., Russell, J. P., DeBerardinis, R. J., Ruchelli, E., & Bevins, C. L. 1996, "Human enteric defensins. Gene structure and developmental expression", *J.Biol.Chem.*, vol. 271, no. 8, pp. 4038-4045.

186. Mannon, P. J., Fuss, I. J., Mayer, L., Elson, C. O., Sandborn, W. J., Present, D., Dolin, B., Goodman, N., Groden, C., Hornung, R. L., Quezado, M., Neurath, M. F., Salfeld, J., Veldman, G. M., Schwertschlag, U., Strober, W., & Yang, Z. 2004, "Anti-interleukin-12 antibody for active Crohn's disease", *N.Engl.J.Med.*, vol. 351, no. 20, pp. 2069-2079.

187. Marcus, R. & Watt, J. 1969, "Seaweeds and ulcerative colitis in laboratory animals", *Lancet*, vol. 2, no. 7618, pp. 489-490.

188. Martin, S. J. 2001, "Dealing the CARDs between life and death", *Trends Cell Biol.*, vol. 11, no. 5, pp. 188-189.

189. Martin, T. M., Doyle, T. M., Smith, J. R., Dinulescu, D., Rust, K., & Rosenbaum, J. T. 2003, "Uveitis in patients with sarcoidosis is not associated with mutations in NOD2 (CARD15)", *Am.J.Ophthalmol.*, vol. 136, no. 5, pp. 933-935.

190. Martinon, F., Agostini, L., Meylan, E., & Tschopp, J. 2004, "Identification of bacterial muramyl dipeptide as activator of the NALP3/cryopyrin inflammasome", *Curr.Biol.*, vol. 14, no. 21, pp. 1929-1934.

191. Mashimo, H., Wu, D. C., Podolsky, D. K., & Fishman, M. C. 1996, "Impaired defense of intestinal mucosa in mice lacking intestinal trefoil factor", *Science*, vol. 274, no. 5285, pp. 262-265.

192. Matsumoto, S., Okabe, Y., Setoyama, H., Takayama, K., Ohtsuka, J., Funahashi, H., Imaoka, A., Okada, Y., & Umesaki, Y. 1998, "Inflammatory bowel disease-like enteritis and caecitis in a senescence accelerated mouse P1/Yit strain", *Gut*, vol. 43, no. 1, pp. 71-78.

193. McDonald, C., Inohara, N., & Nunez, G. 2005, "Peptidoglycan signaling in innate immunity and inflammatory disease", *J.Biol.Chem.*, vol. 280, no. 21, pp. 20177-20180.

194. McDowell, J. M. & Woffenden, B. J. 2003, "Plant disease resistance genes: recent insights and potential applications", *Trends Biotechnol.*, vol. 21, no. 4, pp. 178-183.

195. McGovern, D. P., Van Heel, D. A., Ahmad, T., & Jewell, D. P. 2001, "NOD2 (CARD15), the first susceptibility gene for Crohn's disease", *Gut*, vol. 49, no. 6, pp. 752-754.

196. McGovern, D. P., Van Heel, D. A., Negoro, K., Ahmad, T., & Jewell, D. P. 2003, "Further evidence of IBD5/CARD15 (NOD2) epistasis in the susceptibility to ulcerative colitis", *Am.J.Hum.Genet.*, vol. 73, no. 6, pp. 1465-1466.

197. McGovern, D. P., Hysi, P., Ahmad, T., Van Heel, D. A., Moffatt, M. F., Carey, A., Cookson, W. O., & Jewell, D. P. 2005, "Association between a complex insertion/deletion polymorphism in NOD1 (CARD4) and susceptibility to inflammatory bowel disease", *Hum.Mol.Genet.*, vol. 14, no. 10, pp. 1245-1250.

198. Miceli-Richard, C., Lesage, S., Rybojad, M., Prieur, A. M., Manouvrier-Hanu, S., Hafner, R., Chamaillard, M., Zouali, H., Thomas, G., & Hugot, J. P. 2001, "CARD15 mutations in Blau syndrome", *Nat.Genet.*, vol. 29, no. 1, pp. 19-20.

199. Minami, T., Tojo, H., Shinomura, Y., Matsuzawa, Y., & Okamoto, M. 1994, "Increased group II phospholipase A2 in colonic mucosa of patients with Crohn's disease and ulcerative colitis", *Gut*, vol. 35, no. 11, pp. 1593-1598.

200. Moller, P., Walczak, H., Reidl, S., Strater, J., & Krammer, P. H. 1996, "Paneth cells express high levels of CD95 ligand transcripts: a unique property among gastrointestinal epithelia", *Am.J.Pathol.*, vol. 149, no. 1, pp. 9-13.

201. Mombaerts, P., Mizoguchi, E., Grusby, M. J., Glimcher, L. H., Bhan, A. K., & Tonegawa, S. 1993, "Spontaneous development of inflammatory bowel disease in T cell receptor mutant mice", *Cell*, vol. 75, no. 2, pp. 274-282.

202. Monsen, U., Bernell, O., Johansson, C., & Hellers, G. 1991, "Prevalence of inflammatory bowel disease among relatives of patients with Crohn's disease", *Scand.J.Gastroenterol.*, vol. 26, no. 3, pp. 302-306.

203. Monteleone, G., Biancone, L., Marasco, R., Morrone, G., Marasco, O., Luzza, F., & Pallone, F. 1997, "Interleukin 12 is expressed and actively released by Crohn's disease intestinal lamina propria mononuclear cells", *Gastroenterology*, vol. 112, no. 4, pp. 1169-1178.

204. Morris, G. P., Beck, P. L., Herridge, M. S., Depew, W. T., Szewczuk, M. R., & Wallace, J. L. 1989, "Hapten-induced model of chronic inflammation and ulceration in the rat colon", *Gastroenterology*, vol. 96, no. 3, pp. 795-803.

205. Moxey, P. C. & Trier, J. S. 1978, "Specialized cell types in the human fetal small intestine", *Anat.Rec.*, vol. 191, no. 3, pp. 269-285.

206. Murray, P. J. 2005, "NOD proteins: an intracellular pathogen-recognition system or signal transduction modifiers?", *Curr.Opin.Immunol.*, vol. 17, no. 4, pp. 352-358.

207. Neu, J., Chen, M., & Beierle, E. 2005, "Intestinal innate immunity: how does it relate to the pathogenesis of necrotizing enterocolitis", *Semin.Pediatr.Surg.*, vol. 14, no. 3, pp. 137-144.

208. Nevalainen, T. J., Laine, V. J., & Grass, D. S. 1997, "Expression of human group II phospholipase A2 in transgenic mice", *J.Histochem.Cytochem.*, vol. 45, no. 8, pp. 1109-1119.

209. Newman, B., Rubin, L. A., & Siminovitch, K. A. 2003, "NOD2/CARD15 gene mutation is not associated with susceptibility to Wegener's granulomatosis", *J.Rheumatol.*, vol. 30, no. 2, pp. 305-307.

210. O'Neil, D. A., Porter, E. M., Elewaut, D., Anderson, G. M., Eckmann, L., Ganz, T., & Kagnoff, M. F. 1999, "Expression and regulation of the human beta-defensins hBD-1 and hBD-2 in intestinal epithelium", *J.Immunol.*, vol. 163, no. 12, pp. 6718-6724.

211. Ogura, Y., Bonen, D. K., Inohara, N., Nicolae, D. L., Chen, F. F., Ramos, R., Britton, H., Moran, T., Karaliuskas, R., Duerr, R. H., Achkar, J. P., Brant, S. R., Bayless, T. M., Kirschner, B. S., Hanauer, S. B., Nunez, G., & Cho, J. H. 2001, "A frameshift mutation in NOD2 associated with susceptibility to Crohn's disease", *Nature*, vol. 411, no. 6837, pp. 603-606.

212. Ogura, Y., Inohara, N., Benito, A., Chen, F. F., Yamaoka, S., & Nunez, G. 2001a, "Nod2, a Nod1/Apaf-1 family member that is restricted to monocytes and activates NF-kappaB", *J.Biol.Chem.*, vol. 276, no. 7, pp. 4812-4818.

213. Ogura, Y., Saab, L., Chen, F. F., Benito, A., Inohara, N., & Nunez, G. 2003, "Genetic variation and activity of mouse Nod2, a susceptibility gene for Crohn's disease", *Genomics*, vol. 81, no. 4, pp. 369-377.

214. Ogura, Y., Lala, S., Xin, W., Smith, E., Dowds, T. A., Chen, F. F., Zimmermann, E., Tretiakova, M., Cho, J. H., Hart, J., Greenson, J. K., Keshav, S., & Nunez, G. 2003a, "Expression of NOD2 in Paneth cells: a possible link to Crohn's ileitis", *Gut*, vol. 52, no. 11, pp. 1591-1597.

215. Ohmen, J. D., Yang, H. Y., Yamamoto, K. K., Zhao, H. Y., Ma, Y., Bentley, L. G., Huang, Z., Gerwehr, S., Pressman, S., McElree, C., Targan, S., Rotter, J. I., & Fischel-Ghodsian, N. 1996,

"Susceptibility locus for inflammatory bowel disease on chromosome 16 has a role in Crohn's disease, but not in ulcerative colitis", *Hum.Mol.Genet.*, vol. 5, no. 10, pp. 1679-1683.

216. Okayasu, I., Hatakeyama, S., Yamada, M., Ohkusa, T., Inagaki, Y., & Nakaya, R. 1990, "A novel method in the induction of reliable experimental acute and chronic ulcerative colitis in mice", *Gastroenterology*, vol. 98, no. 3, pp. 694-702.

217. Olaison, G., Sjodahl, R., & Tagesson, C. 1988, "Increased phospholipase A2 activity of Ileal mucosa in Crohn's disease", *Digestion*, vol. 41, no. 3, pp. 136-141.

218. Orholm, M., Munkholm, P., Langholz, E., Nielsen, O. H., Sorensen, I. A., & Binder, V. 1991, "Familial occurrence of inflammatory bowel disease", *N.Engl.J.Med.*, vol. 324, no. 2, pp. 84-88.

219. Ouellette, A. J., Miller, S. I., Henschen, A. H., & Selsted, M. E. 1992, "Purification and primary structure of murine cryptdin-1, a Paneth cell defensin", *FEBS Lett.*, vol. 304, no. 2-3, pp. 146-148.

220. Ouellette, A. J., Hsieh, M. M., Nosek, M. T., Cano-Gauci, D. F., Huttner, K. M., Buick, R. N., & Selsted, M. E. 1994, "Mouse Paneth cell defensins: primary structures and antibacterial activities of numerous cryptdin isoforms", *Infect.Immun.*, vol. 62, no. 11, pp. 5040-5047.

221. Ouellette, A. J. & Selsted, M. E. 1996, "Paneth cell defensins: endogenous peptide components of intestinal host defense", *FASEB J.*, vol. 10, no. 11, pp. 1280-1289.

222. Ouellette, A. J. 1997, "Paneth cells and innate immunity in the crypt microenvironment", *Gastroenterology*, vol. 113, no. 5, pp. 1779-1784.

223. Ouellette, A. J. 1999, "IV. Paneth cell antimicrobial peptides and the biology of the mucosal barrier", *Am.J.Physiol*, vol. 277, no. 2 Pt 1, p. G257-G261.

224. Ouellette, A. J. 2005, "Paneth cell alpha-defensins: peptide mediators of innate immunity in the small intestine", *Springer Semin.Immunopathol.*

225. Palsson-McDermott, E. M. & O'Neill, L. A. 2004, "Signal transduction by the lipopolysaccharide receptor, Toll-like receptor-4", *Immunology*, vol. 113, no. 2, pp. 153-162.

226. Paneth, J. 1888, "Ueber sie secernierenden Zellen des Duenndarmepithels", *Archiv mikroskop.Anat.*, vol. 31, pp. 113-191.

227. Panwala, C. M., Jones, J. C., & Viney, J. L. 1998, "A novel model of inflammatory bowel disease: mice deficient for the multiple drug resistance gene, mdr1a, spontaneously develop colitis", *J.Immunol.*, vol. 161, no. 10, pp. 5733-5744.

228. Papaconstantinou, I., Theodoropoulos, G., Gazouli, M., Panoussopoulos, D., Mantzaris, G. J., Felekouras, E., & Bramis, J. 2005, "Association between mutations in the CARD15/NOD2 gene and colorectal cancer in a Greek population", *Int.J.Cancer*, vol. 114, no. 3, pp. 433-435.

229. Parronchi, P., Romagnani, P., Annunziato, F., Sampognaro, S., Becchio, A., Giannarini, L., Maggi, E., Pupilli, C., Tonelli, F., & Romagnani, S. 1997, "Type 1 T-helper cell predominance and interleukin-12 expression in the gut of patients with Crohn's disease", *Am.J.Pathol.*, vol. 150, no. 3, pp. 823-832.

230. Pauleau, A. L. & Murray, P. J. 2003, "Role of nod2 in the response of macrophages to toll-like receptor agonists", *Mol.Cell Biol.*, vol. 23, no. 21, pp. 7531-7539.

231. Peeters, M., Nevens, H., Baert, F., Hiele, M., de Meyer, A. M., Vlietinck, R., & Rutgeerts, P. 1996, "Familial aggregation in Crohn's disease: increased age-adjusted risk and concordance in clinical characteristics", *Gastroenterology*, vol. 111, no. 3, pp. 597-603.

232. Plant, D., Lear, J., Marsland, A., Worthington, J., & Griffiths, C. E. 2004, "CARD15/NOD2 single nucleotide polymorphisms do not confer susceptibility to type I psoriasis", *Br.J.Dermatol.*, vol. 151, no. 3, pp. 675-678.

233. Podolsky, D. K. 1991, "Inflammatory bowel disease (1)", *N.Engl.J.Med.*, vol. 325, no. 13, pp. 928-937.

234. Podolsky, D. K. 1999, "Mucosal immunity and inflammation. V. Innate mechanisms of mucosal defense and repair: the best offense is a good defense", *Am.J.Physiol*, vol. 277, no. 3 Pt 1, p. G495-G499.

235. Podolsky, D. K. 2002, "Inflammatory bowel disease", *N.Engl.J.Med.*, vol. 347, no. 6, pp. 417-429.

236. Poltorak, A., He, X., Smirnova, I., Liu, M. Y., Van Huffel, C., Du, X., Birdwell, D., Alejos, E., Silva, M., Galanos, C., Freudenberg, M., Ricciardi-Castagnoli, P., Layton, B., & Beutler, B. 1998, "Defective LPS signaling in C3H/HeJ and C57BL/10ScCr mice: mutations in Tlr4 gene", *Science*, vol. 282, no. 5396, pp. 2085-2088.

237. Porter, E. M., Liu, L., Oren, A., Anton, P. A., & Ganz, T. 1997, "Localization of human intestinal defensin 5 in Paneth cell granules", *Infect.Immun.*, vol. 65, no. 6, pp. 2389-2395.

238. Porter, E. M., Poles, M. A., Lee, J. S., Naitoh, J., Bevins, C. L., & Ganz, T. 1998, "Isolation of human intestinal defensins from ileal neobladder urine", *FEBS Lett.*, vol. 434, no. 3, pp. 272-276.

239. Porter, E. M., Bevins, C. L., Ghosh, D., & Ganz, T. 2002, "The multifaceted Paneth cell", *Cell Mol.Life Sci.*, vol. 59, no. 1, pp. 156-170.

240. Poulsen, S. S., Nexo, E., Olsen, P. S., Hess, J., & Kirkegaard, P. 1986, "Immunohistochemical localization of epidermal growth factor in rat and man", *Histochemistry*, vol. 85, no. 5, pp. 389-394.

241. Powrie, F., Leach, M. W., Mauze, S., Caddle, L. B., & Coffman, R. L. 1993, "Phenotypically distinct subsets of CD4+ T cells induce or protect from chronic intestinal inflammation in C. B-17 scid mice", *Int.Immunol.*, vol. 5, no. 11, pp. 1461-1471.

242. Powrie, F., Correa-Oliveira, R., Mauze, S., & Coffman, R. L. 1994, "Regulatory interactions between CD45RBhigh and CD45RBlow CD4+ T cells are important for the balance between protective and pathogenic cell-mediated immunity", *J.Exp.Med.*, vol. 179, no. 2, pp. 589-600.

243. Probert, C. S., Jayanthi, V., Rampton, D. S., & Mayberry, J. F. 1996, "Epidemiology of inflammatory bowel disease in different ethnic and religious groups: limitations and aetiological clues", *Int.J.Colorectal Dis.*, vol. 11, no. 1, pp. 25-28.

244. Qu, H. & Dvorak, A. M. 1997, "Ultrastructural localization of osteopontin immunoreactivity in phagolysosomes and secretory granules of cells in human intestine", *Histochem.J.*, vol. 29, no. 11-12, pp. 801-812.

245. Qu, X. D., Lloyd, K. C., Walsh, J. H., & Lehrer, R. I. 1996, "Secretion of type II phospholipase A2 and cryptdin by rat small intestinal Paneth cells", *Infect.Immun.*, vol. 64, no. 12, pp. 5161-5165.

246. Rioux, J. D., Silverberg, M. S., Daly, M. J., Steinhart, A. H., McLeod, R. S., Griffiths, A. M., Green, T., Brettin, T. S., Stone, V., Bull, S. B., Bitton, A., Williams, C. N., Greenberg, G. R., Cohen, Z., Lander, E. S., Hudson, T. J., & Siminovitch, K. A. 2000, "Genomewide search in Canadian families with inflammatory bowel disease reveals two novel susceptibility loci", *Am.J.Hum.Genet.*, vol. 66, no. 6, pp. 1863-1870.

247. Rivera-Nieves, J., Bamias, G., Vidrich, A., Marini, M., Pizarro, T. T., McDuffie, M. J., Moskaluk, C. A., Cohn, S. M., & Cominelli, F. 2003, "Emergence of perianal fistulizing disease in the SAMP1/YitFc mouse, a spontaneous model of chronic ileitis", *Gastroenterology*, vol. 124, no. 4, pp. 972-982.

248. Rodning, C. B., Wilson, I. D., & Erlandsen, S. L. 1976, "Immunoglobulins within human small-intestinal Paneth cells", *Lancet*, vol. 1, no. 7967, pp. 984-987.

249. Rose, C. D., Doyle, T. M., McIlvain-Simpson, G., Coffman, J. E., Rosenbaum, J. T., Davey, M. P., & Martin, T. M. 2005, "Blau syndrome mutation of CARD15/NOD2 in sporadic early onset granulomatous arthritis", *J.Rheumatol.*, vol. 32, no. 2, pp. 373-375.

250. Rosenstiel, P., Fantini, M., Brautigam, K., Kuhbacher, T., Waetzig, G. H., Seegert, D., & Schreiber, S. 2003, "TNF-alpha and IFN-gamma regulate the expression of the NOD2 (CARD15) gene in human intestinal epithelial cells", *Gastroenterology*, vol. 124, no. 4, pp. 1001-1009.

251. Roussomoustakaki, M., Koutroubakis, I., Vardas, E. M., Dimoulios, P., Kouroumalis, E. A., Baritaki, S., Koutsoudakis, G., & Krambovitis, E. 2003, "NOD2 insertion mutation in a Cretan Crohn's disease population", *Gastroenterology*, vol. 124, no. 1, pp. 272-273.

252. Rozenfeld, R. A., Liu, X., DePlaen, I., & Hsueh, W. 2001, "Role of gut flora on intestinal group II phospholipase A2 activity and intestinal injury in shock", *Am.J.Physiol Gastrointest.Liver Physiol*, vol. 281, no. 4, p. G957-G963.

253. Rudolph, U., Finegold, M. J., Rich, S. S., Harriman, G. R., Srinivasan, Y., Brabet, P., Boulay, G., Bradley, A., & Birnbaumer, L. 1995, "Ulcerative colitis and adenocarcinoma of the colon in G alpha i2-deficient mice", *Nat.Genet.*, vol. 10, no. 2, pp. 143-150.

254. Russel, M. G., Pastoor, C. J., Janssen, K. M., van Deursen, C. T., Muris, J. W., van Wijlick, E. H., & Stockbrugger, R. W. 1997, "Familial aggregation of inflammatory bowel disease: a population-based study in South Limburg, The Netherlands. The South Limburg IBD Study Group", *Scand.J.Gastroenterol.Suppl*, vol. 223, pp. 88-91.

255. Sadlack, B., Merz, H., Schorle, H., Schimpl, A., Feller, A. C., & Horak, I. 1993, "Ulcerative colitis-like disease in mice with a disrupted interleukin-2 gene", *Cell*, vol. 75, no. 2, pp. 253-261.

256. Salzman, N. H., Polin, R. A., Harris, M. C., Ruchelli, E., Hebra, A., Zirin-Butler, S., Jawad, A., Martin, P. E., & Bevins, C. L. 1998, "Enteric defensin expression in necrotizing enterocolitis", *Pediatr.Res.*, vol. 44, no. 1, pp. 20-26.

257. Salzman, N. H., Ghosh, D., Huttner, K. M., Paterson, Y., & Bevins, C. L. 2003, "Protection against enteric salmonellosis in transgenic mice expressing a human intestinal defensin", *Nature*, vol. 422, no. 6931, pp. 522-526.

258. Salzman, N. H., Chou, M. M., de Jong, H., Liu, L., Porter, E. M., & Paterson, Y. 2003a, "Enteric salmonella infection inhibits Paneth cell antimicrobial peptide expression", *Infect.Immun.*, vol. 71, no. 3, pp. 1109-1115.

259. Sartor, R. B. 1997, "The influence of normal microbial flora on the development of chronic mucosal inflammation", *Res.Immunol.*, vol. 148, no. 8-9, pp. 567-576.

260. Satoh, Y., Ishikawa, K., Tanaka, H., & Ono, K. 1986, "Immunohistochemical observations of immunoglobulin A in the Paneth cells of germ-free and formerly-germ-free rats", *Histochemistry*, vol. 85, no. 3, pp. 197-201.

261. Satsangi, J., Jewell, D. P., Rosenberg, W. M., & Bell, J. I. 1994, "Genetics of inflammatory bowel disease", *Gut*, vol. 35, no. 5, pp. 696-700.

262. Satsangi, J., Parkes, M., Louis, E., Hashimoto, L., Kato, N., Welsh, K., Terwilliger, J. D., Lathrop, G. M., Bell, J. I., & Jewell, D. P. 1996, "Two stage genome-wide search in inflammatory bowel disease provides evidence for susceptibility loci on chromosomes 3, 7 and 12", *Nat.Genet.*, vol. 14, no. 2, pp. 199-202.

263. Sawada, M., Takahashi, K., Sawada, S., & Midorikawa, O. 1991, "Selective killing of Paneth cells by intravenous administration of dithizone in rats", *Int.J.Exp.Pathol.*, vol. 72, no. 4, pp. 407-421.

264. Sawcer, S., Maranian, M., Hensiek, A., Roxburgh, R., Gray, J., & Compston, A. 2003, "Crohn's associated NOD2 gene variants are not involved in determining susceptibility to multiple sclerosis", *J.Neurol.Neurosurg.Psychiatry*, vol. 74, no. 8, p. 1157.

265. Schmauder-Chock, E. A. & Chock, S. P. 1992, "Prostaglandin E2 localization in the rat ileum", *Histochem.J.*, vol. 24, no. 9, pp. 663-672.

266. Schmauder-Chock, E. A., Chock, S. P., & Patchen, M. L. 1994, "Ultrastructural localization of tumour necrosis factor-alpha", *Histochem.J.*, vol. 26, no. 2, pp. 142-151.

267. Schwalbe, G. 1872, "Beitraege zur Kenntnis der Druesen in den Darmwandungen, in'sBesondere der Brunner'schen Druesen", *Arch.mikroskop.Anat.*, vol. 8, pp. 92-140.

268. Selsted, M. E., Miller, S. I., Henschen, A. H., & Ouellette, A. J. 1992, "Enteric defensins: antibiotic peptide components of intestinal host defense", *J.Cell Biol.*, vol. 118, no. 4, pp. 929-936.

269. Seno, H., Sawada, M., Fukuzawa, H., Morita-Fujisawa, Y., Takaishi, S., Hiai, H., & Chiba, T. 2002, "Involvement of tumor necrosis factor alpha in intestinal epithelial cell proliferation following Paneth cell destruction", *Scand.J.Gastroenterol.*, vol. 37, no. 2, pp. 154-160.

270. Shen, B., Porter, E. M., Reynoso, E., Shen, C., Ghosh, D., Connor, J. T., Drazba, J., Rho, H. K., Gramlich, T. L., Li, R., Ormsby, A. H., Sy, M. S., Ganz, T., & Bevins, C. L. 2005, "Human defensin 5 expression in intestinal metaplasia of the upper gastrointestinal tract", *J.Clin.Pathol.*, vol. 58, no. 7, pp. 687-694.

271. Shull, M. M., Ormsby, I., Kier, A. B., Pawlowski, S., Diebold, R. J., Yin, M., Allen, R., Sidman, C., Proetzel, G., Calvin, D., & . 1992, "Targeted disruption of the mouse transforming growth factor-beta 1 gene results in multifocal inflammatory disease", *Nature*, vol. 359, no. 6397, pp. 693-699.

272. Six, D. A. & Dennis, E. A. 2000, "The expanding superfamily of phospholipase A(2) enzymes: classification and characterization", *Biochim.Biophys.Acta*, vol. 1488, no. 1-2, pp. 1-19.

273. Snapper, S. B., Rosen, F. S., Mizoguchi, E., Cohen, P., Khan, W., Liu, C. H., Hagemann, T. L., Kwan, S. P., Ferrini, R., Davidson, L., Bhan, A. K., & Alt, F. W. 1998, "Wiskott-Aldrich syndrome protein-deficient mice reveal a role for WASP in T but not B cell activation", *Immunity.*, vol. 9, no. 1, pp. 81-91.

274. Spencer, S. D., Di Marco, F., Hooley, J., Pitts-Meek, S., Bauer, M., Ryan, A. M., Sordat, B., Gibbs, V. C., & Aguet, M. 1998, "The orphan receptor CRF2-4 is an essential subunit of the interleukin 10 receptor", *J.Exp.Med.*, vol. 187, no. 4, pp. 571-578.

275. Stack, W. A., Mann, S. D., Roy, A. J., Heath, P., Sopwith, M., Freeman, J., Holmes, G., Long, R., Forbes, A., & Kamm, M. A. 1997, "Randomised controlled trial of CDP571 antibody to tumour necrosis factor-alpha in Crohn's disease", *Lancet*, vol. 349, no. 9051, pp. 521-524.

276. Stamp, G. W., Poulsom, R., Chung, L. P., Keshav, S., Jeffery, R. E., Longcroft, J. A., Pignatelli, M., & Wright, N. A. 1992, "Lysozyme gene expression in inflammatory bowel disease", *Gastroenterology*, vol. 103, no. 2, pp. 532-538.

277. Stappenbeck, T. S., Hooper, L. V., & Gordon, J. I. 2002, "Developmental regulation of intestinal angiogenesis by indigenous microbes via Paneth cells", *Proc.Natl.Acad.Sci.U.S.A*, vol. 99, no. 24, pp. 15451-15455.

278. Stappenbeck, T. S., Hooper, L. V., Manchester, J. K., Wong, M. H., & Gordon, J. I. 2002a, "Laser capture microdissection of mouse intestine: characterizing mRNA and protein expression, and profiling intermediary metabolism in specified cell populations", *Methods Enzymol.*, vol. 356, pp. 167-196.

279. Steer, S., Fisher, S. A., Fife, M., Cuthbert, A., Newton, J., Wordsworth, P., Lewis, C. M., Mathew, C. G., & Lanchbury, J. S. 2003, "Development of rheumatoid arthritis is not associated with two polymorphisms in the Crohn's disease gene CARD15", *Rheumatology.(Oxford)*, vol. 42, no. 2, pp. 304-307.

280. Steinhoff, U., Brinkmann, V., Klemm, U., Aichele, P., Seiler, P., Brandt, U., Bland, P. W., Prinz, I., Zugel, U., & Kaufmann, S. H. 1999, "Autoimmune intestinal pathology induced by hsp60-specific CD8 T cells", *Immunity.*, vol. 11, no. 3, pp. 349-358.

281. Stevens, C., Walz, G., Singaram, C., Lipman, M. L., Zanker, B., Muggia, A., Antonioli, D., Peppercorn, M. A., & Strom, T. B. 1992, "Tumor necrosis factor-alpha, interleukin-1 beta, and interleukin-6 expression in inflammatory bowel disease", *Dig.Dis.Sci.*, vol. 37, no. 6, pp. 818-826.

282. Stewart, T. H., Hetenyi, C., Rowsell, H., & Orizaga, M. 1980, "Ulcerative enterocolitis in dogs induced by drugs", *J.Pathol.*, vol. 131, no. 4, pp. 363-378.

283. Stockton, J. C., Howson, J. M., Awomoyi, A. A., McAdam, K. P., Blackwell, J. M., & Newport, M. J. 2004, "Polymorphism in NOD2, Crohn's disease, and susceptibility to pulmonary tuberculosis", *FEMS Immunol.Med.Microbiol.*, vol. 41, no. 2, pp. 157-160.

284. Sturniolo, G. C., Di, L., V, Ferronato, A., D'Odorico, A., & D'Inca, R. 2001, "Zinc supplementation tightens "leaky gut" in Crohn's disease", *Inflamm.Bowel.Dis.*, vol. 7, no. 2, pp. 94-98.

285. Sundberg, J. P., Elson, C. O., Bedigian, H., & Birkenmeier, E. H. 1994, "Spontaneous, heritable colitis in a new substrain of C3H/HeJ mice", *Gastroenterology*, vol. 107, no. 6, pp. 1726-1735.

286. Takeda, K., Clausen, B. E., Kaisho, T., Tsujimura, T., Terada, N., Forster, I., & Akira, S. 1999, "Enhanced Th1 activity and development of chronic enterocolitis in mice devoid of Stat3 in macrophages and neutrophils", *Immunity.*, vol. 10, no. 1, pp. 39-49.

287. Tan, X., Hsueh, W., & Gonzalez-Crussi, F. 1993, "Cellular localization of tumor necrosis factor (TNF)-alpha transcripts in normal bowel and in necrotizing enterocolitis. TNF gene expression by Paneth cells, intestinal eosinophils, and macrophages", *Am.J.Pathol.*, vol. 142, no. 6, pp. 1858-1865.

288. Tanabe, H., Ayabe, T., Bainbridge, B., Guina, T., Ernst, R. K., Darveau, R. P., Miller, S. I., & Ouellette, A. J. 2005, "Mouse paneth cell secretory responses to cell surface glycolipids of virulent and attenuated pathogenic bacteria", *Infect.Immun.*, vol. 73, no. 4, pp. 2312-2320.

289. Tanabe, T., Chamaillard, M., Ogura, Y., Zhu, L., Qiu, S., Masumoto, J., Ghosh, P., Moran, A., Predergast, M. M., Tromp, G., Williams, C. J., Inohara, N., & Nunez, G. 2004, "Regulatory regions and critical residues of NOD2 involved in muramyl dipeptide recognition", *EMBO J.*, vol. 23, no. 7, pp. 1587-1597.

290. Tani, T., Fujino, M., Hanasawa, K., Shimizu, T., Endo, Y., & Kodama, M. 2000, "Bacterial translocation and tumor necrosis factor-alpha gene expression in experimental hemorrhagic shock", *Crit Care Med.*, vol. 28, no. 11, pp. 3705-3709.

291. Thompson, N. P., Driscoll, R., Pounder, R. E., & Wakefield, A. J. 1996, "Genetics versus environment in inflammatory bowel disease: results of a British twin study", *BMJ*, vol. 312, no. 7023, pp. 95-96.

292. Thornberry, N. A. & Lazebnik, Y. 1998, "Caspases: enemies within", *Science*, vol. 281, no. 5381, pp. 1312-1316.

293. Ting, J. P. & Davis, B. K. 2005, "CATERPILLER: a novel gene family important in immunity, cell death, and diseases", *Annu.Rev.Immunol.*, vol. 23, pp. 387-414.

294. Todd, J. A. 2001, "Human genetics. Tackling common disease", *Nature*, vol. 411, no. 6837, pp. 537, 539.

295. Tomita, Y., Jyoyama, H., Kobayashi, M., Kuwabara, K., Furue, S., Ueno, M., Yamada, K., Ono, T., Teshirogi, I., Nomura, K., Arita, H., Okayasu, I., & Hori, Y. 2003, "Role of group IIA phospholipase A2 in rat colitis induced by dextran sulfate sodium", *Eur.J.Pharmacol.*, vol. 472, no. 1-2, pp. 147-158.

296. Tysk, C., Lindberg, E., Jarnerot, G., & Floderus-Myrhed, B. 1988, "Ulcerative colitis and Crohn's disease in an unselected population of monozygotic and dizygotic twins. A study of heritability and the influence of smoking", *Gut*, vol. 29, no. 7, pp. 990-996.

297. Uyar, F. A., Saruhan-Direskeneli, G., & Gul, A. 2004, "Common Crohn's disease-predisposing variants of the CARD15/NOD2 gene are not associated with Behcet's disease in Turkey", *Clin.Exp.Rheumatol.*, vol. 22, no. 4 Suppl 34, p. S50-S52.

298. van Duist, M. M., Albrecht, M., Podswiadek, M., Giachino, D., Lengauer, T., Punzi, L., & De Marchi, M. 2005, "A new CARD15 mutation in Blau syndrome", *Eur.J.Hum.Genet.*, vol. 13, no. 6, pp. 742-747.

299. van Dullemen, H. M., Van Deventer, S. J., Hommes, D. W., Bijl, H. A., Jansen, J., Tytgat, G. N., & Woody, J. 1995, "Treatment of Crohn's disease with anti-tumor necrosis factor chimeric monoclonal antibody (cA2)", *Gastroenterology*, vol. 109, no. 1, pp. 129-135.

300. van Es, J. H., Jay, P., Gregorieff, A., van Gijn, M. E., Jonkheer, S., Hatzis, P., Thiele, A., van den, B. M., Begthel, H., Brabletz, T., Taketo, M. M., & Clevers, H. 2005, "Wnt signalling induces maturation of Paneth cells in intestinal crypts", *Nat.Cell Biol.*, vol. 7, no. 4, pp. 381-386.

301. Van Heel, D. A., McGovern, D. P., & Jewell, D. P. 2001, "Crohn's disease: genetic susceptibility, bacteria, and innate immunity", *Lancet*, vol. 357, no. 9272, pp. 1902-1904.

302. Vavassori, P., Borgiani, P., D'Apice, M. R., De Negris, F., Del Vecchio, B. G., Monteleone, I., Biancone, L., Novelli, G., & Pallone, E. 2002, "3020insC mutation within the NOD2 gene in Crohn's disease: frequency and association with clinical pattern in an Italian population", *Dig.Liver Dis.*, vol. 34, no. 2, p. 153.

303. Vavricka, S. R., Musch, M. W., Chang, J. E., Nakagawa, Y., Phanvijhitsiri, K., Waypa, T. S., Merlin, D., Schneewind, O., & Chang, E. B. 2004, "hPepT1 transports muramyl dipeptide, activating NF-kappaB and stimulating IL-8 secretion in human colonic Caco2/bbe cells", *Gastroenterology*, vol. 127, no. 5, pp. 1401-1409.

304. Vermeire, S., Wild, G., Kocher, K., Cousineau, J., Dufresne, L., Bitton, A., Langelier, D., Pare, P., Lapointe, G., Cohen, A., Daly, M. J., & Rioux, J. D. 2002, "CARD15 genetic variation in a Quebec population: prevalence, genotype-phenotype relationship, and haplotype structure", *Am.J.Hum.Genet.*, vol. 71, no. 1, pp. 74-83.

305. Viala, J., Chaput, C., Boneca, I. G., Cardona, A., Girardin, S. E., Moran, A. P., Athman, R., Memet, S., Huerre, M. R., Coyle, A. J., DiStefano, P. S., Sansonetti, P. J., Labigne, A., Bertin, J., Philpott, D. J., & Ferrero, R. L. 2004, "Nod1 responds to peptidoglycan delivered by the Helicobacter pylori cag pathogenicity island", *Nat.Immunol.*, vol. 5, no. 11, pp. 1166-1174.

306. Vidal, S., Khush, R. S., Leulier, F., Tzou, P., Nakamura, M., & Lemaitre, B. 2001, "Mutations in the Drosophila dTAK1 gene reveal a conserved function for MAPKKKs in the control of rel/NF-kappaB-dependent innate immune responses", *Genes Dev.*, vol. 15, no. 15, pp. 1900-1912.

307. Walsh, M. C. & Kliegman, R. M. 1986, "Necrotizing enterocolitis: treatment based on staging criteria", *Pediatr.Clin.North Am.*, vol. 33, no. 1, pp. 179-201.

308. Wang, C., Deng, L., Hong, M., Akkaraju, G. R., Inoue, J., & Chen, Z. J. 2001, "TAK1 is a ubiquitin-dependent kinase of MKK and IKK", *Nature*, vol. 412, no. 6844, pp. 346-351.

309. Watanabe, M., Watanabe, N., Iwao, Y., Ogata, H., Kanai, T., Ueno, Y., Tsuchiya, M., Ishii, H., Aiso, S., Habu, S., & Hibi, T. 1997, "The serum factor from patients with ulcerative colitis that induces T cell proliferation in the mouse thymus is interleukin-7", *J.Clin.Immunol.*, vol. 17, no. 4, pp. 282-292.

310. Watanabe, T., Kitani, A., Murray, P. J., & Strober, W. 2004, "NOD2 is a negative regulator of Toll-like receptor 2-mediated T helper type 1 responses", *Nat.Immunol.*, vol. 5, no. 8, pp. 800-808.

311. Wehkamp, J., Harder, J., Weichenthal, M., Schwab, M., Schaffeler, E., Schlee, M., Herrlinger, K. R., Stallmach, A., Noack, F., Fritz, P., Schroder, J. M., Bevins, C. L., Fellermann, K., & Stange, E. F. 2004, "NOD2 (CARD15) mutations in Crohn's disease are associated with diminished mucosal alpha-defensin expression", *Gut*, vol. 53, no. 11, pp. 1658-1664.

312. Willerford, D. M., Chen, J., Ferry, J. A., Davidson, L., Ma, A., & Alt, F. W. 1995, "Interleukin-2 receptor alpha chain regulates the size and content of the peripheral lymphoid compartment", *Immunity.*, vol. 3, no. 4, pp. 521-530.

313. Wilson, C. L., Ouellette, A. J., Satchell, D. P., Ayabe, T., Lopez-Boado, Y. S., Stratman, J. L., Hultgren, S. J., Matrisian, L. M., & Parks, W. C. 1999, "Regulation of intestinal alpha-defensin activation by the metalloproteinase matrilysin in innate host defense", *Science*, vol. 286, no. 5437, pp. 113-117.

314. Wirtz, S., Finotto, S., Kanzler, S., Lohse, A. W., Blessing, M., Lehr, H. A., Galle, P. R., & Neurath, M. F. 1999, "Cutting edge: chronic intestinal inflammation in STAT-4 transgenic mice: characterization of disease and adoptive transfer by TNF- plus IFN-gamma-producing CD4+ T cells that respond to bacterial antigens", *J.Immunol.*, vol. 162, no. 4, pp. 1884-1888.

315. Yamada, T., Sartor, R. B., Marshall, S., Specian, R. D., & Grisham, M. B. 1993, "Mucosal injury and inflammation in a model of chronic granulomatous colitis in rats", *Gastroenterology*, vol. 104, no. 3, pp. 759-771.

316. Yamaoka, S., Courtois, G., Bessia, C., Whiteside, S. T., Weil, R., Agou, F., Kirk, H. E., Kay, R. J., & Israel, A. 1998, "Complementation cloning of NEMO, a component of the IkappaB kinase complex essential for NF-kappaB activation", *Cell*, vol. 93, no. 7, pp. 1231-1240.

317. Yamazaki, K., Takazoe, M., Tanaka, T., Kazumori, T., & Nakamura, Y. 2002, "Absence of mutation in the NOD2/CARD15 gene among 483 Japanese patients with Crohn's disease", *J.Hum.Genet.*, vol. 47, no. 9, pp. 469-472.

318. Yang, R. B., Mark, M. R., Gray, A., Huang, A., Xie, M. H., Zhang, M., Goddard, A., Wood, W. I., Gurney, A. L., & Godowski, P. J. 1998, "Toll-like receptor-2 mediates lipopolysaccharide-induced cellular signalling", *Nature*, vol. 395, no. 6699, pp. 284-288.

319. Young, C., Allen, M. H., Cuthbert, A., Ameen, M., Veal, C., Leman, J., Burden, A. D., Kirby, B., Griffiths, C. E., Trembath, R. C., Mathew, C. G., & Barker, J. N. 2003, "A Crohn's disease-associated insertion polymorphism (3020insC) in the NOD2 gene is not associated with psoriasis vulgaris, palmo-plantar pustular psoriasis or guttate psoriasis", *Exp.Dermatol.*, vol. 12, no. 4, pp. 506-509.

320. Zhang, J., Yang, J., Roy, S. K., Tininini, S., Hu, J., Bromberg, J. F., Poli, V., Stark, G. R., & Kalvakolanu, D. V. 2003, "The cell death regulator GRIM-19 is an inhibitor of signal transducer and activator of transcription 3", *Proc.Natl.Acad.Sci.U.S.A*, vol. 100, no. 16, pp. 9342-9347.

321. Zouiten-Mekki, L., Zaouali, H., Boubaker, J., Karoui, S., Fekih, M., Matri, S., Hamzaoui, S., Filali, A., Chaabouni, H., & Hugot, J. P. 2005, "CARD15/NOD2 in a Tunisian population with Crohn's disease", *Dig.Dis.Sci.*, vol. 50, no. 1, pp. 130-135.

Appendix A: The allele frequencies of Crohn's disease-associated NOD2 variants

Study, First author (year)	Allele frequencies (%)									Patients with at least one NOD2 risk allele		
	Arg702Trp			Gly908Arg			Leu1007fsinsC					
	Crohn's disease	Healthy controls	Ulcerative colitis	Crohn's disease	Healthy controls	Ulcerative colitis	Crohn's disease	Healthy controls	Ulcerative colitis	Crohn's disease	Healthy controls	Ulcerative colitis
Caucasians, non-Jewish descent												
Ogura (2001)	-	-	-	-	-	-	8.2	4	3	-	-	-
Abreu (2002) 2 cohorts	8.1	-	2.9	5.6	-	0.9	5.8	-	1.7	34.4	-	10.9
Ahmad (2002)	12.5	5.2	-	3.3	1.4	-	9.4	1.6	-	38.5	15.8	
Cuthbert (2002)	9.1	3.5	3.7	3.3	0.6	1.6	5.4	2.1	1.5			14.6
Hampe (2002)	4.5	2.7	-	0.9	1.2	-	2.7	1.2	-			
Lesage (2002)	10.8	4.4	3.1	6.1	1	0.3	10.6	1.9	1.3	41.5	14.6	8.8
Mascheretti (2002)	7.9	4.3	-	3.8	2	-	7.6	3.5	-	31.3		
Radlmayr (2002)							13.9	1.7	2.1			

Study, First author (year)	Allele frequencies (%)									Patients with at least one NOD2 risk allele (%)		
	Arg702Trp			Gly908Arg			Leu1007fsinsC					
	Crohn's disease	Healthy controls	Ulcerative colitis	Crohn's disease	Healthy controls	Ulcerative colitis	Crohn's disease	Healthy controls	Ulcerative colitis	Crohn's disease	Healthy controls	Ulcerative colitis
Caucasians, non-Jewish descent, continued												
Vermeire (2002) B+C	11.5	3.2	-	5	0.6	-	7.8	0.9	-	38.7	8.7	
Brant (2003)										3.9		
Cavanaugh (2003)	11.2	4.5	0	2.4	0.7	0	6.7	1	0	36.7	12.5	0
Croucher (2003)	8.5	6.1	-	4.1	1.3	-	11	4.2	3.1	39.7	19.3	
Helio (2003)	3.3	1.8	1.5	0.6	0	0	5	1.7	3	15.5	6.7	9.1
Louis (2003)										45.5		
Mirza (2003)										34.4	14.3	
Murillo (2003)							8.5	1				
Palmieri (2003)	10.6	6.0	3.1	8.5	2.3	3.1	9.6	1.4	3.1			
Roussomoustakaki (2003)							2.7	1.5	0			
Sugimura (2003)	8.4	3.5	-	8.4	3.5	-	5.1	1.4		30.1	13.3	

Study, First author (year)	Allele frequencies (%)									Patients with at least one NOD2 risk allele (%)		
	Arg702Trp			Gly908Arg			Leu1007fsinsC					
	Crohn's disease	Healthy controls	Ulcerative colitis	Crohn's disease	Healthy controls	Ulcerative colitis	Crohn's disease	Healthy controls	Ulcerative colitis	Crohn's disease	Healthy controls	Ulcerative colitis
Caucasians, non-Jewish descent, continued												
Tomer (2003)	2.9	0.7	-	5.7	2.9	-	8.6	1.8	-	31.0	11.0	
van der Linde (2003)							13.9	1.9	1.6			
Mendoza (2003)	13.7	4.3	-	8.3	2.1	-	14.2	4.3	-	32.8	10.7	
Annese (2004)	8.8	3.9	-	6.9	2.0	-	8.3	0.7	-	40.6	13.4	
Nunez (2004)	6.7	5.8	-	4.5	1.0	-	4.5	1.0	-	27.9	15.2	
Buning (2004)	7.2	3.6	2.1	4.2	2.1	2.1	12.2	2.1	4.3	35.6	15.5	14.3
Giachino (2004)	8.9	5.6	10.9	4.9	1.4	2.7	6.3	2.2	0.5	32.6	18.6	33.3
Newman (2004)	10.3	5.0	-	3.7	2.0	-	4.9	3.0	-			

Study, First author (year)	Allele frequencies (%)									Patients with at least one NOD2 risk allele (%)		
	Arg702Trp			Gly908Arg			Leu1007fsinsC					
	Crohn's disease	Healthy controls	Ulcerative colitis	Crohn's disease	Healthy controls	Ulcerative colitis	Crohn's disease	Healthy controls	Ulcerative colitis	Crohn's disease	Healthy controls	Ulcerative colitis
Caucasians, Jewish descent												
Zhou (2002)	5.1	4.5	-	8.3	5.5	-	6.1	3.6	-	31.8	26.3	
Fidder (2003)	5.3	-	2.9	7.9	-	2.9	2.4	-	0.7	27.1	-	10.3
Sugimura (2003)	4.5	3.8		7.6	5.1		5.8	1.3		33	18.9	
Newman (2004)	4.9	3.2		7.3	4.3		8.4	3.7				
Tukel (2004)	6.9	2.8		8.3	4.3		5.6	3.0				
Karban (2004)										38.0		9.1

Study, First author (year)	Allele frequencies (%)									Patients with at least one NOD2 risk allele (%)		
	Arg702Trp			Gly908Arg			Leu1007fsinsC					
	Crohn's disease	Healthy controls	Ulcerative colitis	Crohn's disease	Healthy controls	Ulcerative colitis	Crohn's disease	Healthy controls	Ulcerative colitis	Crohn's disease	Healthy controls	Ulcerative colitis
Asians												
Inoue (2002)	0	0	0	0	0	0	0	0	0	0	0	0
Croucher (2003)	0	0		0	0		0	0		0	0	
Leong (2003)	0	0	0	0	0	0	0	0	0	0	0	0
Sugimura (2003)	0	0		0	0		0	0		0	0	
Guo (2004)							3.3	0.3	1.3	7.1	0.6	2.7

Appendix B: The Vienna Classification of Crohn's disease

Age at diagnosis[1]:	A1, <40 years
	A2, ≥40 years
Location[2]:	L1, Terminal ileum[3]
	L2, Colon[4]
	L3, Ileo-colon[5]
	L4, Upper gastrointestinal[6]
Behavior:	B1, Non-stricturing non-penetrating (i.e. inflammatory)[7]
	B2, Stricturing[8]
	B3, Penetrating[9]

Adapted from Gasche (2000)

1. Age when diagnosis of Crohn's disease was definitively established by radiology, endoscopy, pathology or surgery.
2. The maximum extent of disease involvement at any time before the first resection. Minimum involvement for a location is defined as any aphthous lesion or ulceration. Mucosal erythema and edema are insufficient. For classification at least both, a small bowel and large bowel examination, are required.
3. Disease limited to the terminal ileum (the lower third of the small bowel) with or without spill over into cecum.
4. Any colonic location between cecum and rectum with no small bowel or upper gastrointestinal involvement.
5. Disease of the terminal ileum with/without spill over into cecum, or any location in the colon.
6. Any disease location proximal to the terminal ileum (excluding the mouth) regardless of additional involvement of the terminal ileum or colon.
7. Inflammatory disease which never has been complicated at any time in the course of disease.
8. Stricturing disease is defined as the occurrence of constant luminal narrowing demonstrated by radiologic, endoscopic or surgical-pathologic methods with prestenotic dilatation or obstructive signs/ symptoms without presence of penetrating disease at any time in the course of disease.
9. Penetrating disease is defined as the occurrence of intra-abdominal or perianal fistulas, inflammatory masses and/or abscesses at any time in the course of disease. Perianal ulcers are also included. Excluded are postoperative intra-abdominal complications and perianal skin tags.

Appendix C: List of reagents and suppliers

	Name of reagent	Supplier
1.	β-mercaptoethanol	Sigma
2.	100x Antibiotic antimycotic solution: 10 000 U penicillin, 10 mg streptomycin, and 25 μg amphotericin B per mL	Sigma
3.	10x Trypsin-EDTA solution: 5.0 g porcine trypsin, 2.0 g EDTA·4 Na in 0.9% NaCl	Sigma
4.	1-palmitoyl-2-[1-^{14}C]palmitoyl L-3-phosphaditylcholine (925 kBq/ml, 1.85-2.29 GBq/mmol)	Amersham
5.	^{32}P dCTP (10 mCi/mL) (Redivue deoxycylidine 5' [α ^{32}P] triphosphate, triethylammonium salt; 11TBq/mmol, ~3000 Ci/mmol)	Amersham
6.	5X First Strand Buffer [250 mM Tris-HCl (pH 8.30, 375 mM KCl, 15 mM $MgCl_2$]	Invitrogen
7.	Acetic acid	VWR
8.	Acrylamide	Sigma
9.	Agarose	Sigma
10.	Ammonium acetate (5M)	Sigma
11.	Ammonium persulphate	Sigma
12.	Ampicillin	Sigma
13.	Avidin-biotin peroxidase complex (ABC) reagent	Vector
14.	Bacto-agar	Appleton Woods
15.	Bee venom PLA_2	Sigma
16.	Biotinylated anti-mouse antibody	Vector
17.	Biotinylated anti-rabbit and anti-mouse immunoglobulin antibodies	Vector
18.	Bovine serum albumin	Sigma
19.	Bromophenol blue	Sigma
20.	Calcium chloride ($CaCl_2$)	Sigma
21.	Chloroform	VWR

22.	Chloroform: isoamyl alcohol (24:1 or 49:1)	Sigma
23.	Coomassie blue	Sigma
24.	DAB/ 0.02% hydrogen peroxide	Sigma
25.	Deoxyadenosine triphosphate (dATP) 100 mM	Invitrogen
26.	Deoxycytidine triphosphate (dCTP) 100 mM	Invitrogen
27.	Deoxyguanosine triphosphate (dGTP) 100 mM	Invitrogen
28.	Deoxythymidine triphosphate (dTTP) 100 mM	Invitrogen
29.	Dextran sulphate	Amersham
30.	DH5α E.Coli	Invitrogen
31.	Diethyl ether	VWR
32.	Diethyl-pyrocarbonate (DEPC)	Sigma
33.	DIG RNA labeling Kit	Roche Diagnostics
34.	Dimethyl formamide	VWR
35.	Dipalmitoyl phosphatidylcholine stock solution: 120 mM dipalmitoyl L-α-phosphatidylcholine (1, 2-dipalmitoyl-sn-glycero-3-phosphocholine)	Sigma
36.	Dithiothreitol (DTT)	Sigma
37.	DMEM/F12 medium	Sigma
38.	DNase 1 (10 U/μL; RNase-free)	Sigma
39.	Dulbecco PBS	Royal Free Hospital Pharmacy
40.	Dulbecco's modified Eagle medium (DMEM)	Sigma
41.	Ecl136II restriction endonuclease	Helena Biosciences
42.	EcoRI restriction endonuclease	Invitrogen
43.	Ecoscint A scintillation fluid	Phillip Harris
44.	EDTA (pH 8.0) Ethylenediaminetetraacetic acid	Sigma
45.	Ethanol	VWR
46.	Ethidium bromide	Sigma
47.	Ficoll 400	Sigma
48.	Foetal calf serum	Sigma
49.	Formaldehyde (37%)	Sigma
50.	Formamide	Sigma
51.	Glucose	Sigma
52.	Glycerol	Sigma

53.	Glycine	Sigma
54.	Goat Serum	Sigma
55.	H_2O_2 (30%)	VWR
56.	Haematoxylin	VWR
57.	Hanks' balanced salt solutions (HBSS)	Sigma
58.	HEPES [N-(2-Hydroxyethyl)piperazine-N′-(2-ethanesulfonic acid) hemisodium salt]	Sigma
59.	Hexane	VWR
60.	HindIII restriction endonuclease	Invitrogen
61.	Histopaque® 1077	Sigma
62.	Horse Serum	Sigma
63.	Hydrochloric acid (HCl)	VWR
64.	IPTG (isopropylthio-β-D-galactoside)	Sigma
65.	Isopropanol	VWR
66.	Klenow fragment	Helena Biosciences
67.	L-Glutamine, 200 mM	Sigma
68.	Maleic acid	Sigma
69.	Methanol	VWR
70.	Magnesium chloride ($MgCl_2$)	Sigma
71.	Moloney Murine Leukemia Virus Reverse Transcriptase (M-MLV RT) (200 units/ μL)	Invitrogen
72.	MOPS [3-(N-Morpholino)propanesulfonic acid]	Sigma
73.	Mouse anti-digoxigenin monoclonal antibody	Roche Diagnostics
74.	Neutral buffered formalin (10%)	VWR
75.	Nuclease-free water	Invitrogen
76.	Oligo$(dT)_{12-18}$ primer	Invitrogen
77.	Paraformaldehyde	Sigma
78.	Phenol: chloroform: isoamyl alcohol (25:24:1 or 50:49:1)	Sigma
79.	Phosphate Buffered Solution (PBS)	Sigma
80.	Phytohaemagglutinin (PHA)	Sigma
81.	PIPES (1,4-Piperazinediethanesulfonic acid)	Sigma
82.	Polyvinyl pyrrolidone	Sigma

83.	Pooled human AB serum	Invitrogen
84.	Porcine pancreas PLA_2 (Type IB)	Sigma
85.	Protease inhibitor	Sigma
86.	Proteinase K	Sigma
87.	PstI restriction endonuclease	Invitrogen
88.	pUC 18 plasmid DNA	Helena Biosciences
89.	PvuII restriction endonuclease	Invitrogen
90.	Qiaprep® Spin Miniprep kit	Qiagen
91.	Random hexamers	Invitrogen
92.	RNase A	Sigma
93.	Roswell Park Memorial Institute (RPMI)-1640 Medium	Sigma
94.	Salmon sperm DNA	Sigma
95.	SmaI restriction endonuclease	Invitrogen
96.	Sodium acetate (3M; pH 5.2)	Sigma
97.	Sodium chloride (NaCl)	Sigma
98.	Sodium deoxycholate	Sigma
99.	Sodium dodecyl sulfate (SDS)	Sigma
100.	Sodium hydroxide (NaOH) pellets	VWR
101.	SstI restriction endonuclease	Invitrogen
102.	TEMED (Tetramethylethylenediamine)	Sigma
103.	Transfer RNA (tRNA)	Roche Diagnostics
104.	Tris-Cl (pH 8.0) Tris(hydroxymethyl)aminomethane	Sigma
105.	Tris-HCl (pH 7.4)	Sigma
106.	Triton X-100	Sigma
107.	Trizol reagent	Invitrogen
108.	Tryptone	Appleton Woods
109.	Tween 20	Sigma
110.	X-gal (5-bromo-4-chloro-3-indoyl-β-D-galactoside)	Sigma
112.	Xylene	VWR
113.	Xylene cyanol	Sigma
114.	Yeast extract	Appleton Woods

List of Suppliers:

Amersham Biosciences UK Limited
Amersham Place
Little Chalfont
Buckinghamshire
HP7 9NA
United Kingdom

Anachem Limited
Anachem House
20 Charles Street
Luton
LU2 0EB
United Kingdom
Phone: 01582 747 500
Fax: 01582 745 105
Email: bioscience@anachem-ltd.com

Appleton Woods
Lindon House
Heeley Road
Selly Oak
Birmingham
B29 6EN
United Kingdom
Phone: 01214 727 353
Fax: 01214 141 075

Bio-Rad Laboratories Limited
Bio-Rad House
Maylands Avenue
Hemel Hempstead
Hertfordshire
HP2 7TD
United Kingdom
Phone: 0208 328 2247
Email: techsupport.uk@bio-rad.com

DakoCytomation Limited
Denmark House
Angel Drove
Ely
CB7 4ET
United Kingdom
Phone: 01353 669 911
Fax: 01353 668 989

Eppendorf Scientific Incorporated
One Cantiague Road
P.O. Box 1019
Westbury
New York
11590-0207
USA
Phone: 00 1 800 421 9988
Fax: 00 1 516 876 8599
Email: eppendorf@eppendorfsi.com
UK distributor: VWR International

Helena BioSciences Europe
Colima Avenue
Sunderland Enterprise Park
Sunderland
Tyne & Wear
SR5 3XB
United Kingdom
Phone: 01915 496 064
Fax: 01915 496 271

Invitrogen Limited
3 Fountain Drive
Inchinnan Business Park
Paisley
PA4 9RF
United Kingdom
Phone: 01418 146 100
Fax: 01418 146 260

LCG Promochem
Queen's Road
Teddington
Middlesex
TW11 0LY
London
United Kingdom
Phone: 0208 943 7000

Perbio Science UK Limited
Century House
High Street
Tattenhall
Cheshire
CH3 9RJ
United Kingdom
Phone: 01829 771 744
Fax: 01829 771 644
Email: uk.info@perbio.com

Philip Harris Scientific
Findel House
Excelsior Road
Ashby Park
Ashby de la Zouch
Leicestershire
LE65 1NG
United Kingdom
Phone: 08451 204 520
Fax: 01530 419 492

Qiagen Limited
Qiagen House
Fleming Way
Crawley
West Sussex
RH10 9NQ
United Kingdom
Phone: 01293 422 911
Fax: 01293 422 922

Roche Diagnostics Limited
Bell Lane
Lewes
East Sussex
BN7 1LG
United Kingdom
Phone: 01273 480 444

Sigma-Aldrich Company Limited
The Old Brickyard
New Road
Gillingham
Dorset
SP8 4XT
United Kingdom
Phone: 0800 717 181
Fax: 0800 378 785
Email: ukorders@europe.sial.com

Thermo Electron GmbH
Sedanstrasse 18
89077 Ulm
Germany
Phone: +49 (0)731 935 79 290
Fax: +49 (0)731 935 79 291
Email: sales.oligos@thermo.com

Vector Laboratories Limited
3 Accent Park
Bakewell Road
Orton Southgate
Peterborough
PE2 6XS
United Kingdom
Phone: 01733 237 999
Fax: 01733 237 119

VWR International Limited
Merck House
Poole
Dorset
BH15 1TD
United Kingdom
Phone: 01202 660 444
Fax: 01202 666 856

Publications

Original articles

1. Lala, S., Ogura, Y., Osborne, C., Hor, S. Y., Bromfield, A., Davies, S., Ogunbiyi, O., Nunez, G., & Keshav, S. 2003, "Crohn's disease and the NOD2 gene: a role for Paneth cells", *Gastroenterology*, vol. 125, no. 1, pp. 47-57.

2. Ogura, Y., Lala, S., Xin, W., Smith, E., Dowds, T. A., Chen, F. F., Zimmermann, E., Tretiakova, M., Cho, J. H., Hart, J., Greenson, J. K., Keshav, S., & Nunez, G. 2003a, "Expression of NOD2 in Paneth cells: a possible link to Crohn's ileitis", *Gut*, vol. 52, no. 11, pp. 1591-1597.

Review articles

1. Keshav, S. & Lala, S. 2003, "The Paneth Cell in IBD - New Kid on the Block?" *IBD Monitor*, vol. 5, pp. 2-10.

Poster presentations

2. Lala S.G., Turton D., Keshav S. 2002, "Expression of Tumour Necrosis Factor α (TNFα) and Lysozyme in Necrotizing Enterocolitis (NEC)", *Gut*, vol. 50 (Suppl 2), pp 1-125. Oral presentation at the British Society of Gastroenterology Annual Meeting, Birmingham, UK, 17-20 March 2002.

3. Lala S.G., Ogura Y., Hor S.K., Abeya M., Osborne C., Davies S., Ogunbiyi O. Nunez G., Keshav S. 2003, "Crohn's Disease and the NOD2 Gene: A Role for Paneth Cells", Gut, vol. 52 (Suppl 1), pp 1-130. Plenary poster presentation at the British Society of Gastroenterology Annual Meeting, Birmingham, UK, 23-26 March 2003.

4. Lala S., Bromfield A., Hor S., Osborne C., Ogunbiyi O., Keshav S., 2003, "Paneth cells in the terminal ileum are the main site of local NOD2 gene expression". Oral presentation at Digestive Diseases Week, Orlando, USA 2003, 21 May 2003.

5. Lala S.G., Turton D., Keshav S. 2003, "Expression of secretory phospholipase A_2 in necrotizing enterocolitis", Poster presentation at the European Society of Paediatric Hepatology, Gastroenterology and Nutrition Annual Meeting, Prague, Czech Republic, 2003.

In preparation

1. Abeya M., Bromfield A., Lala S., Sheshappanavar V., Deroide F., Heuschkel R., Ogunbiyi O., Keshav S., "Paneth cells in Crohn's disease: effect of NOD2 gene status", *manuscript in preparation.*